Evolved P450 mutants as general oxidation catalysts for target synthesis via C–H activation

A thesis submitted to the

Board of the Faculty of the Physical Sciences

in partial fulfilment of the requirements for the degree of

Doctor of Philosophy of the University of Oxford

Jonathan Gregory Moloney

Hertford College

Hilary Term 2022

Declaration

The work described in this thesis was carried out in the Chemistry Research Laboratory and the Inorganic Chemistry Laboratory, University of Oxford, from September 2018 until January 2021, under the supervision of Professor Jeremy Robertson and Professor Luet L. Wong. All of the work is my own unless otherwise stated and has not been submitted previously for any other degree at this or any other university.

Jonathan G. Moloney

January 2022

Abstract

Evolved P450 mutants as general oxidation catalysts for target synthesis via C–H activation

Jonathan Gregory Moloney D.Phil.

Hertford College Hilary Term 2022

This thesis describes synthetic studies towards three natural product precursors: the tricyclic core of the abietane diterpenoids, a bicyclic lactone intermediate on Danishefsky's route towards eleutherobin, and the hydrocarbon core of Taxol®. These syntheses were followed by an investigation into biocatalytic oxidation with particular focus on kinetic resolution.

Chapter 1 provides an introduction to contemporary chemical and biocatalytic C–H functionalisation for the introduction of oxygen and its use in natural products synthesis.

Chapter 2 describes the synthesis of an abietane tricycle and an investigation into kinetic resolution through oxidation by CYP102A1 enzymes. In the case of one P450 variant a study was carried out into the origin of the kinetic resolution process alongside the use of this reactivity in the synthesis of a natural product, margocin.

Chapter 3 explores the synthesis of a bicyclic lactone and its biocatalytic oxidation with cytochrome P450 variants. Kinetic resolution was observed with three enzyme variants and, through alteration of the enzyme variant employed, control of the major metabolite and its enantiomeric excess was possible.

Finally, chapter 4 outlines a synthetic study towards a taxane diterpenoid, again with a view to an investigation into its behaviour upon reaction with CYP102A1 variants. Submission of the taxane substrate to biocatalytic conditions showed a complex reaction profile, with clear evidence of kinetic resolution processes again observed.

Table of Contents

Acknowledgements

First thanks must go to my supervisors Jeremy and Luet.

Jeremy, put simply I could not have got through this D. Phil working for anyone else. Not only has your unparalleled knowledge of both theoretical and practical chemistry steered the project through its many rough patches, but your understanding of life outside the lab gave a much-needed sense of perspective and has allowed me to spend time looking towards life after university.

Luet, this project would not have come anywhere without your vast experience within the world of cytochrome P450s. Through working in your lab, I've been able to spend time doing research I never thought I would have the opportunity to carry out and have developed a feel for science outside of organic chemistry!

Next, I must thank Francesco and Andy, without whom this project certainly would not be as far progressed as it is, and Yang, who not only took us to some fantastic restaurants in Suzhou, but also carried out some key experiments after I left.

Thanks to the facilities and analytical service staff in the CRL, my experimental section would be significantly shorter without their help!

To all the members of the Robertson and Wong groups, past and present, thank you for everything. I would not be where I am without the guidance, jokes, tears, music, cakes, coffees, and whatever else we've shared over the last three years.

In particular I must thank Lucy. I would not have made it through the last few years without your help in and out of the lab. Your sense of humour and ability to endlessly sink beers has been instrumental in me keeping my sanity (just!) and our trip to China was the highlight of my D. Phil.

To all my friends, new and old, thank you for the many moments of fun away from the lab that kept me going. The last four years in Oxford would have been significantly harder without switching off from chemistry with you lot.

To Jess, I can't put into words what you've given me over the past five years. Your love and advice have got me through some very difficult times and, as I hope you know, I would have quit this thing a long time ago without your support. Thank you.

Finally, to my family, thank you for everything. You've guided me through the ups and downs of life, not just this D. Phil., and I wouldn't be anything like the man I am now without you. Mum, your endless optimism kept me smiling through the last year, not an easy task! Dad, you're an inspiration. Being able to follow in the footsteps of a scientist (and bloke!) like you kept my faith in science, also not an easy task! Laurence, get the beers out, I'm free!

Abbreviations

% ee	Enantiomeric excess
Ac	Acetyl
BHT	Butylated hydroxytoluene
BINOL	1,1′-Bi-2-naphthol
BM3	Third P450 to be extracted from Bacillus megaterium
Bn	Benzyl
Bu	Butyl
CAL-B	Lipase B from Candida antarctica
COSY	Homonuclear correlation spectroscopy
CuTc	Copper thiophenecarboxylate
CYP	Cytochrome P450
d	Doublet
DBU	1,8-Diazabicyclo[5.4.0]undec-7-ene
DCC	*N*,*N*′-Dicyclohexylcarbodiimide
DCE	Dichloroethane
DIBAL-H	Diisobutyl aluminium hydride
DIPA	Diisopropylamine
DMAP	*N*,*N*-Dimethylaminopyridine
DMDO	Dimethldioxirane
DME	Dimethoxyethane
DMF	Dimethyl formamide
DMP	Dess-Martin periodinane
dmpe	1,2-Bis(dimethylphosphino)ethane

DMPU	N,N′-Dimethylpropyleneurea
DMSO	Dimethylsulfoxide
DNA	Deoxyribonucleic acid
DTBMP	2,6-Di-*tert*-butyl-4-methylpyridine
E. coli	*Escherichia coli*
Eq.	Equivalent
ESI	Electrospray ionisation
Et	Ethyl
FAD	Flavin adenine nucleotide
FMN	Flavin mononucleotide
g	Gram
GC	Gas chromatography
GDH	Glucose dehydrogenase
GDP	Guanosine diphosphate
GTP	Guanosine triphosphate
h	Hour
hept	Heptet
HFIP	Hexafluoroisopropanol
HMBC	Heteronuclear Multiple Bond Correlation
HPLC	High-performance liquid chromatography
HSQC	Heteronuclear Single Quantum Correlation
IMDA	Intramolecular Diels–Alder
IR	Infrared
J	Coupling constant
L	Litre

LC	Liquid chromatography
LDA	Lithium diisopropylamide
LG	Leaving group
LHMDS	Lithium bis(trimethylsilyl)amide
Lit.	Literature value
LUMO	Lowest Unoccupied Molecular Orbital
m	multiplet
M	Mole/litre
m-CPBA	*meta*-chloroperoxybenzoic acid
m.p.	Melting point
m/z	Mass/charge ratio
Me	Methyl
Me	Methyl
mg	Milligram
MHz	Megahertz
mL	Millilitre
mmol	Millimole
MOM	Methoxymethyl
$mP450_{BM3}$	Mutant P450
MS	Mass spectrometry
Ms	Methanesulfonyl
MSA	Microtubule stabilising agent
n-	Normal
NAD	Nicotinamide adenine dinucleotide
NADP	Nicotinamide adenine dinucleotide phosphate

NBS	*N*-Bromosuccinimide
NHC	*N*-heterocyclic carbene
NMR	Nuclear magnetic resonance
nOe	Nuclear Overhauser Effect
NOESY	Nuclear Overhauser Effect Spectroscopy
NPG	*N*-palmitoyl glycine
p	Pentet
p-TSA	*para*-toluenesulfonic acid
PCC	Pyridinium chlorochromate
PCR	Polymerase chain reaction
PDA	Photo Diode Array
PDC	Pyridinium dichromate
PDP	2-({(S)-2-[(S)-1-(pyridin-2-ylmethyl)pyrrolidin-2-yl]pyrrolidin-1-yl}methyl)pyridine]
PFC	Perfluorinated carboxylix acid
Ph	Phenyl
Pr	Propyl
PTAD	(1-Adamantyl)-(N-phthalimido)acetate
PTTL	*N*-phthaloyl-*tert*-leucinate
q	Quarter
R_f	Retention factor
rpm	Rotations per minute
RT	Room temperature
s	Singlet
s-	Secondary

SAR	Structure activity relationship
SFC	Supercritical Fluid Chromatography
t	Triplet
t-	Tertiary
TBAF	Tetrabutylammonium fluoride
TBS	*Tert*-butyldimethylsilyl
TES	Triethylsilyl
Tf	Trifluoromethanesulfonyl
tfa	Trifluoroacetate
THF	Tetrahydrofuran
THF	Tetrahydrofuran
THQ	Tetrahydroquinoline
TLC	Thin layer chromatography
TMS	Trimethylsilyl
UV	Ultraviolet
v/v	volume-to-volume ratio
WT	Wild-type
αKG	Alpha-ketoglutarate
µL	Microlitre

Amino acid codes

Amino acid	Three letter code	One letter code
Alanine	Ala	A
Arginine	Arg	R
Asparagine	Asn	N
Aspartic acid	Asp	D
Cysteine	Cys	C
Glutamic acid	Glu	E
Glutamine	Gln	Q
Glycine	Gly	G
Histidine	His	H
Isoleucine	Ile	I
Leucine	Leu	L
Lysine	Lys	K
Methionine	Met	M
Phenylalanine	Phe	F
Proline	Pro	P
Serine	Ser	S
Threonine	Thr	T
Tryptophan	Trp	W
Tyrosine	Tyr	Y
Valine	Val	V

1 Introduction

1.1 C–H activation

Over the last 50 years, C–H activation has become increasingly important as a tool for the synthesis of organic molecules. The ability to functionalise C–H bonds has had a significant impact on the field of organic chemistry, allowing construction of compounds of interest in a more streamlined fashion, and offering chemists more freedom in their choice of synthetic strategy (***Scheme 1.1***). This broad umbrella of reactivity encompasses a vast array of substrates including sp^3, aromatic and vinylic sp^2, and sp hybridised carbon centres, and a large number of metals, with transition metals being the most common due to their ability to support higher oxidation states – a necessity for oxidative addition of the C–X bond in question.

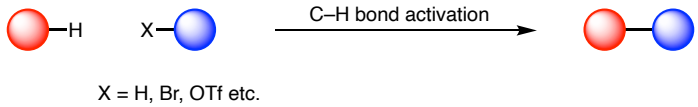

Scheme 1.1. General C–H activation reaction.

The first example of C–H activation by a transition metal complex is attributed to Chatt when he reported that, upon reaction of $Ru(dmpe)_2$ (**1**) with naphthalene (**2**), activation of a C–H bond of a ligand phospinomethyl group or a C–H bond of the naphthalene occurred (***Scheme 1.2***).[1]

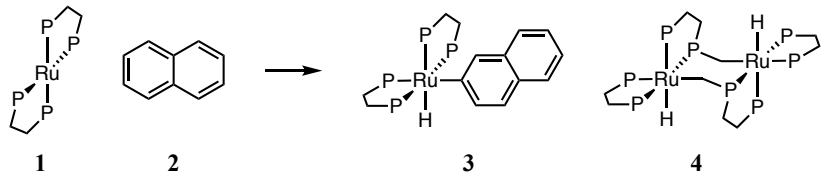

Scheme 1.2. First reported C–H activation; phosphine dimethyl groups have been omitted for clarity.

This concept of using C–H bonds as reactive partners has since been extensively developed; a range of functionality can be inserted including carbon, nitrogen and oxygen (***Figure 1.1***),[2–5] and the use of carbene and nitrene reagents, biologically

inspired and NHC ligands, and biocatalysis, alongside more typical Pd-based catalytic systems, have become commonplace.[6]

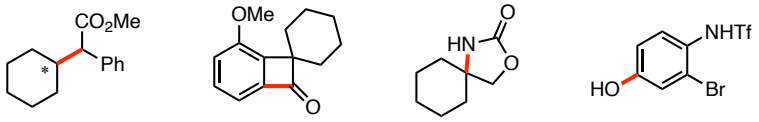

5 **6** **7** **8**

Figure 1.1. Bonds formed by C–H activation reactions; * denotes carbon at which C–H activation occurred.

The ability to functionalise C–H bonds confers a number of benefits to synthetic routes; orthogonality to traditional reactivity, access to otherwise difficult-to-form bonds, and a reduction in the reliance on protecting group strategy through late-stage functionalisation of relatively simple core structures. These advantages make C–H activation chemistry an attractive prospect for synthetic chemists; however, its use can prove difficult, with issues concerning selectivity and reactivity revolving around the strength of the C–H bond and the large numbers of C–H bonds present in organic molecules. In particular, sp^3 hybridised C–H bonds present a challenge due to their bond strength, often unactivated nature, and their tendency to undergo β-hydride elimination when bonded to a metal centre; this is particularly relevant to the work of this thesis and so is discussed in more detail below.

1.1.1 Activation of sp^3 hybridised C–H bonds in synthesis

Activation of sp^3 hybridised C–H bonds is an innately difficult process, with both a high bond dissociation energy (BDE), ~400 kJ/mol, and a high pKa value of ~50, reflecting inactivity towards both homolytic and heterolytic bond cleavage respectively.

Prior to the rapid growth in the use of transition metals across all facets of organic synthesis, C–H activation could be achieved through the use of radicals. The Barton reaction, reported in 1960, made use of these highly reactive species, and their tendency towards 1,5-hydrogen abstraction to functionalise remote C–H bonds.[7] The utility of the reaction was demonstrated in the synthesis of aldosterone acetate, in which a remote,

unactivated methyl group in **9** was converted to oxime **10**, and eventually to the desired steroid **11** (***Scheme 1.3.***).[8]

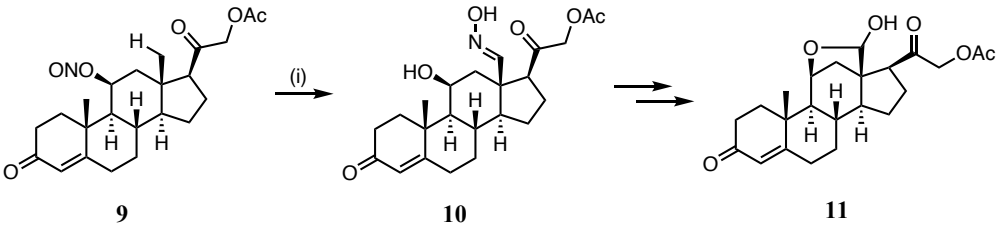

9 **10** **11**

Scheme 1.3. Key step in Barton's synthesis of aldosterone acetate. Conditions: (i) hv, PhMe.

Although arguably less fashionable than transition metal catalysed processes, radical mediated C–H activation is still a useful technique and has been applied more recently to aryl group translocation and the synthesis of a novel carbacephem antibiotic.[9–11] Within this radical reaction manifold, the orbitally controlled 1,5-hydrogen abstraction is often key to the selective formation of the desired product and, in order to achieve a similar effect in transition metal catalysed reaction, directing groups are commonplace. In the late 1930s reports of *ortho*-deprotonation of anisole and fluorobenzene, directed by heteroatom chelation to the organolithium base, led to the broader development of directed *ortho*-metalation processes for the regioselective synthesis of polysubstituted aromatic and heteroaromatic compounds.[12] Although generally applied to the activation of aromatic C–H bonds, activation of *ortho*-methyl groups has been applied in the formation of aromatic small molecules and natural products,[13] and this methodology extends to *ortho*-benzylic centres in general, demonstrated in the synthesis of corydalic acid methyl ester (***Scheme 1.4***).[14] Directed lithiation of the benzylic proton in **12** followed by intermolecular addition to imine **13** forms the key C–C bond, and further manipulation furnishes natural product **16**.

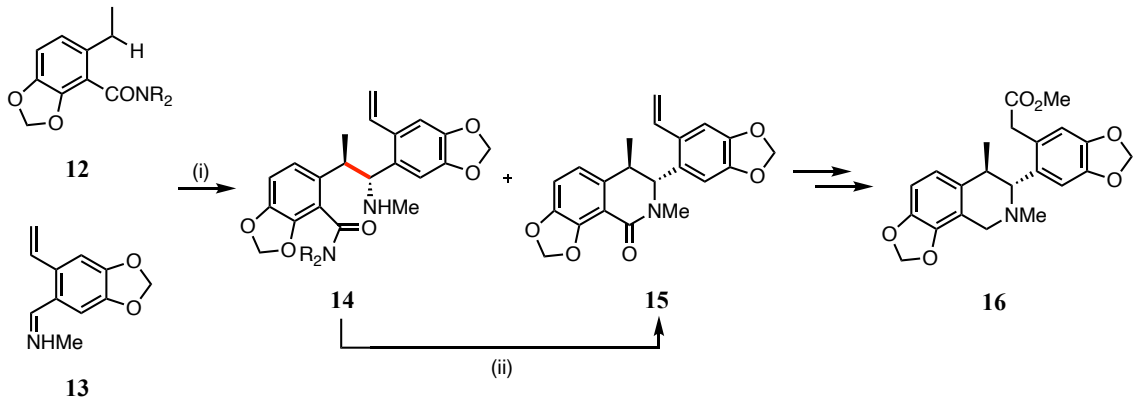

Scheme 1.4. Key directed *ortho*-metalation step in the synthesis of corydalic acid methyl ester. Conditions: (i) LDA, THF; (ii) *t*-BuLi, THF.

This general concept has also been applied in the synthesis of virosaine A (**19**), in which an unactivated proton is metalated; again an amide is necessary to direct the reaction (***Scheme 1.5***).[15]

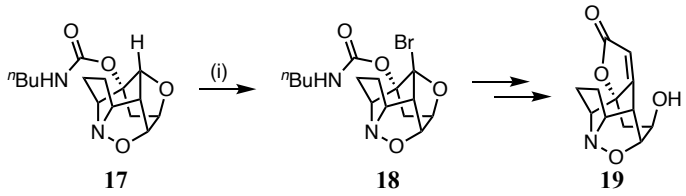

Scheme 1.5. Directed lithiation in the synthesis of virosaine A. Conditions: (i) *s*-BuLi, THF; Br_2.

Although these *ortho*-metalations extend the scope of C–H activation reactions, the deprotonation step necessitates the use of an organolithium base that may not be suitable for highly functionalised substrates.

Transition metal complexes offer a mild alternative to lithium-based *ortho*-metalations, and, unlike organolithium bases, they can be tuned to increase reactivity and selectivity with particular substrates through judicious choice of ligand and solvent. Whilst aromatic C–H activation catalysed by transition metal complexes has been heavily developed,[16] the analogous aliphatic field is perhaps less mature.

1.1.1.1 Directed transition metal catalysed sp^3 C–H activation

As discussed above, directing groups are common within the field of C–H activation; in order to control reactivity and selectivity, the metal catalyst must be in close proximity

to the desired bond for successful reaction to occur.[17] Perhaps unsurprisingly, a large number of intramolecular directing groups have proved to be useful in aliphatic C–H functionalisation reactions, from simple ketones and amides, to more complex ureas, Weinreb amides, and *O*-methyl oximes.[18] More specialised directing groups have also proved useful; the synthesis of aeruginosin 98B (**23**) makes use of the ligating 2-pyridinylisopropyl (PIP) group to direct C–H arylation of **20** (***Scheme 1.6***).[19]

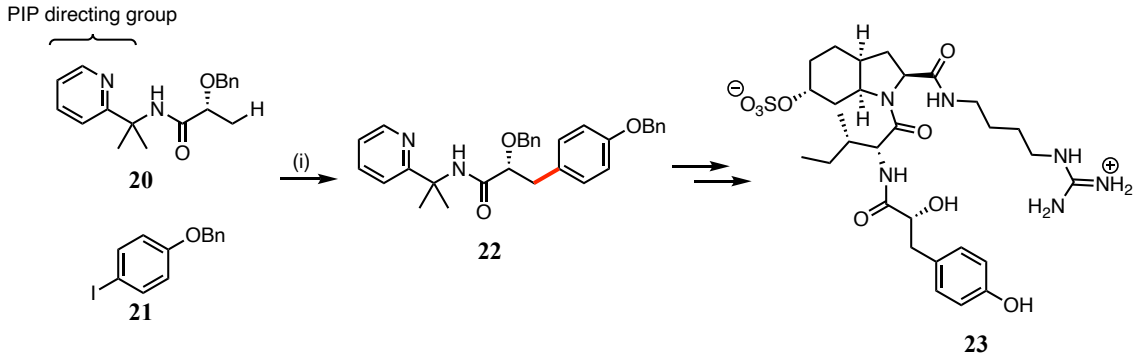

Scheme 1.6. Directed aliphatic C–H activation in synthesis of aeruginosin 98B. Conditions: (i) $Pd(OAc)_2$, K_2CO_3, MeCN.

Interestingly, it has been shown recently that the regioselectivity of sp^3 C–H arylation of heteroaromatic ketones can be controlled by addition of pyridine ligand **27** (**Scheme 1.7**).[20]

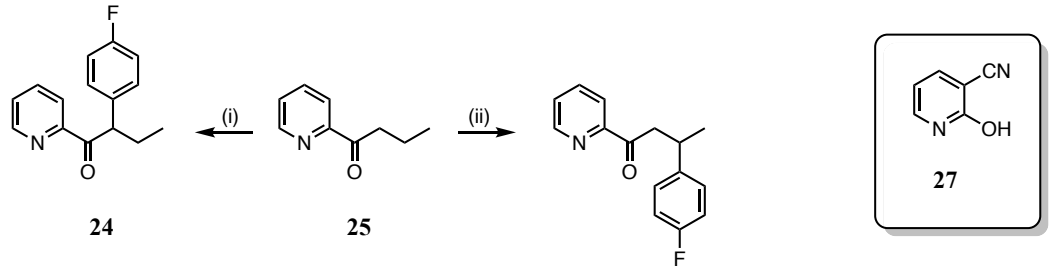

Scheme 1.7. Control of regioselectivity of C–H arylation *via* use, or lack of, pyridone ligand **27**. Reagents: (i) $Pd(OAc)_2$, Cs_2CO_3; (ii) $Pd(OAc)_2$, Rb_2CO_3, **27**.

Alongside C–C bond formation, carbon–heteroatom bond formation is also possible. Sanford has reported the formation of C–O bonds using oxime and pyridine directing groups, alongside iodosobenzene diacetate as a stoichiometric oxidant, to effect the acetoxylation of unactivated C–H bonds. This method achieved the diastereoselective

oxidation of an aliphatic C–H bond in the synthesis of paspaline (**30**).[21] Differentiation of the *gem*-dimethyl unit was attributed to the proximity between the oxime directing group and the C–H bonds in the equatorial methyl group in **28** (***Scheme 1.8***).

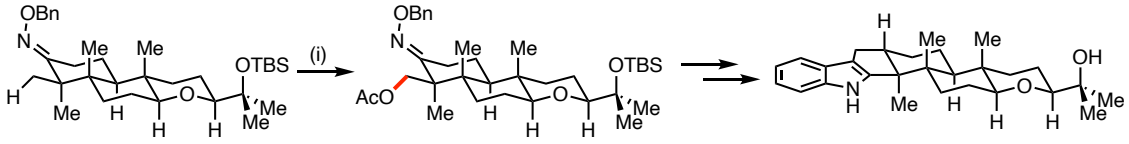

Scheme 1.8. Directed C–H acetoxylation gave a platform for the incorporation of the indole fragment of paspaline. Conditions: (i) $Pd(OAc)_2$, $PhI(OAc)_2$, AcOH, Ac_2O.

C–N bond formation at sp^3 centres has been achieved *via* the use of directing groups, including at the allylic position with rhodium nitrenoids, [22,23] but tethered sulphonamide and carbamate groups are more common (see §**1.1.1.2**).[24]

In addition to the formation of C–C, C–O, and C–N bonds, a large range of other directed C–H activation reactions have been developed including iodination,[25] borylation,[26] carbonylation,[27] and sulphonylation.[28]

1.1.1.2 Tethered transition metal catalysed sp^3 C–H activation

Another method of achieving selectivity in C–H functionalisation reactions is intramolecular tethering.[29] This approach often makes use of carbene and nitrene precursors to form a metal carbene reactive species and therefore C–C and C–N functionalisations are most common.[30,31]

Tethered carbene insertions, often catalysed by rhodium complexes, have been used in the diversification of natural products, as well as in syntheses of natural products themselves.[32] The synthesis of (–)-incarviatone A **33**, a potent monoamine oxidase inhibitor, relied on an intramolecular rhodium carbenoid insertion to form key indane intermediate **32** (***Scheme 1.9***).[33] This was the first example of a catalytic asymmetric synthesis of an indane *via* C–H activation.

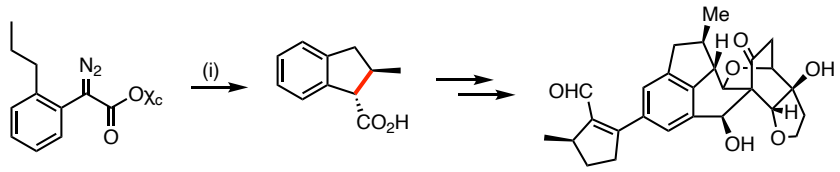

31 **32** **33**

Scheme 1.9. Carbene insertion into an unactivated C–H bond to form indane **32**. Conditions: (i) Rh_2(*R*-PTTL)$_4$.

Alongside carbene insertion processes, metal nitrenoid chemistry has been extensively developed;[22,34] these reactions proceed via highly electrophilic intermediates that insert selectively into electron rich C–H bonds, with the order of reactivity being typically: allylic > α-ethereal ≈ 3° > benzylic > 2° ≫ 1°.[35] Commonly catalysed by rhodium,[36] these transformations have seen application as strategic steps in a range of natural product syntheses,[37] including Yakura's route to myriocin (**36**).[38] This synthesis involves a key intramolecular amination step, inspired by Du Bois' synthesis of (+)-saxitoxcin,[39] to form a fully substituted nitrogen-bearing stereocentre in **35** (***Scheme 1.10***); hydrolysis of the tether occurred readily in a THF/0.1 M phosphate buffer solution.

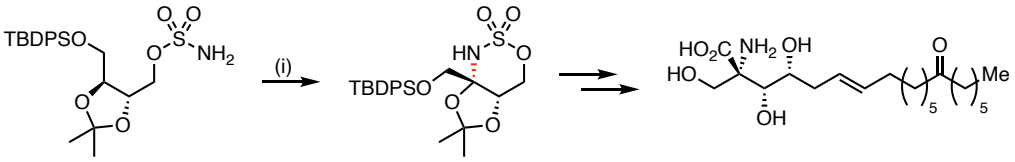

34 **35** **36**

Scheme 1.10 Key tethered C–H amination in Yakura's synthesis of myriocin (**36**). Conditions: (i) $Rh_2(OAc)_4$, $PhI(OAc)_2$.

In addition to C–C and C–N formation, tethered C–O functionalisation has been achieved, for example through the use of Fe(PDP) complex **50** (see §**1.1.1.3**). This method was used to install the lactone functionality in Snyder's synthesis of scaparvins B, C, and D (X = O, OH, and OAc, respectively, ***Scheme 1.11***).[40]

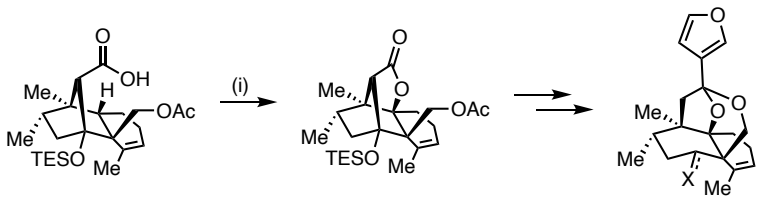

37 **38** **39**

Scheme 1.11. Tethered lactonisation in the synthesis of the scaparvins B, C and D. Conditions: (i) Fe(PDP), H_2O_2.

Although the techniques outlined in this section so far can form varied chemical functionality, the need for directing groups and tethers introduces constraints on these processes; their addition and removal reduce synthetic efficiency and, perhaps of more concern, is the unsuitability of this approach for compounds lacking the required functionality for generation of the required directing group.

1.1.1.3 Directing group free sp^3 C–H activation

Much work has gone into reducing the reliance on directing groups in order to increase the flexibility of C–H functionalisation reactions. In a limited number of cases, geometrical constraints can be used to force intramolecular C–H activations to proceed selectively as exemplified by the formation of the strained tetracyclic core of aplydactone (**43**) (***Scheme 1.12***).[41]

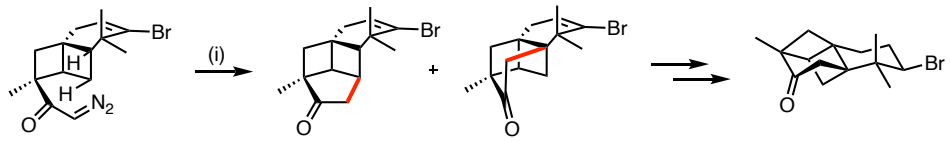

40 **41** **42** **43**

Scheme 1.12. Key step in the synthesis of aplydactone **43**. Conditions: (i) $Rh_2(tfa)_4$.

Electrophilic $Rh_2(tfa)_4$ proved to be a somewhat effective catalyst; however, even after extensive optimisation the ratio of products did not exceed 1.5:1 (**42**:**41**), illustrating the difficulty in differentiating between C–H bonds without a directing group. Clearly this strategy relies on the rigid nature of the substrate and, as in the case of aplydactone **43**, does not necessarily give a high degree of regiocontrol.

Catalytic systems have been found for carbene insertions into a range of substrates, including alkane C–H bonds, allylic and propargylic positions, bonds α- to nitrogen and ethereal C–H bonds.[42] The latter was used as inspiration in the synthesis of a benzo-fused indoxamycin core (**47**), the key carbene insertion step proceeding in 95% yield and >20:1 diastereoselectivity when (+)-**44** was used (***Scheme 1.13***).[43]

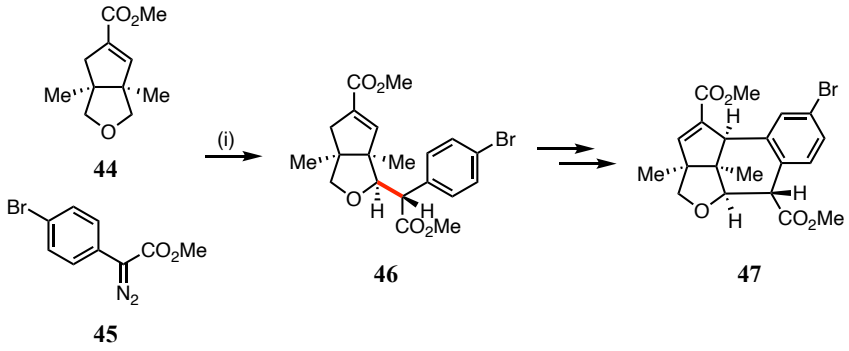

Scheme 1.13. Key carbene C–H functionalisation step in the synthesis of indoxamycin core **47**. Conditions: (i) Rh_2[(*S*)-PTAD]$_4$.

Undirected C–O bond formation has also been reported,[44] which is important due to the possibility of achieving late-stage functionalisation of complex substrates. Much research has been undertaken in order to understand the selectivity of these hydroxylations;[45] the dependence on steric and electronic effects is similar to biological oxidations within protein binding pockets, and makes use of electrophilic iron catalysts with bulky ligands [e.g. Fe((*S*,*S*)-PDP), **50**]. This technique has been demonstrated in the late-stage diversification of natural products, such as cycloheximide **48** to streptovitacin A derivative **49** (***Scheme 1.14***).[46]

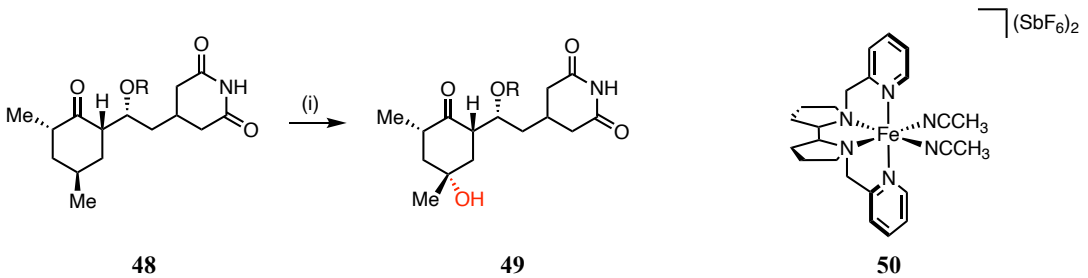

Scheme 1.14. Hydroxylation of a cycloheximide (R = H) derivative (R = C(O)CH_2Cl). Conditions: (i) Fe((*S*,*S*)-PDP, H_2O_2).

Exploitation of steric and electronic effects to achieve selectivity mimics enzyme-catalysed reactions in Nature, where steric, electronic, hydrogen bonding, and other supramolecular effects cooperate to control substrate orientation and therefore subsequent reactivity, so that biological C–H activation reactions can provide inspiration for analogous synthetic processes.

1.2 Enzymes in synthesis

Nature has developed a vast array of enzymes, tailored to specific substrates and processes, which catalyse reactivity ranging from simple ester hydrolysis to more complex steroidal cyclisation reactions and even the Diels–Alder reaction.[47] There are seven broad classes of enzymes and this wide range of catalytic activity gives enzymes great potential in a synthetic setting (***Table 1.1***).

Table 1.1. General classes of reaction catalysed by enzymes.

Class	Reaction catalysed	Enzyme example
EC 1 Oxidoreductase	Oxidation and reduction reactions; transfer of H and O atoms or electrons from one substrate to another	Oxidase, dehydrogenase
EC 2 Transferase	Transfer of a functional group one substrate to another	Transaminase
EC 3 Hydrolase	Hydrolysis of a substrate	Peptidase
EC 4 Lyase	Non-hydrolytic addition or cleavage of a group to or from a substrate	Decarboxylase
EC 5 Isomerase	Isomerisation of a substrate	Isomerase
EC 6 Ligase	Linkage of two molecules through formation of a C–C, C–N, C–O, C–S bond with simultaneous breakdown of ATP	Synthetase
EC 7[a] Translocase	Movement or separation of ions or molecules across membranes	Transporter

[a]EC7 was created in 2018 in order to better categorise a number of enzymes, including some that had been previously classified as EC 3.

The use of enzymes as biocatalysts allows transformations to be accomplished under mild conditions, without toxic metals and complex ligands; reactions are run at room temperature and almost neutral pH in order to stabilise the enzyme. These mild reaction

conditions allow compatibility with delicate functionality and are environmentally friendly, a characteristic which should be at the forefront of contemporary chemical synthesis.

Alongside the benefits that mild reaction conditions confer on a synthetic route, enzymatic reactions are also highly selective; the complex three-dimensional nature of the active site achieves discrimination between different substrates and reactions are often stereoselective, an attribute that is often utilised in kinetic resolution *via* esterification as exemplified in the synthesis of the core of prepluanin A (**53**) (***Scheme 1.15***).[48]

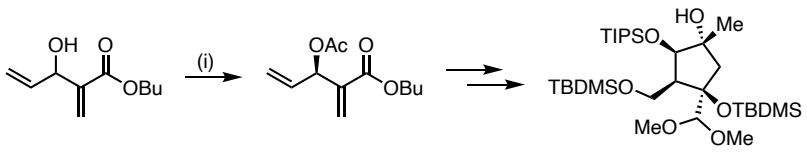

51 **52** **53**

Scheme 1.15. Kinetic resolution of alcohol **51** by enzymatic acetylation. Conditions: (i) Vinyl acetate, CAL-B on Immobead™.

Despite the significant potential benefits of enzymatic reactions, there are difficulties in using biocatalytic approaches in synthesis; thus, submission of non-natural substrates can lead to low conversion, substrates display poor solubility in the polar solvents necessary for enzymes, the high cost of cofactors can make these reactions economically unattractive, and, possibly the largest drawback, substrate specificity means enzymes are not considered as general catalysts and so chemical methods are often preferred. These problems have been solved to some extent; protein engineering allows enzymes to be made more suitable for the substrate in question,[49] solubilising agents and biphasic systems can be employed,[50] and cofactor regeneration systems allow for substoichiometric quantities of expensive cofactors.[51]

By providing a large number of accessible transformations, alongside adaptability through both mutagenesis and computational understanding of substrate binding,

enzymes are being embraced as an important part of chemists' synthetic toolbox, and interest has been renewed in their use as C–H activation catalysts.

1.2.1 C–H activation in Nature

C–H activation is common in Nature and the biosynthesis of terpene natural products is a good example; a cyclase phase, either through the mevalonic or non-mevalonic pathway,[52] forms the carbocyclic core after which heteroatomic functionality is introduced in the oxidase phase, often *via* enzyme catalysed C–H activation.[53] Synthetically, this two-phase strategy has been developed by Baran and, alongside impressive efforts culminating in the synthesis of paclitaxel (see §**4.1**),[54] has been used in the synthesis of five members of the eudesmane natural product family (***Scheme 1.16***).[55]

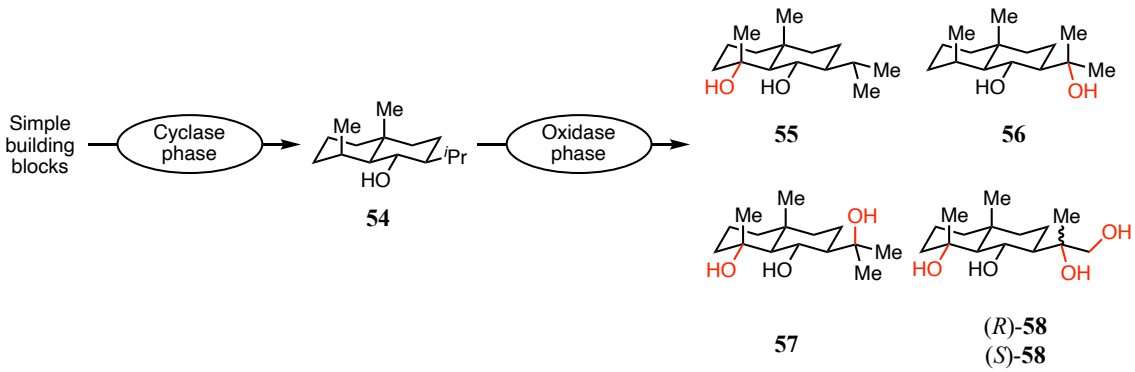

Scheme 1.16. General two-phase strategy towards eudesmane natural products.

Clearly, the application of biological principles provides advantages to synthetic routes towards complex natural products, with diversification of a common intermediate either leading to generation of multiple members of a natural product family or biologically active analogues.

1.2.1.1 Biocatalytic sp^3 C–H activation

Biological inspiration has led to significant research into the use of enzymes to accomplish a large number of synthetic transformations with excellent selectivity and versatility towards natural and unnatural substrates.[56,57] Enzymes are perfectly suited to

C–H activation catalysis; selectivity is controlled by the topography of the active site eliminating the need for directing groups; this active site can be altered through mutagenesis allowing selectivity to be tailored towards specific substrates.[58]

Biocatalysis has been demonstrated to be a successful tool for C–O bond formation;[59,60] C–H oxidation using GriE, a hydroxylase enzyme implicated in griselimycin biosynthesis,[61] enabled the formal synthesis of manzacidin C (**62**) (***Scheme 1.17***).[62]

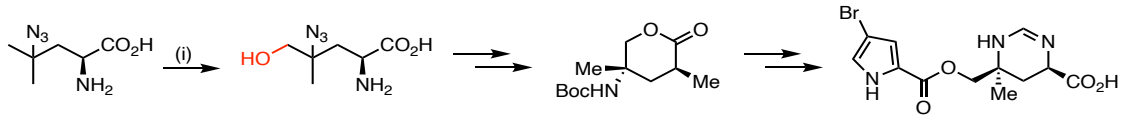

59 **60** **61** **62**

Scheme 1.17. Formal synthesis of manzacidin C with a key biocatalytic hydroxylation. Conditions: (i) GriE, O_2, αKG, Fe^{2+}.

Alongside other oxidases, cytochrome P450 enzymes have emerged as scalable,[63] adaptable,[64] and selective catalysts for late-stage hydroxylation reactions.[65] This family of enzymes has been used in both late-stage diversification of natural products as well as in total synthesis, exemplified by the use of an engineered $P450_{BM3}$ in a route to nigelladine A (**65**) (***Scheme 1.18.***).[66,67]

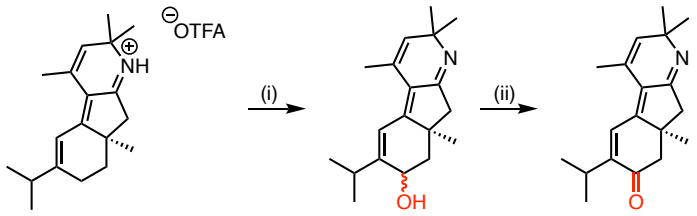

63 **64** **65**

Scheme 1.18. Biocatalytic synthesis of nigelladine A. Conditions: (i) $P450_{BM3}$; (ii) DMP.

1.3 Cytochrome P450

Cytochromes P450 (CYPs) are a superfamily of haem *b*-dependent monooxygenase enzymes. With more than 300,000 sequenced P450 genes, CYP enzymes have been found in all kingdoms of life;[68] however, importantly, they have not be identified in *Escherichia coli* making *E. coli* an ideal host system for expression of P450 enzymes.

Although, collectively, P450 enzymes show low sequence homology (≤ 20%) and contain only one invariant amino acid, a cysteine residue axially bound to the iron centre, they have a highly conserved tertiary structure and share a common protein fold with 12 α-helices and five β-sheets (***Figure 1.2***).[69]

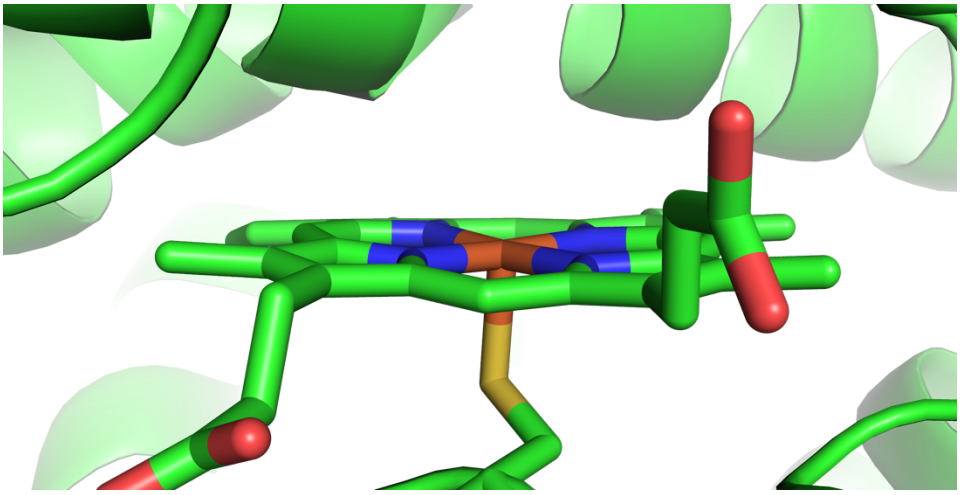

Figure 1.2. Invariant cysteine residue bound to the haem centre in wild-type $P450_{BM3}$.[70]

This prosthetic cysteine is key to C–H activation reactivity, thought to be by electron donation into the Fe=O species (compound **I**, see §**1.3.1.1**) which, in turn, allows hydrogen abstraction at reduction potentials below those at which oxidative degradation of the enzyme would occur.[71]

CYP enzymes carry out important roles in both catabolic and anabolic processes across all the organisms in which they are found. The metabolism of toxins and drugs, such as caffeine *N*3-demethylation, codeine *O*-demethylation, and the demethylenation of methylenedioxymethamphetamine (MDMA), acts as a defence mechanism.[72] The biosynthesis of secondary metabolites in plants and bacteria through late-stage oxidation gives rise to a plethora of interesting and biologically active natural products as exemplified in ***Figure 1.3*** by (+)-menthofuran **66**,[73] tirandamycin B **67**,[74] gibberellin A_{12} **68**,[75] and cyclooctatin **69**,[76] among others.[77]

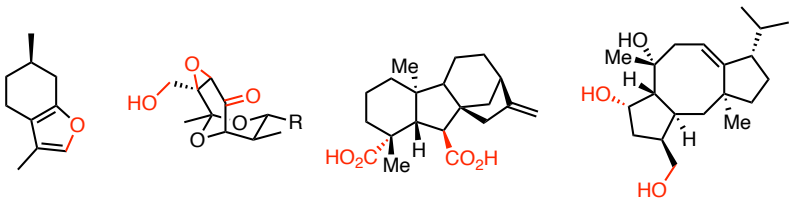

66 **67** **68** **69**

Figure 1.3. A selection of plant and bacterial secondary metabolites. The highlighted oxygen atoms are installed by P450 enzymes.

The ability to catalyse the oxidation of a wide range of substrates, as displayed in particular by microsomal catabolic enzymes which carry out a function requiring adaptability and promiscuity, makes this enzyme class a promising tool for biocatalytic oxidation; however, although microsomal CYPs tolerate a large number of substrates, they are problematic in a practical setting. Eukaryotic P450s react slowly and, as they are membrane bound, are insoluble. This insolubility means that reactions must be performed through the use of whole-cell systems and this presents its own difficulties, such as product isolation, cell permeability of the substrate, and the cell lifetime.

By contrast, bacterial CYPs are typically cytosolic so are soluble, more easily isolated, and more stable, as well as showing higher catalytic activity and better expression rates in recombinant hosts. These attributes have cemented bacterial P450 enzymes as the preferred biocatalysts in CYP mediated synthetic transformations and, within this class, $P450_{BM3}$ has emerged as a powerful tool for C–H oxidation.[78]

1.3.1 $P450_{BM3}$ (CYP102A1)

$P450_{BM3}$ (CYP102A1) is a soluble fatty acid hydroxylase,[79] the third to be isolated from *Bacillus megaterium*,[80] that catalyses the sub-terminal oxidation of a number of saturated and unsaturated fatty acids (***Table 1.2***).[81] $P450_{BM3}$ offers potential access to late-stage oxidation reactivity in a synthetically useful manner[82] because its reactions behave well on preparative and process scale,[63,83] it expresses well in *Escherchia coli*,[84] as a bacterial CYP it is non-membrane bound and soluble, and its self-sufficiency, that

allows electron transfer to the iron centre without the need for a redox partner, leads to high catalytic activity.[85]

Table 1.2. Product distribution of the oxidation of some fatty acids by $P450_{BM3}$.[81]

Fatty acid	**= or ≡ bonds**	**% Hydroxylation**			**Epoxidation**	
		ω–1	ω–2	ω–3	%	Position
Pentadecanoic (C15)	0	32	49	19	0	
Palmitic (C16)	0	31	48	21	0	
Eicosapentenoic (C20)	5	0	0	0	100	17–18
Eicosatrienoic (C20)	3	18	39	43	0	
Octadecynoic (C18)	1	0	100	0	0	

This self-sufficiency derives from the fact that $P450_{BM3}$ is a natural fusion protein comprising a 55 kDa "haem" (BMP) domain and a 65 kDa "reductase" (BMR) domain containing two flavin groups, FMN (ferredoxin reductase-like) and FAD (flavodoxin-like), in equimolar amounts.[86] This reductase domain facilitates two single electron reductions from NADPH in the catalytic cycle (see **Error! Reference source not found.**) and means CYP102A1 is only dependent on NADPH and O_2 to function; activity is not reliant on the enzyme encountering a redox partner. Although $P450_{BM3}$ was the first self-sufficient CYP to be discovered, others have since been isolated (***Figure 1.4***); $P450_{foxy}$ from *Fusarium oxysporum* and $P450_{RhF}$ from *Rhodococcus* sp.[87,88]

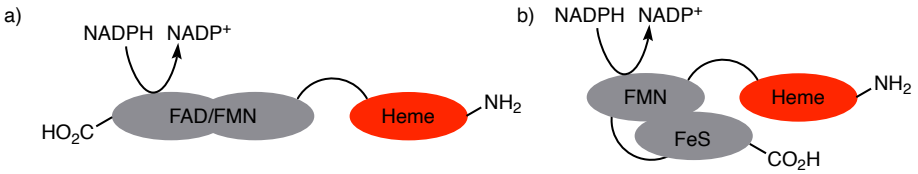

Figure 1.4. Example of self-sufficient P450 architecture. a) $P450_{BM3}$; b) $P450_{RhF}$.

This dependence on NAD(P)H is beneficial for reactivity but comes with the detriment that NADPH is an expensive cofactor; however, use of enzymatic cofactor regeneration systems allows recycling of the NADPH *via* a dehydrogenase at the expense of a cheap co-substrate (***Scheme 1.19***).

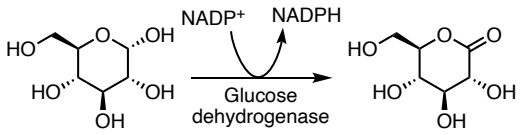

70 **71**

Scheme 1.19. Regeneration of NADPH through the use of glucose dehydrogenase (GDH) and glucose.

1.3.1.1 Catalytic cycle

The P450 catalytic cycle has been heavily researched and is broadly agreed upon for the majority of CYP oxidation reactions (**Error! Reference source not found.**). Much of the insight into the catalytic cycle stems from research undertaken on model metalloporphyrin oxide systems.[89]

Initially, in the resting state **72**, the central Fe (III) atom is hexacoordinate; four nitrogen ligands from the porphyrin system occupy the equatorial binding sites while the thiolato ligand and a water molecule are axially bound. Upon arrival of a substrate into the active site, loss of the axial water molecule is triggered to form **73**, either through induced conformational changes or direct displacement, resulting in an increase of the ferric spin state from low spin ($S = \frac{1}{2}$) to high spin ($S = \frac{5}{2}$). This increase in spin state, measured spectrophotometrically by a shift from ~418 nm to ~390 nm, affects the haem reduction potential making it more oxidising and subsequent reduction of **73** to ferrous **74** occurs through addition of a single electron, often supplied by NADH or NADPH. This electron is transported to the haem iron *via* electron transfer partners; the unique self-sufficient nature of CYP102A1 means this reduction is intramolecular, facilitated by the FAD and FMN domains within the $P450_{BM3}$ reductase module. Dioxygen binds to form oxy-complex **75,** followed by another single electron reduction to generate Fe(III) peroxy species **76**. Hydroperoxy adduct **77**, known as "Compound 0", is formed *via* protonation of the terminal oxygen atom and, following another protonation, water is lost through heterolytic cleavage of the O–O bond generating "Compound I" (**78**). "Compound I", so named because of its history in peroxidase chemistry and

characterisation in 2010,[90,91] is considered to be the active catalytic species in the majority of P450 oxidation reactions.

In hydroxylation reactions, "Compound I" abstracts a hydrogen from the substrate generating **79**, and subsequent "radical rebound" yields the product through recombination of OH and the substrate radical. The hydroxylated product leaves the active site to form **80** which re-enters the catalytic cycle, either through complexation with water and subsequent displacement by more substrate, or direct entry of more substrate into the active site.

A number of side reactions can interrupt the catalytic cycle (shown by dashed arrows in **Error! Reference source not found.**): hindered dioxygen binding can lead to slow reduction of **75** allowing loss of superoxide (superoxide uncoupling); water encroachment due to a loosely fitting substrate can cause protonation at the iron-bound oxygen in **77** which brings about loss of hydrogen peroxide (peroxide uncoupling); binding of a substrate with no hydrogen atoms correctly placed for abstraction promotes reduction of the oxygen "atom" to water in **78** (oxidase uncoupling).

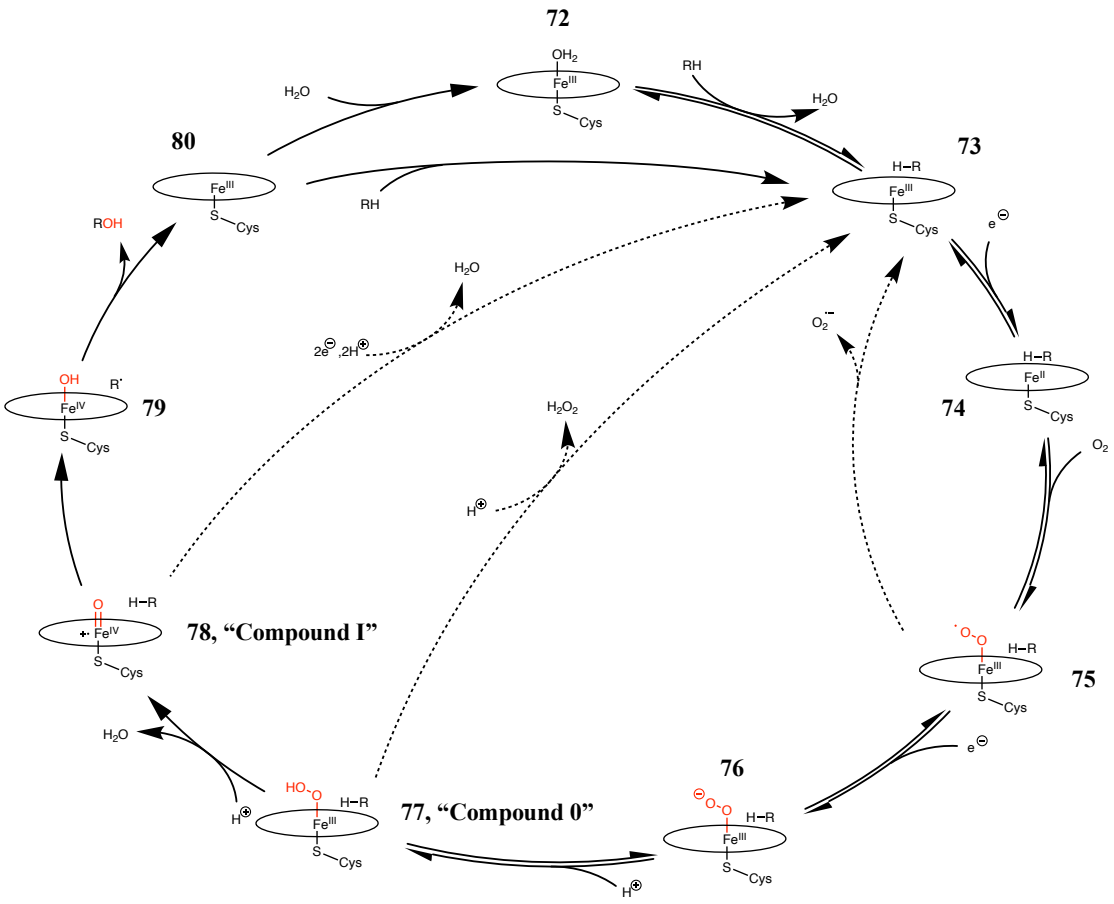

Figure 1.5. P450$_{BM3}$ catalytic cycle.

With some exceptions, and despite difficulties encountered in attempting to expose the nature of the active catalyst, this catalytic cycle is considered to be general across hydroxylation reaction manifolds. Differences in regio- and stereoselectivity then, are attributed to substrate orientation within the active site, itself determined by effects such as hydrogen bonding, hydrophilicity and hydrophobicity, and π-stacking. The selectivity imparted on oxidation reactions by these non-covalent interactions with residues in the catalytic domain, and the ability to alter these residues through mutagenesis, makes P450$_{BM3}$ a powerful tool for biocatalytic C–H oxidation reactions.

1.3.1.2 Key residues

The synthetic utility of P450$_{BM3}$ hinges on the feasibility of mutating specific residues to increase selectivity towards certain substrates, positions, and stereoisomers.

A significant amount of research has aimed to understand the roles of key residues, with a view to tailoring specificity by altering the relevant amino acid.

Arginine-47 (Arg47), tyrosine-51 (Tyr51), and serine-72 (Ser72) provide a hydrophilic region at the mouth of the substrate access channel which controls admission of potential substrates, as well as water, while phenylalanine-42 (Phe42) caps the channel after substrate entry and subsequent binding.[92,93] Within the substrate access channel two residues have key roles; phenylalanine-87 (Phe87) is involved in displacement of the axial water ligand through a 90° movement from the substrate free (SF) to the substrate bound (SB) conformation,[92,94] allowing the substrate into the active site, and leucine-437 (Leu437) acts as a "safety catch" for Phe87, preventing this rotation when no substrate is bound and maintaining the iron centre in its low-spin configuration (***Figure 1.6***).[95]

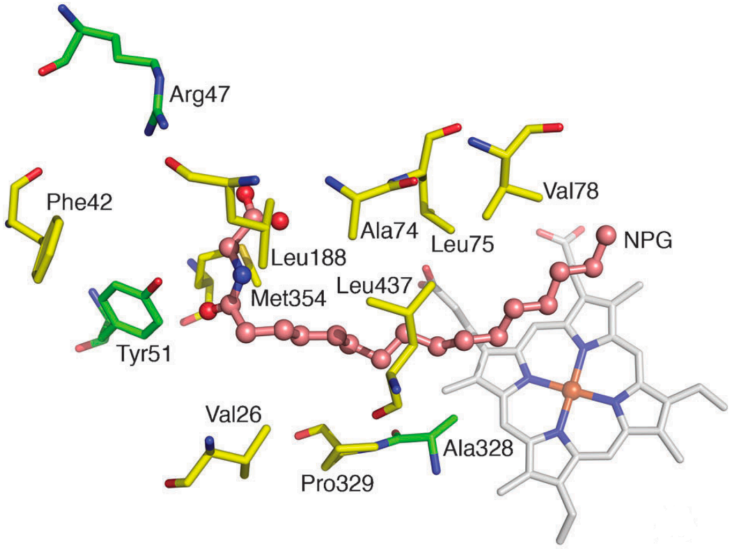

Figure 1.6. The substrate access channel of NPG-bound $P450_{BM3}$.[81]

Unsurprisingly, residues inside the active site also play a key role in substrate binding and specificity. Alanine-264 (Ala264), along with Phe87, aids in displacement of the axial water ligand,[92] while glutamic acid-267 (Glu267) aids in activation of dioxygen,

and threonine-268 (Thr268) is involved in electron transfer, proton delivery, and dioxygen activation (***Figure 1.7***).[96,97]

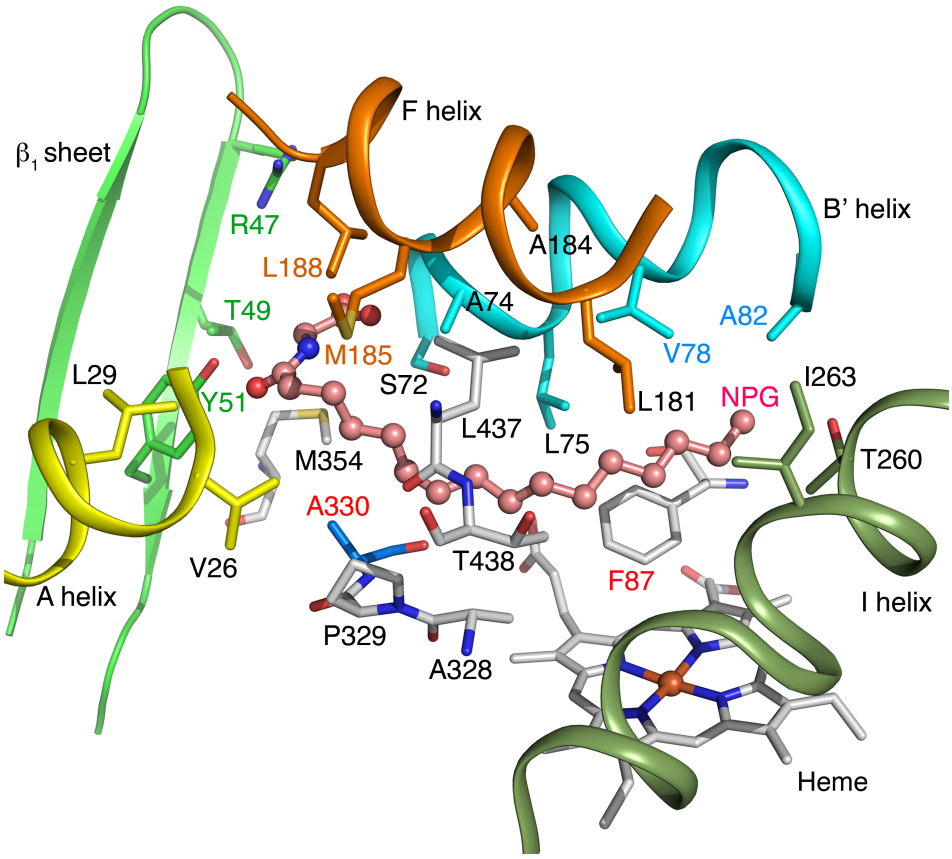

Figure 1.7. The active site of NPG-bound P450$_{BM3}$. Residues A264 and F393 have been omitted for clarity whilst G570 and W1046 are not shown as they are FMN and FAD domain residues. Image generated by L. L. Wong from PDB file 4KPA.

Other key amino acids are phenylalanine-393 (Phe393) which regulates the rate of heme reduction in order to control the oxygen binding rate,[98] glycine-570 (Gly570) which plays a role in FMN binding,[99] and tryptophan-1046 (Trp1046) which modulates co-factor specificity and shields the FAD group.[100]

Knowledge of the function of individual residues has allowed the development of a plethora of P450$_{BM3}$ variants through protein engineering.

1.3.1.3 Protein engineering

Rational design, directed evolution or a combination of the two – 'rational evolution' – and *in silico* design have been used to introduce mutations into the P450$_{BM3}$ DNA sequence.[101,102] Clearly, key residues within the substrate access channel and active site

are candidates for site-directed mutagenesis and indeed Thr268 and Phe87 were among the first to be targeted.[103] These modifications are incorporated into the protein primary structure by substitution of the codon corresponding to the relevant residue in the DNA sequence. With the "mutated" gene sequence in hand, it is expressed in a host, usually *E. coli*; the host organism then biosynthesises the mutated enzyme and, following extraction, the effect of the mutation can be discerned.

Directed evolution is complementary to this approach, and, through the error-prone polymerase chain reaction (PCR), generates random mutations in the protein primary structure.[104,105] This technique generates a library of enzymes with useful mutations at key residues that may not be obvious at first glance but that may have desirable effects on reactivity and selectivity (***Figure 1.8***).

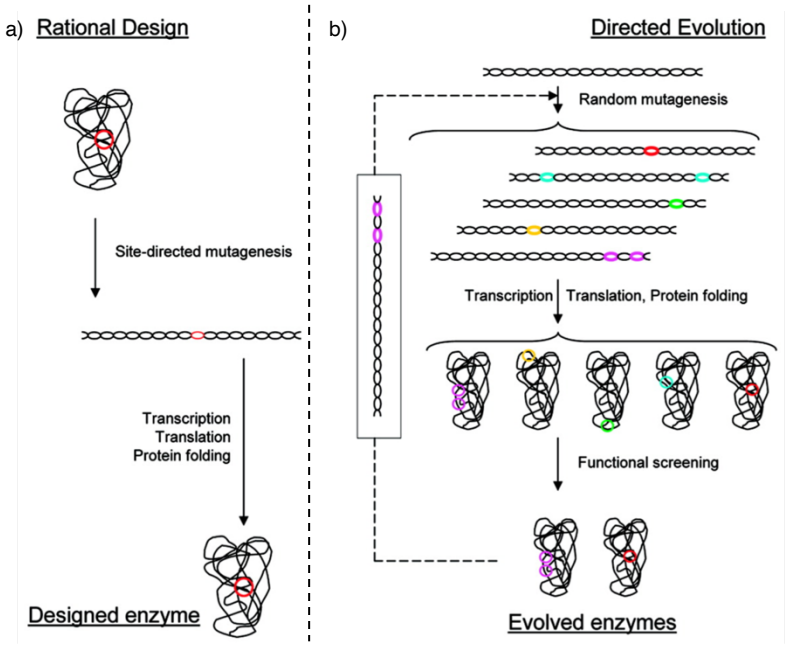

Figure 1.8. Generation of enzyme variants *via* a) rational design; b) directed evolution.[106] Adapted with permission from Strohmeier, G. A.; Pichler, H.; May, O.; Gruber-Khadjawi, M., *Chem. Rev.*, **2011**, 111, 4141. Copyright 2021 American Chemical Society.

The ability to extensively modify the structure of CYP102A1 enzymes has led the Wong group to develop a large library of enzymes which have been employed in the oxidation of a number of substrates including small-ring amines and steroidal cores.

1.3.1.4 Origins of the Wong Group P450 library

The enzyme library contains >500 members, and mutants have been shown to have activity against drugs, aromatic small molecules, terpenes, steroids, various cyclic amines and lactams, and complex natural product precursors. The library originated with four mutants which were identified to have increased reactivity towards a number of substrates: A330P, KT2 (A191T/N239H/I259V/A267T/L353I), KSK19 (F87A/H171L/Q307H/N319Y), and KT5 (F87A/A330P/E377A/D425N). These initial variants were then developed by combination with other mutations including RLYF, R47L/Y51F, and F87A that were already known to boost reactivity. Introduction of these mutations was carried out by genetic modification of the DNA sequence, amplification of the altered gene through PCR, insertion into a plasmid from *E. coli*, and innoculation of *E. coli* cells which biosynthesise the mutant $P450_{BM3}$. Further mutations were introduced through directed evolution and site saturation mutagenesis. In order to identify enzymes with novel beneficial mutations, the indigo method was utilised which can be carried out during colony growth, avoiding time consuming isolation and purification steps.[107] This highlights active $P450_{BM3}$ mutants through colour change; the media turns blue due to the formation of indigo dye (**83**) through oxidation and dimerization of indole **82**, which itself is generated *in situ* from the degradation of L-tryptophan **81** (***Scheme 1.20***).

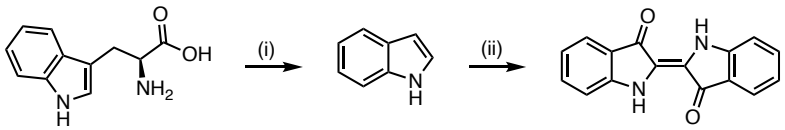

81 **82** **83**

Scheme 1.20. The indigo method. Conditions: (i) Tryptophanase; (ii) $P450_{BM3}$.

With active mutants identified, the enzyme variants were isolated, purified, and subjected to further mutations. Reactions with propylbenzene and naphthalene were used to test the activity and selectivity of the new enzyme variants.[108,109]

The ability to tune $P450_{BM3}$ reactivity and selectivity towards non-natural substrates through protein engineering makes this class of enzymes an ideal candidate for biocatalytic C–H activation reactions, and oxidation of a number of varied substrates has been reported.

1.3.1.5 Use in synthesis

$P450_{BM3}$ variants have been used to incorporate oxy-functionality into a range of C–H bonds by engineering the enzyme towards the substrate. Hydroxylation of tetrahydroquinoline (THQ) with over 30 mutant $P450_{BM3}$ enzymes ($mP450_{BM3}$) has generated an impressive range of products: aromatic and benzylic alcohols, quinoline itself, lactams, and benzylic ketones, and others (***Figure 1.9***).[110]

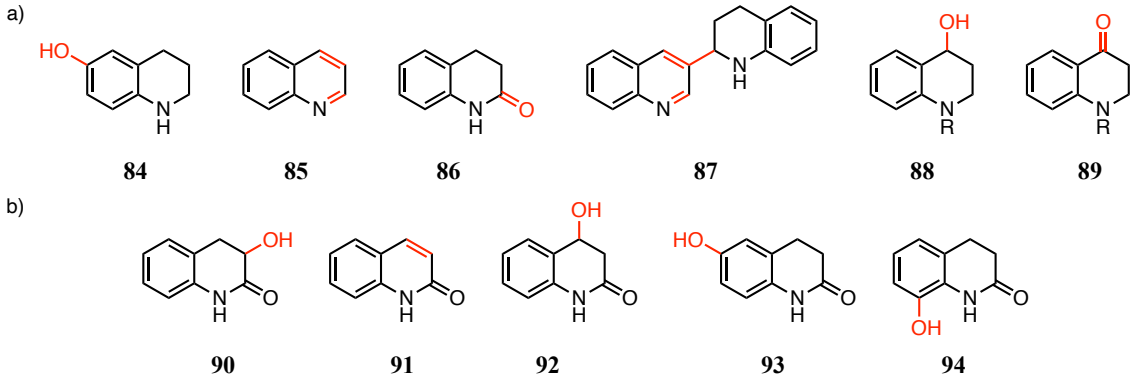

Figure 1.9. A selection of oxidised THQ derivatives. a) Products generated from THQ; b) products generated from 2-oxo-THQ.

Steroids have also been diversified through the use of CYP102A1 variants.[111] Control of diastereoselectivity has been achieved,[112] as well as hydroxylation at unactivated C–H sp^3 bonds.[113]

Oxidation of unactivated C–H bonds is the natural reactivity of $P450_{BM3}$ and, through protein engineering, two remote C–H bonds of artemisinin (**95**) have been hydroxylated (***Scheme 1.21***);[114] this exhibits a key strength of CYP102A1 biocatalysis – the ability to diversify drugs and natural products in order to probe for improved biological properties. $P450_{BM3}$ mutants are ideal for this role; not only are they able to carry out

difficult hydroxylations, but they also allow large, topologically complex, molecules into their active site.

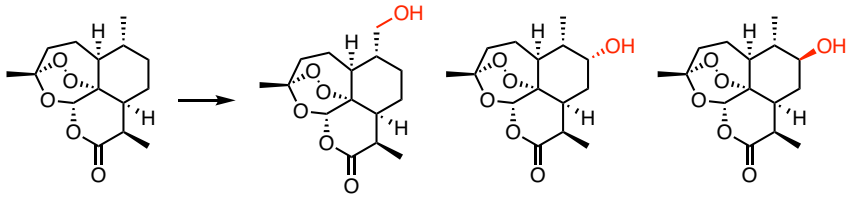

95 **96** **97** **98**

Scheme 1.21. mP450$_{BM3}$-catalysed hydroxylation products of artemisinin **95**.

This quality has been used to study metabolites of Lidocaine, Naproxen, and Chlorzoxazone, among others,[113] as well as diversification of other natural products such as β-cembrenediol and *trans*-polydatin (**99**), and elaboration of monosaccharides (***Scheme 1.22***).[115–117]

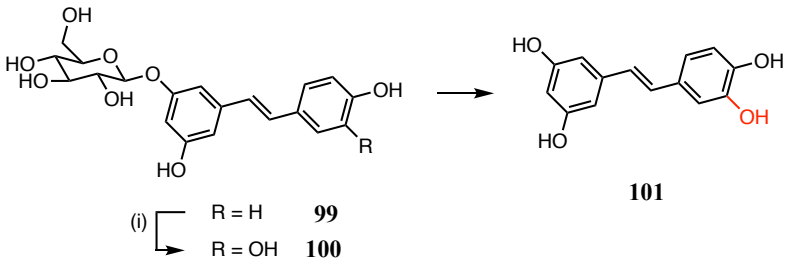

101

Scheme 1.22. CYP102A1 variant mediated diversification oxidation of *trans*-polydatin to (*E*)-astringin **99**, towards a synthesis of piceatannol **101**. Conditions: (i) P450$_{BM3}$ variant.

Although P450$_{BM3}$ biocatalysis is usually tailored towards conventional hydroxylation reactions, more esoteric transformations have proved possible. Tethered C–H amination and even cyclopropanation have been reported, further extending the non-natural reactivity of CYP102A1 variants (***Scheme 1.23***).[118,119]

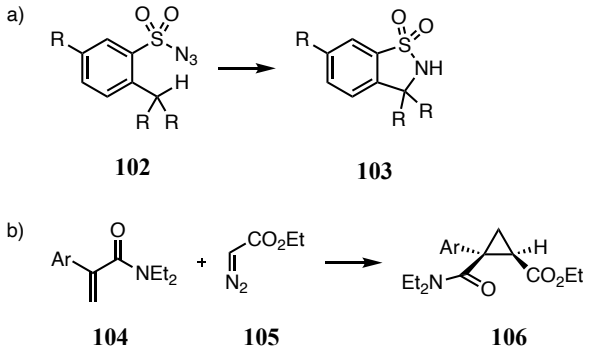

102 **103** **104** **105** **106**

Scheme 1.23. a) P450$_{BM3}$-catalysed C–N bond formation; b) P450$_{BM3}$-catalysed Fe-carbene mediated cyclopropanation.

Complementary to protein engineering is the use of decoy molecules.[120] This relatively recent technique employs, for example, perfluorinated carboxylic acids (PFCs) to "switch on" the $P450_{BM3}$ active site through binding of the acid moiety to Arg47 and Tyr51, allowing ejection of the sixth water ligand, and modifying the Fe centre to the high-spin reactive state. This decoy strategy was pioneered as a means to oxidise gaseous alkanes which, due to their small size coupled with the large $P450_{BM3}$ binding pocket, have a statistically low probability of being correctly oriented near the active oxyferryl centre for oxidation to occur.[121] Perfluoroalkyl compounds were initially used as decoy molecules due to their unreactive C–F bonds,[122] but recently more complex compounds have been exploited; for example, the oxidation of benzene to phenol has been accomplished under whole-cell conditions with a range of fluorine and amino acid based decoy molecules,[123] and both enantiomers of 1-indanol have been produced, with different decoy molecules favouring the production of opposite enantiomers (***Scheme 1.24***).[124]

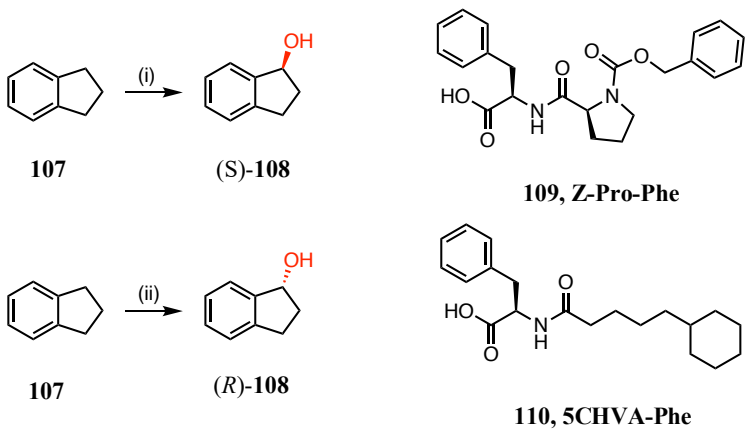

Scheme 1.24. Asymmetric hydroxylation of indane using decoy molecules. Conditions: (i) WT-$P450_{BM3}$, Z-Pro-Phe, 56% ee; (ii) WT-$P450_{BM3}$, 5CHVA-Phe, 53% ee.

Clearly $P450_{BM3}$ enzymes are able to discriminate between diastereotopic and enantiotopic protons (see ***Scheme 1.21*** and ***Scheme 1.24***) and two faces of a π-bond (***Scheme 1.23b***) arising from the three-dimensional nature of the active site and the directionality of the non-bonding interactions within it. This raises the question as to

whether CYP102A1 variants can distinguish substrate enantiomers to perform kinetic resolutions *via* hydroxylation reactions.

1.3.1.6 Kinetic resolution

Asymmetric reactions are central to most modern chemical syntheses, and many chemical and biological strategies have been and continue to be explored, among which is kinetic resolution. Although, in principle, kinetic resolution sacrifices half of the racemic starting material, if the process is carried out on a cheap and readily available substrate, and incorporates difficult to access functionality, this downside is outweighed by the generation of a complex or high-value product. Biocatalytic methods of kinetic resolution have long been known, especially in the hydrolysis of esters, and kinetic resolution using $P450_{BM3}$ enzymes in whole cell systems is known, but the use of isolated CYP102A1 enzymes has not been studied in great detail.[125]

In 1988 kinetic resolution was observed upon submission of an α-pinene derivative to a culture of *Beauveria sulferescens*; however, this study was not expanded upon.[126] Another 24 years passed before further research into this useful property was reported. In this, P450 monooxygenase AurH was used in the synthesis of (+)-aureothin (**112**) in a resolution step (***Scheme 1.25***); however, although displaying the utility of the biocatalytic kinetic resolution approach, the reaction with AurH produces the unusual chiral THF ring in aureothin, which itself is the natural substrate of AurH, so this is not of general synthetic utility.[127]

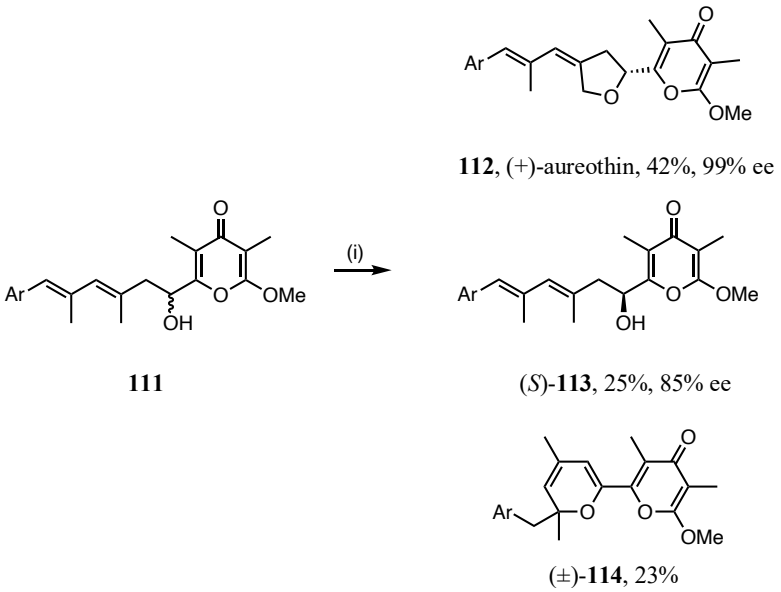

Scheme 1.25. P450-mediated kinetic resolution as the final step of the synthesis of (+)-aureothin **112**.

Wild-type $P450_{BM3}$ has been used in the whole-cell kinetic resolution of β-ionone; however, again this observation has not been studied further.[125]

Improving the enantioselectivity of biocatalytic reactions through protein engineering, as with other site-directed mutagenesis and directed evolution studies, has been demonstrated,[105] and, within the group, the use of modified $P450_{BM3}$ enzymes has led to the kinetic resolution of bicyclic lactone **115**, an intermediate in Danishefsky's enantiospecific synthesis of eleutherobin (***Scheme 1.26***, see §**3.1.2**).[128,129]

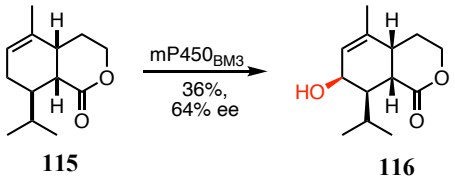

Scheme 1.26. Kinetic resolution of a lactone by a CYP102A1 variant.

Derivatisation of key intermediates like **115** could lead to novel medicinally-useful compounds, and the development of biocatalytic hydroxylation methodology could prove instrumental in gaining access to previously unknown biologically-active compounds. Alongside developing $P450_{BM3}$ catalysis, biocatalytic kinetic resolution is an area that would benefit from more focussed research; increased understanding of the reactivity and chemo-, regio-, and stereoselectivity could lead to $P450_{BM3}$ variants

becoming useful general oxidation catalysts, complementing pre-existing chemical catalysts, and moving towards more selective and environmentally friendly syntheses.

1.4 This project

This project will build on research previously undertaken by the Robertson group. Hydroxylation of tricycle **117** (see ***Figure 1.13***) produced a range of products, and a non-zero specific rotation for alcohol **118** was recorded, indicating kinetic resolution to be operating (***Figure 1.10***).

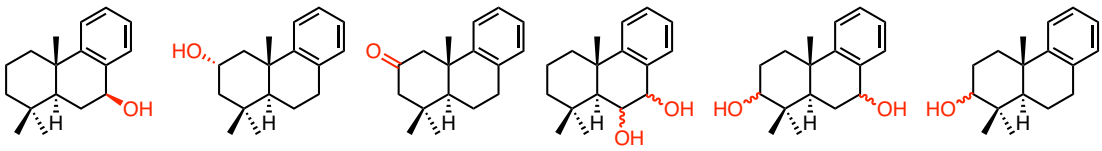

118 **119** **120** **121** **122** **123**

Figure 1.10. Previously isolated oxidised tricycles.

A similar study was undertaken with lactone **115** and five oxidised products were isolated, with **116** displaying a non-zero specific rotation (***Figure 1.11***).

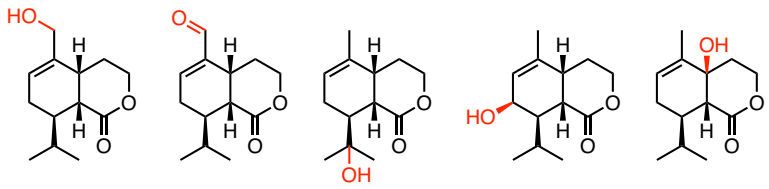

124 **125** **126** **116** **127**

Figure 1.11. Isolated products from hydroxylation of lactone (±)-**115**.

Finally, a significant amount of work was carried out surrounding paclitaxel **234** and its analogues. Syntheses of five derivatives of the core structure were completed and, as before, hydroxylated products were isolated; product **133** was generated as a single enantiomer (***Figure 1.12***).

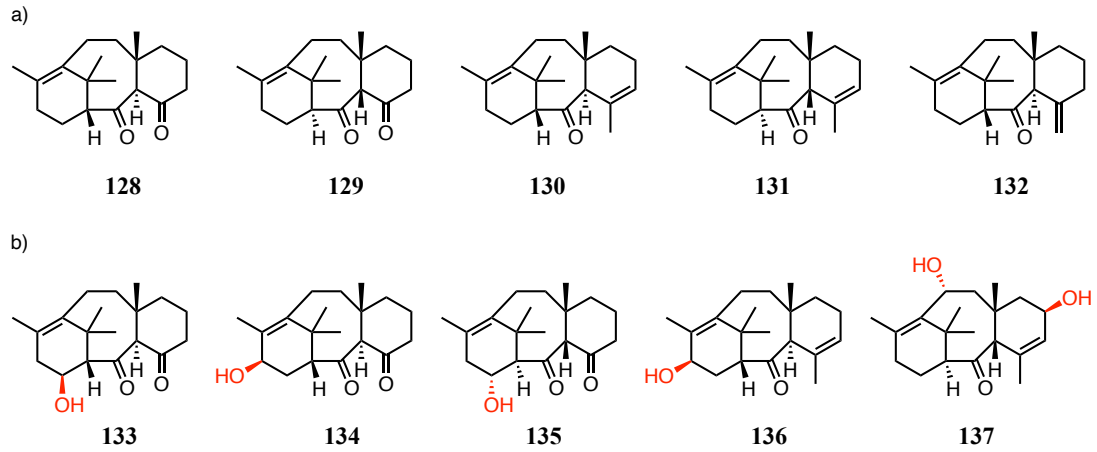

Figure 1.12. a) Five paclitaxel core derivatives previously synthesised in the group; b) subset of isolated hydroxylation products.

These studies showed that the $P450_{BM3}$ enzymes available to our group in Oxford are able to differentiate between the enantiomers of racemic substrates and more focussed research was proposed in order to understand the processes more thoroughly.

Kinetic resolution studies were initiated with **115** and **117**, both small, relatively simple and easily accessible compounds, and then progressed to the more complex *exo*-taxadienone **132**. It was envisaged that the major products from these biocatalytic hydroxylation reactions would be characterised, and scale-up reactions, along with kinetic studies, would be undertaken to understand how the $P450_{BM3}$ variants behave as catalysts at a synthetically useful level (***Figure 1.13***).

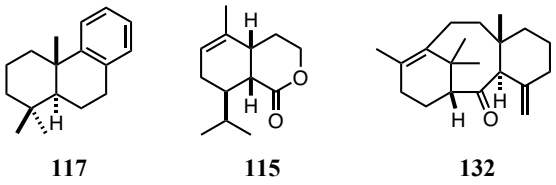

Figure 1.13. The three compounds of interest.

In order for $P450_{BM3}$ enzymes to become widely used as general oxidation catalysts, knowledge of the reactivity profile of each variant is key. Thus, in all these studies, it is intended that submitting novel substrates with non-natural functionality to the $P450_{BM3}$ library will deepen our understanding of the reactivity profile of the Wong group's engineered enzymes.

2 Hydroxylation of an aromatic abietane core

2.1 Background

The abietanes are diterpenoid natural products isolated from a range of terrestrial plant sources including *Salvia rhytidea* and *Plectranthus grandidentatus* (***Figure 2.1***).[130,131]

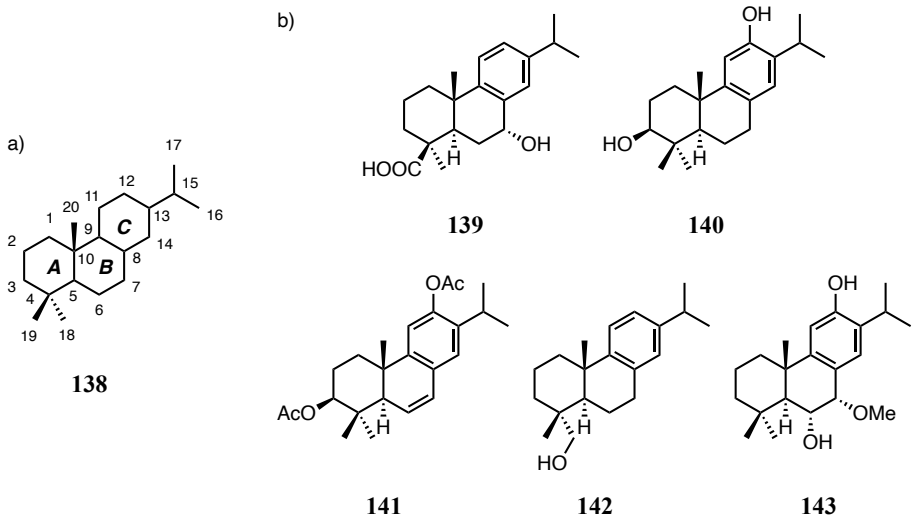

Figure 2.1. a) Structure of abietane family core; b) example aromatic abietane family members.

The abietane core comprises a C_{20} tricyclic reduced phenanthrene structure **138** which arises biosynthetically from two sequential cyclisation and/or rearrangement reactions of geranylgeranyl diphosphate (***Scheme 2.1***);[132] a subclass of this family, the aromatic diterpenoids, have an aromatic C ring.

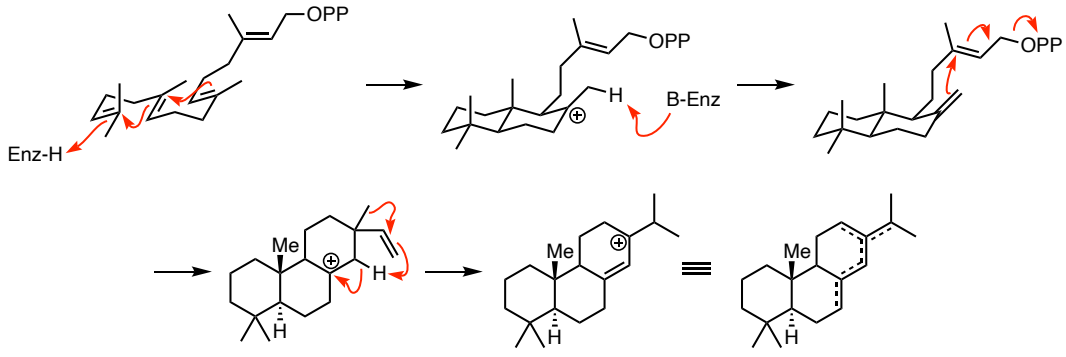

Scheme 2.1. Biosynthetic pathway towards abietante diterpenoids.

Natural products belonging to this family have a wide range of biological activities; 7α-hydroxycallitrisic acid (**139**) exhibits antiviral properties,[133] hinokiol (**140**) shows anti-inflammatory activity through inhibition of NO production,[134] 8-

hydroxydehydroabietane (**142**) presents both antitumour and bactericidal effects,[135] and taxodistine B (**143**) is cytotoxic *via* inhibition of tubulin polymerisation (***Figure 2.1***).[136] Although some SAR has been established for hydroxycallitrisic acid (**139**) and 8-hydroxydehydroabietane (**142**), no clear basis for this wide range of biological activity is known. Efficient access to this core could lead, ultimately, to concise syntheses of natural and unnatural diterpenoids with known or potential clinically-relevant biological properties.

Because of this extensive biological activity, these natural products are interesting synthetic targets, and a large number of syntheses of members of this family have been reported, many of which are based upon a semi-synthetic strategy starting from dehydroabietic acid **145** due to the ready availability of its precursor, abietic acid **144** (***Scheme 2.2***).[137]

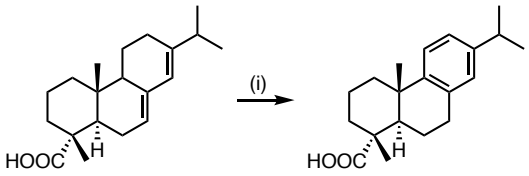

144 **145**

Scheme 2.2. Generation of dehydroabietic acid from abietic acid. Reagents and conditions: (i) Pd/C, 250 °C.

Many of these semi-syntheses have focused on ferruginol **149**, an abietane isolated from *Sequoia sempervirens* with moderate antitumour activity against a range of human cancer cell lines.[138] Matsumoto's route to ferruginol (**149**), and further derivatisation to japonolol (**152**), exemplifies the semi-synthetic strategy; key Friedel–Crafts acylation and Baeyer–Villiger oxidation steps, followed by hydrolysis, gave access to the phenol functionality in **149**, and Wolff–Kischner reduction was employed to generate the required *gem*-dimethyl group (**148**), while the remaining oxyfunctionality was installed *via* benzoyl peroxide mediated aromatic oxidation then by Jones' (benzylic) oxidation (***Scheme 2.3***).[139]

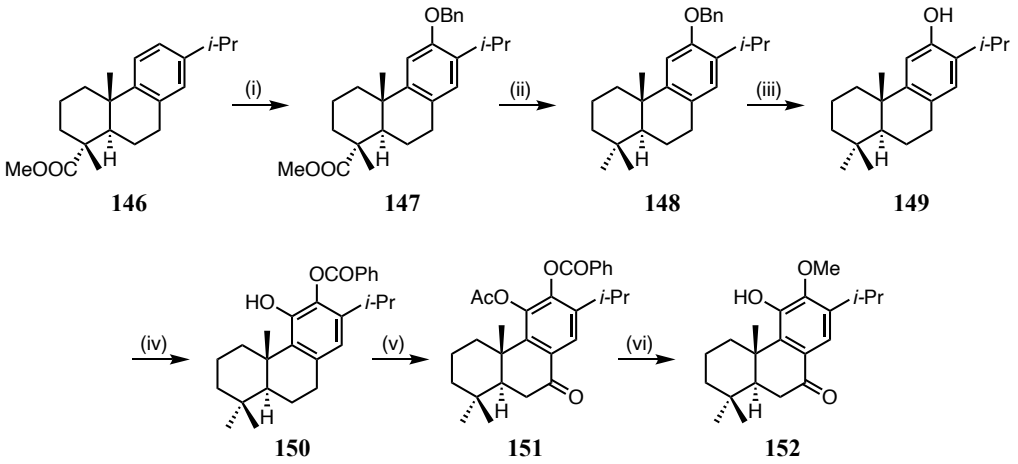

Scheme 2.3. Matsumoto's synthesis of ferruginol **149** and japonolol **152**. Reagents: (i) a. AcCl, $AlCl_3$; b. *m*-CPBA, *p*-TSA; c. aq. $NaHCO_3$; d. BnCl, K_2CO_3; (ii) a. $LiAlH_4$; b. CrO_3, py; c. NH_2NH_2, NaOH; (iii) H_2, Pd/C; (iv) $(PhCO_2)_2$; (v) a. isopropenyl acetate, *p*-TSA; b. CrO_3, AcOH; (vi) a. aq. $NaHCO_3$; b. CH_2N_2.

The elaboration of one natural product into other members of the family, as employed by Matsumoto, is made relatively simple due to functional similarities across the large natural product series; this has been showcased in a number of further syntheses, most notably in a publication by Alvarez-Manzaneda in which six aromatic abietanes were produced (19-hydroxyferruginol **153**, (–)-sugikurojin A **154**, (+)-hanagokenol A **155**, and (+)-fortunins E **157**, G **158**, and H **156**) (***Figure 2.2***).[140]

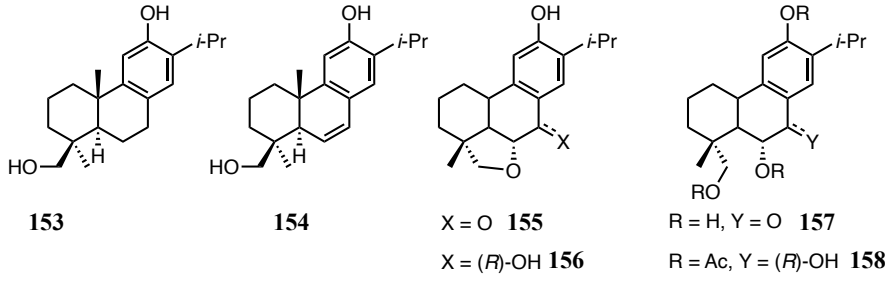

Figure 2.2. Aromatic abietanes produced by Alvarez-Manzaneda's derivatisation strategy.

Recently a semi-synthetic Diels–Alder strategy was used to assemble the highly elaborated aromatic ring present in the *ent*-cleistanthane diterpenoid spruceanol (**162**).[141] This route makes use of the chiral pool by starting from andrographolide (**159**) and allows late stage incorporation of aromatic functionality (***Scheme 2.4***).

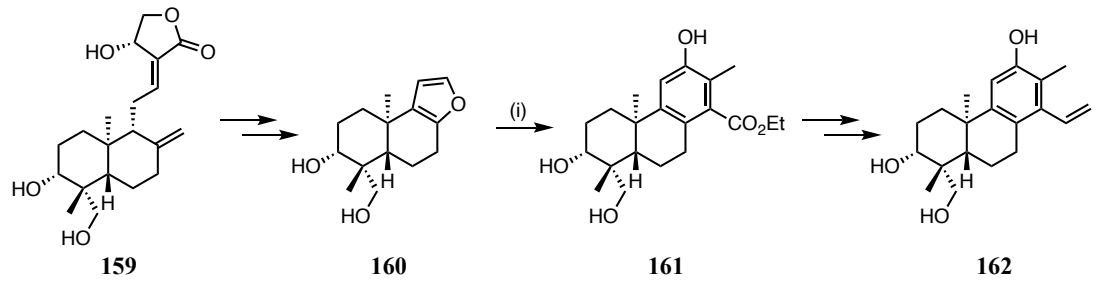

Scheme 2.4. Synthesis of an abietane-like core through the use of a Diels–Alder reaction. Reagents and conditions: (i) ethyl but-2-ynoate, $AlCl_3$, PhMe, 90 °C.

These semi-synthetic strategies avoid steps involved in constructing the tricyclic core, reducing the step count and increasing synthetic efficiency; however, using this pre-prepared core introduces constraints in the process, with oxidations at various positions proving chemically unfeasible and relatively simple functional group transformations requiring lengthy and inefficient routes.

Total synthesis routes have sought to reduce these inefficiencies; although this necessitates formation of the tricyclic core, functionality can be incorporated at more convenient points in the synthesis.

The many strategies reported to give access to the core include relatively simple Robinson ring annulations, acid-catalysed aromatic substitutions, and aldol reactions; more complex domino acylation-cycloalkyation cascade reactions, thermolysis of benzocyclobutene **163**, and radical cascades have also been used (***Scheme 2.5***).[142–147]

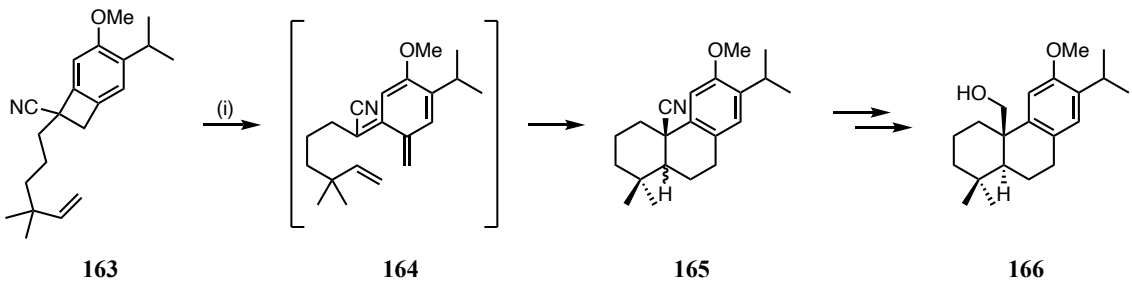

Scheme 2.5. Formation of the tricyclic core through thermolytic IMDA cycloaddition in Honda's synthesis of pisiferol.

Among the various successful cyclisation routes, by far the most common is a biomimetic approach inspired by the conversion of squalene into polycyclic triterpenes

in Nature.[148] This general concept generates cyclic systems rapidly and has been used to great effect in the synthesis aromatic abietanes (***Figure 2.3***).

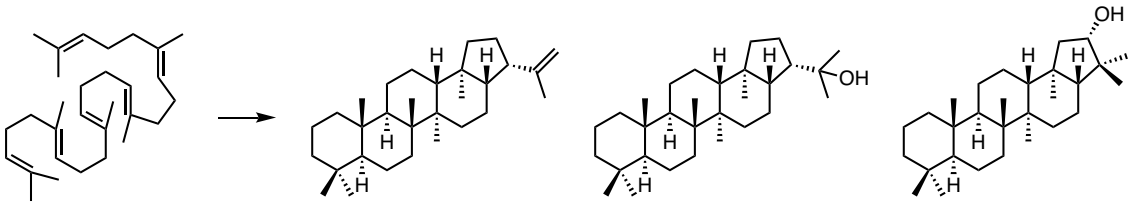

Figure 2.3. Biosynthetic conversion of squalene into triterpenoids.

Corey and Yamamoto advanced this approach by introducing enantioselective catalysts derived from BINOL,[149–151] and Corey applied this strategy to the synthesis of 4-*epi*-podocarpic acid **174** from geranyl acetate (***Scheme 2.6***).[152]

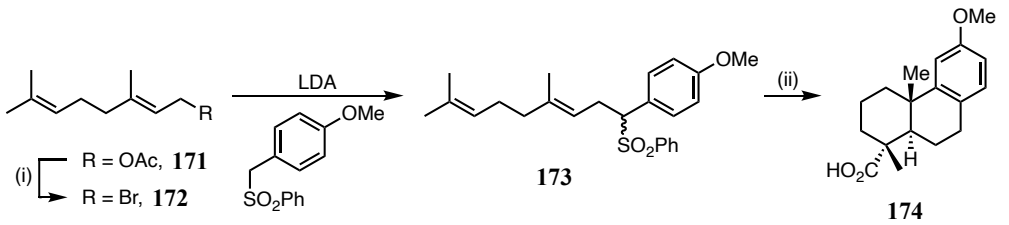

Scheme 2.6. Corey's approach to 4-epipodocarpic acid based on enantioselective biomimetic cyclisation. Reagents: (i) a. aq. K_2CO_3; b. PBr_3; (ii) a. Na/Hg, NaH_2PO_4; b. *o*,*o*′-dichloro-*R*-BINOL, $SbCl_5$; c. $KMnO_4$, $NaIO_4$.

Once access to the core skeleton is established, either through synthesis or procurement of a pre-existing core, control over the subsequent selective oxidation chemistry is crucial, and a variety of late-stage oxidation conditions have been reported: hydroboration, benzylic oxidation, and Sharpless dihydroxylation allow addition of oxygen into the A and B rings, while a frequently-used Friedel–Crafts acylation, Baeyer–Villiger oxidation, hydrolysis procedure gives access to phenol functionality (***Figure 2.4***).[139,153–155]

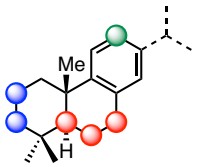

Figure 2.4. Summary of the positions on the aromatic abietane skeleton accessible to chemical oxidising agents. Red indicates oxidation *via* Sharpless dihydroxylation (the benzylic position is also accessible by Cr(VI)-mediated oxidation). Blue indicates oxidation *via* hydroboration. Green indicates the Friedel–Crafts, Baeyer–Villiger, hydrolysis sequence as used in Matsumoto's route to ferruginol **149** (***Scheme 2.3***).

In addition to the chemical methods used to form these diterpenoids, oxidation in fungal culture has also been exploited as a means to oxidise the benzylic position.[156]

2.1.1 Biosynthesis of aromatic abietanes

As discussed briefly in §**2.1**, the biosynthesis of this family of diterpenoids begins with geranyl geranyl diphosphate **175**; an enzyme catalysed cyclisation cascade, either *via* chair-chair-"normal" or chair-boat-"normal" transition states,[i] generates the pimara-15-en-8-yl cation which undergoes rearrangement to a variety of abietadienes.[132] The pimara-15-en-8-yl cation often isomerises to miltiradiene **178** which, following spontaneous aromatisation, is oxidised by cytochrome P450s to the final secondary metabolite. In the case of ferruginol **149**, direct CYP oxidation of the aromatic ring incorporates the phenolic functionality (***Scheme 2.7***).[157]

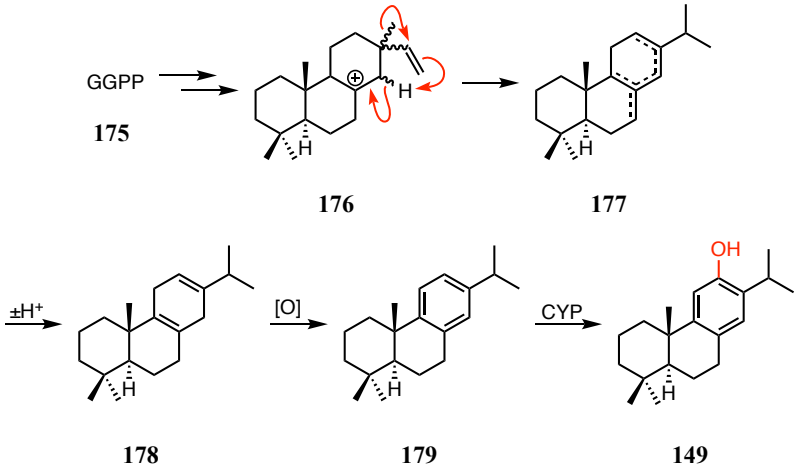

Scheme 2.7. Biosynthesis of ferruginol *via* miltiridiene **178**, a common intermediate in the biosynthesis of many aromatic abietanes.

[i] Chair-chair and chair-boat refer to the conformation of the unsaturated geranyl geranyl chain, while "normal" relates to the absolute stereochemistry observed in the product as compared with the analogous A/B rings in cholesterol.

2.2 Project aims

The aromatic abietane core presents an ideal platform to test mP450$_{BM3}$ reactivity and selectivity; the relatively simple core allows expeditious synthesis and its natural role as a CYP substrate is expected to ensure sufficient reactivity for a study of the metabolites. Importantly, the chirality of the core will enable kinetic resolution processes during enzymatic oxidation to be studied.

In order to keep the synthetic route and the enzymatic products relatively simple, the first reactions were to designed with substrates lacking the aromatic isopropyl group; later, it was expected that this substituent could be incorporated at the start of the synthesis, or before the cyclisation cascade, or post-cyclisation directed by any observed aromatic oxidation.

Initially, a synthesis of the racemic tricyclic core (±)-**117** was planned, based on previously-successful work within the group, followed by synthesis of the separate enantiomers, in order to test for kinetic resolution upon reaction with the mutant P450 library.

The racemic substrate was subsequently to be screened against a panel of P450 variants. Productive reactions were to be scaled up in order to identify the metabolites and measure their specific rotation. Enzyme reactions that produced enantiomerically-enriched products were then to be scaled up using the pure substrate enantiomers and the product distribution analysed; in the cases where the enzymatic reactions with (+)-**117** generate a different product distribution to (–)-**117** then kinetic resolution processes can be inferred. Following any kinetic resolution, analysis of the metabolites by supercritical fluid chromatography was planned in order to determine their % ee.

2.3 Synthesis of the carbocyclic core

2.3.1 Synthesis of racemic carbocycle (±)-117

The investigation began with the synthesis of carbocycle (±)-**117** based on previous work in the group in which acetylation of geraniol **180** and subsequent copper-mediated Grignard coupling with benzyl magnesium chloride produced diene **181**. Subsequent ruthenium catalysed cyclisation, as reported by Sames, generated the desired tricycle (±)-**117** (***Scheme 2.8***).[149,158]

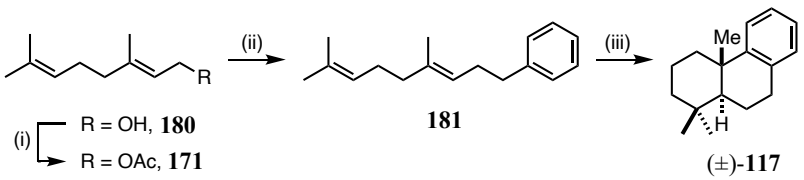

Scheme 2.8. Previous work in the group for the synthesis of carbocycle (±)-**117** based on Corey's copper catalysed Grignard coupling. Conditions: (i) AcCl, py, 0 °C to RT, 5 h, 95%; (ii) BnMgCl, Li_2CuCl_4, THF, 0 °C, 2 h, 81%; (iii) $RuCl_3.xH_2O$, AgOTf, DCE, 60 °C, 5 h, 83%

Upon repetition of the route as described, problems were encountered in the Grignard coupling step. Dimerisation, either through direct reaction of Grignard with halide, or through oxidative coupling of the Grignard, produced bibenzyl **182** as a major side-product to the desired reaction (***Scheme 2.9***).

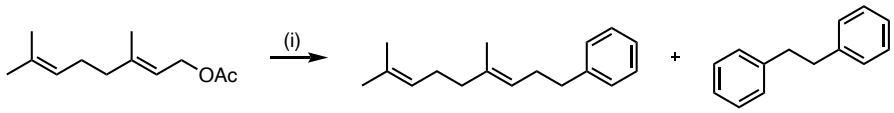

Scheme 2.9. Generation of undesired bibenzyl **182** in Grignard coupling reaction proposed to proceed through a copper catalysed reductive elimination pathway. Reagents and conditions: (i) BnMgCl, Li_2CuCl_4, THF, 0 °C, 2 h.

The so-formed bibenzyl was found to be inseparable from the main product **181** by purification *via* column chromatography and attempts to improve the purification, or to suppress the dimerisation reaction, were only partially successful; therefore, another method of Grignard substitution was required.

In order to avoid dimerisation through the oxidative coupling pathway, the Li_2CuCl_4 catalyst needed to be removed from the reaction mixture. This catalyst increases the

reactivity of the Grignard reagent and its removal would require the electrophilicity of the geranyl derivative to be increased to compensate for this. The reaction between geranyl phosphate **184** and *o*-methoxybenzylmagnesium bromide has been reported in the synthesis of galanal A (**186**) and B (**187**), and this precedent was chosen to test as a new set of conditions (***Scheme 2.10***).[159]

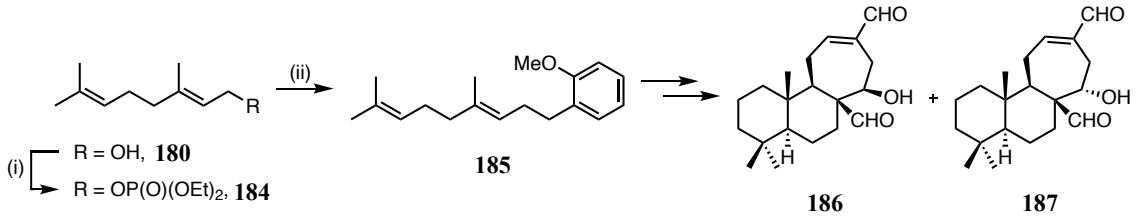

Scheme 2.10. Use of diethyl geranyl phosphate **184** in the synthesis of galanal A (**186**) and B (**187**). Reagents and conditions: (i) $(EtO)_2POCl$, py, Et_2O, –15 °C to RT, 3 h; (ii) *o*-methoxybenzyl bromide, Mg, THF, –40 °C to RT, 12 h.

Synthesis of phosphate **184** was trivial and attention quickly turned to establishing conditions for the Grignard reaction (***Table 2.1***). Initially the conditions reported by Lin *et al*. were tested; however, the major product was derived from an S_N2'-like reaction possibly due to the relatively high reaction temperature promoting fast loss of the phosphate leaving group, followed by non-selective trapping of the so-formed delocalised cation with the nucleophile (Entry **1**).

The temperature of the reaction was decreased to –78 °C and this generated the desired product (**181**) containing inseparable bibenzyl (**182**) (Entry **2**). A move to benzyl chloride, which is less likely to undergo reductive electron transfer than benzyl bromide, coupled with the addition of 1,2-dibromoethane was attempted. Formation of benzylmagnesium chloride is less favourable due to the more negative reduction potential of the C–Cl bond (–0.73 V for benzyl chloride, –0.51 V for benzyl bromide in acetonitrile referenced to the standard calomel electrode) and so mechanically activated Mg, the use of which was pioneered by Brown for the activation of reactive benzylic and allylic chlorides, was employed.[160,161] In the event, these conditions were

unsuccessful in reducing the presence of bibenzyl (**182**), as was a reduction in the number of equivalents of benzyl chloride and Mg (Entries **3** and **4**).

Nevertheless, it was clear that coupling between benzylmagnesium chloride and phosphate **184** was occurring and so the activation phase of the Grignard formation was interrogated. It was proposed that the high temperatures being used for initiation of the exothermic Mg insertion into the C–Cl bond might promote the nucleophilic displacement reaction between benzylmagnesium chloride and unreacted benzyl chloride. When the initiation was carried out at 0 °C the amounts of bibenzyl (**182**) being formed were reduced, so much so that purification by column chromatography, using 1% ethyl acetate in pentane instead of toluene, was effective in removing remaining traces of bibenzyl (**182**) (Entry **5**).

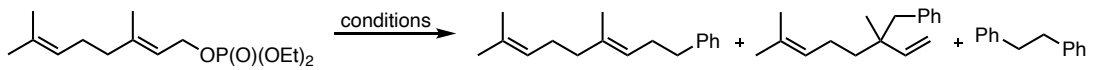

184 **181** **188** **182**

Table 2.1. Optimisation of Grignard addition into phosphate **184**.

Entry	Grignard precursor	Mg activation	Eq. BnX	Eq. Mg	Grignard activation	Reaction temp.	Approx. product ratio[d] 181:188:182
1[a]	BnBr	Oven	2	4	Heat gun then RT	–20 °C	0:52:48
2[a]	BnBr	Oven	2	4	Heat gun then RT	–78 °C	71:21:8
3[a]	BnCl[c]	Brown	2	4	Heat gun then RT	–78 °C	82:18:0
4[a]	BnCl[c]	Brown	0.9	1.2	Heat gun then RT	–78 °C	38:50:12
5[b]	BnCl	Brown	2	4.5	0 °C	–78 °C	99:1:0

[a] Toluene used for purification by column chromatography; [b] 1% ethyl acetate in pentane used as eluent for column chromatography; [c] 1,2-dibromoethane used as initiator; [d] determined by comparison of characteristic resonances in ^{1}H NMR spectra.

These new conditions allowed the efficient synthesis of multigram-quantities of **181** and attention turned to the Brønsted acid catalysed biomimetic cyclisation cascade. The combination of both $RuCl_3 \cdot xH_2O$ and AgOTf in catalytic quantities was proposed by Sames to lead to coordination of Ag(I) to chlorine in the $RuCl_3$ complex, in turn

increasing the electrophilicity of the Ru centre and the acidity of the coordinated water molecules thus providing a proton source for activation of the terminal olefin. Under Sames' reported conditions the reaction progressed smoothly to (±)-**117** in excellent yield and on gram-scale (***Scheme 2.11***)[158] from which point the synthesis of the separate enantiomers was investigated.

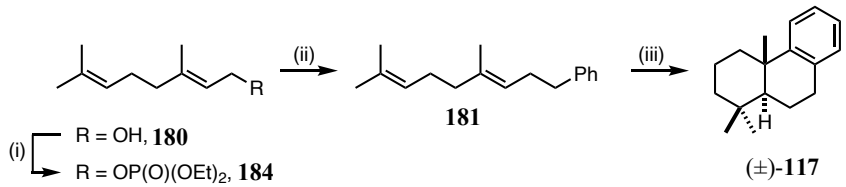

S*cheme 2.11.* Final route to tricycle (±)-**117**. Reagents and conditions: (i) $(EtO)_2POCl$, py, Et_2O, –20 °C to RT, 3 h, 77%; (ii) BnCl, Mg, THF, –78 °C to RT, 16 h, 80%; (iii) $RuCl_3 \cdot xH_2O$, AgOTf, DCE, 60 °C, 4 h, 92%.

2.3.2 Synthesis of (+)-(*S*,*S*)-117 and (–)-(*R*,*R*)-117

A route to (+)-(*S*,*S*)-**117** was reported by Corey that employed a BINOL-derived catalyst combined with $SbCl_5$; the Lewis-acidic $SbCl_5$ increases the acidity of the BINOL hydroxyl groups, in a similar manner to the $RuCl_3 \cdot xH_2O$/AgOTf system, allowing selective protonation of the terminal alkene, while the *R*-BINOL catalyst system promotes formation of (+)-**117** over (–)-**117** by ensuring that protonation takes place within a chiral environment (***Figure 2.5***).[149]

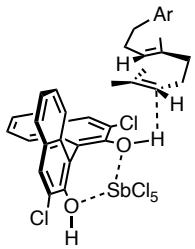

Figure 2.5. Combination of a BINOL-derived catalyst and a Lewis acid ($SbCl_5$) to promote asymmetric Brønsted acid mediated cyclisation.

The rigid BINOL system synergistically protonates one face of the terminal trisubstituted double bond and induces the orientation of the two double bonds as a low-energy π-stacked cationic intermediate; the stereochemistry of further ring closure onto

the so-formed carbocation follows from the initial protonation since the protonation and cyclisation steps are coordinated.

Both (*R*)- and (*S*)-BINOL catalysts were required in order to produce (+)-**117** and (–)-**117**, and these were synthesised following literature precedent (***Scheme 2.12***).[162,163]

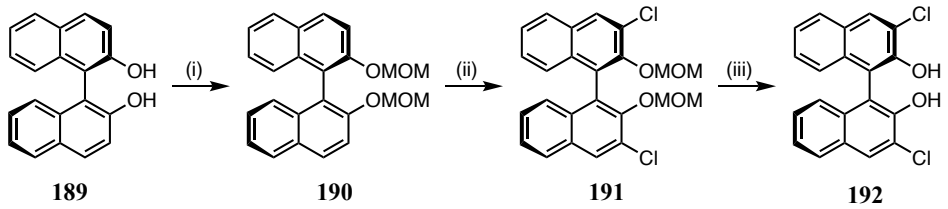

Scheme 2.12. Synthetic route towards (*R*)-*o*,*o*′-dichloro-BINOL. Reagents and conditions: (i) NaH, MOMCl, THF, DMF, 0 °C to RT, 8 h, 87%; (ii) *n*-BuLi, Cl_3CCCl_3, Et_2O, THF, 0 °C to RT, 16 h; (iii) Amberlyst-15, MeOH, THF, 65 °C, 16 h, 32% over two steps. An analogous procedure was carried out in the synthesis of (*S*)-*o*,*o*′-dichloro-BINOL, the yields of which were: (*S*)-**190** 82%; (*S*)-**192** 47% over two steps.

Although the route generated (*R*)-**191** and (*S*)-**191** successfully, their purification was problematic because a ^{1}H NMR silent, viscous yellow oil was present that proved to be inseparable by chromatography from the desired BINOL derivative. Trituration with pentane allowed isolation of pure material for analysis; however, the by-product, most likely tetrachloroethylene, was deemed to be inconsequential in the next step as it was expected that the final BINOL derivative, being polar, would be easily separable from the impurity by chromatography (***Scheme 2.13***).

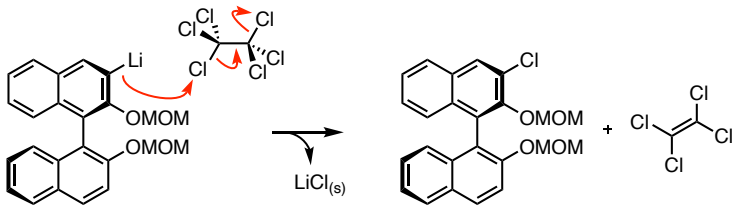

Scheme 2.13. Formation of tetrachloroethylene under the chlorination conditions.

Accordingly, crude (*R*)-**191** and (*S*)-**191** were carried through to the next step and, upon reaction with mildly acidic Amberlyst-15, the desired dichloro-BINOLs were successfully isolated free from impurities.

With both (*R*) and (*S*) catalysts in hand, Corey's reported enantioselective cyclisation was attempted (***Scheme 2.14***).

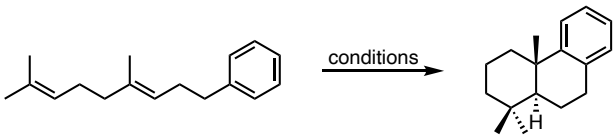

181 **117**

Scheme 2.14. Attempted symmetric cyclisation to carbocycle (+)-**117**.

The originally reported conditions were tested first and, although some of the desired tricycle was produced, it was isolated as a complex mixture (***Table 2.2***, entry 1). Purification by column chromatography led to some separation, with NMR spectroscopic analysis revealing the presence of alkene functionality in one of the fractions. This result, although not referenced in the publication, is perhaps unsurprising since, following protonation and first cyclisation, there are a number of mechanistic possibilities: trapping of the carbocation by the aromatic functionality to produce both desired tricycle **117** and diastereomer **194** (***Scheme 2.15***, k_{cyc}), *endo* or *exo* deprotonation (***Scheme 2.15***, k_{dep}), or even reaction with another molecule of **117**, although this intermolecular reaction is less likely considering the low substrate concentration used in the reaction.

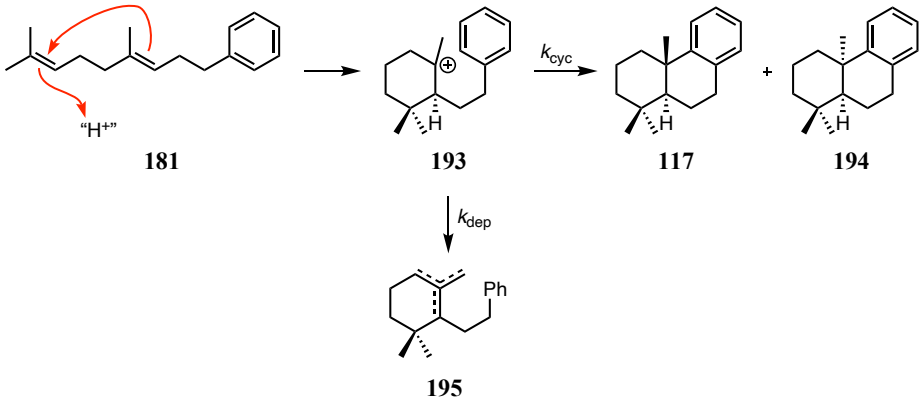

181 **193** **117** **194** **195**

Scheme 2.15. Possible reactivity modes of key carbocation intermediate **193**.

Under these kinetic conditions, the relative rates of each competing process are crucial in determining the product profile. The experimental observation that a mixture of

products was generated implies that $k_{cyc} \approx k_{dep}$, but k_{cyc} needs to be significantly larger than k_{dep} in order for the desired reactivity to dominate. The k_{cyc} pathway requires dearomatisation of the benzene ring with an associated high-energy transition state leading to a reduced relative rate; it seems reasonable, therefore, for k_{cyc} to not be significantly greater than k_{dep}. In short, it appeared the cyclisation of the benzene ring was not sufficiently coordinated with the initial cation formation and the first cyclisation event.

With this in mind, a higher reaction temperature was tested but this led again to a complex product mixture (***Table 2.2***, entry 2). The impurities were difficult to separate because their nonpolar nature led to negligible differences in the TLC R_f values, and ^{1}H NMR resonances overlapped extensively in the aliphatic region with few characterisitic peaks discernible.

It was proposed that the catalytic species might interfere with the reaction since it was used, as in Corey's report, stoichiometrically; accordingly, the loading was reduced to 0.5 equivalents but no improvement was observed. An increase in reaction temperature, necessitating a change of solvent from dichloromethane to DCE, was tested but again with no improvement (***Table 2.2***, entry 3 and 4).

It was proposed the quality of the synthesised (*R*)-**192** may be to blame for the unsuccessful reactivity and, to test if this was the case, the reaction was carried out with (*R*)-BINOL itself. These conditions have been reported and, in our hands, a similar result to the previous attempts was observed (***Table 2.2***, entry 5).[164] In order to test if the underlying reactivity was occurring as expected, the reaction was carried out in the absence of the BINOL catalyst because it was possible that the highly reactive $SbCl_5$ (or adventitious HCl present in it) could competitively catalyse the reaction to give racemic products; however, yet again, a complex mixture was isolated, indicating fundamental

problems with the transformation (***Table 2.2***, entry 6).

Yamamoto, in a report of investigations of a similar system but with a different catalytic entity, highlighted similar problems associated with competing deprotonation of an analogous cationic intermediate and the formation of complex product mixtures (***Scheme 2.16***).[165] A solution was found, in his work, that involved addition of $ClSO_3H$ to the mixture to promote the final ring closure step from any unreacted olefins, pushing the reaction to completion; in practice, treatment of a complex mixture generated from (*R*)-**192**/$SbCl_5$ with $ClSO_3H$ did not improve the outcome (***Table 2.2***, entry 7).

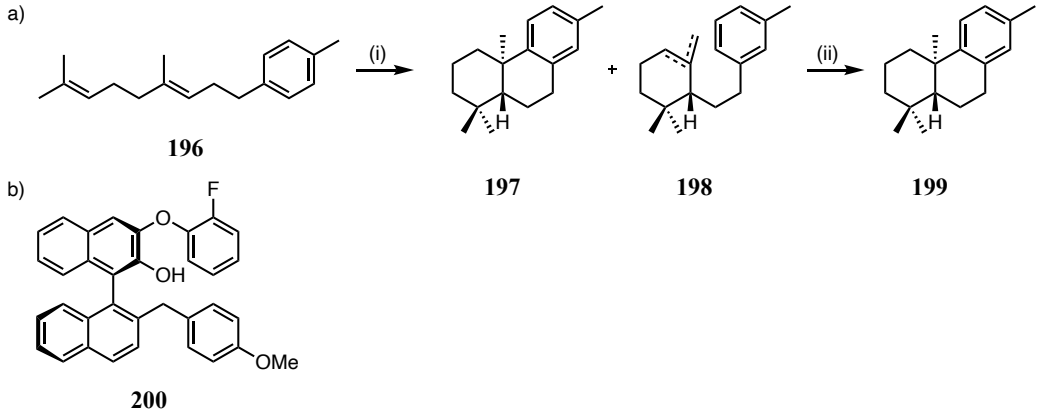

Scheme 2.16. a) Premature deprotonation encountered in Yamamoto's synthesis of (–)-**199**. Conditions: (i) (*S*)-**200**, $SnCl_4$, PhMe, –78 °C 24 h; (ii) $ClSO_3H$, *i*-$PrNO_2$, –78 °C; b) BINOL derived catalyst used by Yamamoto.

A further attempt was made to complete the conversion of unreacted olefinic intermediates into the desired tricycle. A mixture of partially cyclised products was generated through Corey's conditions which was then submitted to Sames' $RuCl_3 \cdot xH_2O$/AgOTf system used in the racemic cyclisation but this yielded no improvement, with another complex olefinic mixture being isolated (***Table 2.2***, entry 8).

Table 2.2. Conditions tested to improve the selectivity of the asymmetric cyclisation reaction.

Entry	T /°C	Time /h	Catalyst	Eq. catalyst	Eq. $SbCl_5$	Solvent
1	–78	6	(*R*)-**192**	1	1	CH_2Cl_2
2	–30	16	(*R*)-**192**	1	1	CH_2Cl_2
3	–78	16	(*R*)-**192**	0.5	0.5	CH_2Cl_2
4	–20 to 60	16	(*R*)-**192**	0.5	0.5	DCE
5	–78	6	(*R*)-BINOL	0.5	0.5	CH_2Cl_2
6	–78	21.5	(*R*)-**192**	0	0.5	CH_2Cl_2
7[a]	–78	18	(*R*)-**192**	0.5	0.5	CH_2Cl_2
8[b]	–78	18	(*R*)-**192**	0.5	0.5	CH_2Cl_2

[a]$ClSO_3H$ added after 6 h to encourage ring closure of olefin intermediate; [b]crude reaction mixture submitted to $RuCl_3 \cdot xH_2O$/AgOTf system to encourage ring closure of olefin intermediate.

Following this, a re-examination of the literature showed that Corey's procedure had not worked as expected in others' hands[159] and, since the focus of this project was not to develop chemical methodology, the decision was made to isolate and resolve the enantiomers by preparative chiral HPLC. This separation was carried out by Andrew Ikin at AstraZeneca. Acquisition of the specific rotation of each enantiomer and comparisons to literature data allowed assignment of the absolute configuration in each case (***Table 2.3***). (–)-**117** was obtained as a pure enantiomer (>99% ee) but the enantiomeric excess of (+)-**117** could not be determined reliably due to the presence of trace impurities; however, this was not deemed to be problematic for future reactions.

Table 2.3. Determination of absolute configuration of separated enantiomers.

Entry	Retention time	Measured $[\alpha]_D^{25}$	Literature $[\alpha]_D^{25}$	Absolute configuration
1	13.30 mins	–53.2 (*c* 0.67, $CHCl_3$)	–[a]	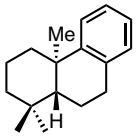
2	15.91 mins	+52.3 (*c* 0.59, $CHCl_3$)	+16.5[149] (*c* 1.0, $CHCl_3$)	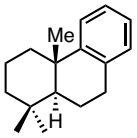

[a] (–)-**117** is unknown in the literature and so there are no specific rotation data available for comparison.

With routes to (±)-**117**, (+)-**117**, and (–)-**117** secured the focus moved on to

investigating the reactivity against the library of $P450_{BM3}$ variants.

2.4 $P450_{BM3}$ screening

The reactivity of (±)-**117** was investigated against a subset of the Wong group's $P450_{BM3}$ enzyme library (see below) in small scale reactions (0.5 μmol of substrate) as a preliminary survey to determine which mutants warrant further examination. At the time of this study the overall enzyme library comprised more than 300 members and it was not feasible to test all of them (see §**1.3.1.4**). Sub-groups of these engineered enzymes show particular activity towards certain substrate types such as cyclic amines, anilides and THQ, and steroids. Carbocycle **117** bears many similarities to steroids, with its *trans*-fused 6,6,6-tricyclic system resembling the A-, B-, and C-rings of the steroid family (***Figure 2.6***), and it was proposed that $P450_{BM3}$ variants that had proven to be active with steroid substrates were the most likely to show significant activity towards **117**.

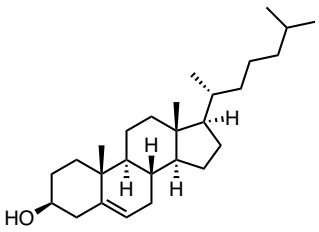

cholesterol, **201**

Figure 2.6. The A,B,C-rings in a representative steroid, cholesterol **201**, bear some structural resemblance to to tricyclic substrate **117**.

Previous group work had found that the hydrophobicity of the tricyclic skeleton reduced its solubility in the aqueous reaction medium for enzymatic transformations and so methyl-β-cyclodextrin (**202**) was added to improve solubility. Cyclodextrins are macrocyclic oligosaccharides commonly containing six (α), seven (β), or eight (γ) glucopyranose units linked through 1,4-glycosidic bonds (***Figure 2.7***). The toroidal topology of cyclodextrins creates an interior that is considerably less hydrophilic than the surrounding aqueous medium, allowing complexation of hydrophobic molecules,

while the hydrophilic exterior confers the cyclodextrin complex enhanced aqueous solubility. Complexation of a guest molecule into a macrocyclic host involves consideration of complex enthalpic and entropic factors which vary depending on the host-guest system and the solvent. Liberation of water molecules from the host cavity upon substrate binding is entropically favourable; however, enthalpic effects have been shown to be at least as important through the increase in participation of ejected water molecules in water-water interactions.[166]

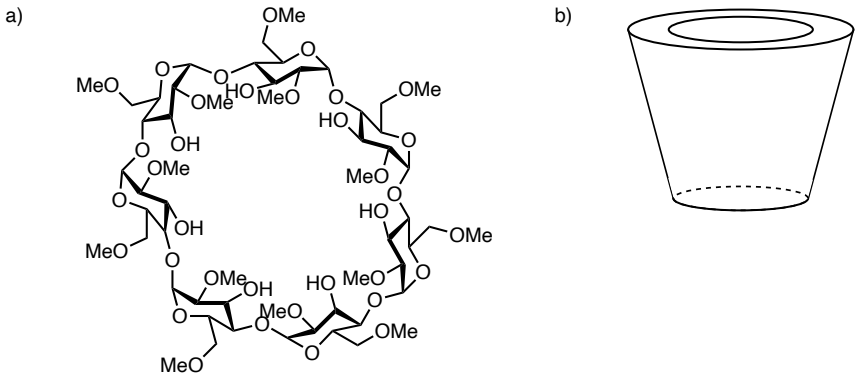

202

Figure 2.7. a) Structure of methyl-β-cyclodextrin **202**; b) toroidal architecture of cyclodextrins; the inner hydrophobic channel allows complexation of the poorly aqueous-soluble substrate.

Screening studies were carried out on a 0.5 mL scale in 24-well plates, with each well containing: 100 mM glucose, 5.0 mM methyl-β-cyclodextrin, 1.0 mM substrate, 2.0 U/mL glucose dehydrogenase, 80 μM $NADP^+$, 2.0 μM CYP102A1 variant, and 200 mM phosphate buffer. The screening reactions were performed in an incubator at 20 °C and, in order to preclude any light-mediated aromatic oxidation pathways, were run in the dark, with the 24-well plates wrapped in aluminium foil. After 24 h the wells were extracted with ethyl acetate and analysed by GC.

As expected on the basis of the mP450s chosen, the majority of the enzymes converted >70% of (±)-**117** into a large number of products (***Graph 2.1***).

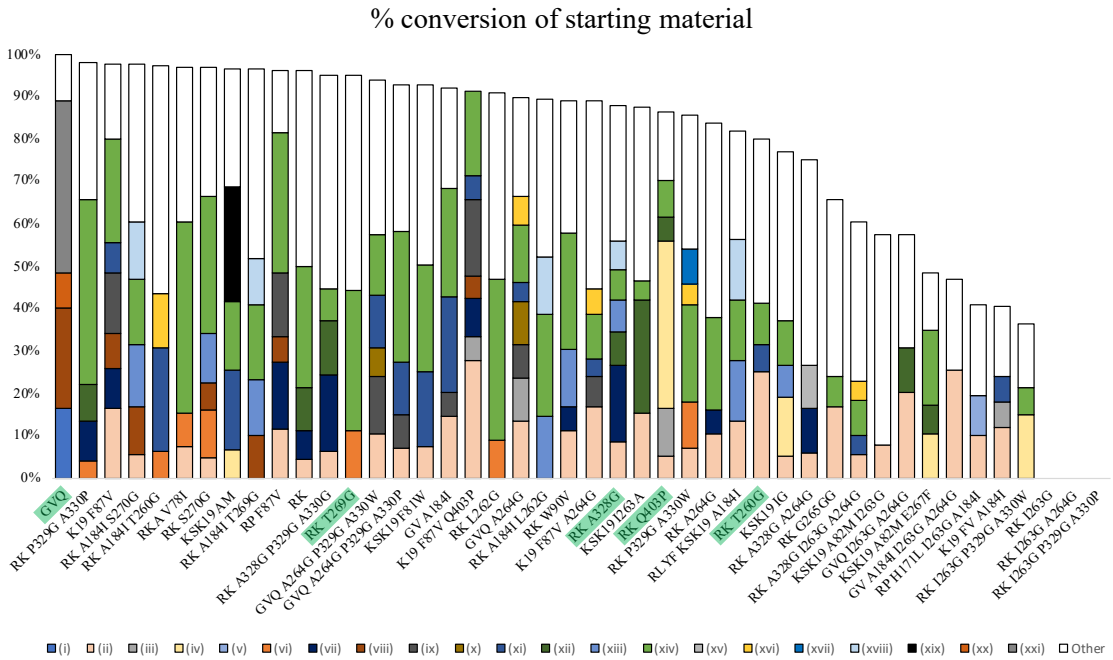

Graph 2.1 Percentage conversion of (±)-**117** into over 20 products.

Analysis of the GC traces for each well was undertaken, and percentage conversion values were calculated from the relative peak integrations. Setting a lower threshold of 5% relative peak area to record the production of a metabolite, in order to reduce the impact of noise, led to the identification of 21 separate unknown metabolites. The overall conversion profile is displayed in ***Graph 2.1*** in which the white regions correspond to trace impurities and products which fell below the 5% cutoff. Inclusion of these "other" metabolites allowed the enzymes to be categorised according to their activity towards (±)-**117** and therefore important residues involved in reactivity towards the substrate might be identified. Unsurprisingly, due to the complex nature of enzymatic processes (see below), no clear correlations could be established at this stage. Very broadly, the GVQ combination (A74G/F87V/L188Q), known to increase activity of CYP102A1s,[107] appeared beneficial for reactivity as did, in general, the A184I mutation. Many of the variants tested included mutations to glycine: S270G, A328G, T269G, among many others. Incorporation of the small glycine residue has the effect of "hollowing out" the active site, potentially allowing larger, non-natural, substrates to

contact the catalytic centre and increasing reactivity; however, the screening results with (±)-**117** indicated no clear relationship between a larger active site and an increase in activity.

A lack of clearly-identifiable key residues merely reflects the complex combination of enthalpic, entropic, and kinetic factors that govern enzymatic reactivity. Hydrogen bonding plays a key role in substrate orientation within the active site but carbocycle **117** is unable to participate in interactions requiring heteroatomic functionality and residues that would usually help to influence reactivity through H-bonding are not able to exert an effect, reducing the impact on reactivity of specific residue changes.

The lack of data for the final three variants shown in ***Graph 2.1*** (RK/I263G, RK/I263G/A264G, and RK/I263G/P329G/A330P) reflects poor-quality GC traces. All three had pA*min values lower than 0.1 (usually ranging from ~1 to ~8) suggesting poor recovery and not necessarily poor enzyme activity; it was determined that the 41 successful results gave sufficient information about the general reactivity profile to begin metabolite characterisation studies.

2.5 Preparative scale $P450_{BM3}$ reactions

In order to characterise the metabolites by NMR spectroscopy and to further investigate individual reactivity profiles, larger-scale reactions were needed. The GC data showed that two products, (ii) and (xiv), were being generated as major components and so these were the first to be scrutinised (***Graph 2.1***).

The reactions with RK/T260G and RK/T269G, which produced (ii) and (xiv), respectively, as major products, were chosen for scale-up on the basis that high conversion of starting material (80% for RK/T260G, 95% for RK/T269G) and reasonable conversion for the product in question (25% for RK/T260G to (ii), 33% for RK/T269G to (xiv)) during screening would allow generation of the required amount of

oxidation product for analysis; furthermore, selectivity for metabolites (ii) and (xiv) separately would aid chromatographic separation of the crude reaction mixture. In general, isolating the individual components of $P450_{BM3}$ reactions can be problematic since the numerous structurally similar hydroxylated metabolites often have comparable R_f values, precluding efficient separation by chromatography on silica, but careful choice of enzyme can minimise the number of products to be separated.

2.5.1 Characterisation of RK/T260G metabolites

To begin, enzyme variant RK/T260G was expressed in *E. coli* and stored as 1.0 mL aliquots in phosphate buffer at –20 °C (see §**6.3**). A preparative scale reaction was carried out on a 100 mL scale in conical flasks and, as in the screening reactions, these were performed in the dark; the concentrations of reagents were also the same as in screening aiming to reproduce the results as closely as possible. After the reaction was complete, in this case 24 h, it was extracted into ethyl acetate and analysed by GC and TLC. Both analysis methods showed the generation of a single major product, assumed to be (ii), alongside a small amount of remaining starting material and a number of trace side-products. This major product was isolated and characterised following purification by column chromatography. The ^{1}H NMR spectrum displayed a resonance at 4.78–4.88 (m, 1H) indicating the presence of an alcohol which was confirmed by a broad peak at 3239 cm^{-1} in the IR spectrum. The high chemical shift of the peak in the NMR spectrum suggested that oxidation had occurred at the benzylic position and, indeed, 2D NMR spectroscopic analysis corroborated this, allowing metabolite (ii) to be characterised as benzylic alcohol (+)-**118** (***Figure 2.8a***). Surprisingly this compound did not fly under ESI^+ or ESI^- MS conditions but EI ionised (±)-**118** succesfully and the mass was found to be 244.1829 ($C_{17}H_{24}O^+$ requires 244.1827) which supported the characterisation. The relative configuration was not determined through the use of coupling constants because

the C**H**OH resonance was an unresolvable multiplet; however, NOESY correlations supported the assignement that (+)-**118** was the product of hydroxylation of the accessible equatorial hydrogen atom (***Figure 2.8b***).

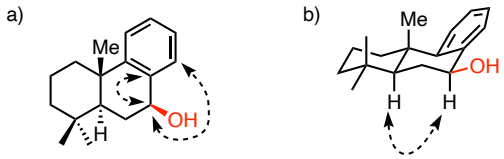

(+)-**118**

Figure 2.8. a) Structure of (ii), the major metabolite of the reaction between RK/T260G and (±)-**118**, showing HMBC correlations confirming the presence of the benzylic alcohol; b) relevant NOESY correlation showing an axial benzylic proton and confirming equatorial oxidation.

2.5.1.1 Kinetic resolution

The non-zero specific rotation of alcohol (+)-**118** obtained from the RK/T260G variant ($[\alpha]_D^{25}$ +44.3 (*c* 0.14, $CHCl_3$)) indicated some degree of kinetic resolution of the racemic substrate. Aiming to probe this further, and to assign the absolute configuration of the major enantiomer of the product, the reactions were repeated with each enantiomer of the substrate. The conditions were repeated exactly and again, after 24 h, the completed reaction was extracted into ethyl acetate and analysed by GC and TLC. These analyses clearly showed that the reaction with (+)-**117** progressed to benzyl alcohol (+)-**118**, as in the racemic case, but (–)-**117** was unreactive. On this basis, it was concluded that the sense of kinetic resolution was for the enzyme to favour reaction with (+)-**117**, the natural enantiomer, over non-natural (–)-**117** (***Scheme 2.17***).

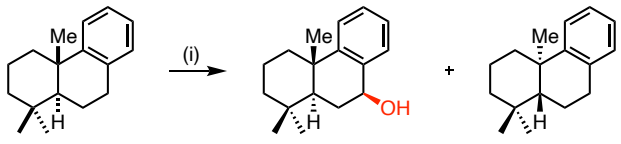

(±)-**117** (+)-**118** (–)-**117**

Scheme 2.17. Overall kinetic resolution reaction of (±)-**117**. Conditions: 2 µM RK/T260G, 1mM (±)-**117**, 100 mM glucose, 2 U/mL GDH, 80 µM $NADP^+$, 5 mM methyl-β-cyclodextrin, 200 mM phosphate buffer 20 °C, 24 h, 22%.

2.5.1.2 Determination of enantiomeric excess

The synthetic utility of these transformations depends heavily on the enantiomeric excess of the metabolite generated, which depends on the selectivity factor – the rate at which the catalyst reacts with one enantiomer over the other.

Efforts to determine the % ee of (+)-**118** began with Mosher's ester derivatisation; the product from the reaction between (±)-**117** and RK/T260G should combine with an excess of a single enantiomer of α-methoxy-α-(trifluoromethyl)phenyl acetyl chloride to produce two diastereomers, expected to be differentiated by NMR spectroscopy (***Scheme 2.18***). Careful integration of any separated peaks in the NMR spectra would allow determination of an approximate % ee value. The ratio of the benzylic proton peaks, C9-$\mathbf{H_{203}}$:C9-$\mathbf{H_{204}}$, equates to the % de of the diastereomers and thus the % ee of the enantiomers, assuming complete conversion of (+)-**118**.

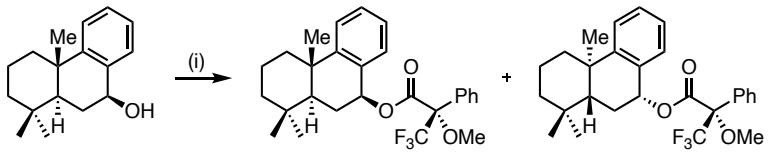

(+)-**118** **203** **204**

Scheme 2.18. Mosher's ester derivatisation of (+)-**118**. Conditions: (*R*)-(–)-α-methoxy-α-(trifluoromethyl)phenyl acetyl chloride, py, CD_2Cl_2.

The small amount, 5.4 mg, of hydroxylated product isolated from the biocatalytic reaction precluded a preparative scale esterification and an NMR-scale reaction was attempted. CD_2Cl_2 was used as a solvent due to its higher purity than $CDCl_3$ while pyridine was employed as a base, since the aromatic proton signals would not interfere with the resonances for the diagnostic aliphatic protons; the (*R*)-(–)-acid chloride was used for the derivatisation on cost grounds. Under these conditions, no significant reaction occurred even after allowing the reaction to stir for two weeks. A number of more polar products were visible by TLC but nothing substantial was observed by ^{1}H NMR spectroscopy and this method of analysis was dismissed. It was proposed that the

adjacent axial proton and the axial methyl group at the bridge position may impart enough steric hindrance on the system to preclude reaction with the bulky Mosher's acid chloride.

With this drawback, it became clear that chiral chromatography would be necessary to determine the % ee value of (+)-**118**, and chiral supercritical fluid chromatography (SFC) was considered. In order to carry out this analysis, a racemic reference sample was required, and a brief synthesis of the racemic alcohol was carried out starting from (±)-**117** (***Scheme 2.19***). Chromic acid oxidation furnished ketone (±)-**205**, and axial-selective $LiAlH_4$ reduction generated the desired alcohol (±)-**118**); no evidence of equatorial reduction was observed by ^1H NMR.

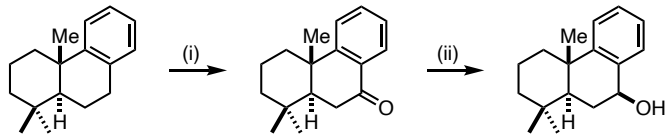

(±)-117 (±)-**205** (±)-**118**

Scheme 2.19. Synthesis of reference sample of (±)-**118** for chromatographic analysis. Conditions: (i) CrO_3, AcOH, RT, 1.5 h, 50%; (ii) $LiAlH_4$, THF, 0 °C to RT, 1.5 h, 56 %.

Using the racemic sample, optimisation of the chromatographic conditions showed that an amylose-based column (Trefoil AMY1) coupled with an isocratic flow of 1.5 mL $CO_{2(l)}$ with 10% methanol showed clear separation of the racemate into its separate enantiomers and the enantiomeric excess of (+)-**118** was determined as 85% (***Figure 2.9***). This analysis was kindly carried out at the Oxford Suzhou Centre for Advanced Research by Yang Cao. With (+)-**118** fully characterised, an investigation into increasing the scale of the reaction was carried out.

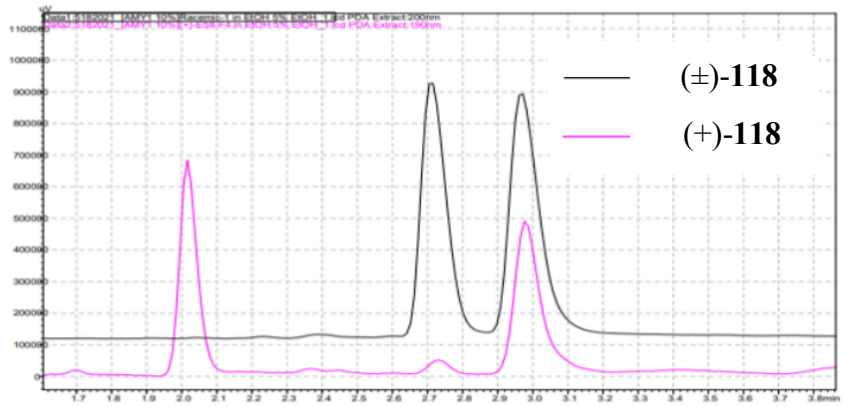

Figure 2.9. Overlaid SFC-PDA chromatogram showing separation of (±)-**118** allowing determination of (+)-**118** % ee. The peak at 2.0 mins is proposed to be a result of aerobic oxidation to (+)-**205**.

2.5.1.3 Large scale reactions

With improved knowledge of the reaction, large scale reactions were undertaken in order to assess the ability of these enzymes to perform C–H hydroxylation reactions at a synthetically useful scale.

Previous work within the group has shown large scale oxidations to be temperamental, often resulting in poor conversion, with the reasons for this erratic reactivity having never been fully ascertained. Large scale reactions are carried out at the same concentration as the reactions used to characterise metabolites and so it has been proposed that difficulty with mass transfer with the larger reaction volume is, in part, responsible for poor conversion. This unreliability was evident in the large scale reaction of (±)-**117** with RK/T260G in which extremely poor conversion was observed. Reactions were carried out at a 500:1 ratio of substrate to enzyme, with cofactor concentrations the same as used in preparative scale procedures and the substrate introduced as a solution in ethanol. The first reaction, carried out at 100 mL scale (substrate concentration = 4 mM), showed no conversion. At this volume, mass transfer is not generally problematic, and it was proposed that the poor solubility of the hydrocarbon substrate was inhibiting reactivity at this high nominal concentration. Accordingly, the substrate concentration was lowered to 0.5 mM but a reaction at 400

mL scale failed to display significant conversion. This large volume, low concentration reaction was carried out in a conical flask on a shaker, as well as in a round-bottom flask equipped with a stirrer bar, in an attempt to investigate differing mass transfer conditions; neither reaction showed promising results and so attention turned to characterisation of further metabolites.

2.5.2 Characterisation of RK/T269G metabolites

A preparative scale reaction with (±)-**117** and RK/T269G was carried out under the same conditions as before. GC and TLC analysis showed that variant RK/T269G produced a greater number of metabolites than RK/T260G but a single major product was evident, corresponding to (xiv) (***Graph 2.1***). Purification by column chromatography led to isolation of the major metabolite but the minor products were not separated either in sufficient quantity or purity to allow characterisation.

Analysis of the ^{1}H NMR spectrum indicated the presence of a diol with two 1H signals at 3.30 (dt, J = 10.0, 4.5 Hz) and 4.83 (dt, J = 10.5, 7.5 Hz) ppm; the signal at 4.83 suggested, as with RK/T260G, that oxidation had occurred at the benzylic position. 2D NMR analysis confirmed the assignment of the benzylic alcohol, and, although no HMBC correlations were discernible for the other alcohol due to the dilute NMR sample (4.2 mg of the metabolite was isolated), COSY and HSQC correlations allowed full elucidation of the structure of metabolite (xiv) as diol (+)-**206** (***Figure 2.10a***). MS data corroborated this assignment, and relative configurations were assigned through both coupling constants and NOESY correlations (***Figure 2.10b***); as before, equatorial hydroxylation was favoured.

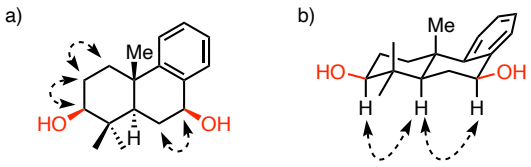

(+)-**206**

Figure 2.10. a) Structure of (xiv), the major metabolite of the reaction between (±)-**117** and RK/T269G, showing relevant COSY correlations confirming the position of the two hydroxyl groups; b) relevant NOESY correlations verifying the equatorial oxidation.

2.5.2.1 Kinetic resolution

Having previously observed kinetic resolution in the formation of (+)-**118**, it was expected that a similar pattern of reactivity would result in the formation of (+)-**206**; that is, favouring the oxidation of one enantiomer over the other. This proved to be the case, with the measured specific rotation of (+)-**206** being $[\alpha]_D^{25}$ +54.1 (*c* 0.21, $CHCl_3$).

Submission of the pure enantiomers separately to the biocatalytic oxidation conditions showed that a parallel kinetic resolution appeared to operate. From GC analysis, the reaction of (+)-**117** with RK/T269G generated (+)-**206** as the major metabolite alongside a small amount of (+)-**118** (***Figure 2.11***).

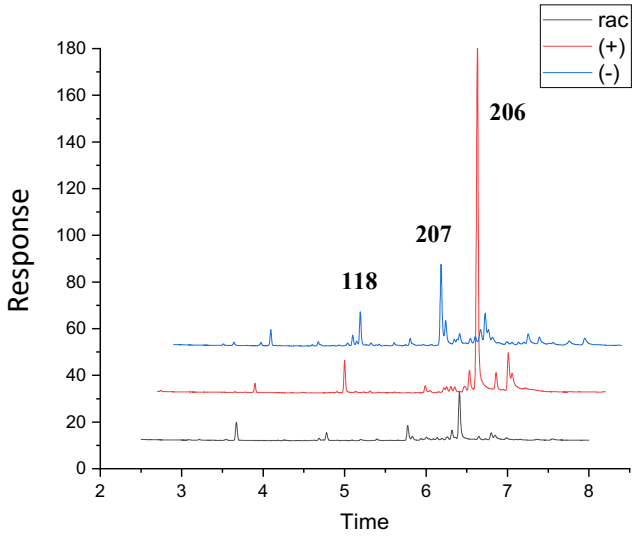

Figure 2.11. GC traces of reaction between RK/T269G and (±)-, (+)-, and (–)-**117** displaying reactivity profiles for the separate enantiomers.

When the analogous reaction was carried out with (–)-**117**, GC and TLC analysis revealed that a number of products were generated, of which none corresponded to the

benzylic alcohol and the diol seen previously. Attempted purification of the complex product mixture by column chromatography was partially successful and just the major product was separated in sufficient quantity and purity to allow full characterisation. NMR spectroscopic analysis of this fraction suggested it to be a vicinal diol (oxidation at the benzylic and homobenzylic sites), and NOESY correlations confirmed the relative stereochemistry, with oxidation occuring equatorially at both sites as before (***Figure 2.12***). The specific rotation was recorded: $[\alpha]_D^{25}$ –49.1 (*c* 0.07, $CHCl_3$).

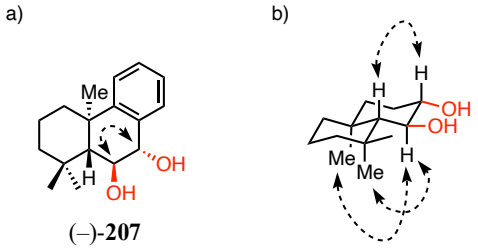

(–)-**207**

Figure 2.12. a) Structure of the major metabolite generated by the reaction between (–)-**117** and RK/T269G showing relevant COSY correlation confirming the vicinal nature of the diol; b) relevant NOESY correlations used in determining the relative stereochemistry, the aromatic ring has been omitted for clarity.

Overall, these studies assigned the absolute stereochemistry of (+)-**206** derived from reaction with (±)-**117** and gave further insight regarding the parallel kinetic resolution in question (***Scheme 2.20***). With this enzyme, selective oxidation of the natural enantiomer (+)-**117** occurred, while poorly-selective hydroxylation of (–)-**117** was observed. These results, alongside the information gained from the RK/T260G study, indicate the natural enantiomer to be more effectively oriented in the active site of both RK/T260G and RK/T269G leading to increased reactivity as well as selectivity.

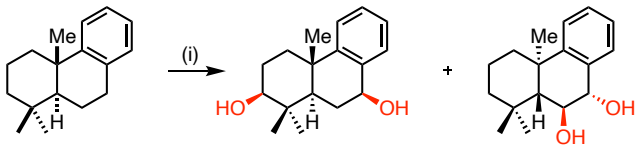

(±)-**117** (+)-**206** (–)-**207**

Scheme 2.20. Overall parallel kinetic resolution reaction. Conditions: 2 µM RK/T269G, 1mM (±)-**117**, 100 mM glucose, 2 U/mL GDH, 80 µM $NADP^+$, 5 mM methyl-β-cyclodextrin, 200 mM phosphate buffer 20 °C, 24 h, 16% (+)-**206**.

2.5.2.2 Determination of enantiomeric excess

As with benzylic alcohol (+)-**118**, in order to assess the synthetic utility of this biocatalytic oxidation, a determination of the enantiomeric excess was sought. In this case a high % ee was expected due to the dioxygenation process proceeding, in principle, through two sequential kinetic resolutions. Mosher's ester derivatisation was deemed to be unsuitable for this substrate due to the previously observed lack of reactivity at the benzylic alcohol alongside possible analytical difficulties arising from partial conversion of diol (+)-**206** to the diester.

As before, application of a chiral-phase SFC technique required a racemic reference sample and a biomimetic process was envisaged, based on the previously used $RuCl_3 \cdot xH_2O$-catalysed carbocyclisation (***Scheme 2.21***).

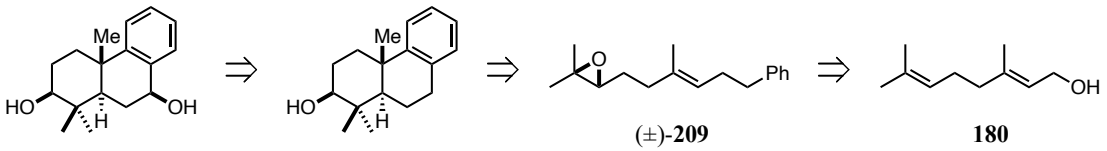

(±)-**206** (±)-**208** (±)-**209** **180**

Scheme 2.21. Retrosynthetic analysis for diol (±)-**206**.

The route began with epoxidation of phosphate **184**, which was already available in large quantity, giving epoxide (±)-**209** (***Scheme 2.22***). The subsequent Grignard addition of benzylmagnesium chloride produced allylic chloride (±)-**211**, perhaps through complexation of the Grignard reagent or $MgCl_2$ to the epoxide facilitating the release of chloride ion as a nucleophile.

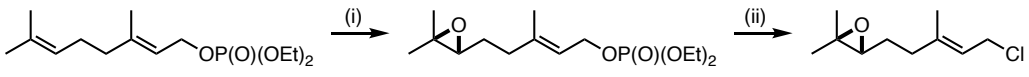

184 (±)-**210** (±)-**211**

Scheme 2.22. Unsuccessful Grignard addition into phosphate (±)-**210**. Reagents and conditions: (i) *m*-CPBA, CH_2Cl_2, 0 °C to RT, 20 h, 68%; (ii) Mg, BnCl, THF, –78 °C to RT, 16 h, 52 %.

The alternative route shown in ***Scheme 2.23*** proceeded instead via acetate **171**, with epoxidation and copper-catalysed Grignard addition delivering the cyclisation substrate

(±)-**209**.[167–169] Tetraphenylphosphonium tetrafluoroborate ($TPP^+BF_4^-$) mediated cyclisation generated alcohol (±)-**208** in reasonable yield.[170] This reaction, carried out in HFIP, is proposed to proceed through epoxide opening to form a 3°-carbocation intermediate, facilitated by the high ionic strength of the polar reaction medium, and subsequent cyclisation to form the desired tricycle. An oxidation/reduction sequence, analogous to that used in the synthesis of (±)-**118** (***Scheme 2.19***), installed the benzylic alcohol and produced (±)-**206**.[171] Although the overall yield of (±)-**206** was poor, the product was only needed as an analytical standard and so no effort was made to optimise the sequence.

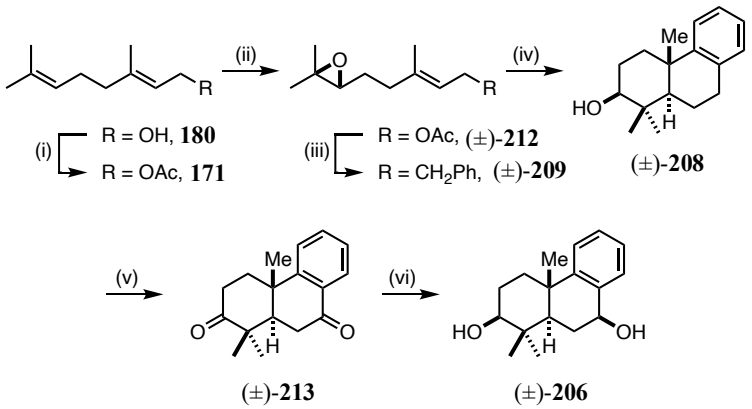

Scheme 2.23. Synthesis of racemic (±)-**206** as a reference for chiral phase SFC analysis. Reagents and conditions: (i)Ac_2O, py, DMAP, 0 °C to RT, 2 h, 82%; (ii) *m*-CPBA, CH_2Cl_2, 0 °C to RT, 24 h, 54%; (iii), Mg, BnCl, Li_2CuCl_4, THF, 0 °C, 2 h , 94%; (iv) $TPP^+BF_4^-$, HFIP, RT, 5 mins, 54%; (v) CrO_3, AcOH, RT, 24 h, 21%; (vi) $LiAlH_4$, THF, 0 °C to RT, 15 h, 17%.

The conditions used previously for the analytical separation of (±)-**118** were succesful, and in the case of (±)-**206** an excellent % ee value of 96% was determined (***Figure 2.13***). This analysis was kindly carried out at the Oxford Suzhou Centre for Advanced Research by Yang Cao. That this value was higher than that of alcohol (+)-**118** (85%) may be a reflection of this stepwise reaction providing at least two opportunities for kinetic resolution.

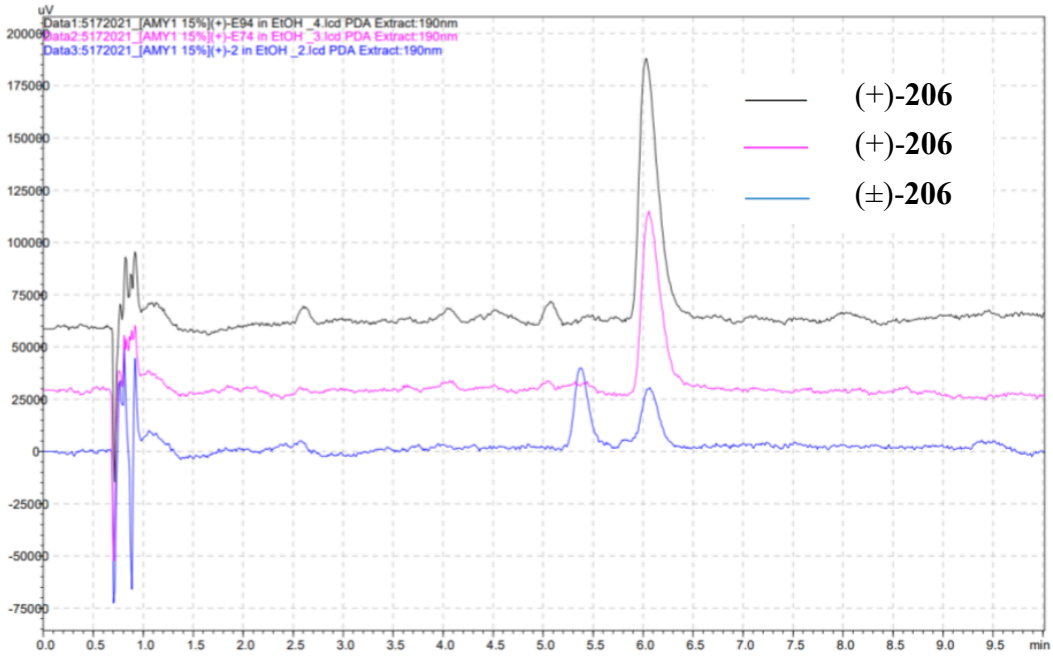

Figure 2.13. Overlaid SFC-PDA chromatogram showing separation of (±)-**206** allowing determination of (+)-**206** %ee for two different samples. Two different samples of (+)-**206** were analysed for reliability purposes.

2.5.2.3 Time course reactions

Because the kinetic resolution had successfully generated a relatively complex compound in excellent % ee, further insight into the kinetic resolution process was sought via a time course study. For this, reactions were carried out with the same ratio of substrate, enzyme, cofactors, and methyl-β-cyclodextrin as in the screening and scale-up reactions, but at a smaller, 25 mL, scale.

The curves in ***Graph 2.2*** clearly illustrate the kinetic resolution process. The left-hand curve shows the reaction of (±)-**117** with RK/T269G which proceeded to approximately 80% conversion by GC over 12 h, with (+)-**206** produced in ~40% yield. The graph on the right-hand side shows the analogous reaction using (+)-**117** as the substrate and in this case (+)-**117** was converted to ~80% of (+)-**206**, double that of the racemic reaction. Interestingly the concentration of intermediate alcohol (+)-**118** in the reaction mixture remains at a steady state during the course of the reaction. The apparent

presence of a small amount of benzylic alcohol at t = 0 is due to a small delay period between initiating the reaction and quenching an aliquot.

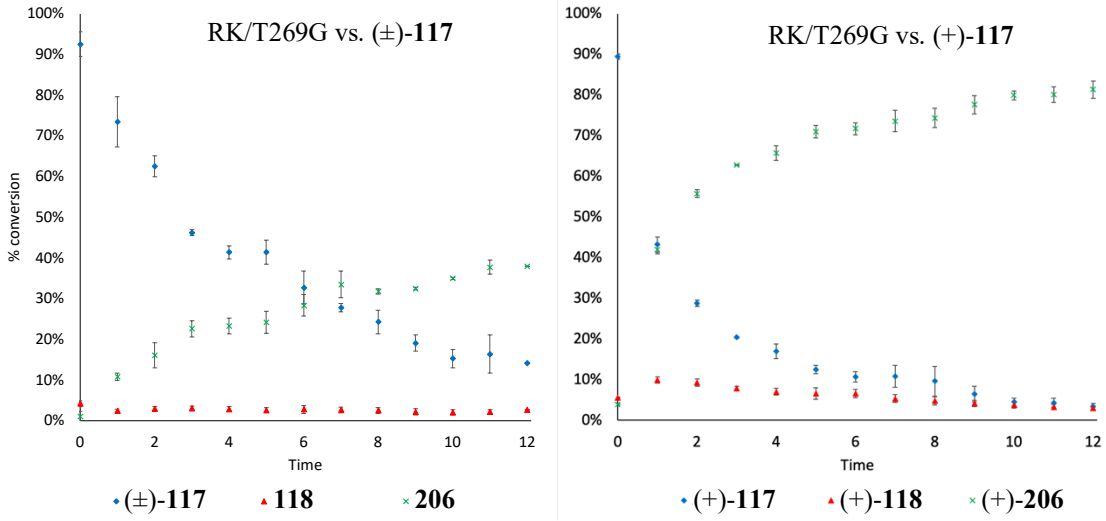

Graph 2.2. Time course data for the reaction between (±)-**117** and RK/T269G, and (+)-**117** and RK/T269G.

2.5.2.4 UV binding assay

A UV binding titration assay was carried out in order to investigate the origins of the parallel kinetic resolution process. This assay probes substrate binding through observing the change in spin state, from low spin to high spin, of the ferric heme centre upon loss of the axial water ligand. From this experiment, the pure enantiomers of **117** were found to bind to a similar extent, with the K_d for both measuring ~14 μM, whilst the racemic substrate bound slightly more strongly with a K_d value of ~12 μM (***Graph 2.3***).

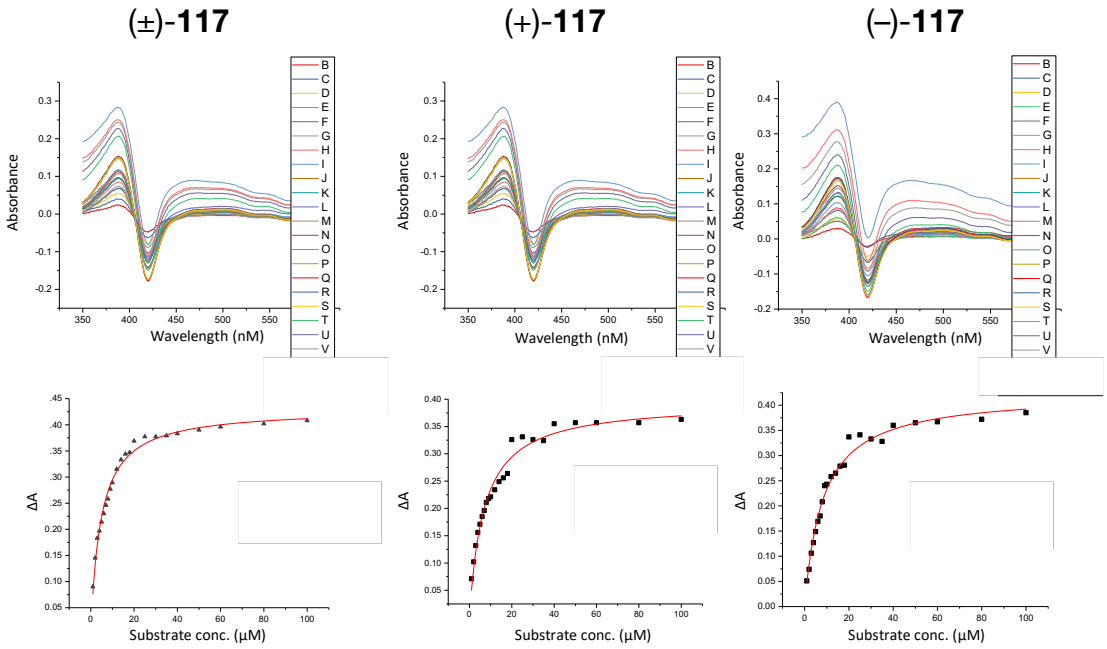

Graph 2.3. Plots showing data from the UV binding titration assay. Raw data are shown above while graphs of peak-to-trough difference are displayed below. Data for (±)-**117** are displayed on the left, (+)-**117** in the middle, and (–)-**117** on the right.

From this it appears that the differing behaviour of the separate enantiomers within the active site is not caused by a difference in binding, and instead must be ascribed to contrasting orientations dictated by substrate-residue interactions. Following this reasoning, a brief computational docking study was carried out; however, a lack of clear substrate-enzyme interactions, as a result of the hydrocarbon substrate, led to unreliable results which showed no correlation with the experimental metabolite profile and therefore further study was aborted.

2.5.2.5 Large scale reactions

As with the RK/T260G study, large scale reactions were evaluated but, here also, gaining reactivity proved to be difficult. Conversion was not observed at a 1000:1 substrate:enzyme ratio at either 100 mL or 400 mL scales; decreasing the substrate:enzyme ratio to 500:1 also failed to induce reactivity, and carrying out the reaction in a round-bottom flask to aid mass transfer did not improve matters. The influence of substrate solubility on conversion was investigated by submitting (±)-**118**

to the 400 mL reaction conditions but, again, poor conversion was observed. Finally, (±)-**117** was added into the reaction as a solution in DMSO; here, a substrate:enzyme ratio of 1000:1 was used with a substrate concentration of 1 mM in 400 mL. This reaction led to a much-improved conversion and (+)-**206** was isolated in 18% yield, reproducing the 16% yield observed at a preparative scale; starting material was recovered in a 3% yield. This significant increase in the efficiency of the reaction upon the switch from ethanol to dimethyl sulfoxide was unexpected and might suggest the former solvent either poisons the enzyme or participates in oxidation reactions itself; however, ethanol behaves well as a solvent at smaller scale and so it may be more likely that dimethyl sulfoxide is more able to solubilise the hydrocarbon substrate.

With the two major metabolites (ii) and (xiv) characterised as (+)-**118** and (+)-**206** respectively, and the nature of the kinetic resolution in each case established, attention was turned to the minor oxidised products. Although less synthetically useful, as these were often generated within mixtures and in smaller amounts, a more complete knowledge of the activity profile of these $P450_{BM3}$ variants towards carbocycle (±)-**117** is crucial to add to our overall understanding of how mutant CYP102A1 enzymes could be used as synthetic biocatalysts more generally.

2.5.3 Characterisation of GVQ metabolites

$P450_{BM3}$ variant GVQ was selected to further probe the metabolites of these reactions because it displayed 100% conversion of starting material and generated a number of novel metabolites. Preparative-scale reactions were carried out with the (±)-**117** as before and, after three hours GC analysis showed complete consumption of the starting material. Four products were isolated as pure compounds following column chromatography, one of which was benzylic alcohol (+)-**118**.

The least polar compound was determined to be a ketone due to diagnostic resonances

in the ^{1}H NMR spectrum at 2.28 (dd, J = 13.5, 2.0 Hz) and 2.38 ppm (d, J = 13.5 Hz,) corresponding to the diastereotopic carbonyl α-protons, as well as at 2.55 (d, J = 13.0 Hz) and 2.90–3.06 ppm (m); this, and the specific rotation, $[\alpha]_{D}^{25}$ –98.3 (c 0.06, $CHCl_3$), allowed this product's characterisation as ketone (–)-**214** (***Scheme 2.24***, see §**2.5.3.1** for assignment of the absolute stereochemistry.). This assignment was backed up by MS, and a clear carbonyl stretch at 1711 cm^{-1} in the IR spectrum was also observed. A compound incorporating the ketone functionality described above as well as a benzylic alcohol was also isolated, assigned as (–)-**215**, ***Scheme 2.24***. Finally, a diol was isolated that differed from both diols (+)-**206** and (–)-**207**. COSY correlations and the specific rotation, $[\alpha]_{D}^{25}$ +8.7 (c 0.15, $CHCl_3$), identified this compound as diol (+)-**216**, the relative stereochemistry being determined by coupling constants and NOESY correlations (***Scheme 2.24***, see §**2.5.3.1** for assignment of absolute stereochemistry.). A sixth metabolite, which was unable to be isolated as a pure sample, was observed and tentatively characterised as alcohol **217**.

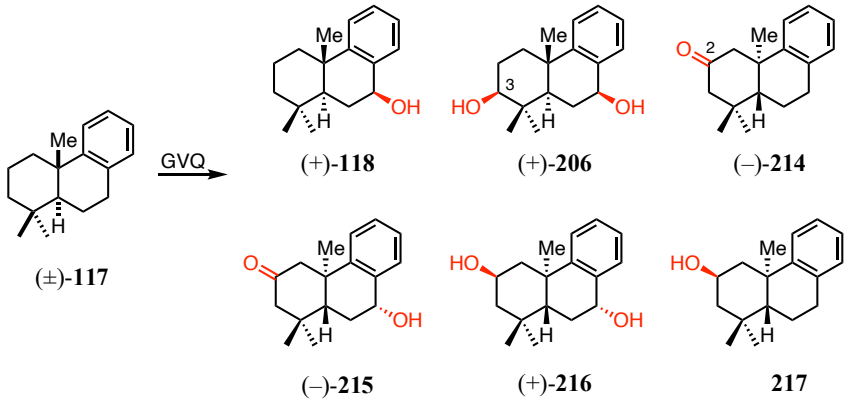

Scheme 2.24. Overall kinetic resolution reaction between (±)-**117** and GVQ. Conditions: 2 μM GVQ, 1mM (±)-**117**, 100 mM glucose, 2 U/mL GDH, 80 μM $NADP^+$, 5 mM methyl-β-cyclodextrin, 200 mM phosphate buffer 20 °C, 24 h, 5% (+)-**118**, 15% (+)-**206**, 5% (–)-**214**, 6% (–)-**215**, 4% (+)-**216**

2.5.3.1 Kinetic resolution

As with the RK/T260G and RK/T269G studies, reactions were carried out with the separate substrate enantiomers with the goal of further understanding the kinetic

resolution and to assign the absolute stereochemistry of the products. GC analysis of the reaction between (+)-**117** and GVQ revealed that both benzylic alcohol (+)-**118** and diol (+)-**206** were produced. The reaction between (–)-**117** and GVQ led to a more complex mixture of products which necessitated purification by column chromatography from which ketone (–)-**214**, keto-alcohol (–)-**215**, and diol (+)-**216** were isolated, allowing assignment of their absolute configurations. A fourth isolated compound was tentatively assigned as alcohol **217**, although impurities and the small amount available precluded unequivocal characterisation of this compound.

This product profile is worthy of comment. First, the regiochemistry of enzymatic oxidation usually relies on substrate orientation within the binding pocket, but benzylic hydroxylation is seen in the majority of compounds isolated. This preference for the electronically-activated benzylic position is likely a consequence of a lack of strong binding within the active site with consequent multiple available binding modes allowing preferential reaction of the most activated C–H bond. Second, the high activity of the CYP102A1 variants, in particular GVQ, towards (±)-**117** allows multiple oxidation reactions through re-entry of hydroxylated products into the active site. Finally, neglecting benzylic oxidation, it is clear that (+)-**117** shows a preference for C3 oxidation, while reaction with (–)-**117** favours C2 oxidation (***Scheme 2.24***. All this confirms by experiment our intuitive expectation that the different enantiomers have contrasting behaviour within the active site.

2.5.4 Characterisation of RK/Q403P metabolites

The screening results (***Graph 2.1***) indicated that variant RK/Q403P produced novel, uncommon product (iv) as a major metabolite and so attention turned to its isolation and characterisation. An analogous scale-up study to those described above was undertaken; however, after three hours and complete consumption of the starting material, the

product profile at preparative scale did not resemble that of the screening reaction. In fact, a similar result to the reaction with variant RK/T269G was observed.

Four fractions were separated by column chromatography, of which the major was characterised as (+)-**206** (38%), and the spectroscopic data for one of the minor metabolites corresponded to those observed for (–)-**207**. The other two fractions comprised inseparable mixtures of hydroxylated products that were not characterised.

The behaviour of the separate enantiomers under the biocatalytic conditions with RK Q403P also mirrored that found with variant RK/T269G. GC analysis of the reaction between (+)-**117** and RK/Q403P showed the major metabolite to be (+)-**206**, with some (+)-**118** also produced. Analysis of the product profile from (–)-**117** revealed a complex mixture of products. These results indicated the operation of a parallel kinetic resolution, as with the RK/T269G reaction (***Scheme 2.25***).

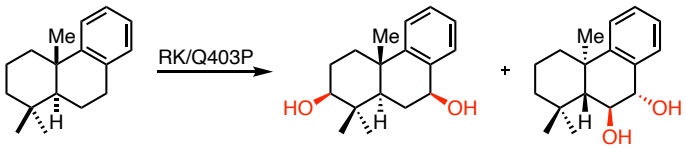

(±)-**117** (+)-**206** (–)-**207**

Scheme 2.25. Overall parallel kinetic resolution reaction with RK Q403P.Conditions: 2 µM RK/Q403P, 1mM (±)-**117**, 100 mM glucose, 2 U/mL GDH, 80 µM $NADP^+$, 5 mM methyl-β-cyclodextrin, 200 mM phosphate buffer 20 °C, 24 h, 38% (+)-**206**, 3% (–)-**207**.

2.5.5 Characterisation of RK/A328G metabolites

With the major metabolites having already been characterised, analysis of the metabolites from reaction with RK/A328G was straightforward. Upon reaction with (±)-**117**, the reactivity profile was observed to be similar to those of RK/T269G and RK/Q403P. Diol (+)-**206** was generated in 45% yield, and reaction with the separate enantiomers confirmed this to be produced solely from (+)-**117**. Diol (–)-**207** was also isolated, in 12% yield, and as before this was formed from reaction with (–)-**117** (***Scheme 2.26***).

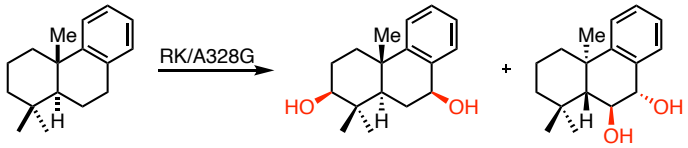

(±)-**117** (+)-**206** (–)-**207**

Scheme 2.26. Overall parallel kinetic resolution reaction with RK/A328G. Conditions: 2 µM RK/A328G, 1mM (±)-**117**, 100 mM glucose, 2 U/mL GDH, 80 µM $NADP^+$, 5 mM methyl-β-cyclodextrin, 200 mM phosphate buffer 20 °C, 24 h, 45% (+)-**206**, 12% (–)-**207**.

With the major metabolites characterised and the reactivity profiles investigated for representative CYP02A1 variants, the application of $P450_{BM3}$ enzymes in a target synthesis was investigated.

2.6 Attempted synthesis of margocin 218

With an understanding of the broad range of metabolites produced through reaction of (±)-**117** with the CYP102A1 variants tested, a simple natural product synthesis was attempted. Due to the established scalability and in-depth analysis undertaken on the RK/T269G system, the diketone margocin (**218**) was targeted in order to probe the utility of $P450_{BM3}$ enzymes in natural product synthesis and shed light on whether model systems are useful for the investigation of CYP102A1 reactivity (***Figure 2.14***).

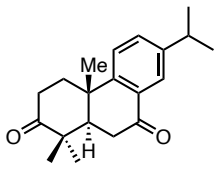

218

Figure 2.14. Structure of the diketone natural product target margocin **218**.

A similar synthetic sequence to that employed in the formation of (±)-**117** was proposed (***Scheme 2.27***), with incorporation of the isopropyl group in the starting material and a similar Grignard addition projected to generate diene **221**. Cyclisation using Sames' $RuCl_3 \cdot xH_2O$/AgOTf system would again be utilised, with the proposal that steric clashing in the chair-like transition state would favour the desired regiochemistry.

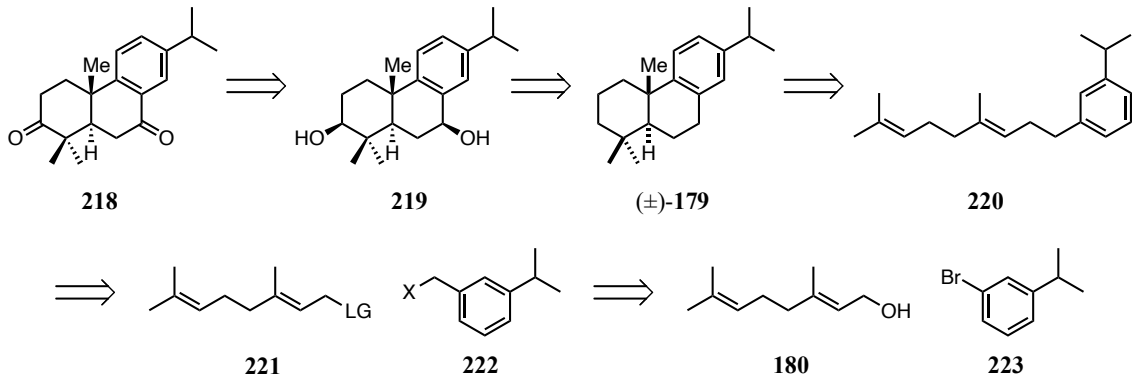

218 **219** (±)-**179** **220** **221** **222** **180** **223**

Scheme 2.27. Retrosynthetic analysis for margocin **218** making use of the previously employed $RuCl_3.xH_2O$ catalysation cascade reported by Sames.

The forward synthesis began with lithiation of bromide **223** and subsequent trapping with DMF to form aldehyde **224**. Aldehyde reduction to **225** and $SOCl_2$ mediated chlorination followed by the previously investigated Grignard addition into geranyl phosphate **184** gave the desired cyclisation precursor diene **220** in 28% overall yield. From diene **220**, the $RuCl_3 \cdot xH_2O$-mediated cyclisation was attempted and it was found that the steric interaction between the *i*-Pr group and the diene side-chain was insufficient to force the reaction to proceed cleanly to the desired product and a 5:2 product ratio in favour of the desired regioisomer resulted. A sample of the major isomer (68 mg, 46%) was obtained through careful column chromatography (***Scheme 2.28***).

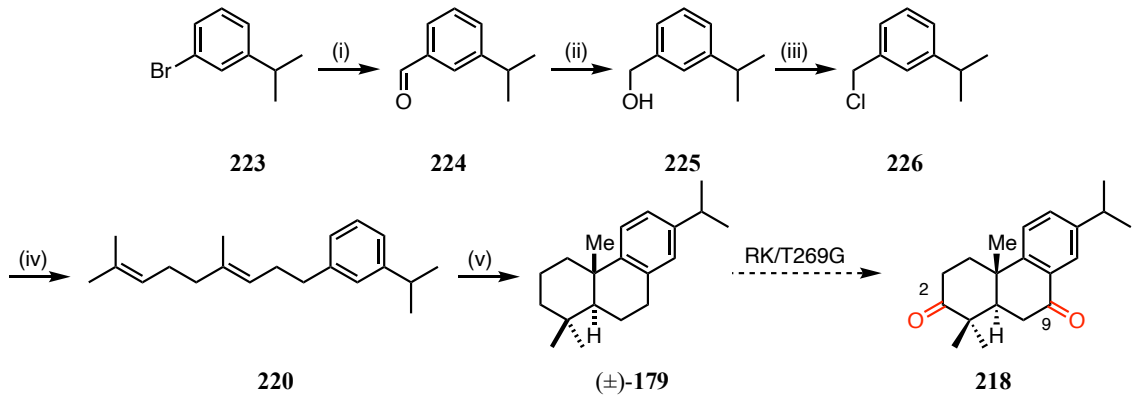

223 **224** **225** **226** **220** (±)-**179** **218**

Scheme 2.28. Synthesis of tricycle (±)-**179** followed by attempted oxidation using CYP102A1 variant RK/T269G. Reagents and conditions: (i) *n*-BuLi, DMF, THF, –78 °C, 1 h, 89%; (ii) $NaBH_4$, MeOH, 0 °C, 2 h , 74%; (iii) $SOCl_2$, py, PhMe, 80 °C, 4 h , 82%; (iv) geranyl phosphate, Mg, THF, –78 °C to RT, 24 h, 45%; (v) $RuCl_3 \cdot xH_2O$, AgOTf, DCE, 60 °C, 4 h, 46%.

Tricycle (±)-**179** was then submitted to enzymatic hydroxylation with RK/T269G in an attempt to oxidise the desired positions (C-2 and C-9) based on the precedent established by the analogous oxidation of tricycle (±)-**117** (§**2.5.2**). From this reaction, a highly complex crude mixture of oxidation products was observed by GC, NMR spectroscopy, and TLC analysis. Some partially-separated fractions were obtained by column chromatography but NMR analysis was not useful in determining their structures due to the presence of impurities coupled with the small amount of material obtained. It was proposed that the additional benzylic site in isopropylated tricycle (±)-**179** was responsible for the large array of metabolites as this theoretically doubles the number of possible oxidation products from the dominant benzylic hydroxylation pathway. This result highlights the high sensitivity of the active site topology towards substrate structure which, in this context, represents a limitation of the application of CYP102A1 enzymes as off-the-shelf oxidation catalysts by extrapolation from reactivity demonstrated in simple model systems.

2.7 Conclusions and future work

Despite the non-selective hydroxylation of tricycle (±)-**179**, this study demonstrates the potential utility of CYP102A1 enzymes in oxidising natural product cores and establishes that kinetic resolution not only occurs but can be harnessed to produce metabolites in excellent enantiomeric excess (***Table 2.4***).

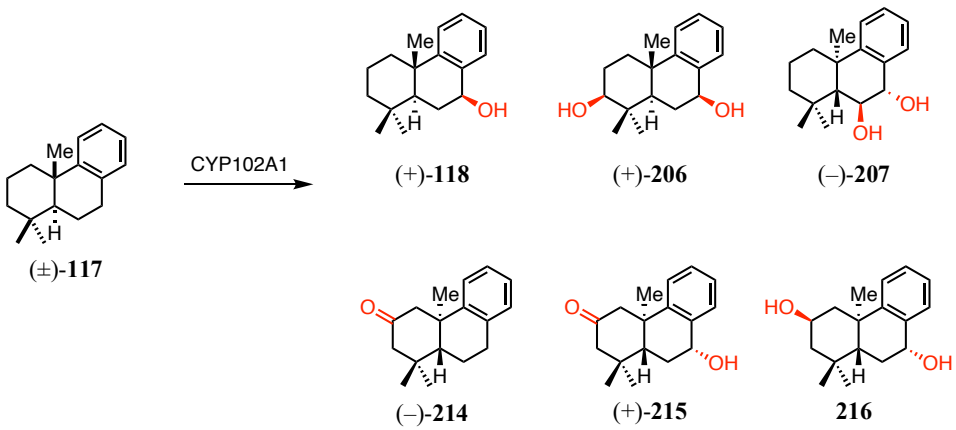

Table 2.4. Overall metabolite profile from catalytic oxidations of (±)-**117** by CYP102A1 variants.

Entry	Variant	(+)-**118** (% ee)	(+)-**206** (% ee)	(–)-**207**	(–)-**214**	(–)-**215**	(+)-**216**
1	RK/T260G	22% (85%)	-	-	-	-	-
2	RK/T269G	-	16% (96%)	-	-	-	-
3	RK/Q403P	-	38%	3%	-	-	-
4	GVQ	5%	15%	-	5%	6%	4%
5	RK/A328G	-	45%	12%	-	-	-

In order to increase the utility of these processes, future work should focus on their scalability. Historically biocatalysis using P450 enzymes has proved inefficient, with enzyme instability and poor expression levels in *E. coli* often to blame; however, recently process engineering efforts, including whole cell reactions, aeration, and pH control have begun to be used with some success.[172]

Additionally, further screening of CYP102A1 variants would expand the metabolite profile and inform which mutations are responsible for reactivity and selectivity. Although the brief computational study in this work proved uninformative, higher level computational studies may aid in understanding the reaction through the substrate binding mode and could inform the design of second-generation enzyme variants with improved conversion and site- and stereoselectivity.

3 Hydroxylation of an eleuthoside synthetic intermediate

3.1 Background

Eleutherobin (**227**), first isolated by Fenical *et al*. in 1995 from a rare alcyonacean thought to be *Eleutherobia albiflora*, is a glycosylated diterpenoid displaying potent cytotoxicity against a variety of cancer cell lines.[173] Classified as an eleuthoside, alongside natural products such as sarcodictyins A–F (A, **230**; B, **231)**, valdivones A (**232**) and B (**233**) and eleuthosides A (**228**) and B (**229**),[174–176] it functions in a biologically similar way to paclitaxel (***Figure 3.1***); that is, through inhibition of the disassembly of microtubules which suppresses cell proliferation.[177,178]

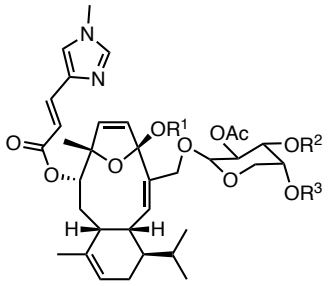

227 eleutherobin: R^1 = Me, R^2 = H, R^3 = H
228 eleuthoside A: R^1 = H, R^2 = Ac, R^3 = H
229 eleuthoside B: R^1 = H, R^2 = H, R^3 = Ac

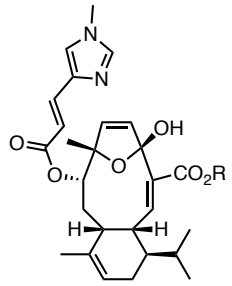

230 sarcodictyin A: R = Me
231 sarcodictyin B: R = Et

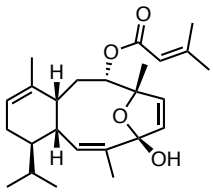

232 valvidone A

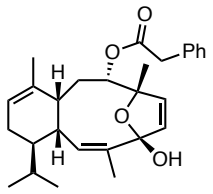

233 valvidone B

Figure 3.1. Structure of eleutherobin (**227**) and related eleuthosides.

3.1.1 Microtubule structure, function, and microtubule stabilising agents

Microtubules, formed through the polymerisation of a heterodimer consisting of α- and β-tubulin, constitute part of the cytoskeleton of eukaryotic cells and are involved in a number of important processes within the cell: maintenance of cell structure, signaling, intracellular transport processes including the movement of macromolecular assemblies,

vesicles and mitochondria, and, importantly in this context, mitosis.[179] The role of microtubules in mitosis, which stems from their involvement in the formation of mitotic spindles, has led to significant interest as a target for cancer therapy.[180]

Structurally consisting of long, thread-like, tubes, the α-tubulin and β-tubulin dimers form microtubules through a nucleation-elongation mechanism; initially, relatively slow oligomerisation of the dimer in a polar head-to-tail fashion generates a short microtubule 'nucleus' comprised of protofilaments, and subsequent elongation through reversible incorporation of tubulin dimers yields the complete microtubule. The cylindrical microtubule wall is composed of 13 parallel protofilaments arranged in a helical structure with a 12 nm pitch. The pitch, combined with the 8 nm longitudinal repeat between dimer subunits, generates a discontinuity in the microtubule wall known as the lattice seam (***Figure 3.2***).[181]

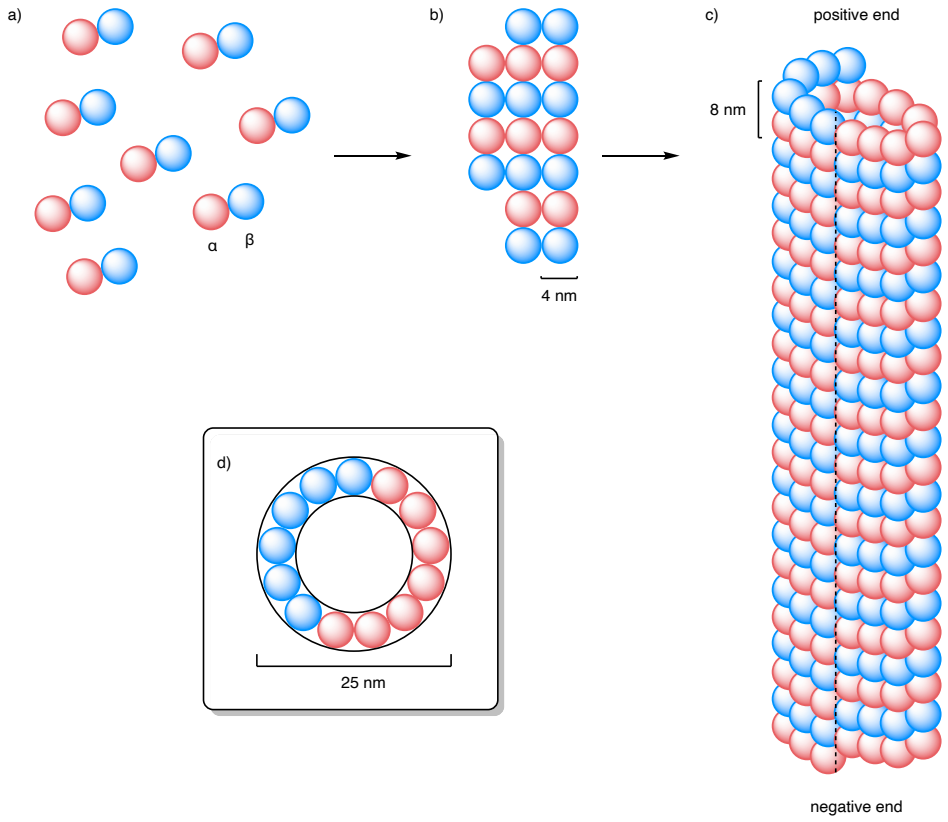

Figure 3.2. Polymerisation of α- and β-tubulin into microtubules. a) α- and β-tubulin heterodimers; b) microtubule 'nucleus' composed of three protofilaments; c) microtubule, dashed line denotes the lattice seam; d) cross-section of microtubule.

Microtubules exist within the cytoplasm in a highly dynamic state; constant addition of tubulin dimers resulting in lengthening is accompanied by shortening through rapid depolymerisation. The ends of the microtubule structure are not equivalent; the terminus bearing an exposed α-tubulin protein is known as the negative end whilst the opposite end, carrying a β-tubulin sub-unit, is termed the positive end and, although dynamic elongation and shortening occurs at both positive and negative ends of the microtubule, these processes take place more rapidly at the positive, β-tubulin, end (***Figure 3.3***).

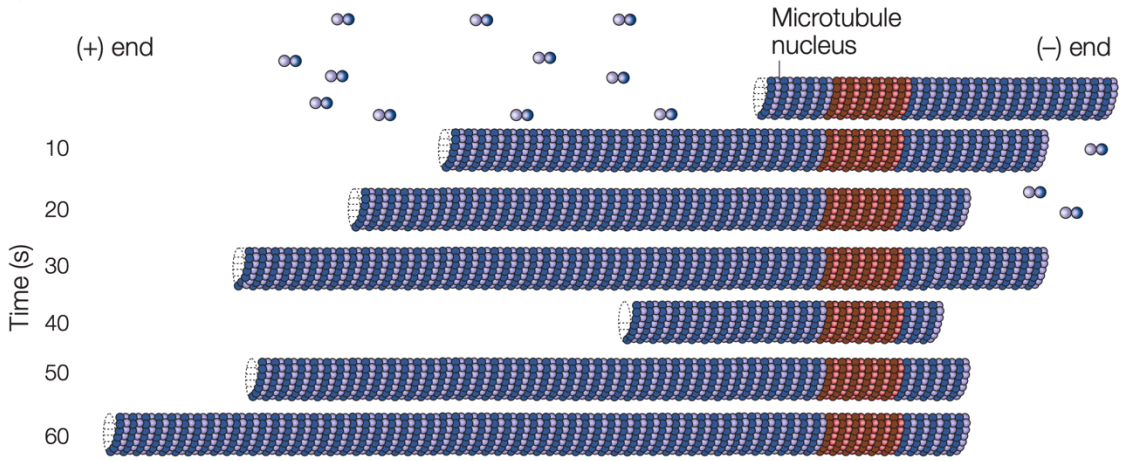

Figure 3.3. Change in the length of a microtubule over time, both lengthening and shortening occur to a greater extent at the positive end. Image adapted from Jordan and Wilson, 2004.[182]

The dynamic instability of these metastable microtubules, which results in stochastic switching between lengthening and shrinking phases both *in vitro* and *in vivo*, arises from differing modes of GTP binding and hydrolysis displayed by the α- and β-tubulin subunits. Each of the two tubulin monomers binds one molecule of GTP; binding at α-tubulin occurs at the N-site and is non-exchangeable whereas GTP binds to β-tubulin at the E-site, which is exchangeable. Polymerisation requires that, upon association with the growing end of the microtubule, the free dimer contains a molecule of GTP at its E-site; the exchangeable GTP is rapidly hydrolysed to GDP and inorganic phosphate and, once formed, this GDP is non-exchangeable while the β-tubulin remains embedded in

the polymer. The need for exchangeable GTP to be present for elongation to occur regulates the dynamics of microtubule polymerisation, and, in particular, the presence of a single layer of GTP at the positive end, termed the GTP cap, dictates whether the microtubule will grow or shrink (***Figure 3.4***).[183]

The GTP cap, then, can be used to explain the unstable behaviour of microtubules; tubulin-GTP exists in a "straight" conformation which allows association to form protofilaments and subsequently microtubules.[184] Elongation requires hydrolysis to tubulin-GDP, and this changes the conformation of the dimer to a "curved" form which imparts strain into the polymer; however, despite the increase in strain disfavouring the polymerised state, the dimer remains embedded within the polymer if the GTP cap persists at the positive end, and lengthening continues. If, however, stochastic loss of the GTP cap occurs, the unstable inner GDP dimers depolymerise leading to shortening (***Figure 3.4***). Transition from the shortening phase to the growth phase is termed "rescue", while the opposite process is called "catastrophe"; complementary to these phases is "treadmilling", a process which involves elongation at one end accompanied by shortening at the other end.[185]

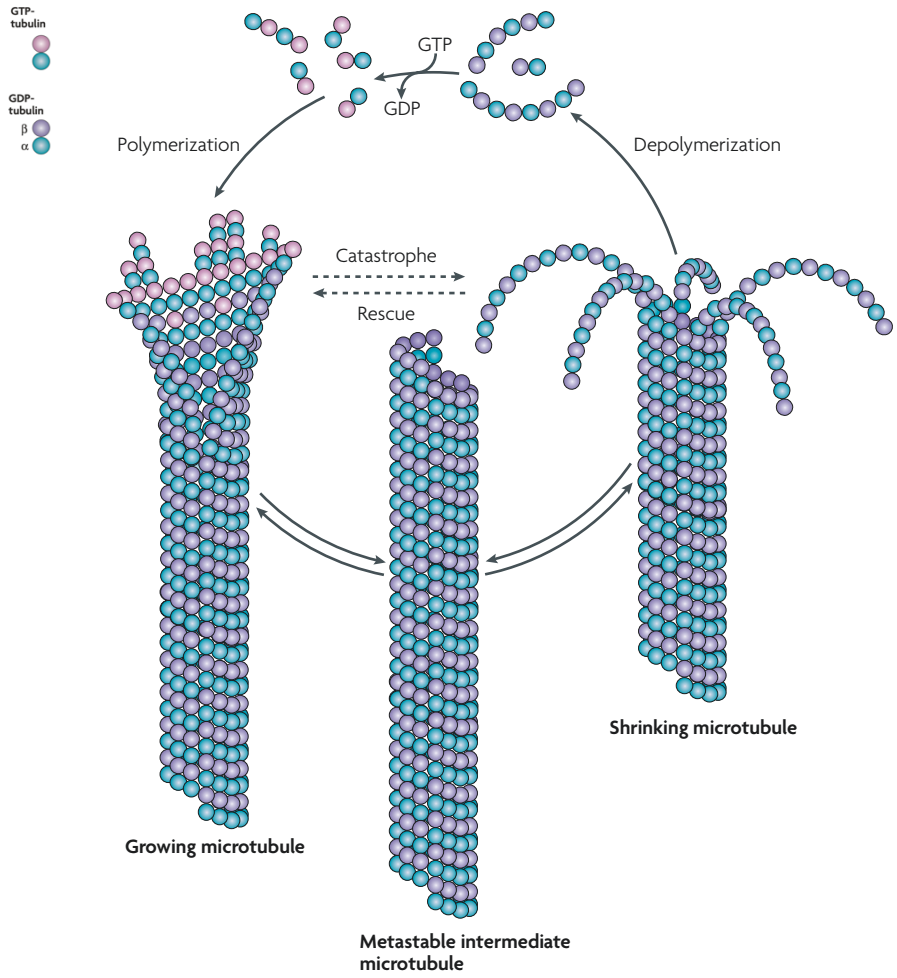

Figure 3.4. Microtubule formation-depolymerisation cycle displaying GTP cap on growing microtubule and lack of GTP cap on shrinking microtubule. Image adapted from Akhmanova and Steinmetz, 2008.[179]

Microtubules are required for all stages of mitosis and therefore microtubule dynamics are crucial to this process. If the inherent instability of microtubules can be overcome, mitosis is unable to take place and eventually the cell undergoes apoptosis. Microtubules, then, present themselves as an ideal target to prevent tumour growth and, importantly, offer selectivity for cancer cells over normal cells; cancer cells divide more often than normal cells and therefore more frequently pass through a cell phase sensitive to mitotic poisons.[182]

Natural products which act as microtubule stabilising agents are known; the most notable, paclitaxel (Taxol®, **234**), was the first to be identified,[186,187] but the epothilone class of natural products, for example epothilone B (**235**), which bind the taxol site on

β-tubulin,[188,189] as well as eleutherobin (**227**) and related natural products,[190] also exhibit similar biological activity (***Figure 3.5***).

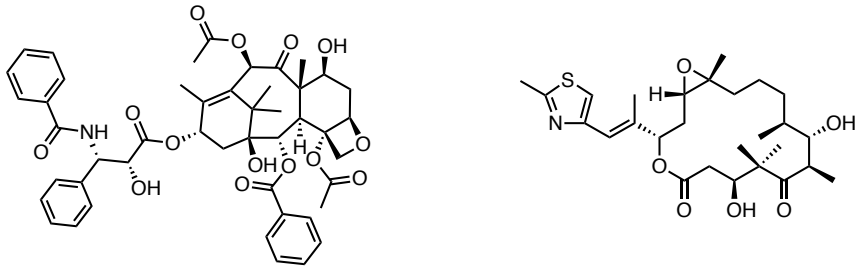

234 paclitaxel **235** epothilone

Figure 3.5. Structures of other microtubule stabilising agents.

3.1.2 Total syntheses

The behavior of eleutherobin (**227**) as a microtubule stabilising agent (MSA), coupled with its chemical complexity and novel tricyclic architecture, has made it an attractive target for synthetic chemists and, to date, total syntheses have been completed by Danishefsky and Nicolaou.[129,191,192]

Danishefsky's route, making use of a chiral pool approach to gain access to the complex stereochemical elements present within eleutherobin (**227**), began with (*R*)-(–)-phellandrene (**236**). Initial [2+2] cycloaddition, through treatment of **236** with dichloroketene formed *in situ*, generated bicyclic ketone **237**, which was elaborated to furan **239**. Key Nozaki–Hiyama–Kishi and Achmatowitz reactions allowed access to **242**, and subsequent rearrangement furnished the eleutherobin core (**244**). Further steps, including a novel oxycarboglycosidation to install the arabinose moiety, generated eleutherobin (**227**) in ~0.4% overall yield (***Scheme 3.1***).

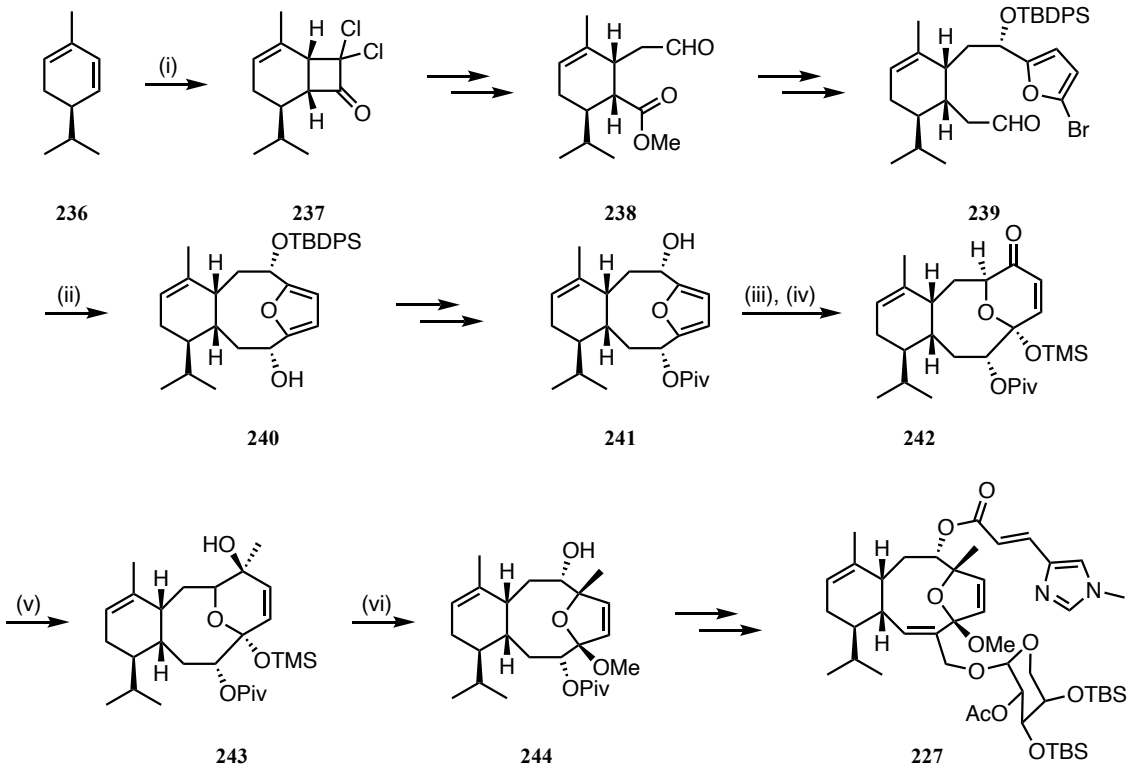

Scheme 3.1. Key steps in Danishefsky's synthesis of eleutherobin (**227**). Conditions: (i) trichloroacetyl chloride, Zn, Et_2O, sonication, 0 °C, 65%; (ii) $CrCl_2$, $NiCl_2$, DMF, 74%; (iii) DMDO/acetone, CH_2Cl_2,– 78 °C, 94%; (iv) TMSOTf, 2,6-lutidine, CH_2Cl_2, –78 °C, 92%; (v) MeLi, THF, – 78 °C, 42%; (vi) *p*-TSA·H_2O, MeOH, RT, 90%.

Nicolaou's approach, again employing the chiral pool to introduce the complex stereochemical elements, allowed not only synthesis of eleutherobin (**227**), but also eleuthosides A (**228**) and B (**229**) *via* derivatisation of eleutherobin (**227**) itself, as well as sarcodictyins A (**230**) and B (**231**) through elaboration of intermediate **248**.[193–195]

The route began with a modified procedure developed by Trost for the synthesis of (–)-dendrobine which transformed (+)-carvone into aldehyde **246**.[196] Subsequent elaboration to key intermediate **248**, followed by glycosidation and acetylide addition generated fused ring system **249**. Installation of the arabinose moiety was accomplished through reaction with trichloroacetimidate **255**, and subsequent reduction of the alkyne functionality placed the tertiary alcohol in a favourable position for ring closure to form the eleutherobin core **252**. A series of protections and deprotections, alongside

incorporation of the methyluraconic acid side chain, furnished eleutherobin **227** in 4.3% overall yield (***Scheme 3.2***).

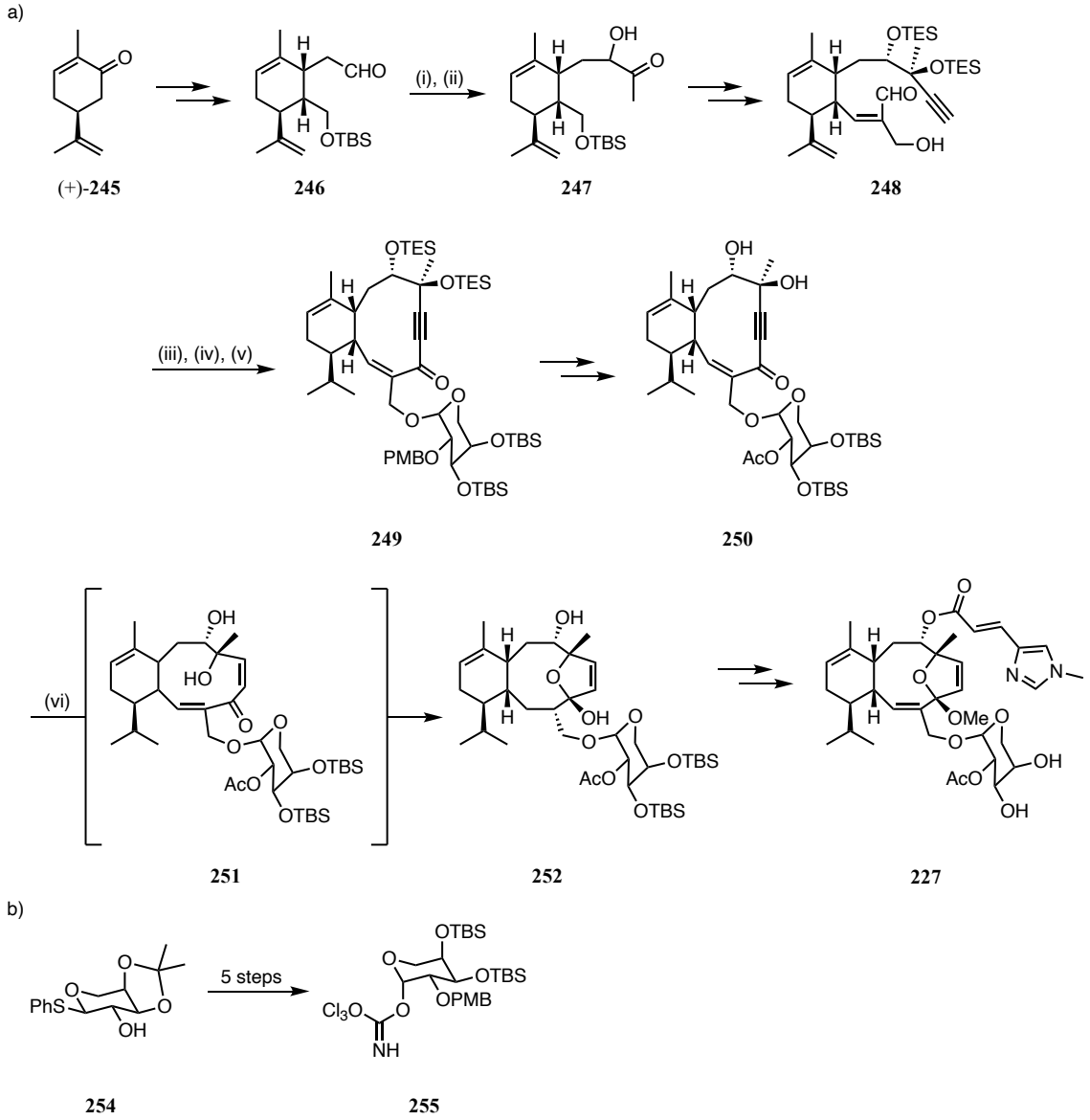

Scheme 3.2. a) Nicolaou's synthesis of eleutherobin. Conditions: (i) Ethyl vinyl ether, *t*-BuLi, THF, –78 °C to 40 °C; (ii) conc. H_2SO_4, Et_2O, 82% for two steps; (iii) **255**, TMSOTf, dioxane/PhMe, 0 °C, 75%; (iv) LiHMDS, THF, –30 °C; (v) DMP, $NaHCO_3$, pyridine, CH_2Cl_2, 0 °C, 93% for two steps; (vi) H_2, Lindlar catalyst, PhMe; b) preparation of trichloroacetimidate **255**.

3.1.3 Formal syntheses

A number of formal syntheses have been completed, intercepting both Danishefsky's and Nicolau's total synthetic routes.

Gennari *et al*. reported the synthesis of tricycle **259**, an intermediate in Danishefsky's route.[197] Beginning with (–)-carvone ((–)-**245**), and utilising a key ring-closing

metathesis to form the C5-C6 double bond, **259** was produced in 24 steps (***Scheme 3.3***).[198] The *E*-selective ring-closing metathesis was probed *via* computational methods, and the preference for the *E*-alkene was found to be a consequence of the increased stability of the *trans*-ruthenocyclobutane intermediate relative to the *cis*-ruthenocyclobutane analogue;[199] this preference proved to be inconsequential as isomerisation to the *Z*-alkene proceeded spontaneously in $CDCl_3$.

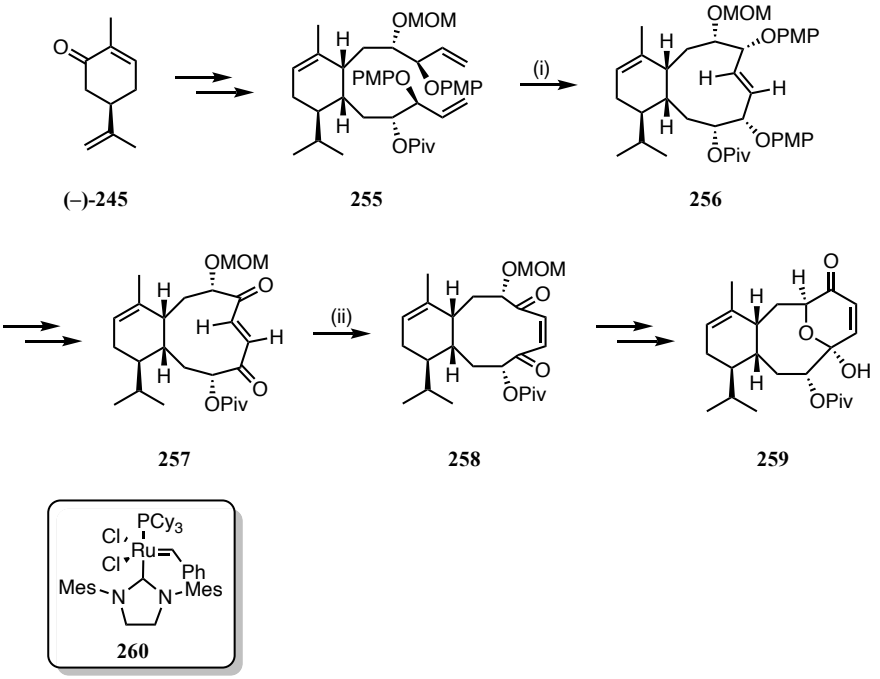

Scheme 3.3. Formal synthesis of eleutherobin reported by Gennari involving key ring-closing metathesis step. Conditions: (i) **260**, PhMe, 110 °C, 64%; (ii) $CDCl_3$.

Another formal route to eleutherobin, intercepting Nicolaou's synthesis, was reported by Metz *et al*. in 2003.[200] A key intramolecular Diels–Alder (IMDA) reaction, inspired by previous work by both Jung and Kurth,[201,202] yielded bicyclic lactone **265**, which, upon further elaboration, generated alkyne **266** (***Scheme 3.4***).

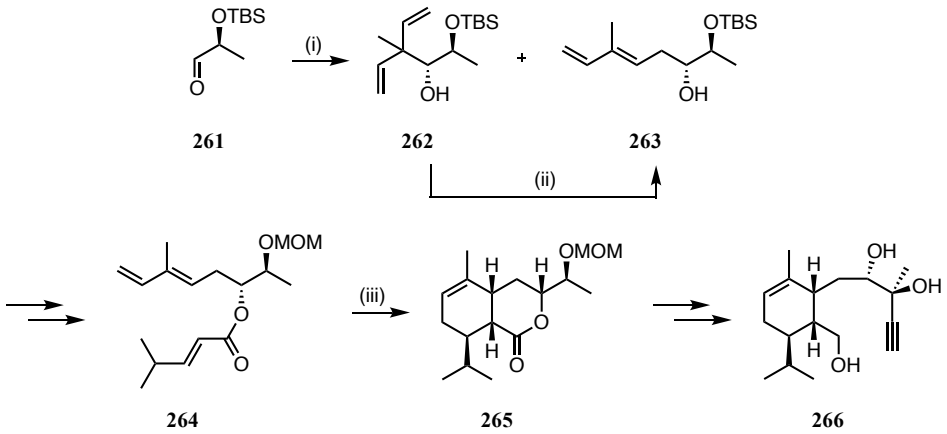

Scheme 3.4. Formal synthesis of eleutherobin *via* Nicolaou's alkyne intermediate. Conditions: (i) 3-methyl-1,4-pentadiene, *n*-BuLi, THF, –78 °C to RT, 40% (**262** + **263**); (ii) NaH, 18-crown-6, THF, 0 °C to RT, 40%; PhMe, BHT, 200 °C, 75%.

Clearly, then, formal synthesis is a valuable tool for the generation of natural products and, on top of building upon the wealth of existing synthetic knowledge, it allows diversification of key intermediates with a view to producing natural product analogues.

3.1.4 Project aims

Previous work within the group has shown bicyclic lactone (±)-**115** to be a good substrate for P450$_{BM3}$ oxidation and one of the metabolites, 2° alcohol **116**, was produced in 36% yield with 64% ee from reaction with variant RT2/IP, revealing that the enzyme was able to discriminate between the two enantiomers present in the reaction (***Scheme 3.5***).[128]

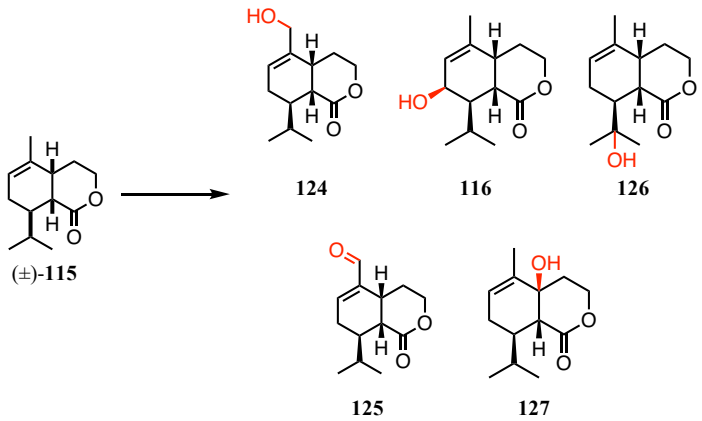

Scheme 3.5. Previously observed metabolite profile in the reaction of bicyclic lactone (±)-**115** with a panel of P450$_{BM3}$ variants. Absolute configurations were unable to be determined.

The potent cytotoxicity of eleutherobin (**227**) towards human cancer cell lines, through microtubule stabilisation (see §**3.1.1**), makes it an attractive target for studies into its use as a chemotherapeutic. Until this point the quantities of eleutherobin (**227**) produced through total and formal syntheses have not been sufficient for a full investigation of its potential as an antitumour agent,[203,204] and medicinal chemical studies into the potency of derivatives have focused around manipulation of the easily accessible side chain components.[205,206] Analogues in which modification of the tricyclic core has been achieved are limited and therefore lactone **115**, which can be further elaborated into aldehyde **238**, an intermediate on Danishefsky's route to eleutherobin (**227**), presents itself as an ideal testbed for investigation of late-stage biocatalytic oxidation.

This project aims to further probe the reactivity of bicyclic lactone **115** towards a panel of $P450_{BM3}$ enzymes, with particular emphasis on kinetic resolution, allowing a reactivity profile to be generated. The metabolites produced have the potential to be elaborated to analogues of eleutherobin (**227**), allowing its biological properties to be further interrogated.

3.2 Synthesis of substrates

In order to adequately probe the metabolite profile and kinetic resolution properties of the $P450_{BM3}$ library, the racemic lactone as well as both separate enantiomers would be required. Bicyclic lactone (±)-**115** is a known compound and so it was thought that the synthesis would proceed smoothly; it was envisaged that the separate enantiomers would be prepared through chemical resolution by aminolysis with a chiral amine, with determination of absolute configuration accomplished through crystallography studies.

3.2.1 Synthesis of the racemate

The racemic lactone had previously been synthesised within the group through an intermolecular Diels–Alder process between alcohol **268** and thioester **270** and so

initially this route was attempted. In this previous work synthesis of the necessary alcohol had been accomplished through an oxy-anion-accelerated [1,3]-sigmatropic shift from 3-methyl-1,4-pentadiene (**267**) (***Scheme 3.6***).

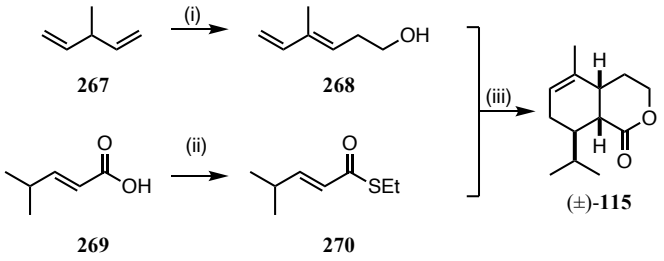

Scheme 3.6. Attempted synthesis of (±)-**115** following literature procedure. Conditions: (i) *n*-BuLi; paraformaldehyde; 18-crown-6, KOTMS, THF, –78 °C to RT, 2 h, 14%; (ii) EtSH, DCC, DMAP, CH_2Cl_2, RT, 24 h, 79%; (iii) Me_2AlCl then *p*-TSA.H_2O, CH_2Cl_2, RT, 41%.

The route began with synthesis of dienyl alcohol **268** through the rearrangement process. Initial test reactions showed formation of alcohol **271**, produced through premature protonation of the lithium alkoxide intermediate (***Scheme 3.7***).

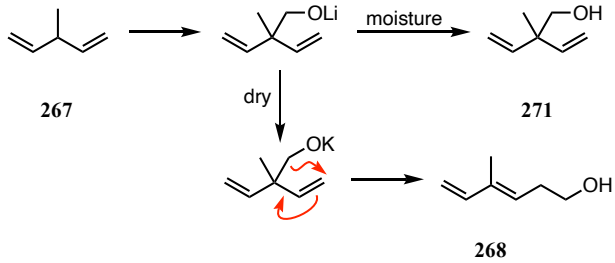

Scheme 3.7. Mechanism of major product formation under moist and dry conditions.

Although rigorous drying of the 18-crown-6 allowed generation of the desired alcohol, purification proved difficult. Isolation of alcohol **268** by bulb-to-bulb distillation was unsuccessful and separation of the crude mixture by column chromatography was unable to furnish **268** in any reasonable yield, with a maximum of 17% achieved. It was clear that another method was needed, especially since the diene starting material **267** is prohibitively expensive for a large-scale synthesis.

Tiglic aldehyde (**272**), a cheaper, more readily available compound, was proposed as a starting material. A combination of three previously reported synthetic steps was carried out beginning with a Horner–Wadsworth–Emmons reaction.[207–209] This furnished

conjugated ester **273** efficiently despite the formation of a small amount of the *Z*-alkene which made purification more difficult. Deconjugation and subsequent $LiAlH_4$ mediated reduction generated the desired alcohol **268** on gram-scale in 66% overall yield. Separately, the preparation of thioester **270** proceeded smoothly on large scale (***Scheme 3.8***).

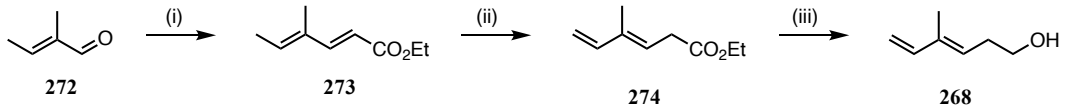

272 **273** **274** **268**

Scheme 3.8. Revised synthesis of dienyl alcohol **268**. Conditions: (i) triethylphosphonoacetate, NaH, THF, 0 °C to RT, 1 h, 87%; (ii) *n*-BuLi, DIPA, DMPU, –78 °C, 4 h, 88%; (iii) $LiAlH_4$, Et_2O, RT, 16 h, 86%.

Formation of the racemic bicyclic lactone ((±)-**115**) following the literature conditions afforded a 41% yield (literature 67%) and, in an attempt to improve the yield, some modifications were attempted (***Table 3.1***).

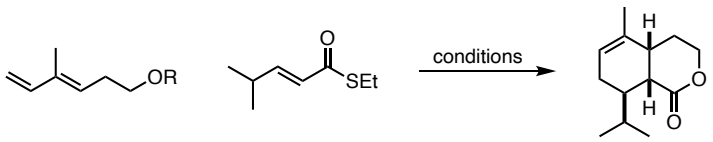

268 R = H
268a R = TES
268b R = TBS

270

(±)-**115**

Table 3.1 Various reaction and work-up conditions attempted to improve yield of the intermolecular Diels–Alder reaction.

Entry	Conditions	Work-up	Yield
1	Me_2AlCl 1 eq., 0.13 M, RT, **268**	Rochelle salt	41%
2	Me_2AlCl 1 eq., CH_2Cl_2 dried over 4 Å molecular sieves, 0.13 M, RT, **268**	Rochelle salt	36%
3	Me_2AlCl 2 eq., 0.13 M, RT, **268**	Rochelle salt	37%
4	Me_2AlCl 2 eq., 0.26 M, 30 °C, **268**	Rochelle salt	22%
5	Me_2AlCl 2 eq., 0.26 M, RT, **268**	Na_2SO_4	20%
6	Me_2AlCl 1.2 eq., 0.13 M, RT, **268**	Rochelle salt, silica	17%
7	Me_2AlCl 1 eq., 0.13 M, RT, **268a**	Rochelle salt	-
8	Me_2AlCl 1 eq., 0.13 M, RT, **268b**	Rochelle salt	-

Initially, it was suspected that moisture within the reaction was reducing the available quantity of the Lewis acid catalyst, Me_2AlCl, but reaction with dichloromethane dried over sieves did not yield the expected results. Despite the superficial appearance that the dry dichloromethane led to a decrease in yield, it was proposed that loss of product during work-up was to blame for the lower yield as the formation of emulsions was problematic throughout the course of this investigation. Neither an increase in the concentration of Lewis acid nor, separately, an increase in the concentration of the reaction as a whole led to an increase in yield (Entries **3** and **4**). Alternative work-up conditions were tested in order to try to avoid emulsion formation, but these were unsuccessful (Entries **5** and **6**). It was theorised that the proton from dienyl alcohol **268**

was interfering with the Me_2AlCl and so variants protected with TES and TBS protecting groups were tested (Entries **7** and **8**). Interestingly, in the case of reaction with the silyl-protected alcohols, no conversion was observed leading to the conclusion that an alkoxyaluminium species may be responsible for the observed reactivity.

An NMR experiment was carried out in order to probe the nature of the reactive intermediates (***Figure 3.6***). The NMR spectra of both alcohol **268** and thioester **270** were recorded and (Spectra **1** and **2**, respectively), then the spectrum of a 1:1 mixture of alcohol and Me_2AlCl was taken (Spectrum **3**). The C**H₂**OH protons, present as a triplet at 3.65 ppm in spectrum **1**, clearly split and shifted to a complex multiplet between 3.8 and 4.4 ppm indicating a bond-forming process between alcohol **268** and the aluminium centre of the Lewis acid. Finally, the spectrum of a 1:1:1 mixture of **268**:**270**:Me_2AlCl was recorded (Spectrum **4**). As was the case in spectrum **3**, a change in the shifts of the alkene protons of the thioester was observed from 6.85 and 6.1 to 6.6 and 6.0 respectively, again indicating the formation an aluminium complex.

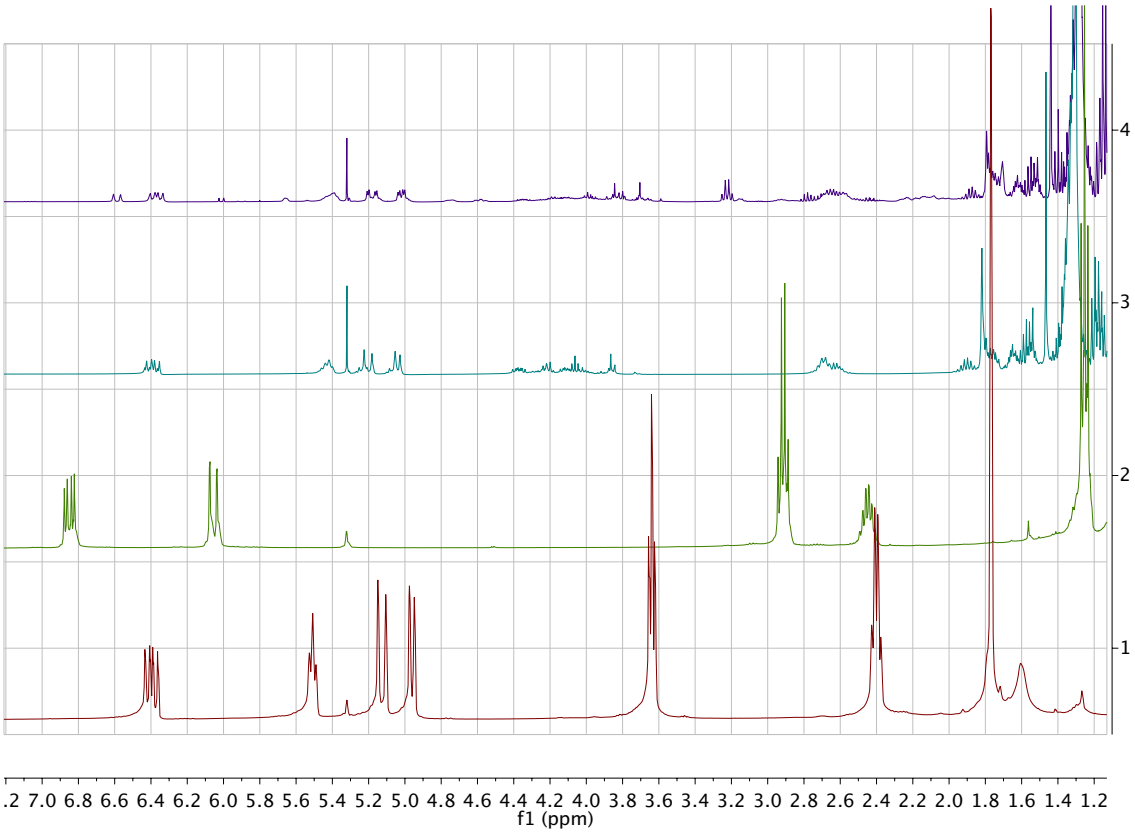

Figure 3.6. NMR spectra recorded to investigate the formation of aluminium intermediates in the Diels–Alder reaction. **1** is the spectrum of pure alcohol **268**, **2** is the spectrum of pure thioester **270**, **3** is the spectrum of a 1:1 mixture of alcohol **268** and Me_2AlCl, and **4** is the spectrum of 1:1:1 mixture of **268**:**270**:Me_2AlCl.

Despite these data giving a better understanding of the reactive intermediates involved in the intermolecular Diels–Alder process, and indeed indicating the potential for the formation of an aluminium complex *in situ* which allows the reaction to progress in an intramolecular sense (**275b**, ***Figure 3.7***), no information was gained to give a clear strategy for improving the yield of the reaction, and so a new route to the lactone was sought.

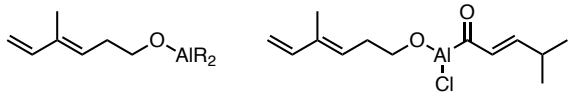

275a **275b**

Figure 3.7. Possible aluminium complexes present within the intermolecular Diels–Alder reaction indicated by changes in certain ^1H NMR shifts.

It was proposed that an intermolecular Diels–Alder (IMDA) process may be better suited to the formation of lactone (±)-**115** and, with this in mind, a previously reported IMDA reaction was attempted.[209]

Esterification of alcohol **268** and 4-methyl-pent-2-enoic acid proceeded smoothly to yield the IMDA precursor, and, making use of a bidentate Lewis acid reported by Taguchi *et al*., the subsequent cycloaddition reaction generated desired lactone (±)-**115** in 75% yield on gram-scale (***Scheme 3.9***).[209]

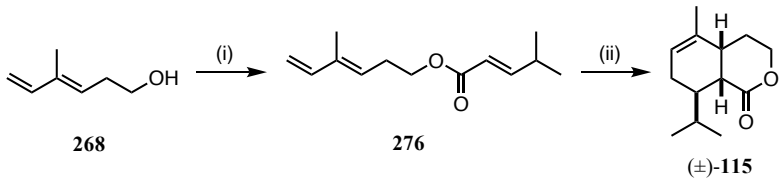

Scheme 3.9. Successful synthesis of bicyclic lactone (±)-**115** utilising key IMDA cyclisation. Conditions: (i) DCC, DMAP, CH_2Cl_2, RT, 24 h, 70%; (ii) $TfNH_2$, Me_2AlCl, DCE, 0 °C to 80 °C, 3 h, 75%.

This unusual catalyst is reported to favour the reactive *cisoid* conformation through coordination with the nitrogen-based ligands, whilst also, like many Lewis acids, lowering the energy of the LUMO allowing improved orbital overlap. The relative stereochemistry of the product, assigned through comparisons with literature data, can be explained through the use of an *endo*-boat transition state (***Figure 3.8***).

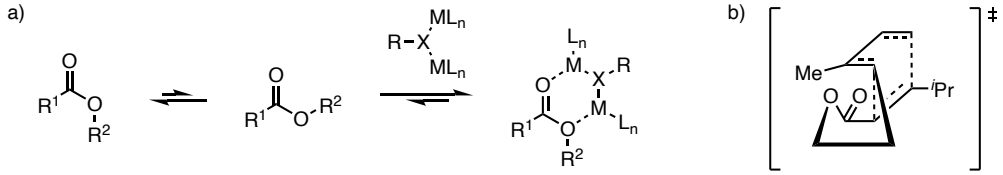

Figure 3.8. a) Stabilisation of reactive *cisoid* conformation by the bidentate Lewis acid; b) *endo*-boat transition state consistent with the observed stereochemistry.

With good quantities of the bicylic lactone (±)-**115** available, attention turned to its chemical resolution.

3.2.2 Chemical resolution of racemic bicyclic lactone

Studies into the resolution of lactone (±)-**115** began with Lewis acid catalysed aminolysis with (*S*)-(–)-α-methylbenzylamine. For this reaction, Ti(O*i*-Pr)$_4$ led to poor

conversion but $AlMe_3$ significantly increased the rate of reaction and purification by column chromatography gave both amide diastereomers in good yield at gram-scale (***Scheme 3.10***).

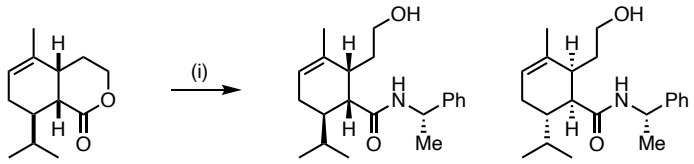

(±)-**115** (+)-**277** (–)-**278**

Scheme 3.10. Successful resolution lactone (±)-**115** *via* aminolysis. Conditions: (i) (*S*)-(–)-α-methylbenzylamine, $AlMe_3$, CH_2Cl_2, 0 °C to RT, 24 h , 81% (+)-**277**, 79% (–)-**278**.

For the ring closure of the separated amide diastereomers back to the lactone enantiomers, a one step process was proposed consisting of amide hydrolysis and *in situ* lactonisation; however, in the event, amide hydrolysis under a range of conditions proved unsuccessful (***Table 3.2***).

Heating under mildly acidic conditions generated an inseparable complex mixture of products (Entry **1**). The use of acidic resin reagents did not improve the outcome (Entries **2** and **3**) and reaction with strong acids, perhaps unsurprisingly, also led to degradation of the amide starting materials (Entries **4** and **5**). Heating under pressurised conditions generated the product in 40% yield, indicating that the presence of acid was the main factor in the failure of the previous reactions, potentially as a consequence of protonation of the electron rich alkene functionality leading to formation of a reactive carbocation.

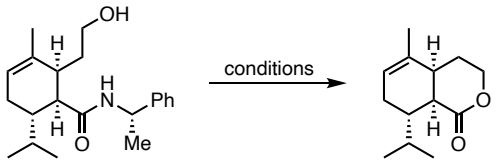

(–)-**278** (+)-**115**

Table 3.2. Conditions attempted for one-step formation of (+)-**115** and (–)-**115**. Test reactions were carried out on (–)-**278**.

Entry	Conditions	Outcome
1	*p*-TSA, PhMe, 110 °C, 1 h	Complex mixture
2	Amberlyst-15, MeOH, THF, reflux, 18 h	No conversion
3	Amberlite IR 120, dioxane, reflux, 6 h	Complex mixture
4	11 M HCl, MeOH, reflux, 24 h	Complex mixture
5	H_2SO_4, dioxane, 80 °C, 6 h	Complex mixture
6	*m*-xylene, 140 °C, sealed tube, 72 h	40%

Although one-step formation of the desired lactone (+)-**115** proved possible, the harsh conditions and poor yield led to further investigation into the ring closure process, with the proposal that either the alcohol may be able to be activated as a leaving group or the amide reactivity towards the pendant alcohol increased. In the event this proved to be the case; reaction of (+)-**277** with $SOCl_2$ generated cyclic imidate (–)-**279** which appeared to be more reactive than amide (–)-**278** (***Scheme 3.11***).

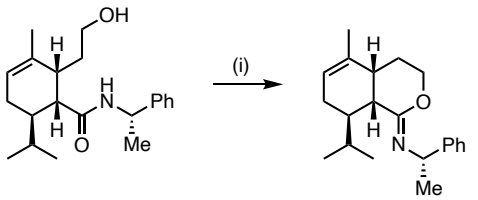

(+)-**277** (–)-**279**

Scheme 3.11. Formation of cyclic imidate (–)-**279** *via* activation of the alcohol with thionyl chloride. Conditions: (i) $SOCl_2$, CH_2Cl_2, RT, 20 mins, 96%.

Hydrolysis of (–)-**279** also proved to be problematic due to a tendency for the imidate to ring-open to the amide starting material (***Table 3.3***).

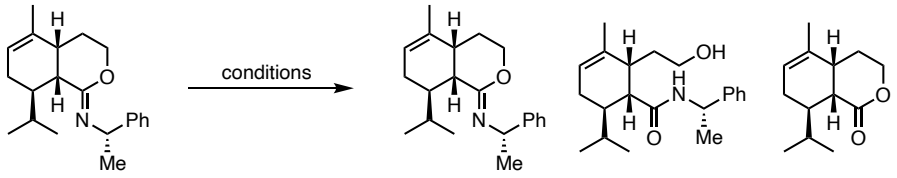

Table 3.3. Attempted conditions for hydrolysis of cyclic imidate (–)-**279**.

Entry	Conditions	(–)-279:(+)-277:(–)-115[a]
1	10% AcOH, THF, 40 °C, 5 h	0:2:1
2	NH_4Cl, MeOH, relux, 7 h	No reaction
3	$Cu(OAc)_2.xH_2O$, THF, H_2O, RT, 4 h	0:5.5:1
4	$Cu(OTf)_2$, THF, H_2O, RT, 72 h	2.5:0:1
5	PhMe, sealed tube, 140 °C, 24 h	0:2:1
6	Oxone, acetone, H_2O, RT, 6 h	Complex mixture
7	Silica gel, CH_2Cl_2, 18 h	0:0:1 (57%)[b]

[a] Estimated by relative peak integrations from ^1H NMR spectra. [b] Isolated yield in brackets.

Neither mild Brønsted acids nor Lewis acids gave positive results, with acetic acid and $Cu(OAc)_2.xH_2O$ favouring reversion reaction to amide (+)-**277** (Entries **1** and **3**), and $Cu(OTf)_2$ generating (–)-**279** as the major product (Entry **4**). Heating in toluene also gave amide (+)-**277** as the major product (Entry **5**) while reaction with Oxone produced an intractable mixture (Entry **6**). Finally, stirring over silica gel was attempted in the hope that the very mildly acidic conditions would allow clean hydrolysis which proved to be the case, forming lactone (–)-**115** in 57% yield; (+)-**115** was generated following the same route in 22% yield.

With a successful route to (±)-**115**, (+)-**115**, and (–)-**115** lactones achieved (***Scheme 3.12***), the synthesis was scaled up to produce sufficient material for biocatalytic testing; however, first it was necessary to determine the absolute configuration of the two enantiomers.

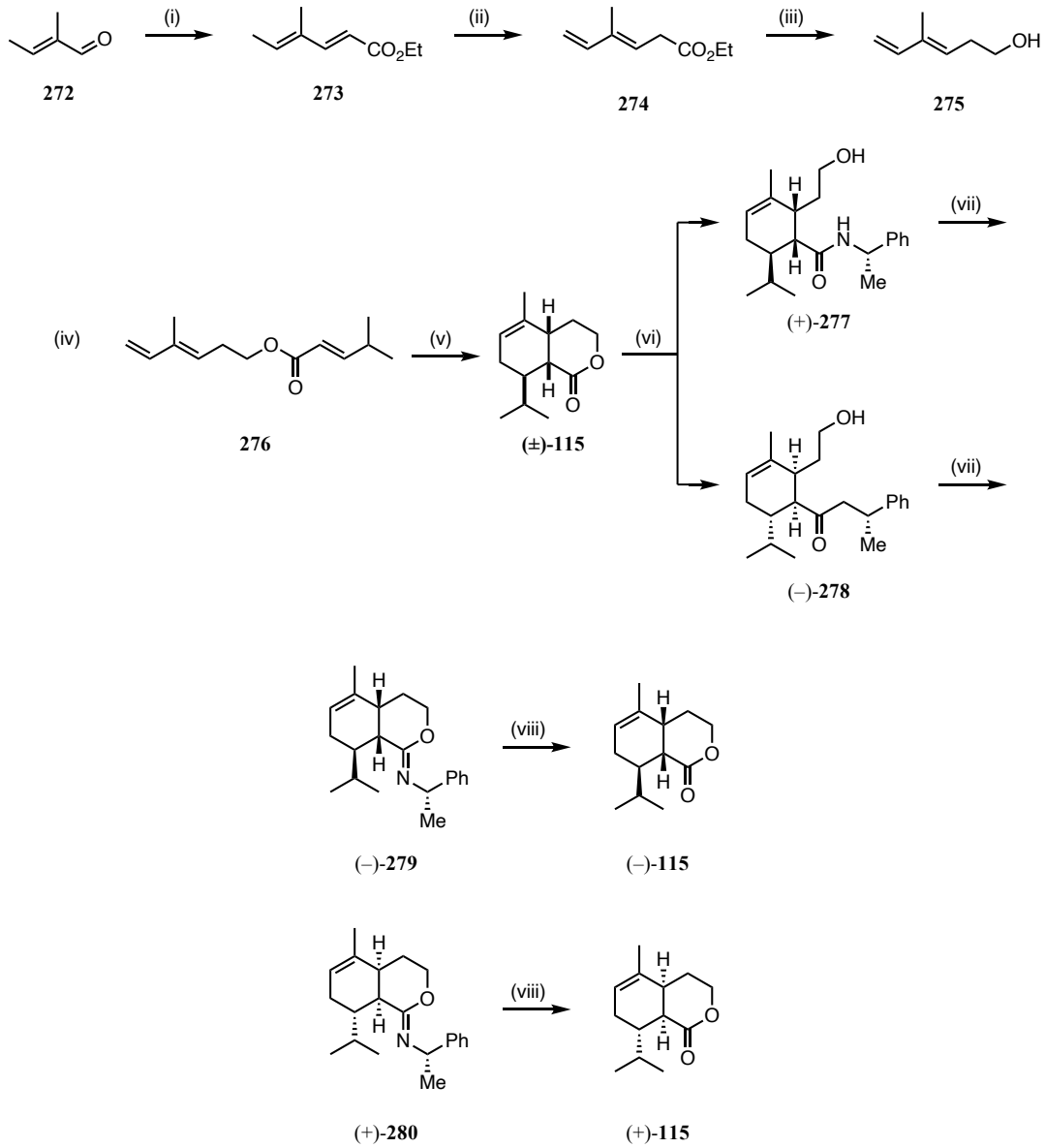

Scheme 3.12. Overall route to both (+)- and (–)-**115** *via* chemical resolution of (±)-**115**. Conditions: (i) triethylphosphonoacetate, NaH, THF, 0 °C to RT, 1 h, 87%; (ii) *n*-BuLi, DIPA, DMPU, –78 °C, 4 h, 88%; (iii) $LiAlH_4$, Et_2O, RT, 16 h, 86%; (iv) DCC, DMAP, CH_2Cl_2, RT, 24 h, 70%; (v) $TfNH_2$, Me_2AlCl, DCE, 0 °C to 80 °C, 3 h, 75%; (vi) (*S*)-(–)-α-methylbenzylamine, $AlMe_3$, CH_2Cl_2, 0 °C to RT, 24 h , 81% (+)-**277**, 79% (–)-**278**; (vii) $SOCl_2$, CH_2Cl_2, RT, 20 mins, (+)-**279** 96%, (–)-**280** 96%; (vii) silica gel, CH_2Cl_2, 18 h; (+)-**115** 22%, (–)-**115** 57%.

3.2.3 Determination of absolute stereochemistry

Amides (+)-**277** and (–)-**278** were obtained as solids; therefore, it was proposed to grow crystalline samples suitable for X-ray crystallographic analysis in order to elucidate the absolute configuration of the amides and, hence, of the lactones (+)- and (–)-**115**. Many crystallisation conditions were tested (evaporation, liquid-liquid diffusion, and vapour diffusion methods from single, binary, and ternary solvent mixtures) but in all cases

where crystallisation occurred, the material was obtained either as a powder or as fine shards.

In the hope of improving the crystallisation properties whilst also incorporating a heavy atom in order to aid the X-ray analysis, the 4-bromobenzoate ester was prepared but all attempted crystallisation conditions failed to produce crystals of sufficiently high quality (***Scheme 3.13***).

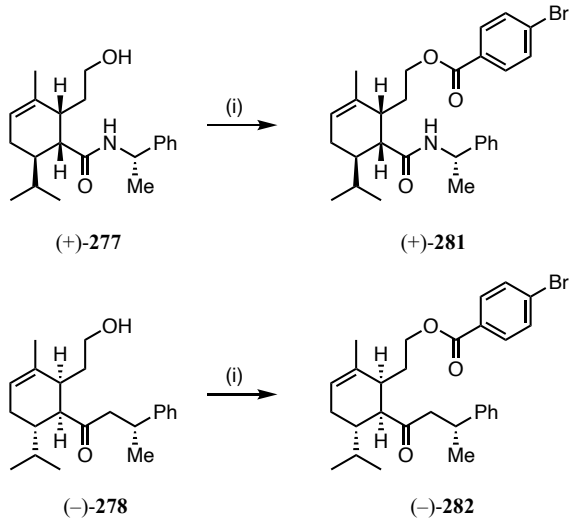

Scheme 3.13. Esterification of (+)-**277** and (–)-**278** in an attempt to improve crystallisation properties. Conditions: 4-bromobenzoic acid, DCC, DMAP, CH_2Cl_2, RT, 3 h, (+)-**281** 89%, (–)-**282** 71%.

In order to avoid the need for crystallisation, chemical correlation was envisaged by converting each lactone, (+)- or (–)-**115**, into a known compound so that comparison with literature data would lead to a determination of absolute configuration. The bicyclic lactone selected for this work was chosen on the basis that it could be used to intercept Danishefky's route to eleutherobin (**227**) and therefore aldehyde (+)-**239**, an intermediate in Danishefsky's synthesis, was proposed as a target.

Lactone (–)-**115** showed low reactivity towards ring-opening with alcohols, probably as a result of the sterically-demanding isopropyl group hindering nucleophilic addition to the ester carbonyl (***Table 3.4***, entries **1** – **5**).

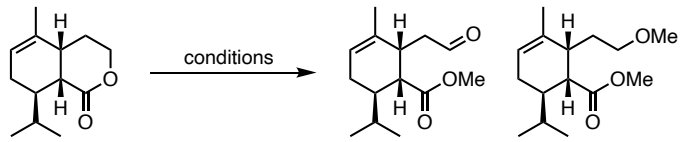

(–)-**115** (+)-**239** **283**

Table 3.4. Conditions tested for formation of aldehyde (+)-**239**. All conditions were tested on (–)-**115**.

Entry	Conditions	Conversion	Product	Yield
1	NaOMe, THF, RT, 2 h	0%	-	-
2	NaOMe, MeOH, 40 °C, 48 h	0%	-	-
3	K_2CO_3, MeOH, 45 °C, 24 h	0%	-	-
4	H_2SO_4, MeOH, 45 °C, 72 h	0%	-	-
5	DMAP, MeOH, 45 °C, 22 h	0%	-	-
6	H_2O_2, $NaHCO_3$; MeI, THF, RT, 2 h	0%	-	-
7	Triton B; MeI, THF, RT, 54 h then PCC, celite, CH_2Cl_2, RT, 3 h	100%	-	-
8	K_2CO_3; MeI, DMF, RT, 3 h then DMP, CH_2Cl_2, 0 °C to RT, 0.5 h	33%	(+)-**239**	33%[a]
9	KOH; MeI (15 eq.), THF, RT, 5 h	66%	**283**	66%[a]
10	KOH, THF then MeI (1.5 eq.), $NaHCO_3$, DMF, RT, 5 h then DMP, CH_2Cl_2, RT, 0.5 h	-	(+)-**239**	43%[b]

[a] Estimated by relative peak integrations from ^{1}H NMR spectra. [b] Isolated yield.

No reactivity was observed for a range of methanolysis conditions and so it was decided to attempt hydrolysis followed by trapping of the so-formed carboxylate with methyl iodide. A three step, one pot, reaction using Triton B for the hydrolysis step was successful in converting the starting lactone; however, oxidation of the crude intermediate was ineffectual in generating the desired aldehyde (***Table 3.4***, entry **7**). The use of K_2CO_3 in DMF allowed partial hydrolysis and, although oxidation with DMP was successful, the slow hydrolysis led to further conditions being tested (***Table 3.4***, entry **8**). Reaction with KOH in THF doubled the amount of hydrolysis product formed;

trapping of the crude with 15 eq. of methyl iodide led to dimethylated compound **283** but, with further optimisation and careful control of reagent and work-up equivalents, aldehyde (+)-**239** was isolated in 46% yield (***Scheme 3.14***).

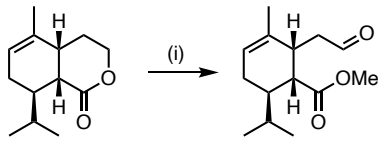

(–)-**115** (+)-**239**

Scheme 3.14. Derivatisation of lactone (–)-**115** to allow elucidation of the absolute stereochemistry. Conditions: KOH, THF, RT, 1 h, then K_2CO_3, MeI, DMF, RT, 1 h, then DMP, $NaHCO_3$, CH_2Cl_2, RT, 0.5 h, 43%.

The specific rotation of aldehyde (+)-**239** was recorded to be +95.7 (*c* 0.55, $CHCl_3$) which, by comparison with the literature value of +59.3 (*c* 0.50, $CHCl_3$), allowed characterisation of the absolute configuration to be the same as the aldehyde derived from (*R*)-(–)-phellandrene in Danishefsky's route. With both lactone enantiomers and the racemate available, biocatalytic hydroxylation studies were initiated.

3.3 $P450_{BM3}$ screening

Initial screening with (±)-**115** was undertaken in order to gain insight into the general reactivity of the lactone towards the $P450_{BM3}$ variants. A panel of 48 enzymes was used which had been developed, with conversion and product selectivity in mind, over a number of iterations in the hydroxylation of cyclic amine systems. Despite the notable differences between these cyclic amines and the lactone, the substrates are of similar molecular weight and overall shape; therefore, it seemed reasonable for the high general reactivity of this P450 panel to translate to the lactone.

Screening reactions were carried out on a 0.5 mL scale in 24-well plates; each well contained: 100 mM glucose, 1.0 mM substrate, 2 U/mL GDH, 80 μM $NADP^+$, 2.0 μM CYP102A1 variant, and 200 mM phosphate buffer. Reactions were performed in an incubator at 20 °C and, in order to preclude any photomediated oxidation pathways,

were run in the dark, with the 24-well plates wrapped in aluminium foil. After 24 h the wells were extracted with ethyl acetate and analysed by GC. In the event, the idea that the high activity of this panel would lead to successful reactions with the lactone was borne out; conversion was generally good, with the majority of variants displaying >60% conversion. From the screening data, four metabolites were commonly formed, two of which were often generated as the major product, and two of which were more frequently present as minor metabolites.

3.4 Preparative scale $P450_{BM3}$ reactions

In order to characterise the metabolites, and to investigate whether kinetic resolution was taking place, scale-up reactions with promising $P450_{BM3}$ variants were carried out. The variants used were chosen based on conversion (> 50%) of starting material and product profile (< four products), keeping in mind that if kinetic resolution was occurring, complete conversion of one enantiomer could be observed at 50% overall conversion in the racemate screening data.

3.4.1 Characterisation of GVQ metabolites

During screening, GVQ displayed excellent conversion to three metabolites and a scale-up reaction (500 μmol substrate, 2 h) allowed isolation and characterisation of all three metabolites. Aldehyde **125** was isolated in 8% yield and was characterised by the diagnostic aldehyde and β-unsaturated proton chemical shifts at 9.37 and 6.95 ppm, respectively. 1° alcohol **124** was isolated in 18% yield with characterisation through the clear disappearance of the allylic methyl peak at 1.66 ppm and the presence of two resonances from diastereotopic protons at 3.90 and 3.99–4.04 ppm. 3° alcohol **126** was isolated in 16% yield and was identified by the singlet resonances at 1.29 and 1.50 ppm for the diastereotopic methyl groups.

The characterisations were confirmed by mass spectrometry and comparison to the literature data (***Scheme 3.15***). The relatively low mass recovery for this reaction was proposed to be caused by loss of material during work-up; however, due to >100% crude mass recovery, this could not be proven categorically.

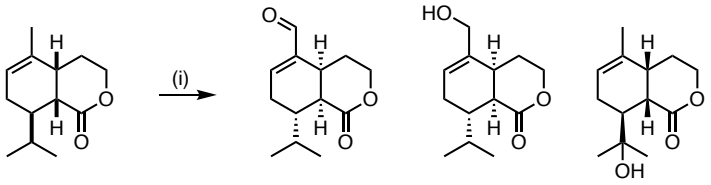

Scheme 3.15. Metabolite profile for the reaction between (±)-**115** and GVQ. Conditions: 2 µM GVQ, 1mM (±)-**115**, 100 mM glucose, 2 U/mL GDH, 80 µM $NADP^+$, 200 mM phosphate buffer, 20 °C, 5 h; 8% (+)-**125**, 18% (+)-**124**, 16% (+)-**126**.

With the structures of the metabolites elucidated, separate screening scale reactions with both pure enantiomers were carried out in order to discover if (+)- and (–)-**115** behaved differently under the reaction conditions due to discrimination within the enzyme catalytic site. In the event, the metabolite profiles of the two reactions, as measured by GC, were different, with (+)-**115** producing only 1° alcohol (+)-**124** and aldehyde (+)-**125** in approximately equal amounts, while (–)-**115** generated 3° alcohol (+)-**126** as the major product with a small amount of (–)-**124**, clearly indicating the separate enantiomers were behaving differently inside the active site (***Graph 3.1***). A small amount of 2° alcohol **124** was observed in the GC trace from the reaction with (±)- and (–)-**115**; however, this was not isolated during the scale-up procedure. These results allowed determination of the absolute configuration of the metabolites.

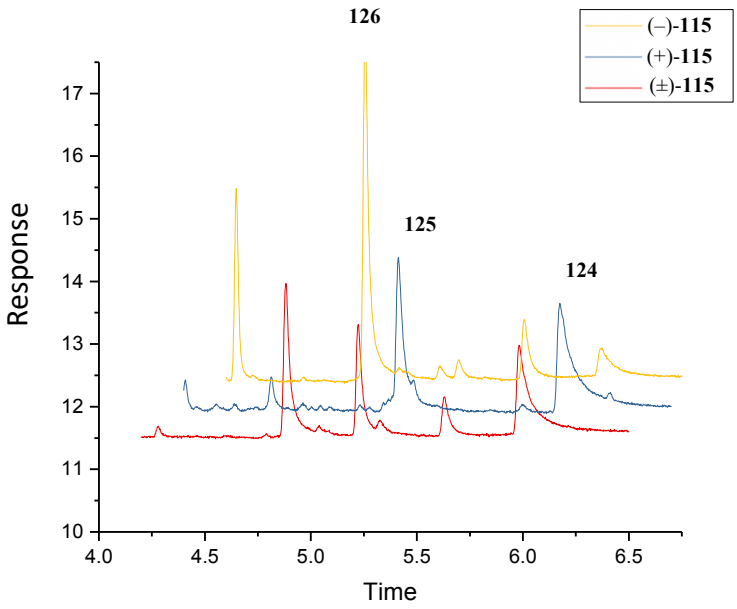

Graph 3.1. Stacked and offset GC traces of the reactions between GVQ and (±)-, (+)-, and (–)-**115** displaying the difference in metabolite profile.

Finally, Mosher's analysis was undertaken to evaluate the enantiomeric excess of the three metabolites from the racemic lactone. Derivatisation of 1° alcohol (+)-**124** and 3° alcohol (+)-**126** was easily carried out as an NMR experiment in CD_2Cl_2; however, it was necessary to reduce aldehyde (+)-**125** for successful Mosher's analysis. DIBAL-H mediated reduction generated a range of products but Luche reduction, with pre-mixing of $NaBH_4$ and $CeCl_3 \cdot 7H_2O$ gave a sufficient quantity of alcohol (+)-**124** for Mosher's esterification. The enantiomeric excess values thus measured were: 18% for 1° alcohol (+)-**124**, 80% for aldehyde (+)-**125**, and 43% for 3° alcohol (+)-**126**.

Reaction with variant KSK19/IA, which had a similar metabolite profile, was next to be probed.

3.4.2 Characterisation of KSK19/I263A metabolites

In order to further understand the kinetic resolution process, a scale-up reaction was carried out with a different $P450_{BM3}$ variant which produced a similar metabolite profile. In this case, the same three metabolites were produced; however, upon Mosher's ester analysis different enantiomeric excess values were obtained: 1° alcohol

(+)-**124** isolated in 27% yield (71% ee), aldehyde (+)-**125** in 17% yield (66% ee), and 3° alcohol (+)-**126** in 12% yield (57% ee) (***Graph 3.2***).

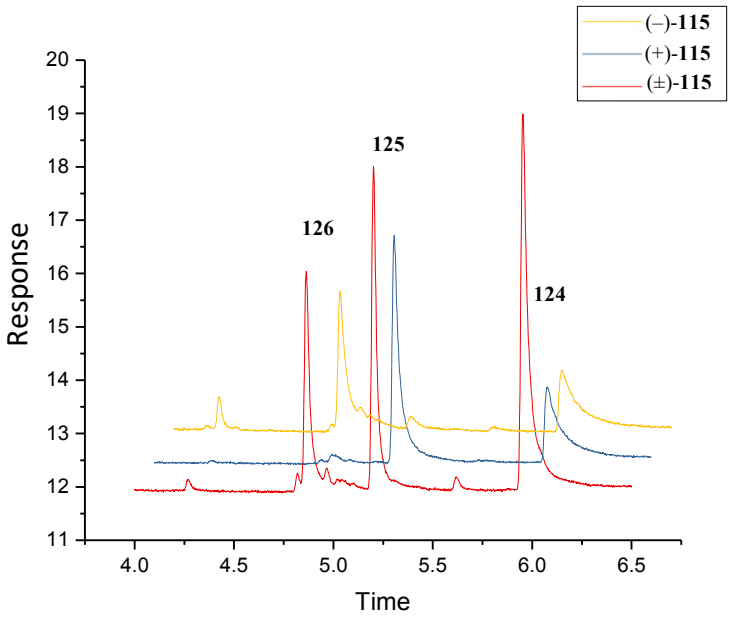

Graph 3.2. Stacked GC traces of the reactions between KSK19/I263A and (±)-, (+)-, and (–)-**115** displaying the difference in metabolite profile; similar relative peak areas for the 1° alcohol peaks in the (+)- and (–)- traces highlights the possibility of competition processes between the two enantiomers in the racemic reaction.

A time course study was carried out. Reaction progress was monitored by GC across a five-hour window which showed that the bulk of the reaction proceeded within the first hour, with the amount of residual (±)-**115** dropping to 2% after three hours and settling at 1% after five hours (***Graph 3.3***). The production of 3° alcohol (+)-**126** behaved as expected, increasing at a decreasing rate over the reaction course; the amounts of 1° alcohol (+)-**124** and aldehyde (+)-**125** rose sharply during the first hour after which time they stayed approximately constant at 46% and 20% respectively. It seems reasonable that the more accessible and chemically-activated nature of the C=C-CH_3 hydrogen atoms was responsible for an increased reaction rate relative to that for oxidation of the $CH(CH_3)_2$ methine hydrogen atom; however, it is interesting to note that conversion from 1° alcohol (+)-**124** to aldehyde (+)-**125** is not observed between hours one and five, possibly due to product inhibition of the enzyme.

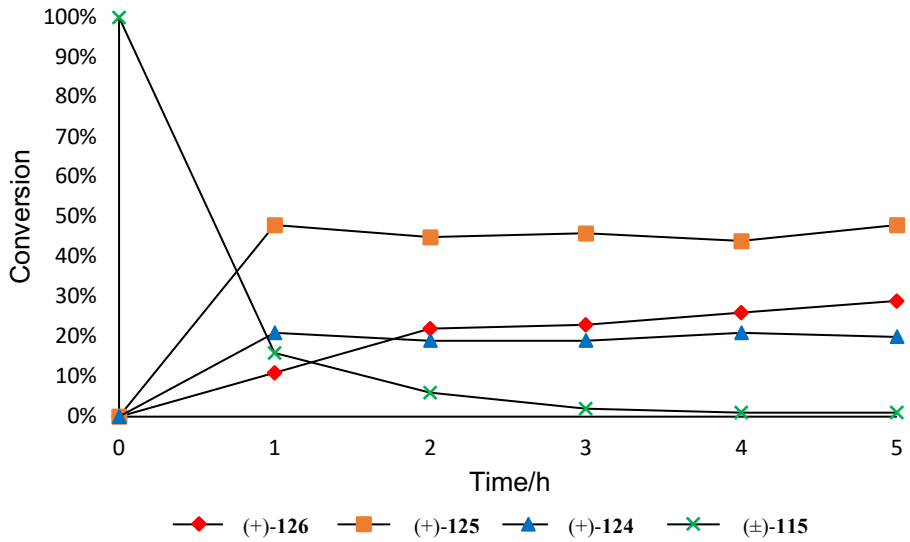

Graph 3.3. Time course data for the reaction between KSK19/I263A and (±)-**115** showing high conversion of the substrate within the first hour.

Next, the change in enantiomeric excess over the course of the reaction was investigated. The metabolites in question were not separable *via* chiral GC so two separate reactions were carried out over one and three hours. The products of these reactions were separated by column chromatography and % ee data were gathered through Mosher's ester analysis. These data were combined with the previously determined % ee values after the five-hour reaction to generate an approximate % ee time course. Due to the inaccuracies associated with Mosher's ester analysis this gave merely a rough insight into the progress of the kinetic resolution. 3° alcohol (+)-**126** showed a slight degradation in enantiomeric excess during the course of the reaction which, due to the nature of kinetic resolution, was understood to be caused by production of the minor enantiomer slowly over time; the behaviour of 1° alcohol (+)-**125** and aldehyde (+)-**125** was more interesting (***Graph 3.4***). Over the course of the first three hours, both 1° alcohol (+)-**124** and aldehyde (+)-**125** were generated approximately racemically; however, during the final two hours of the reaction, when the starting material had been almost completely consumed, the % ee unexpectedly jumped to ~ 70% for both metabolites.

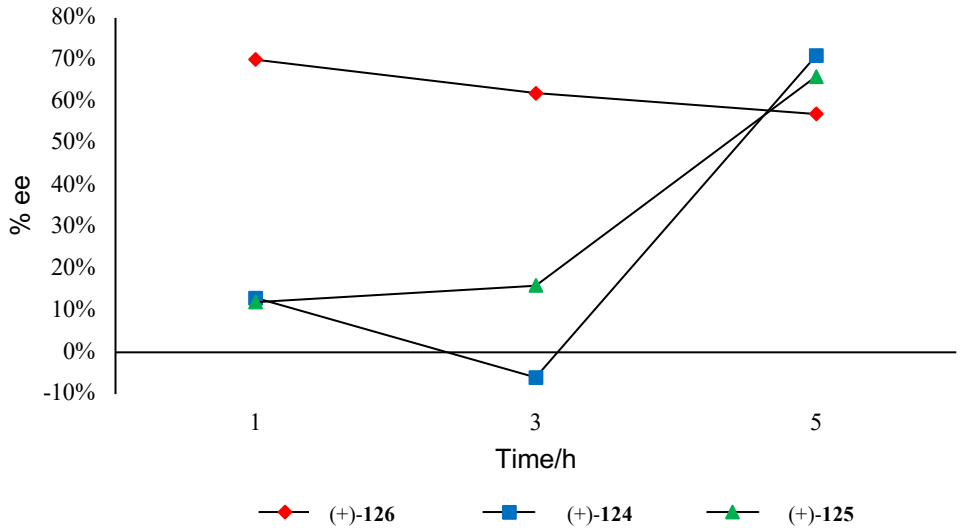

Graph 3.4. Time course data showing change in % ee during the course of the five-hour reaction. A negative value means the ratio favours the opposite enantiomer.

From these time course experiments, it appeared that formation of 3° alcohol (+)-**126** behaved as expected; however, due to the interconnected nature of the formation of 1° alcohol (+)-**124** and aldehyde (+)-**125**, further complexities within the reaction were involved (***Scheme 3.16***).

Computational analysis through docking of the substrate into the enzyme active site was proposed as a useful tool in probing the nature of these kinetic resolution reactions; however, previous work carried out by David Orjonikidze showed that the flexible nature of the *cis*-decalin-like bicyclic lactone led to unreliable results, and so this investigation was not pursued.

Submission of 1° alcohol (±)-**124** and its enantiomers to enzymatic oxidation with KSK19/I263A might shed further light on this two-step process by decoupling the steps; however, time constraints meant that the focus remained with lactone (±)-**115** itself in order to further investigate the metabolite profile, and in particular to isolate 2° alcohol **116** which had been observed in previous group work.

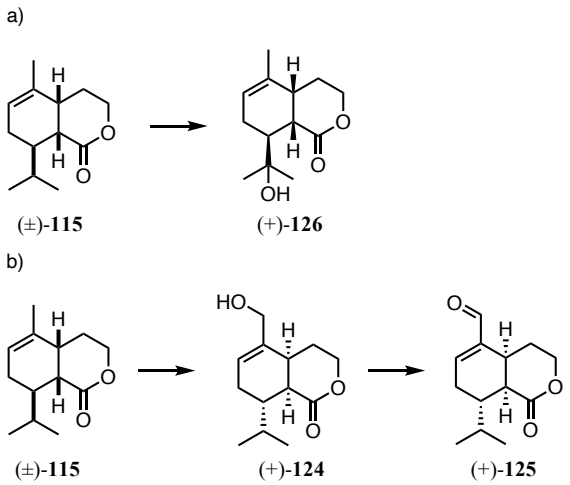

Scheme 3.16. a) One-step oxidation to form 3° alcohol (+)-**126** behaved as expected; ***b)*** two-step formation of aldehyde (+)-**125** *via* 1° alcohol (+)-**124** displayed unexpected reaction progress in terms of both formation and enantiomeric excess.

3.4.3 Characterisation of R19/A330W metabolites

In order to elucidate the structure of the final metabolite, a scale-up reaction with the R19/A330W variant was undertaken.

The unknown compound was isolated alongside 1° alcohol (+)-**124**, obtained in 25% yield (61% ee). The ^{1}H NMR spectrum of the unknown metabolite displayed coupling between the C**H**OH proton at 4.42 ppm (tq, J = 3.0, 1.5 Hz, 1H) and the olefinic proton at 5.61 ppm (dt, J = 3.0, 1.5 Hz, 1H) clearly indicating oxidation had occurred at the alternative allylic position allowing characterisation as secondary alcohol (+)-**116**. This analysis was backed up by the COSY spectrum, mass spectrometry, and literature data, which also allowed assignment of the relative configuration (***Scheme 3.17***). The metabolite was isolated in 44% yield with specific rotation $[\alpha]_{D}^{25}$ +8.6 (c 0.14, $CHCl_3$) but Mosher's ester derivatisation was unsuccessful and so no %ee value was obtained.

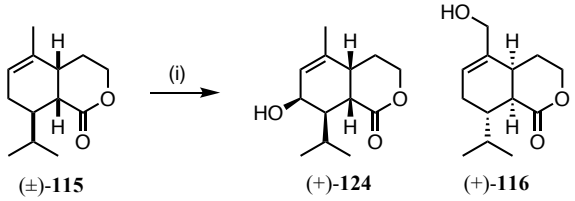

Scheme 3.17. Metabolite profile for reaction of (±)-**115** with R19/A330W. Conditions: 2 µM R19/A330W, 1mM (±)-**115**, 100 mM glucose, 2 U/mL GDH, 80 µM $NADP^+$, 200 mM phosphate buffer, 20 °C, 5 h; 44% (+)-**116**, 25% (+)-**124**.

Reactions with the pure enantiomers were undertaken, analogous to those with the GVQ and KSK19/I263A systems (***Graph 3.5***). The GC trace indicated that the 2° alcohol (+)-**116** is formed preferentially from lactone (–)-**115**, whilst the 1° alcohol (+)-**124** is only formed from lactone (+)-**115** allowing determination of the absolute stereochemistry. Minor components (+)-**125**, present in the GC trace from reactions with (±)-**115** and (+)-**115**, and (+)-**126**, present in all three GC traces, were unable to be isolated.

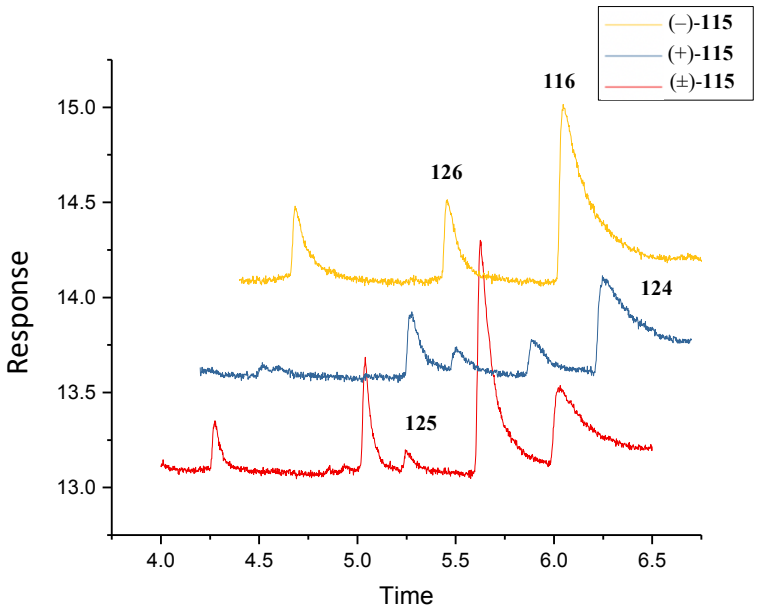

Graph 3.5. Stacked GC traces of the reactions between R19/A330W and (±)-, (+)-, and (–)-**115** displaying the preference for (–)-**115** to form (+)-**116** and (+)-**115** to (+)-**124**.

3.4.4 Characterisation of R19/FI metabolites

The GC data for the screening reaction of (±)-**115** with variant R19/FI was significantly more simple compared to the previous examples. Approximately 50% of **115** remained unconverted after 24 hours, with the only other compound present being 1° alcohol (+)-**124**. A preparative scale reaction over 24 hours with 0.1 mmol (±)-**115** led to 45% conversion and both 1° alcohol (+)-**124** (22%, 44% ee) and residual (–)-**115** (49%, ~30% ee) were isolated. The enantiomeric excess of the residual (–)-**115** was determined through derivatisation with (*S*)-(–)-α-methylbenzylamine and, although slight peak overlap in the ^{1}H NMR spectrum for the diastereomeric mixture precluded

precise measurement, an approximate enantiomeric excess could be calculated (***Scheme 3.18***).

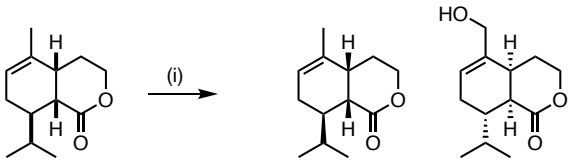

(±)-**115** (–)-**115** (+)-**124**

Scheme 3.18. Metabolite profile for reaction of (±)-**115** with R19/FI. Conditions: 2 µM R19/FI, 1mM (±)-**115**, 100 mM glucose, 2 U/mL GDH, 80 µM $NADP^+$, 200 mM phosphate buffer, 20 °C, 5 h; 49% (–)-**115**, 22% (+)-**125**.

This result means that, not only can CYP102A1 variants be employed in the production of hydroxylated metabolites through kinetic resolution processes, they can also allow enantiomeric enrichment of substrates, further extending their utility.

3.5 Conclusion

This study has shown that biocatalytic C–H oxidation of a bicyclic lactone with $P450_{BM3}$ variants is not only able to produce oxyfunctionalised metabolites in yields up to 27%, but also in enantiomeric excess of between 18% and 80% (***Table 3.5***).

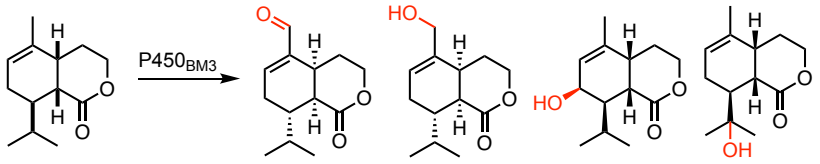

(±)-**115** (+)-**125** (+)-**124** (+)-**116** (+)-**126**

Table 3.5. Overall results from the study into kinetic resolution of bicyclic lactone (+)-**115**.

Entry	Variant	Conv.[a]	% (+)-**125**[b]	% (+)-**124**[b]	% (+)-**116**[b]	% (+)-**126**[b]
1	GVQ	98%	8 (80%)	18 (18%)	-	16 (43%)
2	KSK19/I263A	99%	17 (66%)	27 (71%)	-	12 (57%)
3	R19/A330W	92%	-	25 (61%)	44%[c]	-
4	R19/FI	45%	-	22 (44%)	-	-

[a] Determined through relative peak integrations in the GC traces; [b] isolated yield (% ee); [c] no reactivity was observed with (*R*)-(–)-α-methoxy-α-trifluoromethylphenylacetyl chloride.

These results confirm that mutant $P450_{BM3}$ enzymes are able to effect kinetic resolution processes through discrimination of separate enantiomers within the active site, a property that, once optimised, could allow the asymmetric synthesis of complex medicinally-relevant compounds through late-stage C–H activation, and avoiding inefficient protecting group strategies. Further work is required to understand the origin of these kinetic resolution processes, especially in, for example, the more complex case of the two-step formation of aldehyde (+)-**115**. Use of improved chiral phase analytical techniques, such as LC-MS, would allow more accurate enantiomeric excess data to be gathered, and further work into computational analysis could shed light on modes of binding and key residues. In general, the F87A/H171L/Q307H/N319Y and the A264G mutations improved reactivity of the enzyme towards (±)-**115**; these mutations could be used as a starting point for the design of further variants, with the aim of improving regio- and stereoselectivity.

In the future this reactivity could be employed in the synthesis of eleuthoside derivatives in order to test biological activity and probe key binding motifs, with the goal of developing novel antitumour agents acting *via* microtubule stabilisation.

4 Hydroxylation of a taxane core

4.1 Background

Paclitaxel (Taxol®, **234**), first isolated in 1966 from *Taxus brevifolia* and characterised in 1971, is a potent broad-spectrum anticancer agent currently used for the treatment of a wide range of cancers including ovarian, breast, and non-small cell lung cancer (***Figure 4.1***). [186]

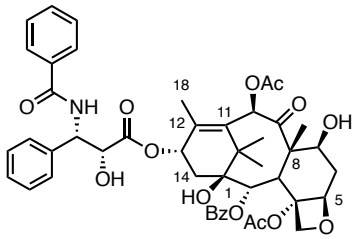

Paclitaxel, **234**

Figure 4.1. Structure and numbering of paclitaxel. (**234**)

Alongside the complex structure and useful biological activity, cross-disciplinary interest in Taxol® (**234**) is centred on its novel mechanism of action which, as elucidated in 1979 by Horwitz and Schiff, is reliant on suppression of mitosis through stabilisation of microtubules (see §**3.1.1**).[187] A significant amount of work was undertaken in order to fully understand the binding properties of paclitaxel (**234**), including the synthesis of Taxol® (**234**) derivatives tagged with photoaffinity probes, and this revealed the binding site to be a hydrophobic pocket in β-tubulin which allows paclitaxel (**234**)l to strengthen the lateral binding between tubulin protofilaments leading to the observed microtubule stabilisation.[178]

Historically paclitaxel (**234**) was isolated from the bark of the pacific yew tree in very small quantities which was highly environmentally destructive; therefore, a semi-synthesis was developed using 10-deacetylbaccatin III (**284**), found in the needles of *Taxus baccata*, and this route is still employed in the commercial synthesis of Taxol® (**234**) by Bristol-Myers-Squibb (***Scheme 4.1***).[210] More contemporary research has

focussed around the use of synthetic biology through plant cell fermentation techonology to produce paclitaxel (**234**) and its precursors without the need for the *Taxus baccata* needles;[211,212] initially scale-up of these enzyme mediated procedures proved difficult, with computational studies, along with high throughput screening, among the methods used to improve the efficacy.[213]

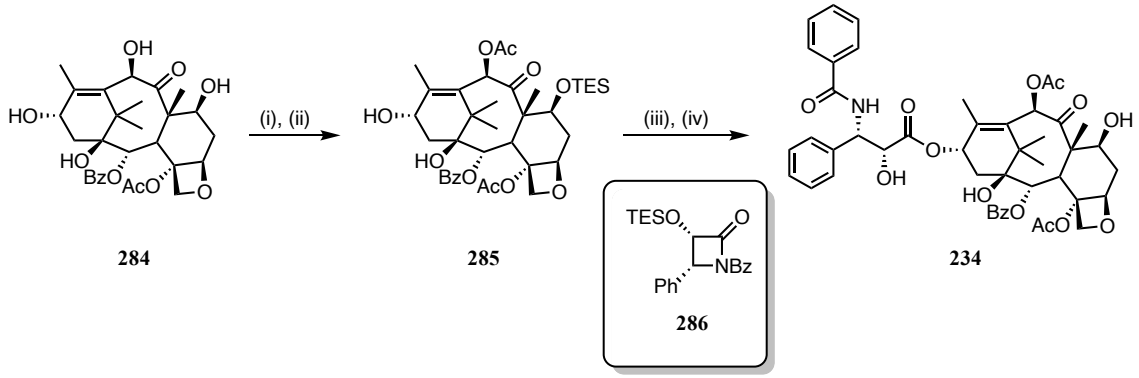

284 **285** **286** **234**

Scheme 4.1. Semi-synthesis of Taxol® from 10-deacetylbaccatin III. Reagents: (i) TESCl, imidazole; (ii) LHMDS, Ac_2O; (iii) LHMDS, lactam **286**; (iv) aq. HF, ~80%.

Due to the highly sought-after biological activity of Taxol® (**234**), alongside its synthetic complexity, many synthetic strategies have been developed leading to nine total syntheses and one formal synthesis, the most recent of which was reported in 2021.[214,215] Despite the significant amount of research undertaken, total synthesis has accounted for less than 105 mgs of man-made paclitaxel (**234**), highlighting the necessity for novel chemical strategies and tactics for the production of this complex diterpene target.[214]

Recently a two-phase concept, pioneered by Baran, has been exploited in the synthesis of intricate terpene natural products.[216] This strategy takes its inspiration from terpene biosynthesis, in which a first cyclase phase constructs the hydrocarbon core through enzyme catalysed additions, cyclisations, and rearrangements. Once the carbocyclic core has been generated, a second phase employs oxidase enzymes to insert oxygen functionality through chemo-, regio-, and stereoselective C–H activation reactions. This

highly efficient and selective generation of terpenes provides an ideal basis for a contemporary synthetic strategy towards these complex targets.

Baran *et al.* originally showcased this strategy in the synthesis of a number of eudasmane derivatives (§**1.2.1**, ***Scheme 1.16***).

This two-phase methodology has been further extended with investigations into the synthesis of taxane derivatives, and has been demonstrated with the formation of (–)-taxuyunnanine D (**292**) from unfunctionalised carbocycle **287** (***Scheme 4.2***).[216,217]

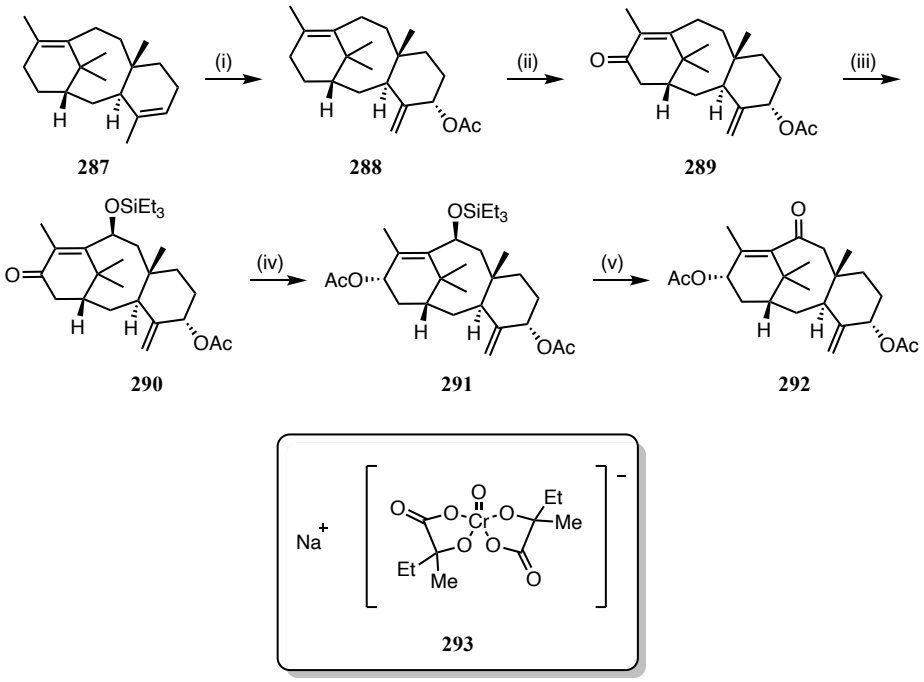

Scheme 4.2. Second phase oxidation of (+)-taxadiene (**287**). Reagents and conditions: (i) $Pd(OAc)_2$, *p*-benzoquinone, anisole, AcOH, 50 °C; (ii) Cr(V) reagent **293**, MnO_2, 15-crown-5, 80 °C; (iii) NBS, benzoyl peroxide, CCl_4, reflux; then AgOTf, Et_3SiOH, PhMe, 0 °C; (iv) DIBAL-H, PhMe, –78 °C; then MeOH, 0 °C; then Ac_2O, DMAP, Et_3N; (v) IBX, DMSO, 80 °C.

Recently, Baran *et al*. have employed this methodology in a total synthesis of paclitaxel (**234**). Diketone **128** was produced in the first cyclase phase, and following a 19 step oxidation phase, Taxol® was produced in 0.0014% overall yield (***Scheme 4.3***).

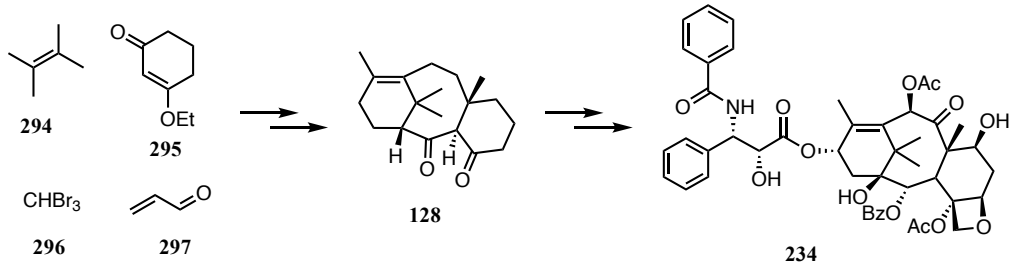

Scheme 4.3. Baran's two-phase total synthesis of Taxol® (**234**) using key diketone intermediate **128**.

The reliance of this two-phase methodology on selective oxidation of a hydrocarbon intermediate provides an opportunity for the use of biocatalysis, and previous group work has displayed the utility of CYP102A1 variants in the oxidation of a number of taxane systems (***Figure 4.2***). Use of this P450-mediated biocatalysis led to a variety of different metabolites incorporating functionalisation at six different positions. Both *endo*-alkenes and both diketones showed good reactivity towards enzymatic oxidation; however, *exo*-methylene compound **132** is yet to be investigated.

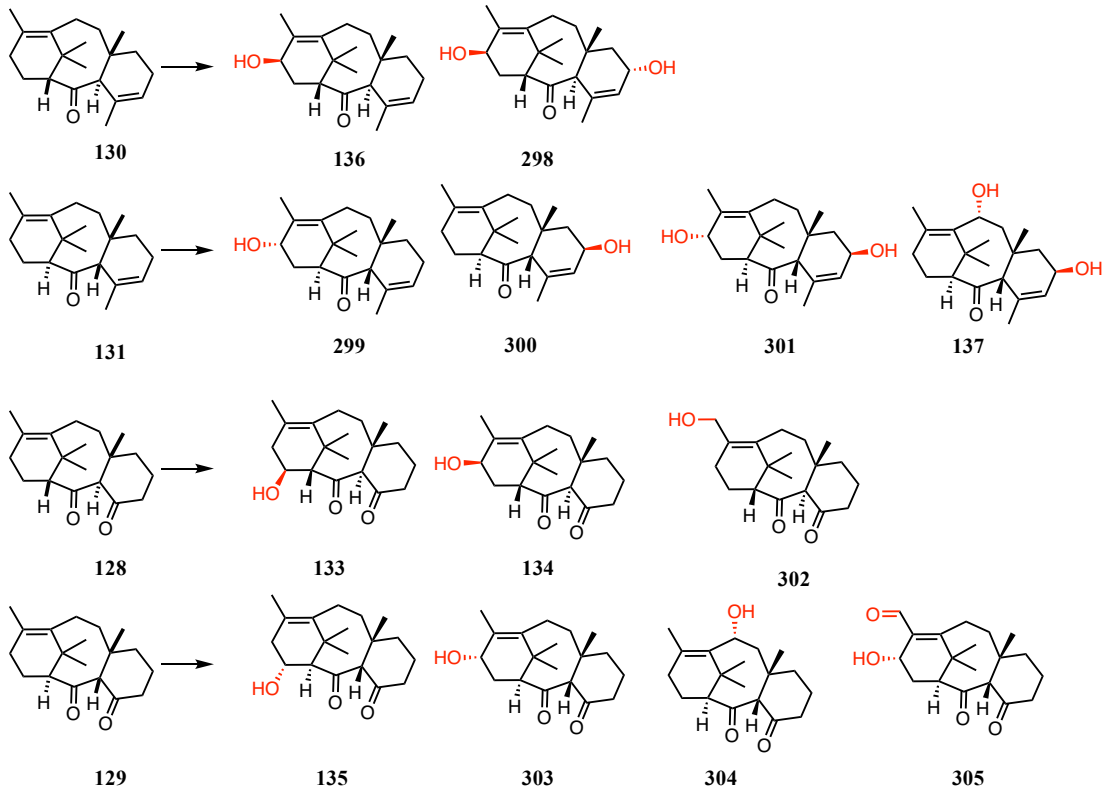

Figure 4.2. Metabolites produced from oxidation of a number of low oxidation-state taxane cores.

Taxane **132**, then, provides an ideal platform to further interrogate the reactivity, as well as the kinetic resolution behaviour, of CYP102A1 variants towards a significantly more complex system than those already studied in ***Chapter 2*** and ***Chapter 3*** (***Figure 4.3***).

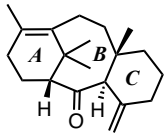

132

Figure 4.3. *Exo*-methylene taxane of interest.

4.2 Synthesis of taxane core (±)-*trans*-132

Synthesis of taxane analogues has been well researched, with a number of cyclisation methods proposed; however, the most common route towards the 6,8,6-ring system is through an IMDA reaction. Despite the fact that the IMDA reaction of *trans*-**306** has not been reported, it was proposed that it would proceed in a similar fashion to diketone *trans*-**307**, and so the synthesis was designed around this key step (***Scheme 4.4***).

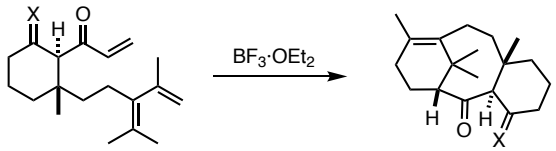

X = CH_2, *trans*-**306**
X = O, *trans*-**307**

X = CH_2, **132**
X = O, **128**

Scheme 4.4. Key IMDA reaction used in previous syntheses of taxane.

4.2.1 Retrosynthetic analysis for taxane *trans*-132

A significant amount of previous group work has been carried out on the synthesis of taxanes *trans*-**128**, *cis*-**129**, *trans*-**130**, *cis*-**131** and *trans*-**132**. IMDA reactions used to form diketones *trans*-**128** and *cis*-**129** proved successful; however, Diels–Alder reaction to form *endo*-alkenes *trans*-**130** and *cis*-**131** were less productive. In order to build on this work it was envisaged that the similarity between *exo*-methylene *trans*-**306** and the precursor to diketones *trans*-**128** and *cis*-**129** would lead to a successful Diels–Alder reaction and so the synthesis of *trans*-**306** was investigated using a key Sakurai

reaction.[218] This new route was able to produce a small amount of desired *trans*-**306** but the Sakurai step proved difficult. This synthesis had explored the possibility of the direct addition of acryloyl chloride; however, the Lewis acid catalysis necessary for reaction led to polymerisation of the highly reactive acryloyl moiety. A move to 3-chloropropionyl chloride improved the reactivity and, alongside the use of $MeAlCl_2$, allowed isolation of the desired β-chloroketone *trans*-**310** in 29% yield with the other 71% made up of protodesilylated alkene regioisomers **309**. Subsequent elimination using DBU generated the key IMDA precursor in a yield of 13% (***Scheme 4.5***). Clearly the low isolated yield of *trans*-**306** from this route would be problematic so some optimisation would have to be carried out.

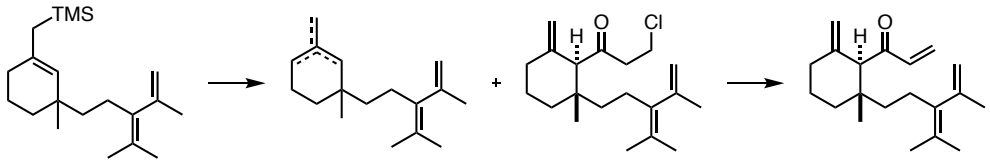

Scheme 4.5. Previous group work on the synthesis of IMDA precursor *trans*-**306** *via* β-chloroketone *trans*-**310**. Reagents: (i) 3-chloropropionyl chloride, $MeAlCl_2$, 29%; (ii) DBU, 13%.

This work aimed to improve the synthesis of *trans*-**306** through optimisation of the Sakurai conditions whilst, with an investigation into kinetic resolution in mind, a route to both the racemate as well as the separate enantiomers would be investigated; key intermediate enone **312** would enable this through conjugate addition under either racemic or asymmetric conditions, both of which have been reported.[219]

Following formation of allyl silane **308** from silyl enol ether **311** *via* a vinyl triflate, Lewis-acid promoted Sakurai reaction with a carbonyl electrophile was proposed as a means to generate IMDA precursor *trans*-**306**. Conjugate addition of a methyl group would be used to produce silyl enol ether **311** and, as discussed earlier, this reaction could be used to generate a racemic compound through the use of CuI, LiCl and methylmagnesium bromide, or separate enantiomers by employing CuTc, a chiral

phosphoramidate ligand, and trimethylaluminium.[219] Enone **312** would arise from addition of halide **313** into 3-ethoxy-2-cyclohexenone **295**; the required halide **313** could be formed through a five-step procedure beginning with γ-butyrolactone **315** (***Scheme 4.6***).

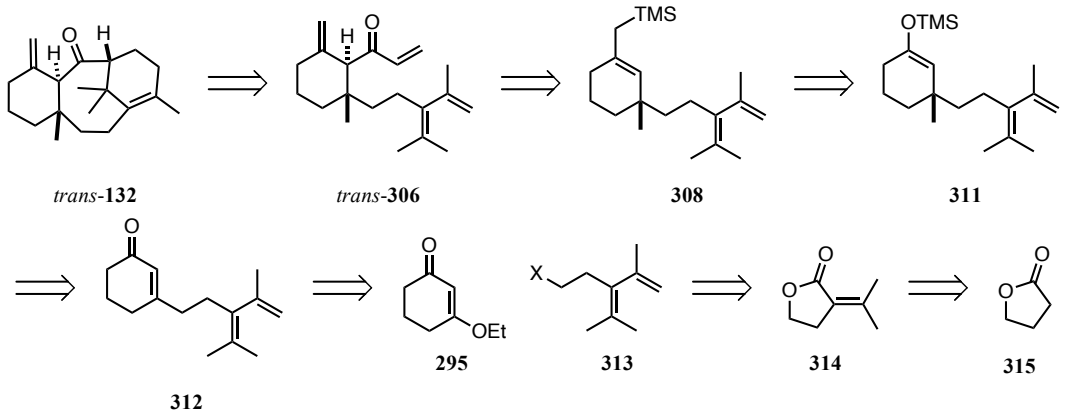

Scheme 4.6. Retrosynthetic analysis for taxane *trans*-**306** utilising an IMDA ring closure and proceeding *via* key enone intermediate **312**.

4.2.2 Synthesis of intermediate enone 312

Formation of mesylate **318** was carried out according to previous group work. The route began with the aldol reaction between γ-butyrolactone (**315**) and acetone. Despite the use of freshly distilled acetone, DIPA, and THF, freshly titrated 1.6 M *n*-butyllithium, and γ-butyrolactone (**315**) that had been passed through a silica gel column, TLC analysis of the reaction showed incomplete consumption of lactone **315**. Previous group work showed retro-aldol reaction of the intermediate tertiary alcohol to complicate purification and so it was proposed this was occurring on the TLC plate, leading to visualisation of a starting material spot. In order to avoid this retro-aldol reaction, the crude residue was carried through to the next reaction without purification. H_2SO_4 mediated dehydration proceeded smoothly to yield the desired α,β-unsaturated enone **314** in 62% yield over two steps. Addition of methylmagnesium bromide furnished acetate **316** in good yield, although during large scale reactions care had to be taken to keep the reaction cool due to the exothermic nature of the Grignard addition. The use of

acetyl chloride to trap the resultant alkoxide fortunately allowed subsequent direct elimination of the so-formed 3º acetate. Trapping of the 3º alkoxide was shown to be necessary during previous group work as aqueous acid-based quenches led to degradation of the electron rich diene system. Hydrolysis of acetate **316** followed by mesylation proceeded as expected to generate mesylate **318** in excellent yield (***Scheme 4.7***).

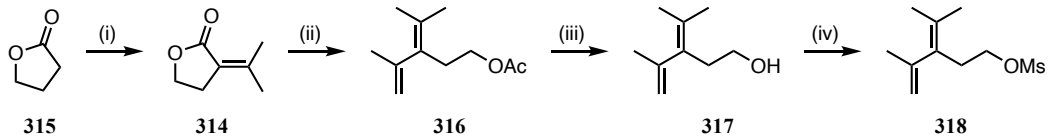

315 **314** **316** **317** **318**

Scheme 4.7. Synthesis of mesylate **318**. Reagents and conditions: (i) DIPA, *n*-BuLi, acetone, THF, –78 °C to RT, 16 h; then H_2SO_4, PhMe, 110 °C, 1 h, 62% over two steps; (ii) MeMgBr, Et_2O; then AcCl, –78 °C to RT 3.5 h, 89%; (iii) K_2CO_3, MeOH, RT, 9 h, 93%; (iv) MsCl, Et_3N, CH_2Cl_2, 0 °C, 2 h, 99%.

Previous work had employed both lithiation and Grignard reactions to produce desired enone **312**. Initially, bromide formation followed by Grignard addition into 3-ethoxy-2-cyclohexenone **295** was proposed as a route to **312** in order to avoid the use of highly reactive *tert*-butyllithium. Reaction with LiBr furnished bromide **319** in reasonable yield, but the following Grignard reaction proved temperamental (***Scheme 4.8***).

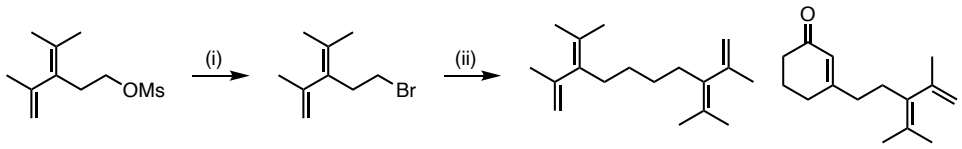

318 **319** **320** **312**

Scheme 4.8. Attempted synthesis of enone **312** through Grignard addition. Reagents and conditions: (i) LiBr, THF, 70 °C, 5 h, 73%; (ii) Mg, I_2, 3-ethoxy-2-cyclohexenone (**295**), THF.

Formation of the Grignard reagent was unsuccessful upon addition of 0.45 M **319** in THF into a suspension of Mg and I_2 in THF; attempted initiation through heating with a heat gun did not improve matters (***Table 4.1,*** entries **1** and **2**). A tenfold increase in the concentration of the bromide solution coupled with a higher overall reaction concentration allowed the reaction to proceed (entry **3**); however, a significant amount of homocoupled tetraene **320** was generated. In order to suppress the homocoupling

reaction pathway the temperature of initiation was reduced to 0 ºC but this precluded the Mg insertion from taking place at all (entry **4**). A slight decrease in concentration of both bromide solution and the overall reaction was successful in reducing the amount of **320** but this did not eliminate it completely (entry **5**).

Table 4.1. Conditions attempted to optimise the Grignard reaction for the formation of enone **312**. [a]Added dropwise over 1.5 h; [b]added in one portion; [c]determined through relative peak area in the proton NMR spectra.

Entry	Bromide solution in THF	Reaction concentration	Temperature	Initiation time	**320**:**312**[c]
1	0.45 M[a]	0.25 M	RT	1 h	No conversion
2	0.45 M[b]	0.25 M	Heat gun	1 h	No conversion
3	4.35 M[b]	0.85 M	RT	0.5 h	1:2
4	4.35 M[b]	0.85 M	0 ºC	0.25 h	No conversion
5	3.35 M[b]	0.5 M	RT	0.25 h	1:3

At this point, due to the temperamental nature of the Grignard reaction, it was proposed a switch to the lithiation reaction previously studied within the group would allow production of the desired enone without loss of yield through side reactions. This lithiation reaction required iodide **321**, readily accessible from mesylate **318**, and, with **321** in hand, the addition reaction was tested.

Initial reactions using 2.1 equiv. of *tert*-butyllithium led to incomplete consumption of starting material. After confirming the concentration of the *tert*-butyllithium solution through titration, an increase to 2.5 equiv. achieved complete consumption of iodide **321** and desired enone **312** was produced in 73% yield with no homocoupled side product observed. (***Scheme 4.9***).

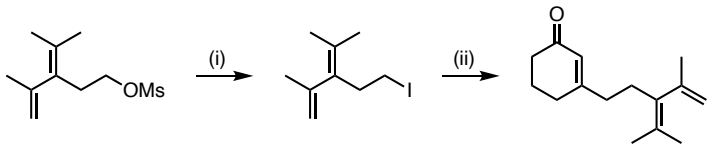

318 **321** **312**

Scheme 4.9. Successful synthesis of key intermediate enone **312**. Reagents and conditions: NaI, acetone, 60 °C, 16 h, 75%; (ii) *t*-BuLi, 3-ethoxy-2-cyclohexenone (**295**), Et_2O, –78 °C to RT, 5 h, 73%.

4.2.3 Sakurai reaction

With enone **312** in hand, investigation into formation of the IMDA precursor was initiated (***Figure 4.4***).

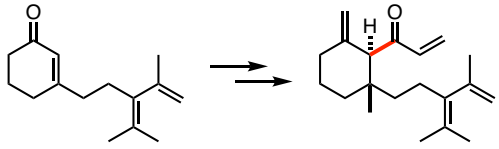

312 (±)-*trans*-**306**

Figure 4.4. Key C–C bond formation in the synthesis of IMDA precursor (±)-*trans*-**306.**

The Sakurai reaction between allylsilanes and carbonyl electrophiles, most commonly aldehydes mediated by Lewis acids, presented itself as a good candidate for the installation of the desired functionality. Despite the fact that formation of β,γ-unsaturated ketones by this method is relatively underdeveloped, the ability to generate the *exo*-methylene functionality in the same step as C–C bond formation would allow rapid generation of chemical complexity.

Two stereochemical models were proposed to account for the stereochemistry of the product (***Figure 4.5)***. Route (a) would proceed *via* a chair-like transition state which would generate the undesired *cis*-diastereomer; however, this would lead to the development of strain within the transition state through 1,3 diaxial interactions with the bulky diene side chain. It was hoped that this strain would increase the transition state energy sufficiently enough to favour formation of the desired *trans*-diastereomer

through the twist-boat transition state (Route (b)). Indeed, the *trans* isomer had been observed in previous group work.

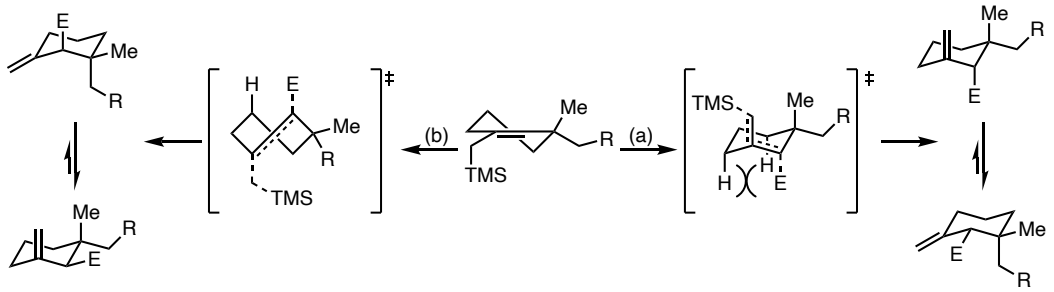

Figure 4.5. Half-chair conformation used to predict the possible stereochemical outcome.

To begin with, optimisation studies were carried out on a simple *gem*-dimethyl model system **325** in order to avoid the complications of side reactions associated with the electron rich diene functionality whilst also simplifying analysis and purification by precluding the formation of diastereomers.

Previous work within the group led to successful synthesis of **325** beginning with copper-catalysed conjugate addition of methylmagnesium bromide to **322**. Silylation of the so-formed enolate *in situ* proceeded smoothly to generate silyl enol ether **323**. Subsequent triflation, which had been extensively investigated in previous group work, was carried out on crude **323** due to stability concerns and produced triflate **324** in reasonable yield. Finally $Pd(PPh_3)_4$-catalysed coupling with trimethylsilyl methylmagnesium chloride generated the required model allyl silane again in reasonable yield (***Scheme 4.10***).

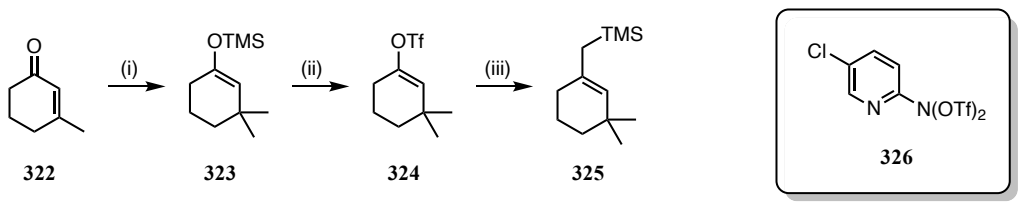

Scheme 4.10. Synthesis of model allyl silane **325**. Reagents and conditions: (i) CuI, LiCl, MeMgBr, TMSCl, Et_3N, THF, –78 °C to RT, 1 h; (ii) MeLi, Comins' reagent **326**, DME, THF, –78 °C to RT, 3 h, 25% over two steps; (iii) $Pd(PPh_3)_4$, trimethylsilyl methylmagnesium chloride, THF, –78 °C, 2 h, 52%.

Although the overall yield of the three step procedure was poor, attributed to the volatility of silyl enol ether **323** and allyl silane **325**, it was sufficient for evaluating the Sakurai reaction, initially with acetyl chloride as the electrophile. An initial attempt with mild $BF_3 \cdot OEt_2$ was unsuccessful; however, use of $MeAlCl_2$, coupled with DTBMP to inhibit any acid-mediated desilylation pathways, allowed isolation of the desired β,γ-ketone **327** in moderate 36% yield. TLC and NMR analysis of crude product showed that this reaction proceeds cleanly to product so the low yield was proposed to arise from the small scale (20 mg) that the reaction was carried out on (***Scheme 4.11***).

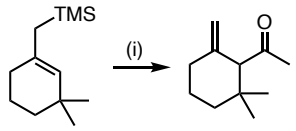

325 **327**

Scheme 4.11. Sakurai reaction on model *gem*-dimethyl system **325**. Reagents and conditions: $MeAlCl_2$, DTBMP, acetyl chloride, CH_2Cl_2, –78 °C to RT, 5 minutes, 36%.

With this, efforts moved on to the real system. Synthesis of dienyl allyl silane (±)-**308** proceeded under the same conditions as *gem*-dimethyl allyl silane **325** but with significantly improved yield due to the reduced volatility of the higher molecular weight compounds (***Scheme 4.12***).

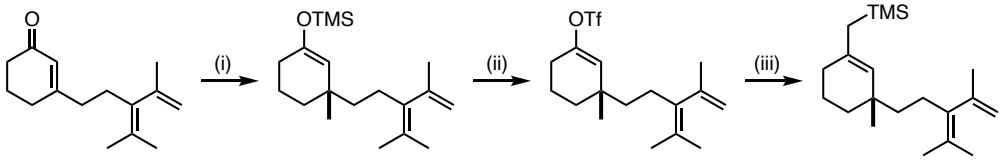

312 (±)-**311** (±)-**328** (±)-**308**

Scheme 4.12. Synthesis of allyl silane (±)-**328**. Reagents and conditions: (i) CuI, LiCl, MeMgBr, TMSCl, Et_3N, THF, –78 °C to RT, 1h; (ii) MeLi, Comins' reagent **326**, –78 °C to RT, 3h, 77% over two steps; (iii) $Pd(PPh_3)_4$, trimethylsilyl methylmagnesium chloride, THF, –78 °C, 2 h, 92%.

From allyl silane (±)-**308**, conditions for the Sakurai reaction were evaluated. It was expected that the reactions with the dienyl system would not be as clean as the *gem*-dimethyl system due to side-reactions involving the electron rich diene; however, it

quickly became clear that the diene seemed to be heavily involved in the reaction with a number of reactions producing highly complex product mixtures (***Scheme 4.13***).

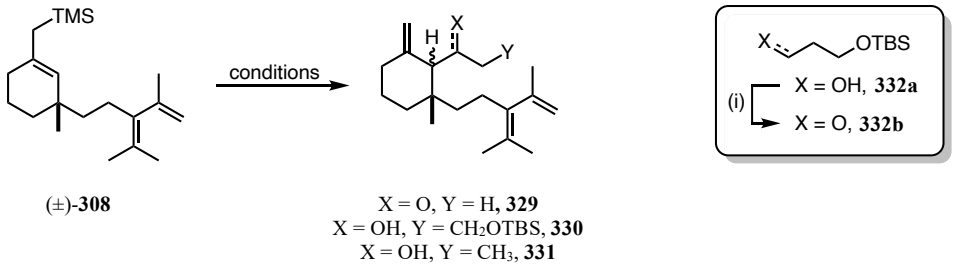

(±)-**308**

X = O, Y = H, **329**
X = OH, Y = CH_2OTBS, **330**
X = OH, Y = CH_3, **331**

Scheme 4.13. Sakurai reaction on real allyl silane system testing four electrophiles: acetyl chloride, triethylorthoacetate, propionaldehyde, and silylated 3-hydroxypropionaldehyde **332b**. Reagents and conditions: (i) $(COCl)_2$, DMSO, then Et_3N, CH_2Cl_2, –78 °C to RT, 18 h, 38%.

An attempt to reproduce the successful conditions found with the model system resulted in no consumption of starting material (***Table 4.2***, entry **1**); however, a reaction without the presence of DTMBP showed high reactivity generating a complex mixture (entry **2**). DTBMP is a solid under the reaction conditions of –78 °C in dichloromethane and so it was proposed that, although vigorous stirring upon addition of the DTMBP resulted in a suspension within the reaction mixture, this was inhibiting reaction with dienyl allyl silane (±)-**308**, possibly due to the more sterically congested, relatively unreactive, nature when compared to the model *gem*-dimethyl system. Use of $LaCl_3 \cdot 2LiCl$, a very mild Lewis acid, led to no reactivity whilst a change in reaction manifold to a fluoride-driven reaction was also unsuccessful (entries **3** and **4**).

It was proposed that a reduction in the reactivity of the electrophile might allow better control of the addition; however, a move to triethylorthoacetate, in the hope it would act as a milder, protected form of acetyl chloride, also displayed no reactivity with both $BF_3 \cdot OEt_2$ and trimethylsilyl triflate (entries **5** and **6**).

Sakurai reactions are most commonly carried out with aldehydes, to generate secondary alcohols; therefore, silylated aldehyde **332** was next to be tested. Although the use of aldehydes would increase the complexity of the product mixture through an increase in

the number of diastereomers, it was envisaged that the reactivity would be tempered enough that purification would be possible or, failing that, oxidation of the crude product could be carried out. $TiCl_4$ and $EtAlCl_2$, commonly reported in these transformations, again led to a complex mixture of products (entries **8** and **9**). It was proposed that the silyl ether protecting group might interact with the strong Lewis acids, allowing the operation of even more reaction pathways. In order to test whether the silyl ether group was indeed participating in the reaction, propionaldehyde was employed as a test substrate; however, as before, $TiCl_4$ led to over-reaction (entry **9**), and both $LaCl_3 \cdot 2LiCl$ and TBAF were unreactive (entries **10** and **11**).

Table 4.2. Conditions attempted to effect Sakurai reaction with dienyl allyl silane (±)-**308**.

Entry	Electrophile	Activating agent	Outcome
1	Acetyl chloride	$EtAlCl_2$, DTBMP	No reaction
2	Acetyl chloride	$EtAlCl_2$	Complex mixture
3	Acetyl chloride	$LaCl_3 \cdot 2LiCl$	No reaction
4	Acetyl chloride	TBAF	No reaction
5	Triethyl orthoacetate	TMSOTf	No reaction
6	Triethyl orthoacetate	$BF_3 \cdot OEt_2$	No reaction
7	**332b**	$TiCl_4$	Complex mixture
8	**332b**	$EtAlCl_2$	Complex mixture
9	Propionaldehyde	$TiCl_4$	Complex mixture
10	Propionaldehyde	$LaCl_3 \cdot 2LiCl$	No reaction
11	Propionaldehyde	TBAF	No reaction

Although it was clear that a middle ground of reactivity must be accessible, the large number of combinations of electrophiles and activating agents that could be envisaged

to mediate the desired reaction, coupled with the difficulties encountered in previous group work, would have led to a time-consuming reaction screening process with limited chance of success. Due to the time-sensitive nature of this project it was decided to move on to another strategy.

4.2.4 Aldol strategy

Previous group work carried out on the synthesis of diketones *trans*-**128** and *cis*-**129** utilised a key aldol reaction with acrolein based on Baran's reported route to taxadienone (***Scheme 4.14a***).[214] In that work, Baran's procedure was found not to be reproducible; however, transformation of the unreactive silyl enol ether **311** to a lithium enolate *via* methyllithium mediated transmetallation allowed addition into acrolein and, following DMP oxidation, key diketone IMDA precursor was isolated in 43% yield (***Scheme 4.14b***).

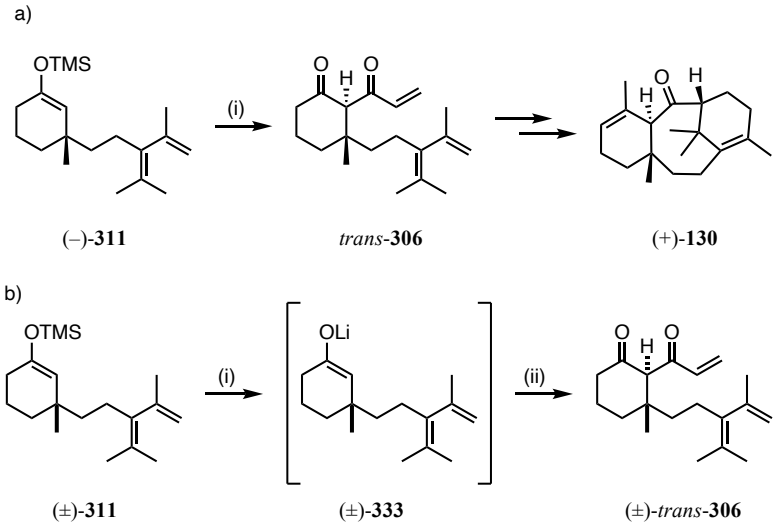

Scheme 4.14. a) Mukaiyama aldol reaction carried out under Kobayashi's conditions reported by Baran in the synthesis of taxadienone. Reagents: (i) $Gd(OTf)_3$, acrolein, 1:10:4 H_2O, EtOH, PhMe then Jones' reagent, 84%. ***b)*** Modification of Baran's aldol reaction as employed in previous group work. Reagents: (i) MeLi, THF; (ii) acrolein; (iii) DMP, CH_2Cl_2, 43% (inseparable mixture of diastereomers).

It was proposed to employ this method to form the key C–C bond but a modification would be required to install the *exo*-methylene group; trapping of aldol alkoxide to form

(±)-**334** followed by Wittig reaction with methylenetriphenylphosphine would complete installation of the desired carbon framework (***Scheme 4.15***).

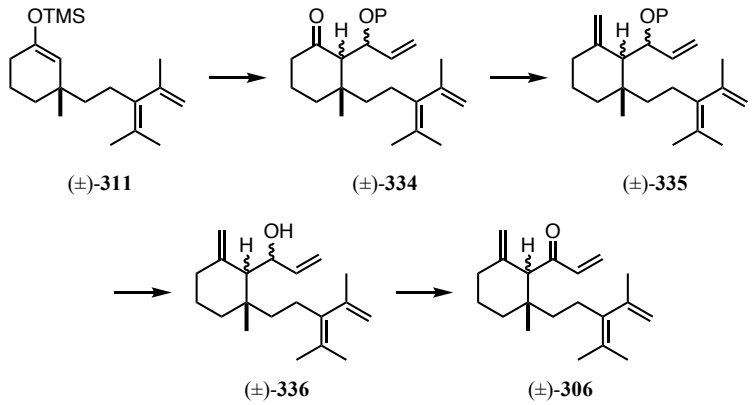

Scheme 4.15. Proposed route towards desired IMDA precursor utilising an aldol reaction with *in situ* trapping of the so-formed alkoxide followed by a Wittig reaction.

It was appreciated that this route would generate a large number of diastereomers due to the formation of secondary alcohol (±)-**336** and it was expected that purification of the intermediate compounds would be problematic; accordingly, the crude products would be carried through until formation of enone (±)-**306** at which point purification and separation of the diastereomers would be carried out.

In order to test reactivity, *gem*-dimethyl system **323** was again employed and, although this system would have fewer intermediate stereoisomers, the crude material would still be carried through until oxidation of secondary alcohol **339** to test the feasibility of this process (***Scheme 4.16***).

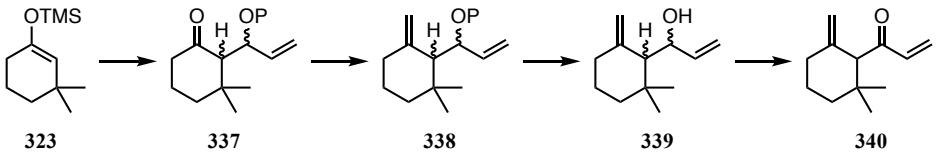

Scheme 4.16. Route towards enone **340** with *gem*-dimethyl model system reducing the number of intermediate stereoisomers.

In the event, with acetyl chloride as the trapping agent, carrying through crude material for four steps proved unsuccessful; the final oxidation reaction yielded no desired enone

340. In order to further investigate this route, purification was carried out as normal after each step.

Despite production of acetate **341** in poor yield, enough was isolated to test the Wittig reaction. In the event, the Wittig reaction was unsuccessful in generating the desired *exo*-methylene compound and, in fact, produced a highly unexpected bicyclic enol ether which was assigned as the *cis*-diastereomer due to a C8-**H**:C9-**H** coupling of J = 10.0 Hz. (***Scheme 4.17***).

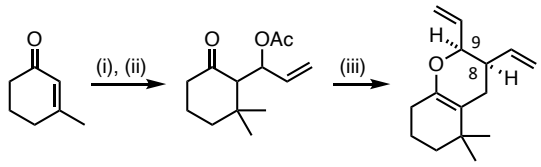

322 **341** **342**

Scheme 4.17. Production of bicyclic enol ether **342** upon submission of acetate **341** to standard Wittig methylation conditions. Reagents and conditions: (i) CuI, LiCl, MeMgBr, TMSCl, Et_3N, THF, –78 °C, 1 h; (ii) MeLi, acrolein, then AcCl, THF, –78 °C to RT, 1.5 h, 14% over two steps; (iii) $MePPh_3Br$, KO*t*-Bu, THF, RT, 2 h, 9%.

Mechanistically, this was proposed to be initiated by deprotonation of one of the acidic acetate α-protons and subsequent loss of diketene to form aldolate **343** which could undergo a retroaldol reaction. 1,4- addition of the so-formed enolate into acrolein followed by 1,2-addition into another molecule of acrolein generated allyl alkoxide **344**. Intramolecular condensation followed by Wittig olefination of the remaining aldehyde generated bicylic enol ether **342** (***Scheme 4.18***).

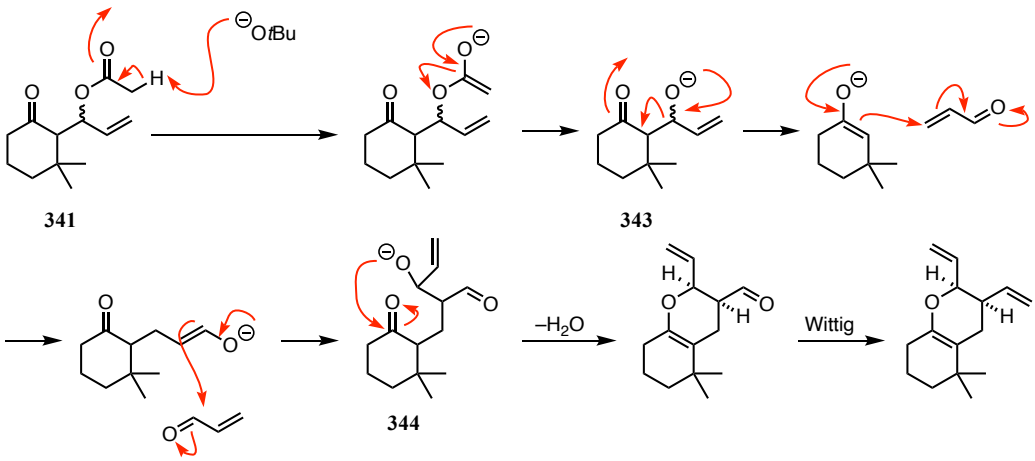

Scheme 4.18. Proposed mechanism for the formation of bicyclic enol ether **342**. Deprotonation followed by retroaldol and subsequent 1,4 addition in to acrolein generates an intermediate enolate which, after a 1,2 addition into another molecule of acrolein, cyclises. Loss of water and final Wittig reaction generate the product.

As with acetate **341**, enol ether **342** was isolated in poor yield; however, analysis of the NMR spectrum of the crude product showed it to be the major component in the reaction mixture and the loss of yield was attributed to the small reaction scale.

It was thought the reversible nature of deprotonation with KO*t*-Bu as a base was contributing to this side reaction and so pre-formation of the ylide with *n*-butyllithium was tested. This reaction progressed slowly and the crude NMR spectrum showed the generation of a complex mixture of products, potentially due to the high basicity of the methylenetriphenylphosphine anion. Despite the isolation of a very small amount of the desired *exo*-methylene acetate, this reaction was unable to produce the quantity necessary for a successful synthetic route and so other methods were tested.

Addition of trimethylsilyl methylmagnesium chloride to acetate **341**, in order to attempt a Peterson olefination, was unsuccessful. The methods tested up to this point had all been base-mediated and the acidity of the acetate protons was leading to side reactions; therefore, different trapping agents were employed. Benzoyl chloride, *para*-nitrobenzoyl chloride, and pivaloyl chloride were all tested due to their lack of acidic protons; however, none of them were successful in forming the desired protected

alcohols, **345**, **346**, or **347** respectively. In fact, analysis of the NMR spectra from crude reaction mixtures showed, in the case of reaction with benzoyl chloride and *para*-nitrobenzoyl chloride, the presence of what was tentatively assigned to be 1,3-diketones **348** and **349**, presumably formed through retroaldol and subsequent trapping of the cyclic enolate. It was proposed that this reaction manifold was operating with the aromatic acid chlorides due to their lower reactivity allowing time for the retroaldol reaction to take place (***Scheme 4.19***).

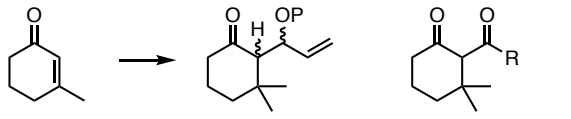

322

P = Bz, **345**
P = *p*-NO_2Bz, **346**
P = C(O)C(Me_3), **347**

R = Ph, **348**
R = *p*-NO_2Ph, **349**

Scheme 4.19. Unsuccessful attempts to trap aldol alkoxide intermediate with benzoyl choride, *para*-nitrobenzoyl chloride, and pivaloyl chloride.

Silylating agents TESCl and TBSCl were next to be tested; however, due to the oxophilicity of silicon these reactions resulted in bis-silylation (***Scheme 4.20***) A brief exploration into the possibility of effecting silyl enol ether hydrolysis without affecting the silyl ether proved unproductive.

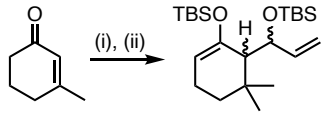

322 **350**

Scheme 4.20. Bis-silylation observed upon use of TBSCl and TESCl as trapping agents (product of TBSCl silylation shown). Reagents: (i) CuI, LiCl, MeMgBr, TMSCl, Et_3N, THF, –78 °C, 1 h; (ii) MeLi, acrolein, then TBSCl, THF, –78 °C, 15 min.

Although this aldol strategy generated the key C–C bond, isolation of the protected alkoxide proved difficult; the trapping electrophiles were not able to protect the alkoxide as cleanly as expected, and the reaction with acrolein, which already generated a number of products from 1,2- and 1,4-addition, formed a pair of diastereomers which complicated purification, a problem which would get significantly worse when attempting this methodology on the real system.

Use of a lithium enolate was clearly important in the formation of the key C–C bond and so it was proposed to continue with this solution whilst altering the electrophile in order to improve the reaction.

4.2.5 Synthesis of model enone 340

Reverting back to an electrophile at the carboxyl oxidation state would avoid formation of a secondary alcohol and attendant stereochemical complications. Cyanoformates were first identified by Mander in 1983 as useful reagents in the regioselective formation of β-ketoesters and so ethyl cyanoformate was proposed as a means to generate ketoester **351**.[220]

This reaction, as with previous work, was first tested on *gem*-dimethyl model system **323**, and, in the event, β-ketoester **351** was produced successfully in moderate yield with subsequent Wittig reaction proceeding smoothly to the desired β,γ-unsaturated ester **352**. Formation of the required Weinreb amide was initially attempted through formation of aminomagnesium chloride reagent **354**; however, this method was unable to completely convert the starting material, with a 1:1 mixture of **352**:**353** observed in the NMR spectrum of the crude product. Reaction with lithium amide **355** was successful, generating amide **353** in 79% yield (***Scheme 4.21***).

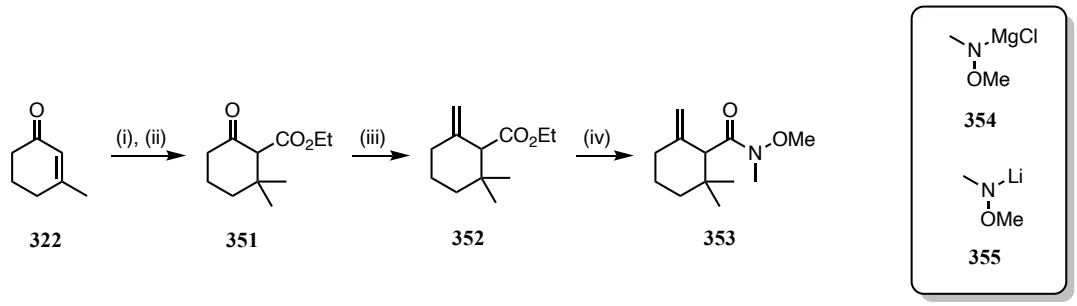

Scheme 4.21. Successful synthesis of Weinreb amide **353**. Reagents and conditions: (i) CuI, LiCl, MeMgBr, TMSCl, Et3N, THF, –78 °C, 1 h; (ii) MeLi then ethyl cyanoformate, THF, –78 °C to RT, 16 h, 45% over two steps; (iii) $MeP(PPh_3)_4Br$, KOt-Bu, THF, 70 °C, 1 h, 57%; (iv) n-BuLi, MeONHMe.HCl, THF, 0 °C to RT, 4 h, 79%.

From amide **353**, addition of vinylmagnesium bromide was evaluated. A first reaction involving $LaCl_3 \cdot 2LiCl$ showed no consumption of starting material. Removal of the

$LaCl_3 \cdot 2LiCl$ allowed the reaction to proceed but **340** was not isolated. Analysis of the ^1H NMR spectrum of crude product showed NCH_3 and OCH_3 resonances assigned to the product of 1,4-addition of MeONHMe to the desired α,β-unsaturated ketone **340** during work-up, although this product was not isolated (***Scheme 4.22***).

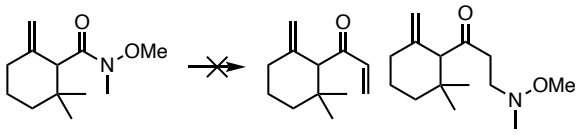

353 **340** **356**

Scheme 4.22. Unsuccessful addition of vinylmagnesium bromide into Weinreb amide **353**.

To circumvent this problematic addition of vinylmagnesium bromide into Weinreb amide **353**, recourse was made to a less redox economical route. Regular alteration of oxidation state is unattractive in contemporary synthesis, but it was important to complete the synthesis of taxane (±)-*trans*-**132** for hydroxylation studies.

In the event, this new route produced the desired enone **340**, albeit in low overall yield. Synthesis of β-ketoester **351** was carried out as before, with subsequent $LiAlH_4$ mediated reduction generating primary alcohol **357** in 63% yield. Oxidation with DMP generated aldehyde **358** in 77% yield which was used without further purification and, following addition of vinylmagnesium bromide, further DMP oxidation produced enone **340** in 10% yield over two steps. Despite the poor yield of the final two steps, this synthesis on the model system showed that, in principle, enone **340** could be accessed from β-ketoester **351** (***Scheme 4.23***).

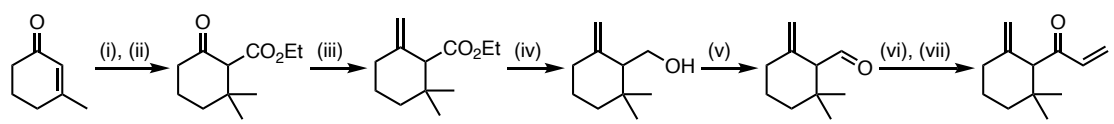

322 **351** **352** **357** **358** **340**

Scheme 4.23. Successful synthesis of enone **340**. Reagents and conditions: (i) CuI, LiCl, MeMgBr, TMSCl, Et_3N, THF, –78 °C, 1 h; (ii) MeLi then ethyl cyanoformate, THF, –78 °C to RT, 16 h, 45% over two steps; (iii) $MePPh_3Br$, KO*t*-Bu, THF, 70 °C, 1 h, 57%; (iv) $LiAlH_4$, THF, 0 °C to RT, 48 h, 63%; (v) DMP, CH_2Cl_2, 0 °C to RT, 2 h, 77%; (vi) vinylmagnesium bromide, Et_2O, 0 °C to RT, 1 h; (vii) DMP, $NaHCO_3$, CH_2Cl_2, 0 °C to RT, 2 h, 10% over two steps.

4.2.6 Construction of taxane (±)-*trans*-132

With the dienyl substrate **312**, use of methyllithium and ethyl cyanoformate did not achieve the formation of β-ketoester (±)-**359**; the ^{1}H NMR spectrum of the crude product showed an alkene resonance at 5.08 ppm but no peak at ~3.1 ppm where C1-**H** is usually found and *O*-acylation was concluded. Upon re-examination of the literature, *O*-acylation has been observed with sterically hindered enolates but this may be avoided through a simple change of solvent to ether.[221] Ether, it is proposed, is less able to chelate Li^{+} ions than THF, meaning that, in ether, the enolate oxygen is more tightly bound by lithium which increases the relative reactivity of the enolate carbon. This change of solvent, along with a switch from methyllithium to *n*-butyllithium, allowed successful generation of β-ketoester (±)-**359**, with no *O*-acylation observed by NMR analysis. Purification of (±)-**359** proved problematic due to co-elution of unidentified impurities so it was submitted to the subsequent Wittig reaction in crude form, after which purification became possible and (±)-**360** was isolated as a mixture of diastereomers in 79% yield over three steps (***Scheme 4.24***).

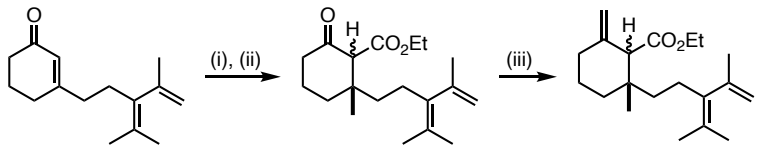

312 (±)-**359** (±)-**360**

Scheme 4.24. Successful synthesis of (±)-**360** *via* β-ketoester (±)-**359.** Reagents and conditions: (i) CuI, LiCl, MeMgBr, TMSCl, Et_3N, THF, –78 °C, 1 h; (ii) *n*-BuLi, ethyl cyanoformate, Et_2O, –78 °C to RT, 16 h; (iii) $MePPh_3Br$, KO*t*-Bu, THF, 70 °C, 1 h, 79% over three steps.

$LiAlH_4$ reduction of ester (±)-**360** generated alcohol (±)-**361** in 95% yield, again as an inseparable mixture of diastereomers, from which DMP oxidation produced aldehyde (±)-**362** as an inseparable mixture of diastereomers. Although not observed with the model system, in the case of DMP oxidation of (±)-**361**, the product appeared as a white solid which was proposed to be a result of aromatic by-products from the DMP. Despite

the presence of this material, the reaction formed the pair of aldehyde diastereomers cleanly, and so the crude mixture was carried through to the next reaction due to concerns that aldehyde (±)-**362** would be unstable on silica gel. Addition of vinylmagnesium bromide generated, as expected, a complex mixture of four diastereomers and so this material also was carried through crude as preparative purification would not have been efficient.

Although enone (±)-**306** was observed in the NMR spectrum of the crude product following oxidation of secondary alcohol (±)-**336**, isolation of the pair of diastereomers was complicated by the presence of a number of products with similar R_f values to (±)-**306**. It was proposed that the DMP was interacting with the electron-rich diene side chain as well as the secondary alcohol to generate a complex mixture of oxidation artifacts. Unsurprisingly, submission of this crude material to $BF_3 \cdot OEt_2$ cycloaddition conditions yield none of the desired taxane (±)-**132**.

Another method was sought to oxidise the secondary alcohol (±)-**336**. MnO_2 was too mild and resulted in no reaction but both PDC and PCC, coupled with NaOAc as a buffer, achieved oxidation and, simply due to a higher rate of reaction, PCC was employed on a preparative scale. The use of crude secondary alcohol (±)-**336** in the reaction was expected to increase the difficulty of purification afterwards and so separation of the four diastereomers into two pairs was attempted. This resulted in isolation of the major pair of diastereomers, epimers at C1-**H** with an unknown relative configuration at C17-**H**, in 58% yield. Submission of the pair of diastereomers of (±)-**336** to PCC oxidation conditions generated enone (±)-**306** in a moderate 40% yield, despite co-elution again complicating purification; recovery of crude material after reaction and work-up was efficient and so it was determined that the loss of yield was arising due to purification by column chromatography, possibly through isomerisation

of the *exo*-methylene olefin into conjugation with the α,β-unsaturated ketone functionality (***Scheme 4.25***).

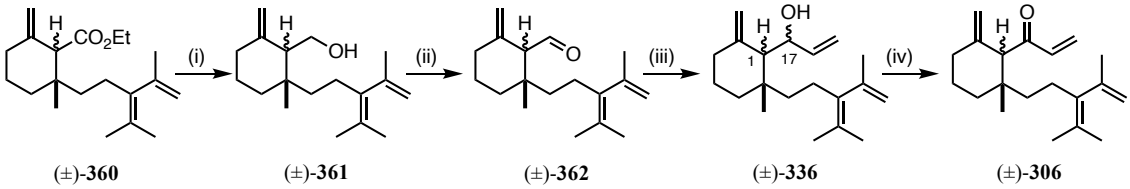

(±)-**360** (±)-**361** (±)-**362** (±)-**336** (±)-**306**

Scheme 4.25. Successful synthesis of enone (±)-**306** as a pair of diastereomers. Reagents and conditions: (i) $LiAlH_4$, THF, 0 °C to RT, 24 h, 90%; (ii) DMP, $NaHCO_3$, CH_2Cl_2, 0 °C, 1 h; (iii) vinylmagnesium bromide, Et_2O, 0 °C, 15 min, 58% over two steps; (iv) PCC, NaOAc, CH_2Cl_2, RT, 1h, 40%.

The key IMDA cycloaddition of enone (±)-**306** was attempted. Submission of (±)-**306**, as a pair of diastereomers, to the cycloaddition conditions resulted in good conversion of starting material; however, co-elution with a number of other products precluded efficient isolation of the desired taxane (±)-**132**. After careful purification by column chromatography, (±)-**132** was isolated in 15% yield.

Due to the difficulty that co-elution presented in the purification of secondary alcohol (±)-**336**, enone (±)-**306**, and taxane (±)-**132**, attention turned to separating the diastereomers at an earlier stage in the synthesis, expecting that this would result in cleaner product profiles and simplified purification steps (***Scheme 4.26***).

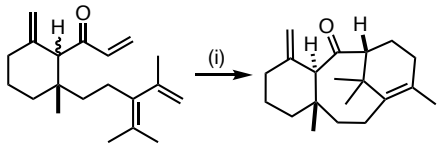

(±)-**306** (±)-**132**

Scheme 4.26. Synthesis of *trans*-taxane (±)-**132** from a mixture of diastereomers of (±)-**306**. Reagents and conditions: $BF_3.OEt_2$, CH_2Cl_2, 0 °C, 3 h, 15%.

At each stage of the synthesis the pairs of diastereomers had very similar, if not the same, R_f values; however, primary alcohol (±)-**361** was chosen as the diastereomers had the biggest difference, 0.43 (5% ethyl acetate in pentane) for (±)-*cis*-**361** and 0.40 (5% ethyl acetate in pentane) for (±)-*trans*-**361**. Purification by column chromatography generated a small amount of separated (±)-*cis*-**361** and (±)-*trans*-**361** along with a large

amount of a mixture of the two; repeated purification of the isolated mixtures generated 0.33 g of (±)-*cis*-**361** (18% yield) and 0.69 g of(±)-*trans*-**361** (37% yield), with a final 0.25 g mixture proving unproductive in further separations due to the decreasing amount of pure material isolated on this smaller scale.

This purification procedure resulted in a significant loss of material; however, it was deemed necessary to improve the subsequent synthetic steps. The relative stereochemistry had not, until this point, been assigned and so it was gratifying to observe that the desired (±)-*trans*-**361**, assigned by NOESY correlations, was the major component of the product mixture.

The later stages of the route were repeated from pure (±)-*trans*-**361** (***Scheme 4.27***). DMP oxidation furnished (±)-*trans*-**362** which, as before, was carried through to the next reaction without purification. Addition of vinylmagnesium bromide yielded secondary alcohol (±)-*trans*-**336** in 27% yield over two steps; purity of (±)-*trans*-**336** was favoured over yield and so, yet again, co-elution reduced the amount of (±)-*trans*-**336** that was able to be isolated in pure form. PCC-mediated oxidation furnished enone (±)-*trans*-**306** as a single diastereomer in an improved 54% yield and, submission of this material to the cycloaddition conditions generated taxane (±)-*trans*-**132** in 26% yield.

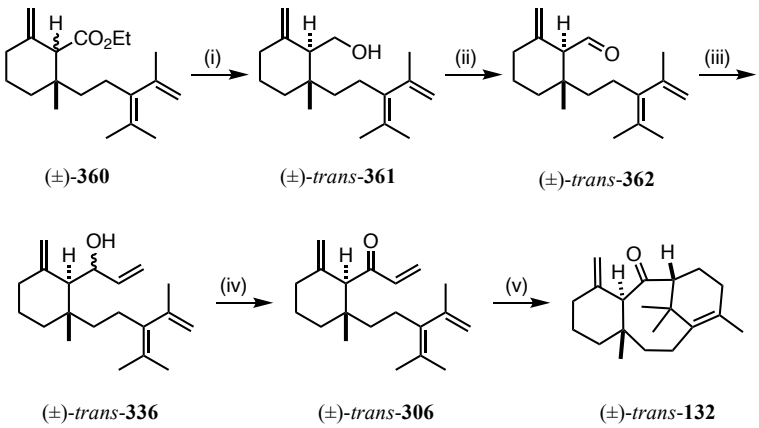

Scheme 4.27. Synthesis of taxane (±)-*trans*-**132** *via* purification of primary alcohol *trans*-**361**. Reagents and conditions: (i) $LiAlH_4$, THF, 0 °C to RT, 24 h, 37%; (ii) DMP, $NaHCO_3$, CH_2Cl_2, 0 °C, 1 h; (iii) vinylmagnesium bromide, Et_2O, 0 °C, 15 min, 27% over two steps; (iv) PCC, NaOAc, CH_2Cl_2, RT, 1h, 54%; (v) $BF_3 \cdot OEt_2$, CH_2Cl_2, 0 °C, 3 h, 26%.

The relative stereochemistry was confirmed by NOESY correlation data and conformed to a model, which lacked the *exo*-methylene group, proposed by Jenkins (***Scheme 4.28***).[222]

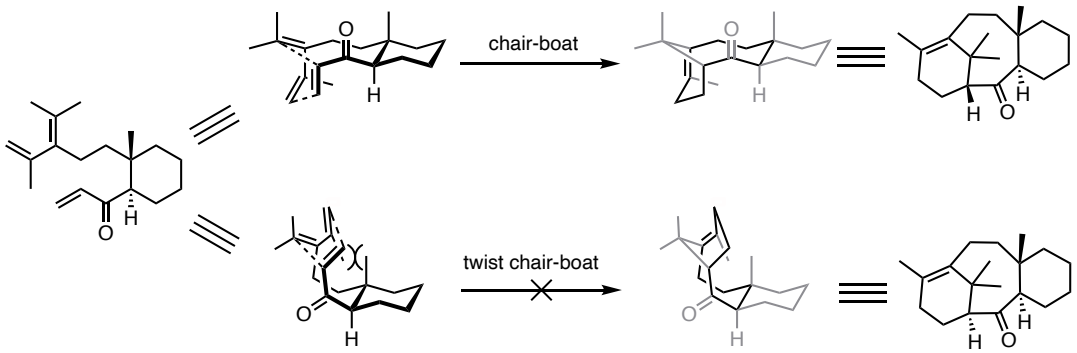

Scheme 4.28. Stereochemical model predicting the relative configuration for cycloaddition products. *Syn*-cycloaddition proceeds through a strained chair-boat-boat transition state precluding formation of the *syn*-taxane.

From the NMR spectrum of the crude product, it was clear that the product was generated along with an unidentified but major product (2:1 undesired:desired). Despite the isolation of a pure sample of the major product, structural assignment still proved impossible [diagnostic peaks: ^{1}H NMR (400 MHz, $CDCl_3$) δ 2.37 (br. s, 2H), 3.52 (s, 1 H), 4.77 (d, J = 5.5 Hz, 1 H, alkene), 5.52 (s, 2H, *exo*-methylene)]. It was proposed that, due to the strained nature of the forming *trans*-fused cyclooctene B-ring, an alternative lower energy pathway was operating. In order to test whether the *trans*-configuration was indeed reducing the efficacy of the Diels–Alder reaction, synthesis of (±)-*cis*-**132** was carried out.

4.2.7 Synthesis of taxane (±)-*cis*-132

The route towards taxane (±)-*cis*-**132** began with the sample of primary alcohol (±)-*cis*-**361** that had been generated during the isolation of (±)-*trans*-**361**.

DMP oxidation was carried out as before; however, in this case β,γ-unsaturated aldehyde (±)-*trans*-**362** was purified *via* column chromatography and, gratifyingly, this extra purification step significantly increased the yields of the following reactions. Addition of vinylmagnesium bromide generated secondary alcohol (±)-*cis*-**336** in 78%

yield and subsequent PCC mediated oxidation furnished enone (±)-*cis*-**306** in 61% yield (***Scheme 4.29***).

Surprisingly, upon submission of (±)-*cis*-**306** to the $BF_3 \cdot OEt_2$ cycloaddition conditions, *endo*-olefin (±)-**131** was produced in 57% yield. This increased yield, almost double that of (±)-*trans*-**132**, reflects the relative ease of the cycloaddition in the less-strained *cis*- system. Isomerisation to the *endo*-alkene present in (±)-**131** was probably facilitated by a small amount of water in the $BF_3 \cdot OEt_2$ which led to generation of a Brønsted acid. The increased flexibility in the *cis*-fused cyclooctene ring then allowed conversion to the *endo*-olefin, not observed with relatively strained taxane (±)-*trans*-**132**.

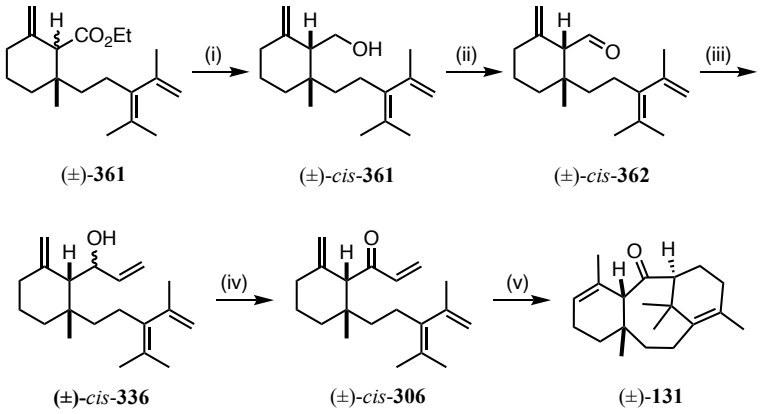

Scheme 4.29. Synthesis of taxane (±)-**131**. Reagents and conditions: (i) $LiAlH_4$, THF, 0 °C to RT, 24 h, 18%; (ii) DMP, $NaHCO_3$, CH_2Cl_2, 0 °C, 1 h, 80%; (iii) vinylmagnesium bromide, Et_2O, 0 °C, 15 min, 78%; (iv) PCC, NaOAc, CH_2Cl_2, RT, 1h, 61%; (v) $BF_3 \cdot OEt_2$, CH_2Cl_2, 0 °C, 3 h, 57%.

With a route established to racemic taxane (±)-*trans*-**132**, and having gained information about the effect of B-ring strain in the cycloaddition, attention turned to the synthesis of the separate enantiomers (+)-*trans*-**132** and (–)-*trans*-**132**.

4.3 Attempted synthesis of (+)-*trans*-132 and (–)-*trans*-132

The asymmetric conjugate addition using trimethylaluminium alongside CuTc and phosphoramidite (+)-**363** has been reported and so this was proposed for the route to (+)-*trans*-**132** and (–)-*trans*-**132** (***Scheme 4.30***).

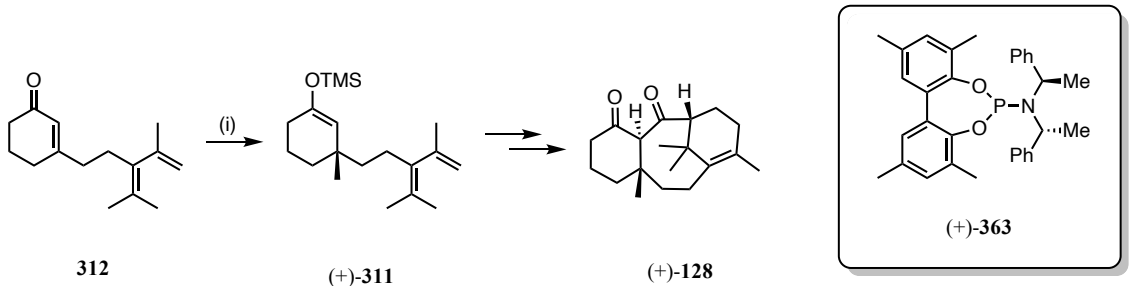

Scheme 4.30. Previously reported asymmetric conjugate addition employed in the synthesis of diketone (+)-**128**. Reagents: Me_3Al, CuTc, phosphoramidite (+)-**363**, TMSCl, THF, Et_2O, 89%, 93% ee.

For this, phosphoramidites (+)-**363** and (–)-**363** had to be prepared, beginning with the synthesis of bis-phenol **365**. Reproduction of the literature precedent,[223] with product purification by Kügelrohr distillation, yielded none of the desired product but purification by column chromatography then recrystallisation furnished **365** in 22% yield (lit. 15%).[223] The subsequent steps to the ligand enantiomers proceeded smoothly according to literature precedent, generating (+)-**363** in 67% yield and (–)-**363** in 70% yield (***Scheme 4.31***).

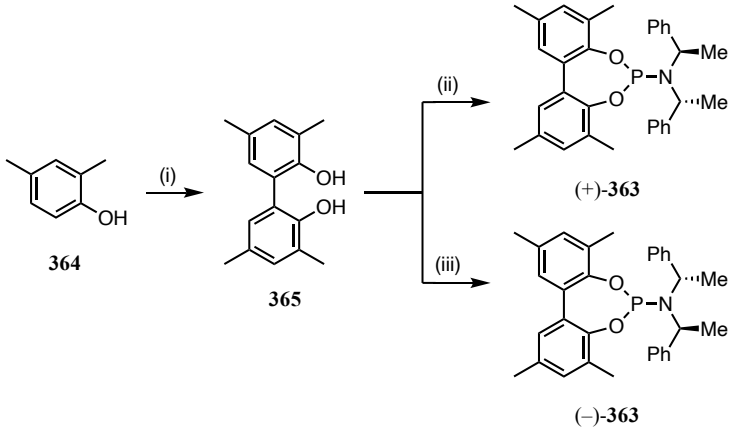

Scheme 4.31. Sythesis of chiral phosphoramidite ligands required for asymmetric conjugate addition reaction. Reagents and conditions: $FeSO_4 \cdot H_2O$, $Na_2S_2O_8$, water, RT, 48 h, 22%; (ii) PCl_3, Et_3N, (+)-bis[(*R*)-1-phenethyl]amine, bis-phenol **365**, CH_2Cl_2, 0 °C to RT, 4.5 h, 67%; PCl_3, Et_3N, (–)-bis[(*S*)-1-phenethyl]amine, bis-phenol **365**, CH_2Cl_2, 0 °C to RT, 4.5 h, 70%.

Initial studies on the asymmetric conjugate addition were carried out with ligand (+)-**363** in an effort to reproduce the literature reaction as closely as possible. In our hands, use of trimethylsilyl chloride to trap the aluminium enolate *in situ* was unsuccessful, with none of the desired silyl enol ether being present. Instead, ketone **366** was

observed and it was proposed that the aluminium enolate was too stable to be silylated at the reaction temperature of –40 ºC (***Scheme 4.32a***). Using trimethylsilyl triflate as a more reactive electrophile, so that the aluminium enolate could be trapped without raising the temperature, the silyl enol ether was generated successfully.

From this point, esterification with ethyl cyanoformate formed **359** as a mixture of diastereomers, and Wittig reaction generated β,γ-unsaturated ester **360**, again as a mixture of diastereomers.

Up to this point no specific rotation data were taken due to the presence of diastereomeric mixtures; however, after $LiAlH_4$-mediated reduction to alcohol (+)-*trans*-**361**, the mixture of diastereomers was separated and analysis undertaken. Although the $LiAlH_4$ reduction resulted in very poor conversion of starting material, sufficient alcohol was obtained to carry out analysis (***Scheme 4.32b***).

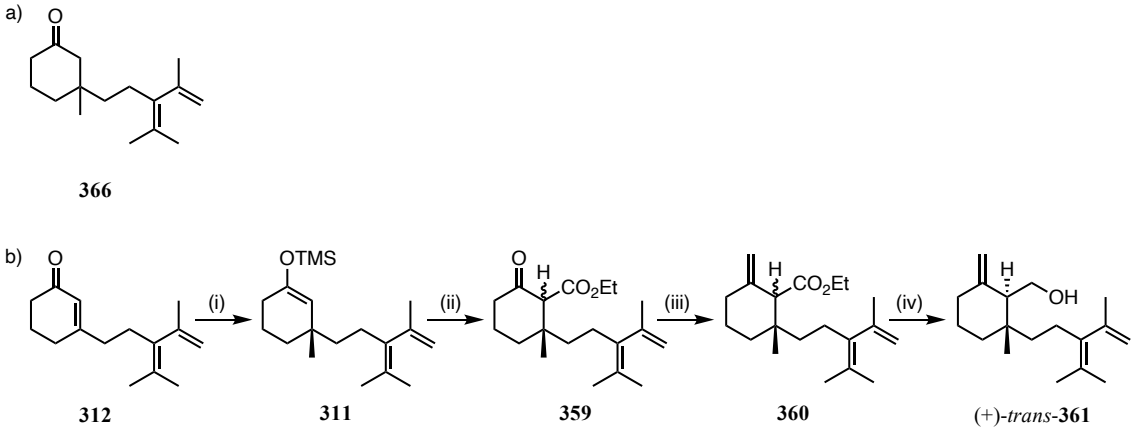

Scheme 4.32a). Ketone **266** formed through prontonation of a stable aluminium enolate. ***b)*** Synthesis of (+)-*trans*-**361**. Reagents and conditions: Me_3Al, CuTc, phosphoramidite (+)-**363**, TMSOTf, Et_2O, THF, –40 °C, 17 h; (ii) *n*-BuLi, ethyl cyanoformate, Et_2O, –78 °C to RT, 16 h; (iii) $MePPh_3Br$, KO*t*Bu, THF, 70 °C, 1 h, 55% over three steps; (iv) $LiAlH_4$, THF, 0 °C to RT, 24 h, 6%.

A specific rotation value of $[\alpha]_D^{25}$ +3.0 (c 0.8, $CHCl_3$) was recorded but, more importantly, reaction with Mosher's acid chloride gave an enantiomeric excess value of ~26%. This low level of enantioenrichment was not expected considering the reported value of 93% and so, since optimisation of this reaction was not within the scope of this

project, and with time constraints in mind, it was decided to move on to CYP102A1 screening of (±)-*trans*-**132**.

4.4 P450$_{BM3}$ screening

The inefficiency of the Diels–Alder cycloaddition of enone (±)-*trans*-**132**, meant that only ~50 mg of the cycloadduct had been isolated; therefore, in order to garner as much information as possible, a panel of 48 screening enzymes was selected whose members had been developed for the oxidation of small saturated heterocyclic amines as well as those developed for larger steroidal cores.

(±)-*Trans*-**132** could not be dissolved in DMSO to generate a 100 mM solution, but a 50 mM solution was obtained by adding sufficient chloroform to the DMSO mixture to dissolve the substrate then removing the chloroform *in vacuo*. The screening reactions were carried out on a 0.5 mL scale in 24-well plates; each well contained: 100 mM glucose, 1.0 mM substrate, 2.0 U/mL GDH, 80 μM $NADP^+$, 2.0 μM CYP102A1 variant, and 200 mM phosphate buffer. Previous group work showed that addition of β-cyclodextrin reduced the reactivity of taxane systems towards oxidation and so no cyclodextrin was added. After 24 h the wells were extracted with ethyl acetate and analysed by GC. Conversion was, in general, poor and only the variants with more open active sites were able to oxidise the large taxane system (see §**8.3**). In particular glycine mutations, which act to "hollow out" the active site, acted to increase reactivity; however, there were a number of exceptions to this, with RKAI/TG/A328G and GVQ/I263G both converting <25% of the substrate.

4.5 Preparative scale CYP102A1 reactions

Scale-up reactions were carried out in order to characterise the metabolites and, due to the small amount of material available for testing, two variants that showed good reactivity and complex but differing product profiles, RK/A328G and GV/AI, were

chosen in order to gain access to as many oxidation products as possible. Both of these variants contain residues that create space within the active site: F87A and A328G in RKA328G, and A74G in GV/AI.

Scale-up reactions were carried out at a concentration of 2.0 μM in a reaction volume of 40 mL with reagent concentrations the same as those used for screening. GC analysis of the reaction mixtures after 24 h showed incomplete consumption of starting material for both RK/A328G and GV/AI; therefore, addition of the relevant enzyme variant, $NADP^+$, GDH, and glucose was repeated, and the reactions were shaken for a further 24 h, to complete the consumption of starting material. The reaction mixtures were saturated with NaCl in order to aid extraction of the dilute solution with ethyl acetate

4.5.1 Characterisation of GV/AI metabolites

Following the above protocol with GV/AI, eight separate fractions were isolated by column chromatography but only one was sufficiently clean to be characterised by NMR analysis. A lack of any C**H**OH resonances implied that oxidation to a carbonyl had taken place, confirmed by a resonance at 171.0 ppm in the ^{13}C NMR spectrum; the relatively low chemical shift of this resonance suggested that the ketone could be α,β-unsaturated. COSY and HMBC NMR experiments were employed to reveal the position of the carbonyl within the molecule, confirming the unsaturated nature of ketone (+)-**367** (***Figure 4.6***). High resolution mass spectrometry data (found: 301.2162, $C_{20}H_{29}O_2$ requires 301.2162) agreed with the assignment. The specific rotation value was measured to be $[\alpha]_D^{25}$ +7.4 (*c* 0.07, $CHCl_3$) but the small amount of material isolated (0.7 mg) precluded analysis by Moshers' esterification so no approximate % ee value was obtained. Due to the lack of pure enantiomer substrates, absolute configuration was unable to be assigned.

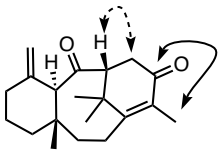

(+)-**367**

Figure 4.6. Structure of α,β-unsaturated ketone isolated from reaction of (±)-*trans*-**132** with GV/AI. Conditions: 2 μM GV/AI, 1mM (±)-**132**, 100 mM glucose, 2 U/mL GDH, 80 μM $NADP^+$, 200 mM phosphate buffer, 20 °C, 48 h; 6%. The dashed arrow denotes a COSY NMR correlation and the solid arrow denotes an HMBC NMR correlation.

4.5.2 Characterisation of RK/A328G metabolites

Following the same protocol with RK/A328G, purification by column chromatography generated nine fractions, of which three were able to be characterised by NMR analysis. It was clear that all three products were diols with characteristic C**H***O*H resonances between 3.9 and 4.25 ppm.

The first diol (**368**) to be characterised was identified within a 2:1 mixture of compounds with the diol as the major component, diagnostic resonances being observed at 3.91 (dd, J = 11.5, 5.5 Hz, 1H, C8-**H**) and 4.08 (dd, J = 8.5, 6.0 Hz, 1H, C19-**H**). The regiochemistry was assigned through use of COSY and HMBC spectra and NOESY was employed to determine the relative stereochemistry; nOe correlations were observed between C19-**H**, C1-**H** and C8-**H**, C7-$\mathbf{H_3}$ (***Figure 4.7***). The specific rotation value was measured to be $[\alpha]_D^{25}$ +32.2 (*c* 0.18, $CHCl_3$); however, due to the presence of alcohol **369** in the mixture, this value is not accurate for diol **368**.

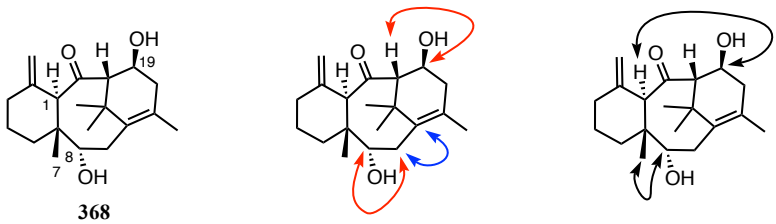

368

Figure 4.7. Structure of diol **368** isolated from reaction of (±)-*trans*-**132** with RK/A328G. The red arrows denote a COSY NMR correlation, the blue arrow denotes an HMBC NMR correlation, and the black arrows show nOe correlations.

The minor compound was tentatively assigned to be mono-alcohol **369**, with the

regiochemistry being assigned through the similarity of the coupling constants of the C**H**OH resonance to those in diol **368** [4.02 (dd, *J* = 12.0, 5.0 Hz) for mono-alcohol **369**, 3.91 (dd, *J* = 11.5, 5.5 Hz) for diol **368**]. COSY data reinforced this assignment with coupling between C8-**H** and two resonances which, according to the HSQC spectrum, belonged to the diastereotopic protons within a methylene group. The stereochemistry was assigned by analogy with that of diol **368**, with the possibility that mono-alcohol **369** is an intermediate in the formation of **368** (***Figure 4.8***).

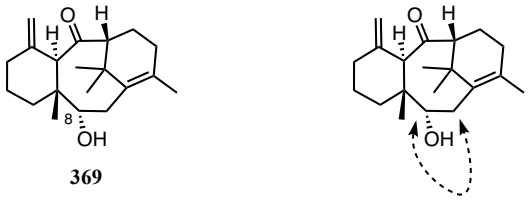

369

Figure 4.8. Tentative structure of alcohol **369** isolated from reaction of (±)-*trans*-**132** with RK/A328G. The dashed arrow denotes a key COSY NMR correlation.

The next diol (**370**) to be characterised again displayed oxidation on the A- and B-rings, with C**H***O*H resonances at 4.03 (dt, *J* = 11.0, 5.0 Hz, 1H, C9-**H**) and 4.23 (td, *J* = 9.5, 4.5 Hz, 1H, C19-**H**). As with **368**, COSY and HMBC NMR correlations were key in determining the regiochemistry, and NOESY shed light on the stereochemistry, with the presence of nOe correlation between C19-**H**, C1-**H** and lack of nOe correlation between C9-**H**, C7-**H₃** allowing characterisation of the relative stereochemistry. This diol **370**, like diol **368**, was identified within a 2:1 mixture of compounds; however, the NMR data were insufficiently clear to assign the minor metabolite, even tentatively. As with diol **368**, a specific rotation value was obtained despite the presence of this unknown impurity, $[\alpha]_{\mathrm{D}}^{25}$ +53.6 (*c* 0.03, $CHCl_3$) (***Figure 4.9***).

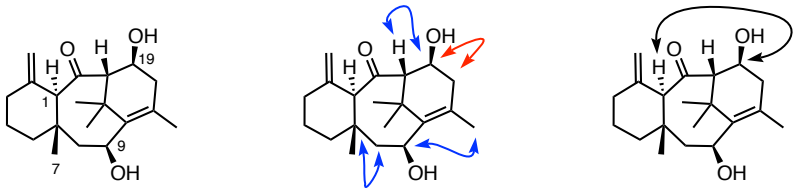

370

Figure 4.9. Structure of diol **370** isolated from reaction of (±)-*trans*-**132** with RK/A328G. The red arrow denotes a COSY NMR correlation, the blue arrow denote HMBC NMR correlations, and the black arrow shows an nOe correlation.

The final metabolite ((+)-**371**) to be identified was another product of oxidation of both the A- and B- rings. Diagnostic C**H**OH resonances appeared at 3.92–3.98 (m, 1H, C8-**H**) and 4.21 (d, J = 9.0 Hz, 1H, C12-**H**), and COSY and HMBC NMR spectra allowed determination of the regiochemistry (***Figure 4.10***). The NOESY spectrum showed the nOe correlations between C7-$\mathbf{H_3}$, C8-**H** and C12-**H**, C13-$\mathbf{H_3}$ supporting the assigned relative stereochemistry. The specific rotation value was measured to be $[\alpha]_{\mathrm{D}}^{25}$ +19.3 (c 0.06, $CHCl_3$).

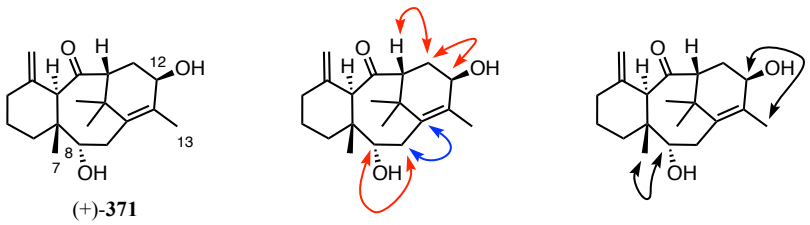

(+)-**371**

Figure 4.10. Structure of diol (+)-**371** isolated from reaction of (±)-*trans*-**132** with RK/A328G. The red arrows denote COSY NMR correlations, the blue arrow denotes an HMBC NMR correlation, and the black arrows show nOe correlations.

The non-zero specific rotation values for the isolated taxane metabolites indicated that kinetic resolution processes were occurring with the reaction mixture; however, due to the small amounts of material isolated, no Mosher's analysis was undertaken and no % ee values were obtained. Again, due to the lack of pure enantiomer substrates, no absolute configurations were able to be assigned.

The prevalence of double oxidation in the isolated metabolites is of interest. Although **369** was tentatively characterised as an alcohol in a mixture with **368**, no mono-alcohols were isolated as pure samples. This observation was proposed to be a consequence of

the low reactivity of RK/A328G towards (±)-**132**. The reaction was carried out over a 48 h period, with an additional aliquot of enzyme added after 24 h. This extended reaction time would have allowed further oxidation to occur, resulting in the observed product profile. Quenching of the reaction after 24 h, before complete consumption of (±)-**132**, could allow isolation of singly hydroxylated products, further filling out the product profile of this reaction.

4.5.3 Conclusions and future work

A preliminary investigation of the hydroxylation of taxane (±)-*trans*-**132** with CYP102A1 variants produced a number of metabolites; these reactions need to be carried out on larger scale in order to identify all the metabolites produced and, in particular, to look for C-ring oxidation products (***Scheme 4.33***).

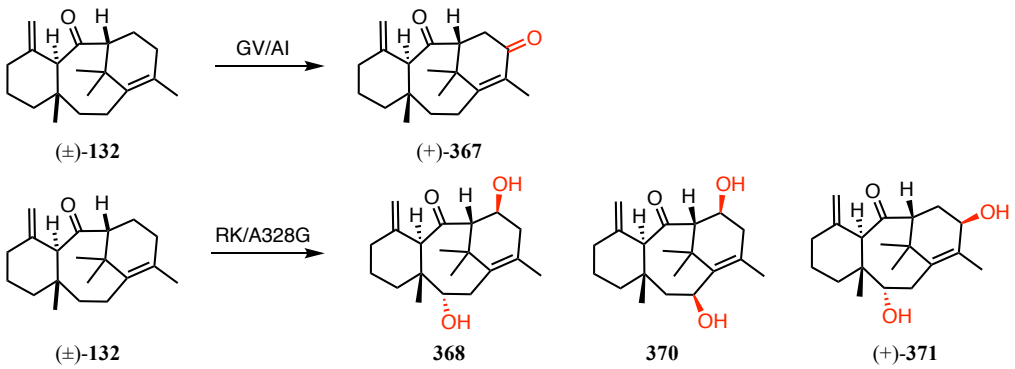

Scheme 4.33. Overall metabolite profile of the reactions between (±)-*trans*-**132** and CYP102A1 variants GV/AI and RK/A328G. Conditions: 2 µM CYP102A1 variant, 1mM (±)-**132**, 100 mM glucose, 2 U/mL GDH, 80 µM $NADP^+$, 200 mM phosphate buffer, 20 °C, 48 h; 6% (+)-**367**, 14% **368**, 2% **370**, (+)-**371** 5%.

Kinetic resolution was clearly taking place with this complex substrate but further investigation, as was carried out with tricycle **117** and lactone **115**, is required to understand this process in greater detail. In order to isolate quantities of substrate sufficient for a thorough examination of the biocatalytic hydroxylation of the racemate, optimisation of the IMDA cycloaddition to taxane (±)-*trans*-**132** is required; however, separation of mixtures of diastereomers, a problem which is difficult to overcome, was

the overriding factor in the poor overall yield. The synthesis of (+)-*trans*-**132** and (–)-*trans*-**132** also requires more work, with these compounds being needed in order to understand the nature of the kinetic resolution process through UV binding titrations; chiral preparative HPLC separation of a racemic sample may be the most efficient way to achieve these separate enantiomers.

5 Conclusions and future work

This work has probed the efficacy of cytochrome P450 variants as oxidation catalysts towards three difference substrates, with clear evidence of kinetic resolution being observed.

Investigation into the oxidation of non-natural hydrocarbon substrate, racemic tricycle (±)-**117**, showed that the CYP102A1 variants were able to hydroxylate a wide range of positions (***Table 5.1***). Variants RK/T260G and RK/T269G were further investigated with respect to kinetic resolution which revealed that the oxidised metabolites were produced in high enantiomeric excess (85% and 96% respectively). The origins of this kinetic resolution process were probed using UV binding titration; however, no difference in K_d was observed implying that the differing reactivity between the enantiomers must be a product of contrasting orientations within the active site. An attempt to utilise this reactivity in the synthesis of margocin (**218)** was complicated by the presence of an additional *i*-Pr group, highlighting the difficulty in using model systems to probe enzyme reactivity. Future work will focus on improving the scalability of these oxidation reactions in order to assess their viability as useful synthetic procedures.

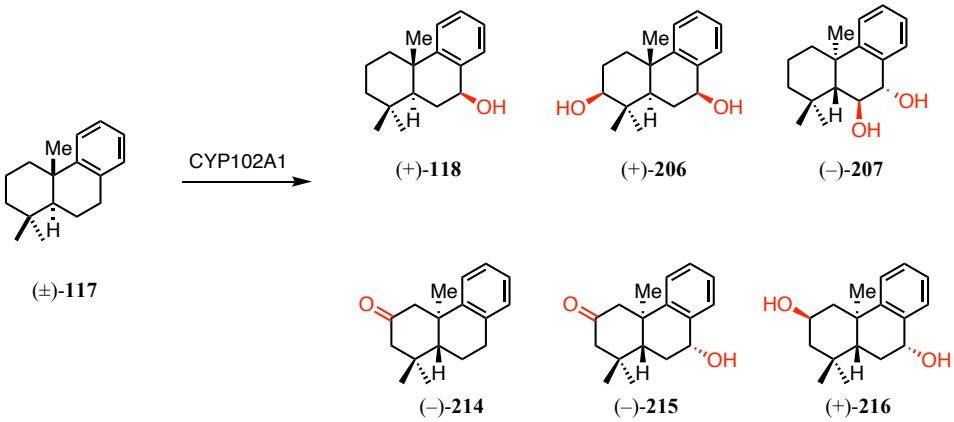

Table 5.1. Overall metabolite profile from catalytic oxidations of (±)-**117** by CYP102A1 variants.

Entry	Variant	Conv.	(+)-**118** (% ee)	(+)-**206** (% ee)	(–)-**207**	(–)-**214**	(–)-**215**	(+)-**216**
1	RK/T260G	80%	22% (85%)	-	-	-	-	-
2	RK/T269G	95%	-	16% (96%)	-	-	-	-
3	RK/Q403P	86%	-	38%	3%	-	-	-
4	GVQ	100%	5%	15%	-	5%	6%	4%
5	RK/A328G	88%	-	45%	12%	-	-	-

Cytochrome P450s have also been shown to be reactive towards bicyclic lactone (±)-**115**, an eleutherobin precursor. Reaction with four enzyme variants produced four metabolites and again kinetic resolution was observed. Modification of the enzyme variant employed allowed control of the reaction profile and access to (+)-**125**, (+)-**124**, (+)-**126**, and (+)-**116** metabolites in >57% ee (***Table 5.2***). Future work will involve investigating the origins of the kinetic resolution with this substrate, as well as possible derivatisation towards eleutherobin-like compounds in order to probe the biological activity of these hydroxylated analogues.

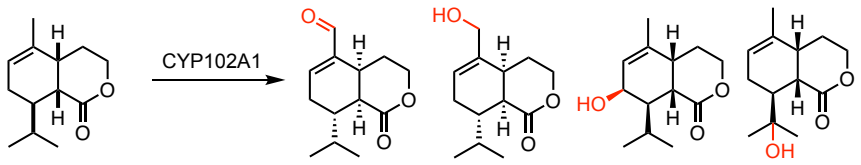

Table 5.2. Overall metabolite profile from catalytic oxidations of (±)-**115** by CYP102A1 variants.

Entry	Variant	Conv.	% (+)-**125**[a]	% (+)-**124**[a]	% (+)-**116**[a]	% (+)-**126**[a]
1	GVQ	98%	8 (80%)	18 (18%)	16 (43%)	-
2	KSK19/I263A	99%	17 (66%)	27 (71%)	12 (57%)	-
3	R19/A330W	92%	-	25 (61%)	-	44%
4	R19/FI	45%	-	22 (44%)	-	-

[a] % ee shown in brackets.

In order to investigate the reactivity of CYP102A1 variants towards more complex substrates, especially with respect to kinetic resolution, synthesis of taxadienone (±)-*trans*-**132** was carried out. The synthetic route generated enough material to begin initial investigations into the behaviour of (±)-*trans*-**132** as a substrate in CYP102A1 catalysed oxidations; however, the overall yield was poor (11% from known enone (±)-**306**) and further work will be necessary to improve this. In particular a large amount of material was lost through the formation, and the separation from (±)-*trans*-**361**, of the undesired (±)-*cis*-**361**. The synthesis of the enantiomers, (+)-*trans*-**132** and (–)-*cis*-**132**, following Baran's asymmetric conjugate addition procedure, was unsuccessful and future work will attempt to gain access to these compounds in order to assign the absolute configuration of isolated metabolites (***Scheme 5.1***).

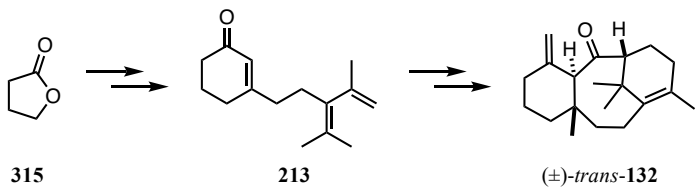

Scheme 5.1. Synthesis of taxane (±)-*trans*-**132** *via* known enone **312.**

Submission of (±)-*trans*-**132** to P450 catalysed oxidation conditions led to the isolation of four metabolites from complex mixtures of products (***Table 5.3***). Despite non-zero specific rotation values indicating the non-racemic nature of these products, the material isolated was insufficient for Mosher's analysis and larger scale reactions will be necessary to determine enantiomeric excess values.

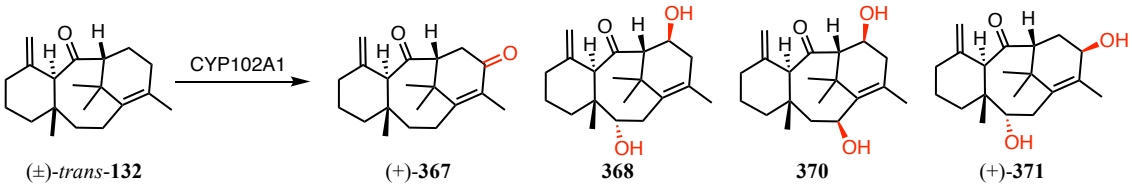

Table 5.3. Overall metabolite profile from catalytic oxidations of (±)-*trans*-**132** by CYP102A1 variants.

Entry	Variant	Conv.	% (+)-**367**	**368**	% **370**	% (+)-**371**
1	GV/AI	100%	6%	-	-	-
2	RK/A328G	100%	-	14%[a]	2%[a]	5%

[a]Isolated as a mixture of two metabolites.

The diversity of products isolated displays the strengths of this biocatalytic methodology; four different C–H bonds were oxidised of which two are chemically unactivated. A broader screen, alongside larger scale reactions, would allow isolation of more metabolites, with oxidation of the *C* ring of particular interest. The use of GC analysis in this work may have precluded the detection of polyhydroxylated products which are of interest due to their similarity to paclitaxel (**234**) itself. Future work would benefit from the use of LC-MS analysis to detect the presence of these highly polar metabolites, if they are indeed formed.

These hydroxylated metabolites could, in principle, be taken forward to investigate the biological behaviour of oxidised taxanes and taxol analogues, as well as acting as useful starting points for further elaboration to naturally occurring taxanes. Overall, CYP102A1 variants have been shown to catalyse oxidative kinetic resolution reactions

of complex non-natural substrates, and have the potential to be developed into useful reagents for the late-stage incorporation of oxygen in a stereocontrolled manner.

6 Experimental

6.1 Materials and Methods

Atom numbering illustrate peak assignments and does not necessarily correspond to IUPAC nomenclature. Solvents and reagents were used as commercially supplied or purified by standard techniques. Acetonitrile, Et_2O, CH_2Cl_2 and benzene were obtained from Grubbs canisters, with the solvent passing through an activated alumina column under argon. THF was freshly distilled over Na/ benzophenone. DIPA was distilled over KOH and stored under Ar. All glassware was oven-dried overnight or flame dried before use.

Merck aluminium-backed DC60 F254 plates (0.2 mm) were used for TLC analysis and were visualised with long wave ultra-violet light before staining with potassium permanganate, iodine or vanillin and developed with heat. Merck silicagel 60 (43- 60 μm) was used for column chromatography and the solvent system used and retention factors are recorded with experimental data.

Proton ^{1}H, carbon ^{13}C NMR spectra were recorded on a Bruker AVIII400 MHz, 500 MHz or 700 MHz spectrometer as specified. δH and δC are recorded to the nearest 0.01 ppm and 0.1 ppm respectively; coupling constants have been rounded to the nearest 0.5 Hz. Peak multiplicities are described as apparent (app.), broad (br.), singlet (s), doublet (d), triplet (t), quartet (q), pentet (p), heptet (hept) or as combinations or multiplets (m). Solvents are referenced as C_6D_6: δH 7.16, δC 128.06 ppm; $CDCl_3$ δH 7.26, 77.16 ppm. Peak assignments were made based on chemical shift, integration, coupling constants, COSY and HSQC spectra. HMBC and NOESY spectra were obtained if required. Infra-red spectra were recorded using a Bruker Tensor 27 FT-IR spectrometer. Absorption maxima are reported in wavenumbers/cm^{-1} and described as strong (s), medium (m), weak (w) and broad (br.) relative to the most intense peak. Low resolution mass spectra

were recorded using a Micromass LCT Premier spectrometer (ESI±). High resolution mass spectra were obtained for novel compounds on a Bruker Daltronics MicroTOF spectrometer (ESI/FI). Mass to charge ratios (*m/z*) are reported in Daltons and intensities are recorded as a percentage relative to the most intense peak. The injector temperature was 280 °C and the FID was at 250 °C. Melting points are recorded in degree Celsius using a Griffin melting point apparatus, where relevant a range may be specified.

6.2 Synthesis of substrates

(*R*)-2,2'-Bis(methoxymethoxy)-1,1'-binaphthalene[162] (*R*)-**190**

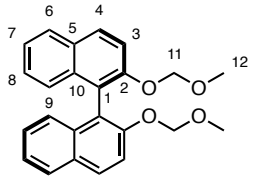

NaH (1.75 g, 60% oil emulsion, 43.6 mmol) was added to a flask under Ar and washed with dry pentane (3 × 10 mL) then the flask was filled with dry THF (75 mL) and dry DMF (35 mL) at 0 °C. A solution of (*R*)-BINOL (5.00 g, 17.5 mmol) in THF (25 mL) was added slowly to the suspension and stirred at RT for 2 h. After this time chloromethyl methyl ether (3.3 mL, 43.6 mmol) was added slowly and stirring continued for 6 h at RT. The reaction was quenched with water (100 mL) and extracted with ethyl acetate (3 × 100 mL). The combined organic layers were washed with water (50 mL) and brine (50 mL), dried over Na_2SO_4, and concentrated *in vacuo* to obtain a pale-yellow oil. Purification by trituration with 10% CH_2Cl_2 in pentane (15 mL) gave the title compound as a white solid (5.69 g, 87%). ^{1}H NMR (400 MHz, $CDCl_3$) δ 3.15 (s, 6H, C12-**H$_3$**), 4.98 (d, *J* = 7.0 Hz, 2H, C11-**H$_a$**H$_b$), 5.08 (d, *J* = 7.0 Hz, 2H, C11-H$_a$**H$_b$**), 7.13 – 7.18 (m, 2H, C9-**H**), 7.22 (ddd, *J* = 8.5, 6.5, 1.5 Hz, 2H, C7-**H**), 7.35

(ddd, *J* = 8.0, 6.5, 1.5 Hz, 2H, C8-**H**), 7.58 (d, *J* = 9.0 Hz, 2H, C3-**H**), 7.87 (dt, *J* = 9.5, 1.5 Hz, 2H, C6-**H**), 7.95 (dd, *J* = 9.0, 1.5 Hz, 2H, C4-**H**); ^{13}C NMR (101 MHz, $CDCl_3$) δ 56.0 (C-12), 95.4 (C-11), 117.5 (C-3), 121.5 (C-1), 124.2 (C-8), 125.7 (C-9), 126.4 (C-7), 128.0 (C-6), 129.5 (C-4), 130.0 (C-5), 134.2 (C-10), 152.8 (C-2); *m/z* ([ESI$^+$]): 297.2 ([M+Na]$^+$).

(*R*)-3,3'-Dichloro-2,2'-bis(methoxymethoxy)-1,1'-binaphthalene[163] (*R*)-**191**

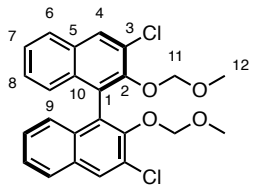

To a solution of (*R*)-**190** (5.00 g, 13.35 mmol) in Et_2O (230 mL) was added *n*-BuLi (16 mL, 2.5 M in hexanes, 40.1 mmol) at RT. After stirring for 3 h the reaction was cooled to 0 °C and hexachloroethane (9.50 g, 40.1 mmol) was added as a solution in THF (150 mL). Stirring continued as the mixture was left to warm to RT overnight after which the reaction was quenched with NH_4Cl. The layers were separated, and the aqueous layer was extracted with CH_2Cl_2 (3 × 50 mL). The combined organic layers were dried over Na_2SO_4 and concentrated *in vacuo* to yield a yellow oil. The crude mixture was inseparable by column chromatography and so was used without further purification. A small amount of the crude yellow oil was triturated with pentane to yield a white solid for analytical purposes. ^{1}H NMR (400 MHz, $CDCl_3$) δ 2.59 (s, 6H, C12-**H$_3$**), 4.81 – 4.84 (m, 2H, C11-**H$_a$**H$_b$), 4.84 – 4.87 (m, 2H, C11-H$_a$**H$_b$**), 7.19 (dd, *J* = 8.5, 1.5 Hz, 2H, C9-**H**), 7.26 (ddd, *J* = 8.0, 7.0, 1.5 Hz, 2H, C7-**H**), 7.41 (ddd, *J* = 8.5, 8.0, 1.0 Hz, 2H, C8-**H**), 7.78 (dd, *J* = 7.0, 1.0 Hz, 2H, C6-**H**), 8.06 (s, 2H, C4-**H**); ^{13}C NMR (101 MHz, $CDCl_3$) δ 56.3 (C-12), 99.0 (C-11), 126.1, 126.5, 126.8, 127.0, 127.6, 127.7, 129.5, 131.0, 132.7, 149.4 (Ar**C**); *m/z* ([ESI$^+$]): 465.0 ([M+Na]$^+$).

(*R*)-3,3'-Dichloro-2,2'-dihydroxy-1,1'-binaphthalene[163] (*R*)-**192**

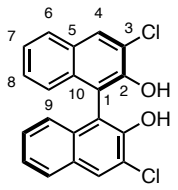

(*R*)-**191** (4.00 g, 9.0 mmol) was dissolved in 1:1 (v/v) MeOH:THF (280 mL) and Amberlyst-15 (4.00 g, 100% w/w). The mixture was stirred at reflux overnight after which time it was cooled to RT and filtered. The filtrate was concentrated *in vacuo* and the residue was purified by flash column chromatography (pentane:EtOAc 10:1) to give the title compound as an off-white solid (1.51 g, 32% over two steps). ^{1}H NMR (400 MHz, $CDCl_3$) δ 7.05 – 7.14 (m, 2H, C9-**H**), 7.30 (ddd, *J* = 8.0, 7.0, 1.5 Hz, 2H, C7-**H**), 7.39 (ddd, *J* = 8.5, 7.0, 1.5 Hz, 2H, C8-**H**), 7.77 – 7.84 (m, 2H, C6-**H**), 8.07 (s, 2H, C4-**H**); ^{13}C NMR (101 MHz, $CDCl_3$) δ 115.1 (C-1), 122.3 (C-3), 124.8 (C-9), 125.1 (C-8), 127.6 (C-7), 127.6 (C-6), 129.3 (C-5), 129.3 (C-4), 132.5 (C-10), 147.6 (C-2); *m/z* ([ESI$^+$]): 355.0 ([M+H]$^+$).

(*S*)-2,2'-Bis(methoxymethoxy)-1,1'-binaphthalene[224] (*S*)-**190**

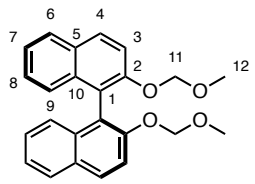

NaH (1.75 g, 60% oil emulsion, 43.6 mmol) was added to a flask under Ar and washed with dry pentane (3 × 10 mL) then the flask was filled with dry THF (75 mL) and dry DMF (35 mL) at 0 °C. A solution of (*S*)-BINOL (5.00 g, 17.5 mmol) in THF (25 mL) was added slowly to the suspension and stirred at RT for 2 h. After this time chloromethyl methyl ether (3.3 mL, 43.6 mmol) was added slowly and stirring

continued for 6 h at RT. The reaction was quenched with water (100 mL), the layers separated, and the aqueous layer extracted with EtOAc (3 × 100 mL). The combined organic layers were washed with water (50 mL) and brine (50 mL), dried over Na_2SO_4, and concentrated *in vacuo* to obtain a pale-yellow oil. Purification by trituration with pentane gave the title compound as a white solid (5.37 g, 82%). ^{1}H NMR (400 MHz, $CDCl_3$) δ 3.15 (s, 6H, C12-**H$_3$**), 4.98 (d, *J* = 7.0 Hz, 2H, C11-**H$_a$**H$_b$), 5.09 (d, *J* = 7.0 Hz, 2H, C11-H$_a$**H$_b$**), 7.16 (app. d, *J* = 8.5 Hz, 2H, C9-**H**), 7.23 (ddd, *J* = 8.0, 6.5, 1.5 Hz, 2H, C7-**H**), 7.35 (ddd, *J* = 8.5, 6.5, 1.5 Hz, 2H, C8-**H**), 7.58 (d, *J* = 9.0 Hz, 2H, C3-**H**), 7.88 (app. d, *J* = 8.0 Hz, 2H, C6-**H**), 7.92 – 7.99 (m, 2H, C4-**H**); ^{13}C NMR (101 MHz, $CDCl_3$) δ 56.0 (C-12), 95.4 (C-11), 117.5 (C-3), 121.5 (C-1), 124.2 (C-8), 125.7 (C-9), 126.4 (C-7), 128.0 (C-6), 129.5 (C-4), 130.0 (C-5), 134.2 (C-10), 152.8 (C-2); *m/z* ([ESI$^+$]): 397.2 ([M+H]$^+$).

(*S*)-3,3'-Dichloro-2,2'-bis(methoxymethoxy)-1,1'-binaphthalene[163] (*S*)-**191**

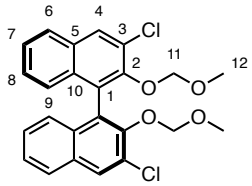

To a solution of (*S*)-**190** (5.00 g, 13.4 mmol) in Et_2O (230 mL) was added *n*-BuLi (16 mL, 2.5 M in hexanes, 40.1 mmol) at RT. After stirring for 3 h the reaction was cooled to 0 °C and hexachloroethane (9.50 g, 40.1 mmol) was added as a solution in THF (150 mL). Stirring continued as the mixture was left to warm to RT overnight after which the reaction was quenched with NH_4Cl. The layers were separated, and the aqueous layer was extracted with CH_2Cl_2 (3 × 50 mL). The combined organic layers were dried over Na_2SO_4, filtered, and concentrated *in vacuo* to yield a yellow oil. The crude mixture was inseparable by column chromatography and so was used without further

purification. A small amount of the crude yellow oil was triturated with pentane to yield a white solid for analytical purposes. ^{1}H NMR (400 MHz, $CDCl_3$) δ 2.59 (s, 6H, C12-**H$_3$**), 4.82 (d, *J* = 6.0 Hz, 2H, C11-**H$_a$**H$_b$), 4.86 (d, *J* = 6.0 Hz, 2H, C11-H$_a$**H$_b$**), 7.19 (app. d, *J* = 8.5 Hz, 2H, C9-**H**), 7.29 (ddd, *J* = 8.5, 7.0, 1.5 Hz, 2H, C7-**H**), 7.45 (ddd, *J* = 8.5, 7.0, 1.5 Hz, 2H, C8-**H**), 7.81 (app. d, *J* = 8.5 Hz, 2H, C6-**H**), 8.07 (s, 2H, C4-**H**); ^{13}C NMR (101 MHz, $CDCl_3$) δ 56.4 (C-12), 99.1 (C-11), 126.2 (C-8), 126.6 (C-9), 126.9 (C-7), 127.1 (C-6), 127.6, 127.8 (Ar**C**), 129.6 (C-4), 131.1, 132.7 (Ar**C**), 149.5 (C-2); *m/z* ([ESI$^+$]): 465.0 ([M+Na]$^+$).

(*S*)-3,3'-Dichloro-2,2'-dihydroxy-1,1'-binaphthalene[163] (*S*)-**192**

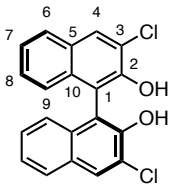

Crude (*S*)-**191** (75 mg, 0.17 mmol) was dissolved in 1:1 (v/v) MeOH:THF (5.6 mL) and Amberlyst-15 (75 mg, 100% w/w). The mixture was stirred at reflux overnight after which time it was cooled to RT and filtered. The filtrate was concentrated *in vacuo* and the residue was purified by flash column chromatography (pentane:EtOAc 10:1) to give the title compound as an off white solid (49 mg, 82%). ^{1}H NMR (400 MHz, $CDCl_3$) δ 7.06 – 7.14 (m, 2H, C9-**H**), 7.30 (ddd, *J* = 8.0, 7.0, 1.5 Hz, 2H, C7-**H**), 7.39 (ddd, *J* = 8.5, 7.0, 1.5 Hz, 2H, C8-**H**), 7.75 – 7.88 (m, 2H, C6-**H**), 8.07 (s, 2H, C4-**H**); ^{13}C NMR (101 MHz, $CDCl_3$) δ 115.0 (Ar**C**), 122.2 (Ar**C**) 124.7 (C-9), 124.9 (C-8), 127.4 (C-7), 127.5 (C-6), 129.1(Ar**C**), 129.2 (C-4), 132.4 (Ar**C**), 147.4 (C-2); *m/z* ([ESI$^-$]): 353.0 ([M–H]$^-$).

(*E*)-3,8-Dimethylocta-2,7-dien-1-yl diethyl phosphate[159] **184**

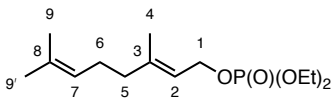

To a solution of geraniol (5.7 mL, 32.4 mmol) and pyridine (7.9 mL, 97.2 mmol) in Et_2O (17 mL) was added diethyl chlorophosphate (7.0 mL, 48.6 mmol) dropwise at –20 °C. The reaction was warmed to RT over 3 h at which point it was quenched with 1M HCl. The layers were separated, and the aqueous phase was extracted with EtOAc (3 × 10 mL). The combined organic layers were washed with $NaHCO_3$ (10 mL) then brine (10 mL) and dried over Na_2SO_4, filtered and concentrated *in vacuo*. The residue was purified by column chromatograpy (10% → 60% EtOAc in hexane) to give the title compound as a pale-yellow oil (7.20 g, 77%). ^{1}H NMR (400 MHz, $CDCl_3$) δ 1.31 (td, *J* = 7.0, 3.0 Hz, 6H, P(O)(OCH$_2$C**H$_3$**)$_2$), 1.57 (s, 3H, C9-**H$_3$**), 1.65 s, 3H, C9′-**H$_3$**), 1.68 (s, 3H, C4-**H$_3$**), 1.98 – 2.15 (m, 4H, C5-**H$_2$**, C6-**H$_2$**), 3.94 – 4.18 (m, 4H, P(O)(O**CH$_2$**CH$_3$)), 4.54 (t, *J* = 7.5 Hz, 2H, C1-**H$_2$**), 5.06 (tq, *J* = 5.0, 1.5 Hz, 1H, C7-**H**), 5.38 (ddt, *J* = 7.5, 4.5, 1.5 Hz, 1H, C2-**H**); ^{13}C NMR (101 MHz, $CDCl_3$) δ 16.2 (d, *J* = 6.5 Hz, P(O)(OCH$_2$**C**H$_3$)), 16.5 (C-4), 17.8, 25.7 (C-9, C-9′), 26.3, 39.6 (C-5, C-6), 63.7 (d, *J* = 5.5 Hz, P(O)(O**C**H$_2$CH$_3$)), 64.2 (d, *J* = 5.5 Hz, C-1), 119.1 (d, *J* = 6.5 Hz, C-2), 123.8 (C-7), 132.0, 142.6 (C-3, C-8); *m/z* ([ESI$^+$]): 313.2 ([M+Na]$^+$).

(*E*)-(3,8-Dimethylnona-3,7-dien-1-yl)benzene[149] **181**

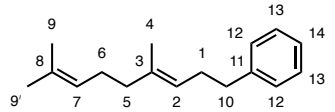

A solution of BnCl (0.4 mL, 3.4 mmol) in THF (8.5 mL) was added to Mg turnings (activated by vigorous stirring under Ar overnight) under Ar at 0 °C. The mixture was

stirred for 1 h after which time it was cannulated into a solution of phosphate **184** (0.50 g, 1.7 mmol) in THF (4.0 mL) under Ar at –78 °C. This solution was stirred for 1 h at –78 °C then warmed to RT and stirred overnight. The reaction was quenched with half saturated aqueous NH_4Cl (5 mL), the layers separated, and the aqueous layer extracted with Et_2O (3 × 10 mL). The combined organic layers were dried over $MgSO_4$, filtered, and concentrated *in vacuo*. The residue was purified by column chromatography (1% EtOAc in pentane) to give the title compound as a colourless oil (0.32 g, 80 %). ν_{max} (thin film)/cm^{-1}: 2966w, 2921w, 1855w, 1496w, 1453w, 1377w, 746m, 697s; ^{1}H NMR (400 MHz, $CDCl_3$) δ 1.57 (s, 3H, C4-**H$_3$**), 1.62 (s, 3H, C9-**H$_3$**), 1.70 (s, 3H, C9′-**H$_3$**), 1.96 – 2.03 (m, 2H, C5-**H$_2$**), 2.08 (app. q, *J* = 7.5 Hz, 2H, C6-**H$_2$**), 2.32 (app. q, *J* = 7.5 Hz, 2H, C1-**H$_2$**), 2.59 – 2.73 (m, 2H, C10-**H$_2$**), 5.11 (app. ddt, *J* = 7.5, 5.5, 2.0 Hz, 1H, C7-**H**), 5.20 (tt, *J* = 7.5, 1.5 Hz, 1H, C2-**H**), 7.16 – 7.23 (m, 3H, C12-**H**, C14-**H**), 7.26 – 7.32 (m, 2H, C13-**H**); ^{13}C NMR (101 MHz, $CDCl_3$) δ 16.1 (C-4), 17.8, 25.8 (C-9, C-10), 26.9 (C-6), 30.1 (C-1), 36.3 (C-11), 39.9 (C-5), 123.7 (C-2), 124.5 (C-7), 125.8 (C-15), 128.3 (C-14), 128.6 (C-13), 131.5, 135.9, 142.6 (C-3, C-8, C-12).

(±)-1,1,4a-Trimethyl-1,2,3,4,4a,9,10,10a-octahydrophenanthrene[149] (±)-**117**

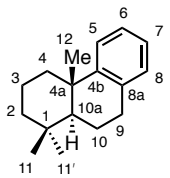

$RuCl_3.xH_2O$ (18 mg, 1 mol%) and AgOTf (45 mg, 2 mol%) were stirred in DCE (13 mL) vigorously for 1 h at RT after which time **181** (2.00 g, 8.8 mmol) was added as a solution in DCE (31 mL). The mixture was stirred for 4 h at 60 °C, cooled to RT, and the solvent removed *in vacuo*. The residue was purified directly by column chromatography (pentane) to give the title compound as a colourless oil (1.84 g, 92%).

ν_{max} (thin film)/cm^{-1}: 2924s, 1488m, 1458m, 1388m, 1040w, 760s, 722s; ^{1}H NMR (400 MHz, $CDCl_3$) δ 0.94 (s, 3H, C11-**H$_3$**), 0.96 (s, 3H, C11′-**H$_3$**), 1.20 (s, 3H, C12-**H$_3$**), 1.25 (dd, *J* = 13.5, 4.0 Hz, 1H, aliphatic), 1.33 – 1.46 (m, 2H, aliphatic), 1.46 – 1.52 (m, 1H, aliphatic), 1.57 – 1.83 (m, 3H, aliphatic), 1.89 (m, 1H, aliphatic), 2.26 – 2.33 (m, 1H, aliphatic), 2.81 – 3.00 (m, 2H, aliphatic), 7.02 – 7.15 (m, 3H, Ar**H**), 7.25 – 7.28 (m, 1H, Ar**H**); ^{13}C NMR (101 MHz, $CDCl_3$) δ 19.2, 19.5 (aliphatic), 21.8 (C-11), 25.0 (C-12), 30.5 (C-9), 33.5 (C-11′), 33.6, 38.0, 39.0, 41.8, (aliphatic), 50.4 (C-10a), 124.5, 125.3, 125.7, 129.1, 135.4, 150.3 (ArC).

Chromatographic resolution of (±)-1,1,4a-trimethyl-1,2,3,4,4a,9,10,10a-octahydrophenanthrene (±)-117

The enantiomers were resolved using preparative HPLC by Andrew Ikin at AstraZeneca. The racemic sample was diluted up to 20.0 mL in EtOH and a CHIRALCEL OD 20-micron (250 x 50mm) column was used (1.0% *i*-PrOH in hexanes; 35.00 mL/min).

(–)-(4a*R*,10a*R*) -1,1,4a-Trimethyl-1,2,3,4,4a,9,10,10a-octahydrophenanthrene (–)-117

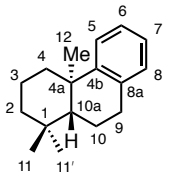

Retention time 13.30 mins; >99% ee; $[\alpha]_D^{25}$ –53.2 (*c* 0.67, $CHCl_3$); ^{1}H NMR (400 MHz, $CDCl_3$) δ 0.94 (s, 3H, C11-**H$_3$**), 0.96 (s, 3H, C11′-**H$_3$**), 1.20 (s, 3H, C12-**H$_3$**), 1.22 – 2.01 (m, 8H, aliphatic), 2.30 (ddt, *J* = 12.8, 4.7, 2.1, Hz, 1H, aliphatic), 2.78 – 3.05 (m, 2H, aliphatic), 7.01 – 7.16 (m, Ar**H**), 7.24 – 7.30 (m, 1H, Ar**H**); ^{13}C NMR (101 MHz,

$CDCl_3$) δ 19.2, 19.5 (aliphatic), 21.8 (C-11), 25.0 (C-12), 30.5 (C-9), 33.5 (C-11′), 33.6, 38.0, 39.0, 41.8, (aliphatic), 50.4 (C-10a), 124.5, 125.3, 125.7, 129.1, 135.4, 150.3 (ArC).

(+)-(4a*S*,10a*S*)-1,1,4a-Trimethyl-1,2,3,4,4a,9,10,10a-octahydrophenanthrene[149] (+)-117

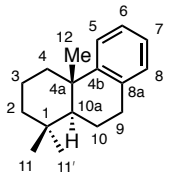

Retention time 15.91 mins; % ee not determined due to trace impurities; $[\alpha]_D^{25}$+52.3 (*c* 0.59, $CHCl_3$); ^{1}H NMR (400 MHz, $CDCl_3$) δ 0.94 (s, 3H, C11-**H$_3$**), 0.96 (s, 3H, C11′-**H$_3$**), 1.20 (s, 3H, C12-**H$_3$**), 1.22 – 2.01 (m, 8H, aliphatic), 2.30 (ddt, *J* = 12.8, 4.7, 2.1, Hz, 1H, aliphatic), 2.78 – 3.05 (m, 2H, aliphatic), 7.01 – 7.16 (m, Ar**H**), 7.24 – 7.30 (m, 1H, Ar**H**); ^{13}C NMR (101 MHz, $CDCl_3$) δ 19.2, 19.5 (aliphatic), 21.8 (C-11), 25.0 (C-12), 30.5 (C-9), 33.5 (C-11′), 33.6, 38.0, 39.0, 41.8, (aliphatic), 50.4 (C-10a), 124.5, 125.3, 125.7, 129.1, 135.4, 150.3 (ArC).

1,1,4a-trimethyl-2,3,4,4a,10,10a-hexahydrophenanthren-9(1*H*)-one [225] (±)-205

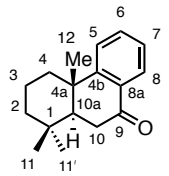

Tricycle (±)-**117** (0.10 g, 0.44 mmol) was added to a solution of CrO_3 (44 mg, 0.44 mmol) in AcOH (4.4 mL) at RT. The reaction mixture was stirred for 30 minutes after which time it was neutralised with sat. aq. $NaHCO_3$. The mixture was extracted with Et_2O (3 × 5 mL), washed with sat. brine (5 mL) and dried over Na_2SO_4. The combined

organic layers were concentrate *in vacuo* and the crude residue was purified by column chromatography (5% Et_2O in pentane) to yield the title compound as a colourless oil (53 mg, 50%). ^{1}H NMR (400 MHz, $CDCl_3$) δ 0.94 (s, 3H, C11-**H$_3$**), 1.01 (s, 3H, C11′-**H$_3$**), 1.25 (s, 3H, C12-**H$_3$**), 1.30 (dd, *J* = 13.5, 4.0 Hz, 1H, C2-**H$_a$**H$_b$), 1.50 – 1.61 (m, 2H, C2-H$_a$**H$_b$**, C4-**H$_a$**H$_b$), 1.70 (dp, *J* = 10.5, 4.0 Hz, 1H, C3-**H$_a$**H$_b$), 1.79 (tt, *J* = 13.0, 4.0 Hz, 1H, C3-H$_a$**H$_b$**), 1.89 (dd, *J* = 13.5, 4.5 Hz, 1H, C10a-**H**), 2.35 (dq, *J* = 13.0, 3.0 Hz, 1H, C4-H$_a$**H$_b$**), 2.60 – 2.79 (m, 2H, C10-**H$_2$**), 7.26 – 7.31 (m, 1H, C7-**H**), 7.38 (dd, *J* = 8.0, 1.0 Hz, 1H, C5-**H**), 7.49 – 7.55 (m, 1H, C6-**H**), 8.01 (dd, *J* = 7.0, 1.5 Hz, 1H, C8-**H**); ^{13}C NMR (101 MHz, $CDCl_3$) δ 19.0 (C-3), 21.5 (C-11), 23.6 (C-12), 32.7 (C-11′), 33.5 (C-1), 36.4 (C-10), 38.1 (C-4), 38.3 (C-4a), 41.5 (C-2), 49.4 (C-10a), 123.8 (C-5), 126.2 (C-7), 127.5 (C-8), 131.0 (C-8a), 134.2 (C-6), 156.3 (C-4b), 199.7 (C-9); *m/z* ([ESI$^+$]): 243.2 ([M+H]$^+$).

1,1,4a-Trimethyl-1,2,3,4,4a,9,10,10a-octahydrophenanthren-9-ol (±)-118

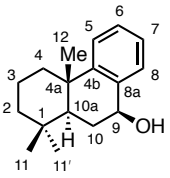

To a solution of ketone (±)-**205** (50 mg, 0.21 mmol) in THF (0.62 mL) was added $LiAlH_4$ (6.0 mg, 0.16 mmol) at 0 °C. After 1.5 h the reaction was quenched with H_2O (0.1 mL) followed by 15% aq. NaOH (0.1 mL) then H_2O (0.3 mL) at 0 °C. The mixture was warmed to RT and stirred for 15 minutes after which time $MgSO_4$ was added. Stirring continued for 15 minutes and then the mixture was filtered. The filtrate was concentrated *in vacuo* and the crude residue was purified by column chromatography (20% Et_2O in pentane) to yield the title compound as a white solid (28 mg, 56%). Data are consistent with alcohol (+)-**118**.

(±)-(*E*)-5-(8,8-dimethyloxiran-6-yl)-3-methylpent-2-en-1-yl diethyl phosphate 210

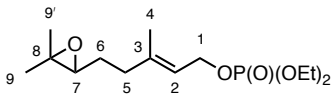

To a solution of olefin **184** (50 mg, 0.17 mmol) in CH_2Cl_2 (0.9 mL) was added 3-chloroperoxybenzoic acid (31 mg, 0.18 mmol) at 0 °C. The reaction mixture was warmed to RT and stirred for 20 h after which time it was quenched with sat. aq. $NaHCO_3$ (2 mL), extracted with CH_2Cl_2 (3 × 2 mL), dried over $MgSO_4$, and concentrated *in vacuo*. The crude residue was purified by column chromatography (3:7 pentane:EtOAc) to yield the title compound as a colourless oil (36 mg, 68%). R_f 0.29 (3:7 pentane:EtOAc); ν_{max} (thin film)/cm^{-1}: 2986w, 2908w, 1329w, 2121w, 1676w, 1218m, 1167m, 1032s, 819w, 749w; ^{1}H NMR (400 MHz, $CDCl_3$) δ 1.26 (s, 3H, C9-**H₃**), 1.30 (s, 3H, C9′-**H₃**), 1.33 (td, *J* = 7.0, 1.0 Hz, 6H, P(O)(OCH$_2$C**H₃**)$_2$), 1.62 – 1.70 (m, 2H, C6-**H₂**), 1.72 (d, *J* = 1.5 Hz, 3H, C4-**H₃**), 2.08 – 2.29 (m, 2H, C5-**H₂**), 2.70 (t, *J* = 6.0 Hz, 1H, C7-**H**), 4.10 (p, *J* = 7.0 Hz, 4H, P(O)(OC**H₂**CH$_3$)$_2$), 4.56 (app. t, *J* = 7.5 Hz, 2H, C1-**H₂**), 5.44 (tq, *J* = 7.5, 1.5 Hz, 1H, C2-**H**); ^{13}C NMR (101 MHz, $CDCl_3$) δ 16.3 (d, *J* = 6.5 Hz, OCH$_2$**C**H$_3$), 16.6 (C-4), 18.9 (C-9), 25.0 (C-9′), 27.2 (C-6), 36.3 (C-5), 58.5 (C-8), 63.8 (d, *J* = 5.5 Hz, O**C**H$_2$CH$_3$), 64.0 (C-7), 64.0 (d, *J* = 5.5 Hz, C-1), 119.7 (d, *J* = 6.5 Hz, C-2), 141.7 (C-3); *m/z* ([ESI$^+$]): 307.2 ([M+H]$^+$), 329.1 ([M+Na]$^+$); HRMS: 307.1671 found, $C_{14}H_{28}O_3P$ requires 307.1669.

(±)-(*E*)-7-(1-chloro-3-methylpent-2-en-6-yl)-8,8-dimethyloxirane[226] 211

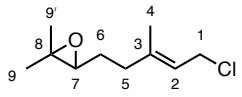

To a suspension of activated Mg (14 mg, 0.59 mmol) in THF (0.3 mL) was added BnCl (30 μL, 0.26 mmol) under Ar at 0 °C. The mixture was stirred for 1 h at 0 °C after which time it was added to a solution of phosphate **210** (30 mg, 0.10 mmol) in THF (0.3 mL) at –78 °C. The reaction mixture was stirred at –78 °C for 1 h then warmed to RT and stirring continued overnight. The reaction was quenched with half sat. aq. NH_4Cl (2 mL) and extracted with Et_2O (3 × 2 mL). The combined organic layers were dried over $MgSO_4$ and concentrated *in vacuo*. The crude residue was purified by column chromatography (3% EtOAc in pentane) to yield the title compound as a colourless oil (10 mg, 52%). ^{1}H NMR (400 MHz, $CDCl_3$) δ 1.26 (s, 3H, C9-**H₃**), 1.31 (s, 3H, C9′-**H₃**), 1.63 – 1.72 (m, 2H, C6-**H₂**), 1.75 (d, *J* = 1.5 Hz, 3H, C4-**H₃**), 2.06 – 2.30 (m, 2H, C5-**H₂**), 2.70 (t, *J* = 6.0 Hz, 1H, C7-**H**), 4.09 (d, *J* = 8.0 Hz, 2H, C1-**H₂**), 5.49 (app. ddq, *J* = 9.5, 8.0, 1.5 Hz, 1H, C2-**H**); ^{13}C NMR (101 MHz, $CDCl_3$) δ 16.2 (C-4), 18.9 (C-9), 25.0 (C-9′), 27.2 , (C-6), 36.3 (C-5), 41.0 (C-1), 58.6 (C-8), 64.0 (C-7), 121.0 (C-2), 141.9 (C-3); *m/z* ([ESI$^+$]): 154.2 ([M–Cl]$^+$).

(*E*)-3,7-dimethylocta-2,6-dien-10-yl acetate[167] 171

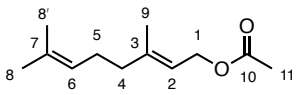

To a solution of geraniol (2.0 mL, 11.4 mmol) and Ac_2O (2.2 mL, 22.8 mmol) in freshly distilled pyridine (1.9 mL, 22.8 mmol) was added DMAP (0.14 g, 1.14 mmol) under Ar

at 0 °C. The reaction mixture was warmed to RT and stirred for 2 h after which time it was quenched with 6 M HCl (10 mL). The layers were separated, and the aqueous layer was extracted with Et_2O (3 × 10 mL). The combined organic layers were washed with $NaHCO_3$, dried over $MgSO_4$, and concentrated *in vacuo* to yield the title compound as a colourless oil (1.81 g, 81%). ν_{max} (thin film)/cm^{-1}: 2968w, 2917w, 1740s, 1444w, 1378w, 1366w, 1231s, 1023m ; ^{1}H NMR (400 MHz, $CDCl_3$) δ 1.60 (s, 3H, C8-**H₃**), 1.68 (s, 3H, C8′-**H₃**), 1.70 (s, 3H, C9-**H₃**), 2.05 (s, 3H, C11-**H₃**), 2.05 – 2.15 (m, 4H, C4-**H₂**, C5-**H₂**), 4.58 (d, *J* = 7.0 Hz, 2H, C1-**H₂**), 5.08 (m, 1H, C6-**H**), 5.34 (tq, *J* = 7.0, 1.5 Hz, 1H, C2-**H**); ^{13}C NMR (101 MHz, $CDCl_3$) δ 16.6 (C-9), 17.8 (C-8), 21.2 (C-11), 25.8 (C-8′), 26.4 (C-5), 39.7 (C-4), 61.5 (C-1), 118.4 (C-2), 123.9 (C-6), 132.0 (C-7), 142.4 (C-3), 171.3 (C-10).

(*E*)-5-(3,7-dimethyloxiran-6-yl)-3-methylpent-2-en-1-yl acetate[168] (±)-212

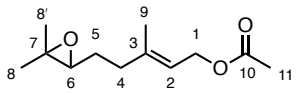

To a solution of olefin **171** (0.10 g, 0.51 mmol) in CH_2Cl_2 (1 mL) was added *m*-CPBA (92 mg, 0.54 mmol) under Ar at 0 °C. The reaction was warmed to RT and stirred for 24 h after which time it was quenched with 3 M NaOH (1 mL), extracted with CH_2Cl_2 (3 × 1 mL), and concentrated *in vacuo*. The crude residue was purified by column chromatography to yield the title compound as a colourless oil (59 mg, 54%). ^{1}H NMR (400 MHz, $CDCl_3$) δ 1.26 (s, 3H, C8-**H₃**), 1.30 (s, 3H, C8′-**H₃**), 1.61 – 1.69 (m, 2H, C5-**H₂**), 1.72 (s, 3H, C9-**H₃**), 2.05 (s, 3H, C11-**H₃**), 2.07 – 2.28 (m, 3H, C4-**H₂**), 2.70 (t, *J* = 6.0 Hz, 1H, C6-**H**), 4.59 (d, *J* = 7.0 Hz, 2H, C1-**H₂**), 5.38 (tq, *J* = 7.0, 1.5 Hz, 1H, C2-**H**); ^{13}C NMR (101 MHz, $CDCl_3$) δ 16.6 (C-9), 18.9 (C-8), 21.2 (C-11), 25.0 (C-8′),

27.2 (C-5), 36.3 (C-4), 58.5 (C-7), 61.4 (C-1), 64.1(C-6), 119.1 (C-2), 141.4 (C-3), 171.2 (C-10); *m/z* ([ESI$^+$]): 235.2 ([M+Na]$^+$).

(*E*)-2,2-dimethyl-3-(3-methyl-9-phenylhex-6-en-4-yl)oxirane[169] **(±)-209**

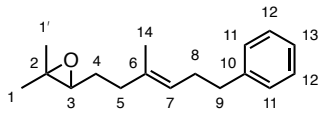

To a suspension of Mg (1.56 g, 64.4 mmol) in THF (28 mL) was added BnCl (3.3 mL, 28.3 mmol) at 0 °C under Ar. The mixture was stirred at 0 °C for 1 h after which time it was added to a solution of acetate (±)-**212** (3.00 g, 14.1 mmol) and Li_2CuCl_4 (14 mL, 0.1 M in THF, 1.41 mmol) in THF (28 mL) at 0 °C. The reaction mixture was stirred for 1 h and then quenched with half sat. aq. NH_4Cl. The layers were separated, the aqueous layer extracted with Et_2O (3 × 40 mL), and the combined organic layers were washed with brine, dried over Na_2SO_4, and concentrated *in vacuo*. The crude residue was purified by column chromatography (5% EtOAc in pentane) to yield the title compound (3.26 g, 94%). ν_{max} (thin film)/cm^{-1}: 2062w, 2026w, 2960w, 2923w, 2856w, 1496w, 1454m, 1377m, 1077wm 747m, 698s; ^{1}H NMR (400 MHz, $CDCl_3$) δ 1.26 (s, 3H, C1-**H₃**), 1.30 (s, 3H, C1′-**H₃**), 1.57 (d, *J* = 1.5 Hz, 3H, C14-**H₃**), 1.58 – 1.70 (m, 2H, C4-**H₂**), 2.03 – 2.21 (m, 2H, C5-**H₂**), 2.32 (q, *J* = 8.0 Hz, 2H, C8-**H₂**), 2.65 (app. d, *J* = 8.0 Hz, 2H, C9-**H₂**), 2.69 (t, *J* = 6.5 Hz, 1H, C3-**H**), 5.24 (tq, *J* = 8.0, 1.5 Hz, 1H, C7-**H**), 7.14 – 7.21 (m, 3H, C11-**H**, C13-**H**), 7.23 – 7.31 (m, 2H, C12-**H**); ^{13}C NMR (101 MHz, $CDCl_3$) δ 16.1 (C-14), 18.9 (C-1), 25.0 (C-1′), 27.6 (C-4), 30.1 (C-8), 36.2 (C-9), 36.4 (C-5), 58.4 (C-2), 64.3 (C-3), 124.4 (C-7), 125.8 (C-13), 128.4 (C-12), 128.6 (C-11), 135.0 (C-10), 142.4 (C-6).

1,1,4a-trimethyl-1,2,3,4,4a,9,10,10a-octahydrophenanthren-2-ol[170] **(±)-208**

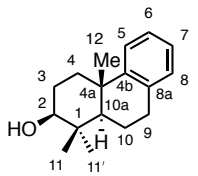

Epoxide (±)-**209** (1.00 g, 4.1 mmol) was added to a solution of TPP BF_4 (1.75 g, 4.1 mmol) in HFIP (41 mL) under Ar. After 5 minutes EtOAc (40 mL) was added, the suspension filtered under vacuum and the filtrate concentrated *in vacuo*. The crude residue was purified by column chromatography (10% EtOAc in pentane) to yield the title compound as a white solid (0.54 g, 54%). ν_{max} (thin film)/cm^{-1}: 3389m br., 2966m, 1945m, 1870m, 1837w, 1488m, 1447m, 1375m, 1091m, 1071m, 1007s, 970m, 761s, 723m; ^{1}H NMR (400 MHz, $CDCl_3$) δ 0.91 (s, 3H, C11-**H$_3$**), 1.09 (s, 3H, C11′-**H$_3$**), 1.21 (s, 3H, C12-**H$_3$**), 1.34 (dd, *J* = 12.0, 2.5 Hz, 1H, C10a-**H**), 1.41 – 1.47 (br. s, 1H, *O***H**), 1.56 (td, *J* = 13.0, 5.0 Hz, 1H, C4-**H$_a$**H$_b$), 1.71 – 1.87 (m, 3H, C3-**H$_2$**, C10-**H$_a$**H$_b$), 1.91 (dt, *J* = 12.0, 7.5 Hz, 1H, C10-H$_a$**H$_b$**), 2.33 (dt, *J* = 13.0, 3.5 Hz, 1H, C4-H$_a$**H$_b$**), 2.82 – 3.03 (m, 2H, C9-**H$_2$**), 3.32 (dd, *J* = 11.0, 5.0 Hz, 1H, C2-**H**), 7.03 – 7.16 (m, 3H, Ar**H**), 7.23 – 7.27 (m, 1H, Ar**H**); ^{13}C NMR (101 MHz, $CDCl_3$) δ 15.5 (C-11), 18.9 (C-10), 25.0 (C-12), 28.1 (C-3), 28.3 (C-11′), 30.8 (C-9), 37.0 (C-4), 37.7 (C-4a), 39.2 (C-1), 49.9 (C-10a), 78.9 (C-2), 124.6, 125.5, 125.9, 129.1 (C-5, C-6, C-7, C-8), 135.2, 149.5 (C-4b, C-8a).

1,1,4a-trimethyl-4,4a,10,10a-tetrahydrophenanthrene-2,9(1*H*,3*H*)-dione[171] (±)-213

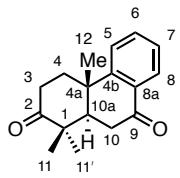

Alcohol (±)-**208** (0.30 g, 1.2 mmol) was added to a solution of CrO_3 (0.49 g, 4.9 mmol) in AcOH (12 mL). The reaction mixture was stirred at RT for 24 h after which time it was neutralised with 3 M NaOH, extracted with Et_2O (3 × 10 mL). The combined organic layers were washed with brine (20 mL), dried over Na_2SO_4, and concentrated *in vacuo*. The crude residue was purified by column chromatography (20% EtOAc in pentane) to yield the title compound as a colourless oil (66 mg, 21%). ^{1}H NMR (400 MHz, $CDCl_3$) δ 1.15 (s, 3H, C11-**H$_3$**), 1.22 (s, 3H, C11′-**H$_3$**), 1.46 (s, 3H, 21, C12-**H$_3$**), 2.04 (td, *J* = 13.0, 5.5 Hz, 1H, C4-**H$_a$**H$_b$), 2.35 (dd, *J* = 14.0, 4.0 Hz, 1H, C10a-**H**), 2.52 – 2.73 (m, 3H, C3-**H$_a$**H$_b$, C4-H$_a$**H$_b$**, C10-**H$_a$**H$_b$), 2.77 – 2.96 (m, 2H, C3-H$_a$**H$_b$**, C10-H$_a$**H$_b$**), 7.31 – 7.39 (m, 2H, C5-**H**, C6-**H**), 7.56 (ddd, *J* = 8.0, 7.0, 1.5 Hz, 1H, C7-**H**), 8.04 (dd, *J* = 8.0, 1.5 Hz, 1H, C8-**H**); ^{13}C NMR (101 MHz, $CDCl_3$) δ 21.6 (C-11), 22.9 (C-12), 25.1 (C-11′), 34.7 (C-3), 36.5 (C-10), 37.0 (C-3), 37.8 (C-4a), 47.5 (C-1), 49.5 (C-10a), 124.3 (C-5), 127.0 (C-6), 127.7 (C-8), 130.7 (C-8a), 134.5 (C-7), 153.6 (C-4b), 198.1 (C-9), 214.4 (C-2); *m/z* ([ESI$^+$]): 257.2 ([M+H]$^+$).

1,1,4a-trimethyl-1,2,3,4,4a,9,10,10a-octahydrophenanthrene-2,9-diol (±)-206

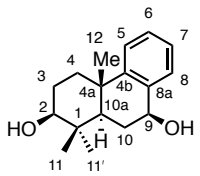

To a suspension of $LiAlH_4$ (14 mg, 0.36 mmol) in THF (0.77 mL) under Ar was added diketone (±)-**213** (66 mg, 0.26 mmol) at 0 ºC. The reaction mixture was warmed to RT and stirred for 15 h. Water (0.01 mL), aq. NaOH (15% w/v, 0.01 mL), and water 0.03 mL were added, and the mixture stirred for 15 minutes. $MgSO_4$ was added and the mixture was stirred for 15 minutes, filtered, and concentrated *in vacuo*. The crude residue was purified by column chromatography (40% EtOAc in pentane) and then further purified by column chromatography (30% EtOAc in pentane). Further purification by recrystallisation from EtOAc yielded the title compound as a white solid (18 mg, 17%). Data were consistent with diol (+)-**206**.

4-Isopropylbenzaldehyde[227] **224**

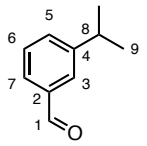

To a solution of aryl bromide **223** (2.3 mL, 15.0 mmol) in THF (30 mL) was added *n*-BuLi (1.6 M in hexanes, 11 mL, 16.5 mmol) dropwise at –78 ºC. The mixture was stirred at –78 ºC for 40 minutes after which time DMF (1.3 mL, 16.5 mmol) was added dropwise. Stirring continued for 15 minutes while warming to –10 ºC and then the reaction was quenched with water (20 mL). The reaction was extracted with Et_2O (3 × 30 mL), and the combined organic layers were washed with brine and dried over Na-

$_2SO_4$, filtered, and concentrated. The crude compound, isolated as an orange oil, was used without further purification (2.38 g, 89%). ^{1}H NMR (400 MHz, CD_2Cl_2) δ 1.29 (d, *J* = 7.0 Hz, 6H, C9-**H₃**), 3.00 (hept, *J* = 7.0 Hz, 1H, C8-**H**), 7.46 (t, *J* = 7.5 Hz, 1H, Ar**H**), 7.49 – 7.52 (m, 1H, Ar**H**), 7.70 (dt, *J* = 7.5, 1.5 Hz, 1H, Ar**H**), 7.75 (t, *J* = 1.5 Hz Hz, 1H, Ar**H**), 10.01 (s, 1H, C1-**H**); ^{13}C NMR (101 MHz, $CDCl_3$) δ 24.0 (C-9), 34.1 (C-8), 127.5, 127.9, 129.1, 133.1, 136.8, 150.0 (Ar**C**), 192.8 (C-1); *m/z* ([ESI$^+$]): 149.0 ([M+H]$^+$).

(4-Isopropylphenyl)methanol[227] **225**

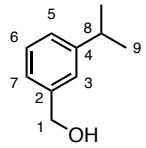

To a solution of aldehyde (1.98 g, 13.4 mmol) in MeOH (67 mL) was added $NaBH_4$ (1.01 g, 26.7 mmol) at 0 ºC. The mixture was stirred at 0 ºC for 2 h after which time it was poured into 1 M HCl (50 mL) and extracted with EtOAc (3 × 50 mL). The combined organic layers were washed with brine, dried over Na_2SO_4, filtered and concentrated *in vacuo*. The crude residue was purified by column chromatography (20 % EtOAc in pentane) to yield the title compound as a pale-yellow oil (1.48 g, 74 %). ν_{max} (thin film)/cm^{-1}: 3320m br., 3027s, 2870m, 1608w, 1488m, 1464m, 1444m, 1363m, 1177w, 1018m, 891w, 790m, 723w, 703s; ^{1}H NMR (400 MHz, $CDCl_3$) δ 1.26 (d, *J* = 7.0 Hz, 6H, C9-**H₃**), 2.92 (hept, *J* = 7.0 Hz, 1H, C8-**H**), 4.68 (s, 2H, C1-**H₂**), 7.18 (ddt, *J* = 7.5, 5.5, 1.5 Hz, 2H, Ar**H**), 7.24 (m, 1H, Ar**H**), 7.30 (t, *J* = 7.5 Hz, 1H, Ar**H**); ^{13}C NMR (101 MHz, $CDCl_3$) δ 24.1 (C-9), 34.3 (C-8), 65.8 (C-1), 124.6, 125.3, 126.0, 128.7, 141.0, 149.5 (Ar**C**).

1-(Chloromethyl)-3-isopropylbenzene 226

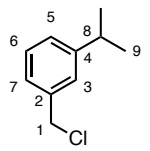

To a solution of alcohol **225** (2.00 g, 13.3 mmol) and pyridine (1 drop) in PhMe (14 mL) under argon was added $SOCl_2$ (1.6 mL, 21.3 mmol). The reaction was heated at 80 ºC for 4 h after which time it was concentrated *in vacuo*. The residue was redissolved in Et_2O (20 mL), washed with water (10 mL) and brine (10 mL), dried over $MgSO_4$, filtered, and concentrated *in vacuo*. The crude residue was purified by column chromatography (2% EtOAc in pentane) to yield the title compound as a colourless oil (1.83 g, 82%). ν_{max} (thin film)/cm^{-1}: 3022w, 2961m, 1870w, 1605w, 1487w, 1463w, 1444w, 1266w, 1179w, 1050w, 794m, 706s; ^{1}H NMR (400 MHz, $CDCl_3$) δ 1.27 (d, *J* = 7.0 Hz, 6H, C9-**H$_3$**), 2.92 (hept, *J* = 7.0 Hz, 1H, C8-**H**), 4.59 (s, 2H, C1-**H$_2$**), 7.21 (tt, *J* = 7.5, 1.5 Hz, 2H, Ar**H**), 7.25 (t, *J* = 1.5 Hz, 1H, Ar**H**), 7.27 – 7.32 (t, 7.5 Hz, 1H, Ar**H**); ^{13}C NMR (101 MHz, $CDCl_3$) δ 23.9 (C9), 34.0 (C-8), 46.5 (C-1), 126.1, 126.6, 126.7, 128.7, 137.4, 149.5 (Ar**C**).

(*E*)-11-(3,8-dimethylnona-2,7-dien-1-yl)-15-isopropylbenzene 220

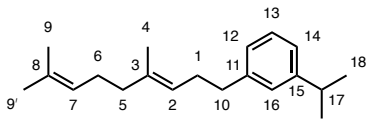

A solution of aryl chloride **226** (0.80 g, 4.7 mmol) in THF (13 mL) was added to Mg turnings (activated by vigorous stirring under Ar overnight) under Ar at 0 °C. The mixture was stirred for 1 h after which time it was cannulated into a solution of phosphate **184** (0.69 g, 2.4 mmol) in THF (7.0 mL) under Ar at –78 °C. This solution

was stirred for 1 h at –78 °C then warmed to RT and stirred overnight. The reaction was quenched with half saturated aqueous NH_4Cl (5 mL), the layers separated, and the aqueous layer extracted with Et_2O (3 × 10 mL). The combined organic layers were dried over $MgSO_4$, filtered, and concentrated *in vacuo*. The residue was purified by column chromatography (pentane) to give the title compound as a colourless oil (0.29 g, 45%). ν_{max} (thin film)/cm^{-1}: 2961s, 2924s, 2856m, 1606w, 1488w, 1444m, 1382w, 1108w, 1050w, 921w, 887w, 791m, 705s; ^{1}H NMR (400 MHz, $CDCl_3$) δ 1.26 (d, *J* = 7.0 Hz, 6H, C18-**H$_3$**), 1.57 (s, 3H, C4-**H$_3$**), 1.61 (s, 3H, C9′-**H$_3$**), 1.70 (s, 3H, C9-**H$_3$**), 1.99 (m, 2H, C5-**H$_2$**), 2.03 – 2.12 (m, 2H, C6-**H$_3$**), 2.31 (app. q, *J* = 7.5 Hz, 2H, C1-**H$_2$**), 2.63 (app. dd, *J* = 9.0, 7.5 Hz, 2H, C10-**H$_2$**), 2.89 (hept, *J* = 7.0 Hz, 1H, C17-**H**), 5.11 (t, *J* = 7.0 Hz, 1H, C7-**H**), 5.21 (t, *J* = 7.5 Hz, 1H, C2-**H**), 7.00 – 7.08 (m, 3H, Ar**H**), 7.21 (t, *J* = 8.0 Hz, 1H, C13-**H**); ^{13}C NMR (101 MHz, $CDCl_3$) δ 16.1 (C-4), 17.8 (C-9′), 24.2 (C-18), 25.8 (C-9), 26.9 (C-6), 30.2 (C-1), 34.3 (C-17), 36.4 (C-10), 39.9 (C-5), 123.8 (C-2), 123.9 (Ar**C**), 124.5 (C-7), 126.0, 126.8 (Ar**C**), 128.3 (C-13), 131.5, 135.8, 142.5, 148.9 (C-3, C-8, C-11, C-15); HRMS: 271.2422 found, $C_{20}H_{31}^+$ requires 271.2420.

Abietatriene[228] **(±)-179**

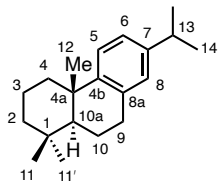

$RuCl_3.xH_2O$ (1 mg, 1 mol%) and AgOTf (3 mg, 2 mol%) were stirred in DCE (1 mL) vigorously for 1 h at RT after which time **220** (0.15 g, 0.6 mmol) was added as a solution in DCE (1.5 mL). The mixture was stirred for 2 h at 60 °C, cooled to RT, and the solvent removed *in vacuo*. The residue was purified directly by column chromatography (pentane) to give the title compound as a colourless oil (69 mg, 46%).

ν_{max} (thin film)/cm^{-1}: 2956s, 2934s, 2866m, 1570m, 1498m, 1387w, 1375m, 1364w, 1084w, 996w, 944w ,858s; ^{1}H NMR (400 MHz, $CDCl_3$) δ 0.94 (s, 3H, C11-**H$_3$**), 0.96 (s, 3H, C11′-**H$_3$**), 1.20 (s, 3H, C12-**H$_3$**), 1.21 – 1.26 (m, 7H, C14-**H$_3$**, C4-**H$_a$**H$_b$), 1.34 – 1.39 (m, 1H, C10a-**H**), 1.40 – 1.46 (m, 1H, C2-**H$_a$**H$_b$), 1.49 (m, 1H, C4-H$_a$**H$_b$**), 1.57 – 1.65 (m, 1H, C3-**H$_a$**H$_b$), 1.66 – 1.83 (m, 2H, C3-H$_a$**H$_b$**, C10-**H$_a$**H$_b$), 1.85 – 1.93 (m, 1H, C10-H$_a$**H$_b$**), 2.29 (dtd, *J* = 12.5, 3.5, 1.5 Hz, 1H, C2-H$_a$**H$_b$**), 2.78 – 2.99 (m, 3H, C9-**H$_2$**, C13-**H**), 6.90 (d, *J* = 2.0 Hz, 1H, C8-**H**), 7.00 (dd, *J* = 8.0, 2.0 Hz, 1H, C6-**H**), 7.19 (d, *J* = 8.0 Hz, 1H, C5-**H**); ^{13}C NMR (101 MHz, $CDCl_3$) δ 19.3 (C-10), 19.5 (C-3), 21.8 (C-11), 24.1 (C-14), 25.0 (C-12), 30.7 (C-9), 33.5 (C-1), 33.6 (C-1, C11′), 37.7 (C-4a), 39.0 (C-2), 41.9 (C-4), 50.6 (C-10a), 123.9 (C-6), 124.4 (C-5), 127.0 (C-8), 135.1, 145.5, 147.8 (Ar**C**).

_S_-Ethyl (2_E_)-4-Methylpent-2-enethioate[229] 270

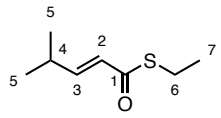

To a solution of 4-methyl-2-pentenoic acid (3.1 mL, 26.3 mmol), EtSH (2.5 mL, 34.2 mmol), and DMAP (0.32 g, 2.64 mmol) in CH_2Cl_2 (132 mL) was added DCC (5.76 g, 27.9 mmol) at 0 °C. The mixture was stirred and allowed to warm to RT overnight. The reaction was filtered through celite and the celite was washed with CH_2Cl_2. The filtrate was washed with $NaHCO_3$ (25 mL), water (25 mL), and brine (25 mL), dried over $MgSO_4$, filtered, and concentrated *in vacuo*. The residue was purified by flash column chromatography (pentane:Et_2O 60:1) to give the title compound as a yellow oil (3.30 g, 79%). ^{1}H NMR (400 MHz, $CDCl_3$) δ 1.07 (d, *J* = 7.0 Hz, 6H, C5-**H$_3$**), 1.27 (t, *J* = 7.5 Hz, 3H, C7-**H$_3$**), 2.39 – 2.51 (m, 1H, C4-**H**), 2.94 (q, *J* = 7.5 Hz, 2H, C6-**H$_2$**), 6.05 (dd, *J* = 15.5, 1.5 Hz, 1H, C2-**H**), 6.86 (dd, *J* = 15.5, 6.5 Hz, 1H, C3-**H**); ^{13}C NMR (101

MHz, $CDCl_3$) δ 15.0 (C-7), 21.3 (C-5), 23.2 (C-6), 31.1 (C-4), 126.2 (C-2), 151.4 (C-3), 190.6 (C-1); *m/z* ([ESI^+]): 159.0 ([$M+H]^+$).

Ethyl (2*E*,4*E*)-3-methylhexa-2,4-dienoate[230] 273

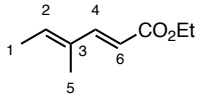

Triethyl phosphonoacetate (7.7 mL, 38.8 mmol) was added to a suspension of NaH (60% oil emulsion, 1.34 g, 33.6 mmol) in THF (50 mL) under Ar at 0 °C. The mixture was stirred for 30 mins at RT after which time the temperature was reduced to 0 °C and tiglic aldehyde (2.5 mL, 25.9 mmol) was added slowly. The reaction was stirred for 1 h at RT and then it was quenched with H_2O dropwise. The reaction was extracted with Et_2O (3 × 30 mL) and the combined organic layers were washed with brine, dried over $MgSO_4$, filtered, and concentrate under a stream of nitrogen. The crude residue was purified by column chromatography (2% → 5% EtOAc in pentane) to yield the title compound as a pale-yellow oil (2.17 g, 54%). ν_{max} (thin film)/cm^{-1}: 2926s, 2869m, 2161wm 2032w, 1728s, 1456m, 1378m, 1303m, 1238m, 1174, 1037m; ^1H NMR (400 MHz, $CDCl_3$) δ 1.29 (t, *J* = 7.0 Hz, 3H, C**H₃**CH_2O), 1.77 (s, 3H, C5-**H₃**), 1.81 (d, *J* = 7.0 Hz, 3H, C1-**H₃**), 4.20 (q, *J* = 7.0 Hz, 2H, CH_3C**H₂**O), 5.77 (d, *J* = 15.5 Hz, 1H, C6-**H**), 5.98 (q, *J* = 7.0 Hz, 1H, C2-**H**), 7.31 (d, *J* = 15.5 Hz, 1H, C4-**H**); ^{13}C NMR (101 MHz, $CDCl_3$) δ 11.9 (**C**H_3CH_2O), 14.5 (C-5), 14.7 (C-1), 60.3 (CH_3**C**H_2O), 115.4 (C-6), 133.9 (C-3), 136.4 (C-2), 149.6 (C-4), 167.8 (**C**O_2Et).

Ethyl (*E*)-3-methylhexa-1,3-dienoate[230] 274

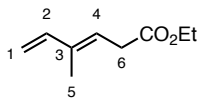

To a solution of dry DIPA (2.4 mL, 16.9 mmol) in dry THF (13 mL) under argon was added *n*-BuLi (6.1 mL, 2.35 M in hexanes, 14.3 mmol) dropwise at –78 °C. DMPU (2.7 mL, 22.7 mmol) was added dropwise and the mixture stirred for 10 mins. Diene **273** was added dropwise and the solution was stirred for 4 h at –78 °C. After this time the reaction mixture was poured into AcOH in ice water (5 mL, 25 mL water), the layers separated, and the aqueous layer extracted with pentane (3 × 10 mL). The combined organic layers were washed with satd. aq. $NaHCO_3$ solution (10 mL) and brine (10 mL) then dried over $MgSO_4$ and the solvent removed *in vacuo* to give the title compound as a colourless oil (1.64 g, 83%). The product was used in the next reaction without purification. ν_{max} (thin film)/cm^{-1}: 2926w, 1737s, 1320w, 1259w, 1161m, 1020w, 849w; ^{1}H NMR (400 MHz, $CDCl_3$) δ 1.26 (t, *J* = 7.0 Hz, 3H, C**H$_3$**CH_2O), 1.76 (s, 3H, C5-**H$_3$**), 3.18 (d, *J* = 7.5 Hz, 2H, C6-**H$_2$**), 4.15 (q, *J* = 7.0 Hz, 2H, CH_3C**H$_2$**O), 5.01 (d, *J* = 10.5 Hz, C1-**H**$_{cis}$), 5.16 (d, *J* = 17.5 Hz, C1-**H**$_{trans}$), 5.66 (t, *J* = 7.5 Hz, 1H, C4-**H**), 6.41 (dd, *J* = 17.5, 10.5 Hz, 1H, C2-**H**); ^{13}C NMR (101 MHz, $CDCl_3$) δ 12.1 (C-5), 14.3 (**C**H_3CH_2O), 34.2 (C-6), 60.9 (CH_3**C**H_2O), 112.3 (C-1), 123.6 (C-4), 137.0 (C-3), 140.8 (C-2), 171.9 (**C**O_2Et).

(*E*)-3-Methylhexa-1,3-dien-6-ol[231] **268**

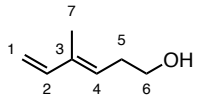

Method A

To a solution of 3-methyl-1,4-pentadiene (2.8 mL, 22.9 mmol) under Ar in dry THF (63 mL) was added *n*-BuLi (8.8 mL, 2.35 M in hexanes, 20.7 mol) dropwise at –78 °C. The mixture was warmed to RT over 40 mins and then cooled again to –78 °C. Paraformaldehyde (0.96 g, 32.1 mmol) was added as a suspension in THF (7 mL). The mixture was warmed to RT and once the reaction was complete, judged by disappearance of the red colour, 18-crown-6 (5.46 g, 20.7 mmol) then KOTMS (5.30 g, 41.3 mmol) were added. The solution was stirred at RT for 15 mins after which time brine (15 mL) was added. The layers were separated and the aqueous layer extracted with Et_2O (3 × 15 mL). The combined organic layers were washed with water (15 mL) and brine (15 mL), dried over $MgSO_4$, filtered, and the solvent removed *in vacuo*. The crude residue was purified by column chromatography (30%→50% Et_2O in pentane) to give the title compound as a pale-yellow oil (0.56 g mg, 22%).

Method B

To a suspension of $LiAlH_4$ (0.60 g, 15.9 mmol) in dry Et_2O (30 mL) was added ester **274** (1.75 g, 11.35 mmol) as a solution in dry Et_2O (10 mL). The reaction mixture was stirred for 16 h at RT after which time 0.6 mL water was added at 0°C, followed by 0.6 mL 3 M NaOH and 1.8 mL water. The mixture was warmed to RT and stirred for 15 mins. $MgSO_4$ was added and, after stirring for another 15 mins, the mixture was filtered and the solvent removed *in vacuo* to give the title compound without further

purification (1.02 g, 80%). ν_{max} (thin film)/cm^{-1}: 3325m br. (alcohol), 2926m, 2877m, 1643w, 1607m, 1415m, 1389m, 1046s, 990m, 894s; ^{1}H NMR (400 MHz, $CDCl_3$) δ 1.78 s, 3H, C7-**H$_3$**), 2.43 (app. q, *J* = 7.0 Hz, 2H, C5-**H$_2$**), 3.68 (t, *J* = 7.0 Hz, 2H, C6-**H$_2$**), 4.98 (d, *J* = 10.5 Hz, 1H, C1-**H**$_{cis}$), 5.13 (d, *J* = 17.5 Hz, 1H, C1-**H**$_{trans}$), 5.50 (t, *J* = 7.0 Hz, 1H, C4-**H**), 6.39 (dd, *J* = 17.5, 10.5 Hz, 1H, C2-**H**); ^{13}C NMR (101 MHz, $CDCl_3$) δ 12.0 (C-7), 31.9 (C-5), 62.4 (C-6), 111.6 (C-1), 128.4 (C-4), 136.9 (C-3), 141.3 (C-2).

(*E*)-3-Methylhexa-1,3-dien-1-yl (*E*)-11-methylpent-9-enoate[209] 276

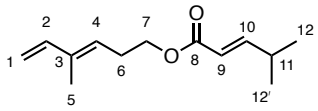

To a solution of (*E*)-4-methylpent-2-enoic acid (0.37 mL, 3.08 mmol), alcohol **268** (0.23 g, 2.05 mmol), and DMAP (50 mg, 0.41 mmol) in CH_2Cl_2 (9 mL) under argon was added DCC (0.64 g, 3.08 mmol) at 0 °C. The solution was stirred at 0 °C for 30 mins then at RT for 18 h. After this time the reaction mixture was filtered through celite, washed with satd. aq. $NaHCO_3$ solution (5 mL) then brine (5 mL), dried over $MgSO_4$ and the solvent removed *in vacuo*. The residue was purified by column chromatography (5% Et_2O in pentane) to give the title compound as a yellow oil (337 mg, 79%). ν_{max} (thin film)/cm^{-1}: 2962m, 2926m, 2161w, 1978w, 1719s, 1653m, 1465w, 1299m, 1262m, 1188m, 1165s, 987m; ^{1}H NMR (400 MHz, $CDCl_3$) δ 1.05 (s, 3H, C12-**H$_3$**), 1.07 (s, 3H, C12′-**H$_3$**), 1.77 (s, 3H, C5-**H$_3$**), 2.41 – 2.48 (m, 1H, C11-**H**), 2.51 (app. q, *J* = 7.5 Hz, 2H, C6-**H$_2$**), 4.15 (t, *J* = 7.5 Hz, 2H, C7-**H$_2$**), 4.98 (d, *J* = 10.5 Hz, 1H, C1-**H**$_{cis}$), 5.13 (d, *J* = 17.5 Hz, 1H, C1-**H**$_{trans}$), 5.48 (t, *J* = 7.5 Hz, 1H, C4-**H**), 5.76 (d, *J* = 15.5 Hz, 1H, C9-**H**), 6.38 (dd, *J* = 17.5, 10.5 Hz, 1H, C2-**H**), 6.94 (dd, *J* = 15.5, 6.5 Hz, 1H, C10-**H**); ^{13}C NMR (101 MHz, $CDCl_3$) δ 11.9 (C-5), 21.4 (C12, C12′), 28.0 (C-

6), 31.1 (C-11), 63.6 (C-7), 111.6 (C-1), 118.6 (C-9), 127.6 (C-4), 136.6 (C-3), 141.2 (C-2), 155.9 (C-10), 167.2 (C-8).

(±)-(8-Isopropyl-5-methyl-3,4,4a,7,8,8a-hexahydro-1*H*-isochromen-1-one[231] (±)-**115**

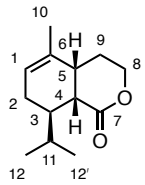

Method A

To a solution of diene **268** (30 mg, 0.27 mmol) and thioester **270** (0.17 g, 1.1 mmol) in CH_2Cl_2 (2 mL) was added Me_2AlCl (0.27 mL, 1.0 M in hexanes, 0.27 mmol). The reaction was stirred at RT for 60 h, diluted with CH_2Cl_2 (2 mL), then sat. aq. NaH_2PO_4 (0.3 mL) was added and the mixture stirred for 10 mins. 3 M HCl was added to dissolve the white precipitate, the layers separated, and the aqueous layer extracted with CH_2Cl_2 (3 × 2 mL). The combine organic layers were washed with brine (5 mL), dried over Na_2SO_4, and concentrated under a stream of nitrogen. The resultant mixture was dissolved in CH_2Cl_2 (2 mL) and *p*-toluenesulfonic acid monohydrate (25 mg, 0.134 mmol) was added. Stirring continued for 3 h at RT then the mixture was diluted with CH_2Cl_2 (2 mL), sat. aq. $NaHCO_3$ solution (5 mL) was added, and the layers separated. The aqueous layer was extracted with CH_2Cl_2 (3 × 5 mL), and the combined organic layers were washed with brine (10 mL), dried over Na_2SO_4, and concentrated under a stream of nitrogen. The residue was purified by flash column chromatography (20% EtOAc in pentane) to give the title compound as a pale-yellow oil (28 mg, 51%).

Method B

To a solution of $TfNH_2$ (0.40 g, 2.64 mmol) in DCE (24 mL) was added Me_2AlCl (5.3 mL, 1.0 M in hexanes, 5.3 mmol) at 0 °C under Ar. The solution was stirred for 30 mins at RT after which time triene **276** (0.50 g, 2.40 mmol) was added as a solution in DCE (12 mL). The reaction mixture was heated to 80 °C and stirred for a further 4 h after which time it was cooled to RT and gently quenched with 1M HCl (5 mL), the layers separated, and the aqueous layer extracted with Et_2O (3 × 10 mL). The combined organic phases were washed with brine, dried over $MgSO_4$, and concentrated *in vacuo*. The residue was purified by column chromatography (20% Et_2O in pentane) to give the title compound as a yellow oil (0.37 g, 75%). ^{1}H NMR (400 MHz, C_6D_6) δ 0.75 (d, *J* = 6.5 Hz, 3H, C12-**H$_3$**), 0.86 (d, *J* = 6.5 Hz, 3H, C12′-**H$_3$**), 1.16 – 1.25 (m, 2H, C9-**H$_2$**), 1.30 (app. dq, *J* = 2.5, 1.5 Hz, 3H, C10-**H$_3$**), 1.48 (dhept, *J* = 9.0, 6.5 Hz, 1H, C11-**H**), 1.82 (app. dddt, *J* = 18.0, 5.0, 3.0, 1.5 Hz, 1H, C2-**H$_a$**H$_b$), 1.95 (t, *J* = 4.5 Hz, 1H, C5-**H**), 2.06 – 2.15 (m, 1H, C3-**H**), 2.22 (app. ddq, *J* = 18.0, 5.0, 2.0 Hz, 1H, C2-H$_a$**H$_b$**), 2.50 (ddd, *J* = 6.5, 4.5, 2.0 Hz, 1H, C4-**H**), 3.52 – 3.64 (m, 1H, C8-**H$_a$**H$_b$), 3.62 – 3.76 (m, 1H, C8-H$_a$**H$_b$**), 5.20 – 5.30 (m, 1H, C1-**H**); ^{13}C NMR (101 MHz, C_6D_6) δ 20.4 (C-12), 20.5 (C-10), 21.0 (C-12′), 24.6 (C-2), 26.2 (C-9), 27.2 (C-11), 33.2 (C-5), 39.5 (C-3), 43.1 (C-4), 65.5 (C-8), 124.0 (C-1), 132.5 (C-6), 172.1 (C-7); *m/z* ([ESI$^+$]): 209.2 ([M+H]$^+$), 231.2 ([M+Na]$^+$).

Chemical resolution of bicyclic lactone

To a solution of lactone (±)-**115** (0.75 g, 3.6 mmol) and (*S*)-1-phenethylamine (0.93 mL, 7.2 mmol) in CH_2Cl_2 (11 mL) under Ar was added $AlMe_3$ (3.6 mL, 2M in hexanes, 7.2 mmol) at 0 °C. The reaction mixture was allowed to warm to RT and stirred for 24 h after which time it was quenched with water (5 mL). 1M HCl was added to dissolve the

white precipitate, the layers separated, and the aqueous layer extracted with CH_2Cl_2 (3 × 5 mL). The combined organic layers were dried over $MgSO_4$, filtered, and concentrate *in vacuo*. The residue was purified by column chromatography (40% EtOAc in pentane) to yield the desired diastereomers.

(–)-(1*R*,2*R*,6*R*)-2-(2-hydroxyethyl)-6-isopropyl-3-methyl-*N*-((*S*)-1-phenylethyl)cyclohex-3-ene-1-carboxamide (–)-**278**

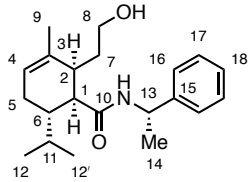

White solid; 0.47 g, 79%; R_f 0.27 (40% EtOAc in pentane); m.p. 107 – 109 °C; $[\alpha]_D^{25}$ 124.0 (*c* 0.78, $CHCl_3$); ν_{max} (thin film)/cm^{-1}: 3287w, 2958w, 2932w, 1637s, 1537m, 1449w, 1236w, 1033w, 699m; ^{1}H NMR (400 MHz, $CDCl_3$) δ 0.77 (d, *J* = 6.5 Hz, 3H, C12-**H$_3$**), 0.91 (d, *J* = 6.5 Hz, 3H, C12′-**H$_3$**), 1.50 (d, *J* = 7.0 Hz, 3H, C14-**H$_3$**), 1.52 – 1.61 (m, 1H, C7-**H$_a$**H$_b$), 1.66 (m, 3H, C9-**H$_3$**), 1.69 – 1.86 (m, 1H, C5-**H$_a$**H$_b$), 1.92 – 2.03 (m, 2H, C5-H$_a$**H$_b$**, C7-H$_a$**H$_b$**), 2.03 – 2.11 (m, 2H, C2-**H**, C11-**H**), 2.19 (app. q, *J* = 6.0 Hz, 1H, C1-**H**), 2.31 (dd, *J* = 10.5, 6.0 Hz, 1H, C6-**H**), 3.35 – 3.53 (m, 2H, C8-**H$_2$**), 5.13 (p, *J* = 7.0 Hz, 1H, C13-**H**), 5.40 (app. tt, *J* = 3.0, 1.5 Hz, 1H, C4-**H**), 5.93 (d, *J* = 7.0 Hz, 1H, *N***H**), 7.27 – 7.39 (m, 5H, Ar**H**); ^{13}C NMR (101 MHz, $CDCl_3$) δ 16.0 (C-12), 21.2 (C-12′), 21.7 (C-14), 22.3 (C-9), 23.6 (C-5), 27.8 (C-11), 32.8 (C-7), 35.4 (C-2), 39.7 (C-1), 48.7 (C-13), 49.2 (C-6), 61.4 (C-8), 122.0 (C-4), 126.5 (C-16), 127.6 (C-18), 128.8 (C-17), 135.7 (C-3), 143.2 (C-15), 173.9 (C-10); *m/z* ([ESI$^+$]): 330.2 ([M+H]$^+$); HRMS: 330.2427 found, $C_{21}H_{32}O_2N$ requires 330.2428.

(+)-(1*S*,2*S*,6*S*)-2-(2-hydroxyethyl)-6-isopropyl-3-methyl-*N*-((*S*)-1-phenylethyl)cyclohex-3-ene-1-carboxamide (+)-**277**

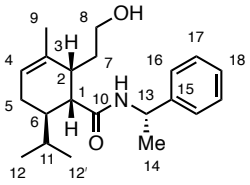

White solid; 0.48 g mg, 81%; R_f 0.15 (40% EtOAc in pentane); m.p. 55 – 57 °C; $[\alpha]_D^{25}$ +10.3 (*c* 1.17, $CHCl_3$); ν_{max} (thin film)/cm^{-1}: 3320m, 2958w, 2907w, 1640s, 1523s, 1450w, 1383w, 1237w, 1066w, 1031w, 699m; ^1H NMR (500 MHz, $CDCl_3$) δ 0.67 (d, *J* = 7.0 Hz, 3H, C12-**H$_3$**), 0.85 (d, *J* = 7.0 Hz, 3H, C12′-**H$_3$**), 1.49 (d, *J* = 7.0 Hz, 3H, C14-**H$_3$**), 1.58 – 1.66 (m, 1H, C7-**H$_a$**H$_b$), 1.68 (d, *J* = 2.0 Hz, 3H, C9-**H$_3$**), 1.70 – 1.83 (m, 1H, C5-**H$_a$**H$_b$), 1.86 – 1.95 (m, 1H, C11-**H**), 1.95 – 2.01 (m, 1H, C5-H$_a$**H$_b$**), 2.01 – 2.07 (m, 1H, C6-**H**), 2.07 – 2.14 (m, 1H, C7-H$_a$**H$_b$**), 2.27 (app. q, *J* = 5.0 Hz, 1H, C2-**H**), 2.32 (dd, *J* = 10.5, 5.0 Hz, 1H, C1-**H**), 2.51 (s, 1H, *O***H**), 3.56 (dt, *J* = 11.0, 6.0 Hz, 1H, C8-**H$_a$**H$_b$), 3.65 (ddd, *J* = 11.0, 7.5, 6.0 Hz, 1H, C8-H$_a$**H$_b$**), 5.15 (p, *J* = 7.0 Hz, 1H, C13-**H**), 5.41 (br. s, 1H, C4-**H**), 5.95 (d, *J* = 7.0 Hz, 1H, *N***H**), 7.23 – 7.27 (m, 1H, C18-**H**), 7.27 – 7.36 (m, 4H, Ar**H**); ^{13}C NMR (126 MHz, $CDCl_3$) δ 15.9, 21.2 (C-12, C-12′) , 21.7 (C-14), 22.2 (C-9), 23.6 (C-5), 27.6 (C-11), 32.9 (C-7), 35.5 (C-2), 40.1 (C-1), 48.6 (C-13), 49.2 (C-6), 61.8 (C-8), 122.0 (C-4), 126.2 (C-16), 127.5 (C-18), 128.7 (C-17), 135.6 (C-3), 143.3 (C-15), 174.1 (C-10); *m/z* ([ESI$^+$]): 330.2 ([M+H]$^+$); HRMS: 330.2427 found, $C_{21}H_{32}O_2N$ requires 330.2428.

(–)-2-(5-Isopropyl-2-methyl-6-(((*S*)-1-phenylethyl)carbamoyl)cyclohex-2-en-1-yl)ethyl 4-bromobenzoate (–)-**282**

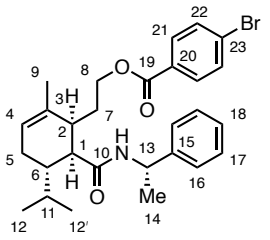

To a solution of alcohol (–)-**278** (50 mg, 0.15 mmol) and 4-bromobenzoic acid (46 mg, 0.38 mmol) in CH_2Cl_2 (0.9 mL) was added DCC (47 mg, 0.23 mmol) followed by DMAP (4 mg, 0.03 mmol). The reaction mixture was stirred at RT for 3 h after which time it was filtered through celite. The filtrate was washed with $NaHCO_3$ (3 × 2 mL), dried over Na_2SO_4, and concentrated *in vacuo*. The residue was purified by column chromatography (5% → 7.5% EtOAc in pentane) to give the title compound as a white solid (56 mg, 71%). R_f 0.73 (20% EtOAc in pentane); m.p. 136 – 138 °C; $[\alpha]_D^{25}$ – 99.5 (*c* 0.79, $CHCl_3$); ν_{max} (thin film)/cm^{-1}: 3322w, 3032w, 2960w, 2361w, 1725m, 1635m, 1590w, 1527m, 1483w, 1397w, 1270s, 1233w, 1117m, 1103m, 1011m, 756m; ^{1}H NMR (400 MHz, $CDCl_3$) δ 0.78 (d, *J* = 7.0 Hz, 3H, C12-**H$_3$**), 0.91 (d, *J* = 7.0 Hz, 3H, C12′-**H$_3$**), 1.51 (d, *J* = 7.0 Hz, 3H, C14-**H$_3$**), 1.68 (app. q, *J* = 2.0 Hz, 3H, C9-**H$_3$**), 1.70 – 1.77 (m, 1H, C7-**H$_a$**H$_b$), 1.77 – 1.85 (m, 1H, C5-**H$_a$**H$_b$), 1.94 – 2.04 (m, 3H, C2-**H**, C5-H$_a$**H$_b$**, C11-**H**), 2.10 (qd, *J* = 7.0, 4.0 Hz, 1H, C11-**H**), 2.16 – 2.24 (m, 2H, C6-**H**, C7-H$_a$**H$_b$**), 2.30 (dd, *J* = 10.5, 4.0 Hz, 1H, C1-**H**), 4.09 (ddd, *J* = 11.0, 8.0, 6.5 Hz, 1H, C8-**H$_a$**H$_b$), 4.19 (ddd, *J* = 11.0, 8.0, 5.0 Hz, 1H, C8-H$_a$**H$_b$**), 5.15 (p, *J* = 7.0 Hz, 1H, C13-**H**), 5.39 (br. s, 1H, C4-**H**), 5.77 (d, *J* = 7.0 Hz, 1H, *N***H**), 7.18 – 7.25 (m, 1H, C18-**H**), 7.27 – 7.36 (m, 4H, C16-**H**, C17-**H**), 7.52 – 7.58 (m, 2H, C22-**H**), 7.82 – 7.88 (m, 2H, C21-**H**); ^{13}C NMR (101 MHz, $CDCl_3$) δ 16.1, 21.2 (C-12, C-12′), 21.7 (C-14), 22.4 (C-9), 23.6

(C-5), 27.7 (C-11), 29.3 (C-7), 35.5 (C-2), 39.1 (C-6), 48.8 (C-1, C-13), 64.9 (C-8), 122.2 (C-4), 126.4 (C-16), 127.6 (C-18), 128.0 (C-20), 128.9 (C-17), 131.2 (C-21), 131.8 (C-22), 135.5 (C-3), 165.8 (C-19), 172.8 (C-10); *m/z* ([ESI$^+$]): 534.2 ([M+Na]$^+$); HRMS: 534.1614 found, $C_{28}H_{34}O_3N^{79}Br^{23}Na$ requires 534.1614.

(+)-2-(5-Isopropyl-2-methyl-6-(((*S*)-1-phenylethyl)carbamoyl)cyclohex-2-en-1-yl)ethyl 4-bromobenzoate (+)-**281**

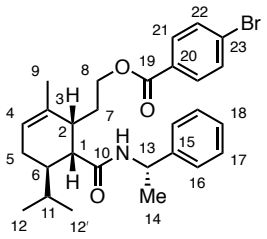

To a solution of of alcohol (+)-**277** (50 mg, 0.15 mmol) and 4-bromobenzoic acid (46 mg, 0.23 mmol) in CH_2Cl_2 (0.9 mL) was added DCC (47 mg, 0.23 mmol) followed by DMAP (4 mg, 0.03 mmol). The reaction mixture was stirred for 3 h after which time it was filtered through celite. The filtrate was washed with $NaHCO_3$ (3 × 2 mL), dried over Na_2SO_4, and concentrated *in vacuo*. The residue was purified by column chromatography (5% → 7.5% EtOAc in pentane) to give the title compound as a white solid (70 mg, 89%). R_f 0.84 (40% EtOAc in pentane); m.p. 124 – 126 °C; $[\alpha]_D^{25}$ + 9.2 (*c* 0.75, $CHCl_3$); ν_{max} (thin film)/cm^{-1}: 3296w, 303w, 2959w, 1721m, 1633m, 1591w, 1535w, 1271s, 1117w, 1104w, 1013w, 757m; ^{1}H NMR (400 MHz, $CDCl_3$) δ 0.68 (d, *J* = 6.5 Hz, 3H, C12-**H$_3$**), 0.85 (d, *J* = 6.5 Hz, 3H, C12′-**H$_3$**), 1.49 (d, *J* = 7.0 Hz, 3H, C14-**H$_3$**), 1.72 (d, *J* = 2.0 Hz, 3H, C9-**H$_3$**), 1.75 – 1.88 (m, 2H, C5-**H$_a$**H$_b$, C7-**H$_a$**H$_b$), 1.91 – 2.05 (m, 3H, C5-H$_a$**H$_b$**, C2-**H**, C11-**H**), 2.20 – 2.36 (m, 3H, C1-**H**, C6-**H**, C7-H$_a$**H$_b$**), 4.22 – 4.38 (m, 2H, C8-**H$_2$**), 5.17 (p, *J* = 7.0 Hz, 1H, C13-**H**), 5.40 (s, 1H, C4-**H**), 5.84 (d, *J* = 7.0 Hz, 1H, *N***H**), 7.21 – 7.25 (m, 1H, C18-**H**), 7.27 – 7.35 (m, 4H, C16-**H**, C17-

H), 7.55 – 7.59 (m, 2H, C22-**H**), 7.87 – 7.92 (m, 2H, C21-**H**); ^{13}C NMR (101 MHz, $CDCl_3$) δ 16.0, 21.1 (C-12, C-12′), 21.7 (C-14), 22.4 (C-9), 23.6 (C-5), 27.5 (C-2) 29.3 (C-7), 35.5 (C-11), 39.2 (C-6), 48.5 (C-13), 48.6 (C-1), 65.2 (C-8), 122.1 (C-4), 126.2 (C-16), 127.4 (C-18), 128.0 (C-20), 128.7 (C-17), 129.6 (C-23), 131.2 (C-21), 131.8 (C-22), 135.4 (C-3), 143.5 (C-15), 166.0 (C-19), 172.8 (C-10); *m/z* ([ESI$^+$]): 534.2 ([M+Na]$^+$); HRMS: 534.1614 found, $C_{28}H_{34}O_3N^{79}Br^{23}Na$ requires 534.1614.

(+)-(3a*R*,7*R*,7a*R*,*Z*)-8-Isopropyl-5-methyl-*N*-((*S*)-1'-phenylethyl)-2,3,3a,6,7,7a-hexahydro-1*H*-isochromen-1-imine (+)-**280**

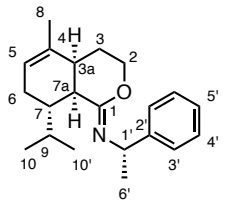

To a solution of (–)-**278** (20 mg, 0.06 mmol) in CH_2Cl_2 (0.92 mL) was added $SOCl_2$ (7 μL, 0.09 mmol) under argon at RT. The reaction mixture was stirred for 20 mins after which time it was quenched with sat. aq. $NaHCO_3$ (1 mL). The layers were separated, the aqueous layer extracted with CH_2Cl_2 (3 × 1 mL), and the combined organic layers were dried over Na_2SO_4, filtered and concentrated *in vacuo* to give the title compound as a yellow oil without further purification (7 mg, 36%). $[\alpha]_D^{25}$ +83.7 (*c* 0.64, $CHCl_3$); ν_{max} (thin film)/cm^{-1}: 3026m, 2957m, 2361w, 1672s, 1466m, 1384w, 1248m, 1217m, 1085m, 1061s, 760m, 700s; ^{1}H NMR (400 MHz, $CDCl_3$) δ 0.94 (d, *J* = 7.0 Hz, 3H, C10-**H$_3$**), 0.97 (d, *J* = 7.0 Hz, 3H, C10-**H$_3$**), 1.36 (d, *J* = 6.5 Hz, 3H, C6'-**H$_3$**), 1.64 (d, *J* = 2.0 Hz, 3H, C8-**H$_3$**), 1.75 – 1.85 (m, 3H, C9-**H**, C3-**H$_2$**), 1.85 – 1.91 (m, 1H, C6-**H$_a$**H$_b$), 1.92 – 1.99 (m, 1H, C7-**H**), 2.00 – 2.09 (m, 1H, C6-H$_a$**H$_b$**), 2.30 (q, *J* = 6.5 Hz, 1H, C3a-**H**), 2.56 (dd, *J* = 10.5, 6.5 Hz, 1H, C7a-**H**), 3.66 – 3.75 (m, 1H, C2-**H$_a$**Hb),

4.20 (dt, *J* = 11.0, 4.5 Hz, 1H, C2-H$_a$**H$_b$**), 5.00 (q, *J* = 6.5 Hz, 1H, C1'-**H**), 5.44 (br. s, 1H, C5-**H**), 7.16 – 7.22 (m, 1H, C5'-**H**), 7.27 – 7.34 (m, 2H, C4'-**H**), 7.39 – 7.44 (m, 2H, C3'-**H**); ^{13}C NMR (101 MHz, $CDCl_3$) δ 16.4 (C-10), 21.4 (C-8), 21.6 (C-10'), 24.4 (C-6), 24.5 (C-6'), 27.1 (C-3), 28.0 (C-9), 37.0 (C-7), 38.8 (C-3a), 43.7 (C-7a), 54.3 (C-1'), 68.7 (C-2), 122.3 (C-5), 126.3 (C-5'), 126.8 (C-3'), 128.4 (C-4'), 134.7 (C-4), 147.3 (C-2'), 158.9 (C-1); *m/z* ([ESI$^+$]): 312.2 ([M+H]$^+$), 313.2 ([M+2H]$^+$); HRMS: 312.2325 found, $C_{21}H_{30}NO$ requires 312.2322.

(–)-(3a*S*,7*S*,7a*S*,*Z*)-7-Isopropyl-4-methyl-*N*-((*S*)-1'-phenylethyl)-2,3,3a,6,7,8a-hexahydro-1*H*-isochromen-1-imine (–)-279

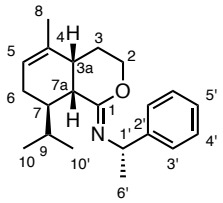

To a solution of (+)-**277** (20 mg, 0.06 mmol) in CH_2Cl_2 (0.9 mL) was added $SOCl_2$ (7 μL, 0.09 mmol) under argon at RT. The reaction mixture was stirred for 20 mins after which time it was quenched with sat. aq. $NaHCO_3$ (1 mL). The layers were separated, the aqueous layer extracted with CH_2Cl_2 (3 × 1 mL), and the combined organic layers were dried over Na_2SO_4, filtered and concentrated *in vacuo* to give the title compound as a yellow oil without further purification (14 mg, 73%). $[\alpha]_D^{25}$ –172.1 (*c* 0.96, $CHCl_3$); ν_{max} (thin film)/cm^{-1}: 2958m, 2926m, 2869w, 1668s, 1449m, 1384w, 1367w, 1248m, 1216m, 1085m, 1061s, 1034m, 759m, 699s; ^{1}H NMR (400 MHz, $CDCl_3$) δ 0.76 (d, *J* = 7.0 Hz, 3H, C10-**H$_3$**), 0.83 (d, *J* = 7.0 Hz, 3H, C10'-**H$_3$**), 1.40 (d, *J* = 6.5 Hz, 3H, C6'-**H$_3$**), 1.42 – 1.50 (m, 1H, C9-**H**), 1.66 (app. q, *J* = 2.0 Hz, 3H, C8-**H$_3$**), 1.74 – 1.94 (m, 4H, C3-**H$_2$**, C6-**H$_a$**H$_b$, C7-**H**), 1.92 – 2.03 (m, 1H, C6-H$_a$**H$_b$**), 2.39 (dt, *J* = 10.5, 5.5 Hz,

1H, C3a-**H**), 2.57 (dd, *J* = 10.5, 5.5 Hz, 1H, C7a-**H**), 3.91 (ddd, *J* = 11.0, 10.0, 4.0 Hz, 1H, C2-**H$_a$**H$_b$), 4.27 (ddd, *J* = 11.0, 5.0, 4.0 Hz, 1H, C2-H$_a$**H$_b$**), 5.07 (q, *J* = 6.5 Hz, 1H, C1'-**H**), 5.42 (br. s, 1H, C5-**H**), 7.13 – 7.22 (m, 1H, C5'-**H**), 7.23 – 7.32 (m, 2H, C4'-**H**), 7.34 – 7.42 (m, 2H, C3'-**H**); ^{13}C NMR (101 MHz, $CDCl_3$) δ 16.4 (C-10), 21.4 (C-10'), 21.4 (C-8), 24.3 (C-6), 25.2 (C-6'), 27.1 (C-3), 27.6 (C-9), 37.1 (C-7), 38.7 (C-3a), 43.8 (C-7a), 53.9 (C-1'), 68.9 (C-2), 122.3 (C-5), 126.2 (C-5'), 126.8 (C-3'), 128.1 (C-4'), 134.6 (C-4), 146.8 (C-2'), 159.3 (C-1); *m/z* ([ESI$^+$]): 312.2 ([M+H]$^+$), 313.2 ([M+2H]$^+$); HRMS: 312.2321 found, $C_{21}H_{30}NO$ requires 312.2322.

(+)-(3a*R,7*R**,7a*R**)-7-Isopropyl-4-methyl-2,3,3a,6,7,7a-hexahydro-1*H*-isochromen-1-one** (+)-**115**

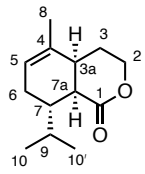

To a solution of iminoether (+)-**280** (0.48 g, 1.54 mmol) in CH_2Cl_2 (20 mL) was added silica gel (4.80 g, 10:1 w/w). The reaction mixture was stirred at RT for 55 h. The mixture was filtered, and the silica gel washed with EtOAc (3 × 5 mL). The combined organic layers were concentrated *in vacuo* and the crude residue purified by column chromatography (20% EtOAc → EtOAc) to yield the title compound as a yellow oil (69 mg, 22%). R_f 0.64 (40% EtOAc in pentante); $[\alpha]_D^{25}$ +124.5 (*c* 1.0, $CHCl_3$); ^{1}H NMR (400 MHz, C_6D_6) δ 0.75 (d, *J* = 6.5 Hz, 3H, C10-**H$_3$**), 0.86 (d, *J* = 6.5 Hz, 3H, C10′-**H$_3$**), 1.23 (app. pd, *J* = 6.5, 2.5 Hz, 2H, C3-**H$_2$**), 1.31 (d, *J* = 2.5 Hz, 3H, C8-**H$_3$**), 1.49 (dhept, *J* = 9.0, 6.5 Hz, 1H, C9-**H**), 1.77 – 1.87 (m, 1H, C6-**H$_a$**H$_b$), 1.97 (br. s, 1H, C3a-**H**), 2.05 – 2.14 (m, 1H, C7-**H**), 2.15 – 2.27 (m, 1H, C6-H$_a$**H$_b$**), 2.51 (ddd, *J* = 6.5, 4.5, 1.5 Hz, 1H, C7a-**H**), 3.54 – 3.63 (m, 1H, C2-**H$_a$**H$_b$), 3.63 – 3.76(m, 1H, C2-H$_a$**H$_b$**), 5.26 (s,

1H, C5-**H**); ^{13}C NMR (101 MHz, C_6D_6) δ 20.4 (C-10), 20.5 (C-8), 21.0 (C-10′), 24.6 (C-6), 26.3 (C-8), 27.2 (C-9), 33.2 (C-3a), 39.5 (C-7), 43.1 (C-7a), 65.5 (C-2), 124.0 (C-5), 132.6 (C-4), 172.1 (C-1); *m/z* ([ESI$^+$]): 209.4.

(–)-(3a*S,7*S**,7a*S**)-7-Isopropyl-4-methyl-2,3,3a,6,7,7a-hexahydro-1*H*-isochromen-1-one** (–)-**115**

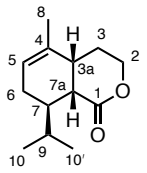

To a solution of iminoether (–)-**279** (0.60 g, 1.93 mmol) in CH_2Cl_2 (25 mL) was added silica gel (6.00 g, 10:1 w/w). The reaction mixture was stirred at RT for 63 h. The mixture was filtered, and the silica gel washed with EtOAc (3 × 5 mL). The combined organic layers were washed with 1 M HCl (10 mL), concentrated *in vacuo* and the crude residue purified by column chromatography (20% EtOAc → EtOAc) to yield the title compound as a yellow oil (230 mg, 57%). R_f 0.64 (40% EtOAc in pentane); $[\alpha]_D^{25}$ – 123.5 (*c* 1.0, $CHCl_3$); ^{1}H NMR (400 MHz, C_6D_6) δ 0.75 (d, *J* = 6.5 Hz, 3H, C10-**H$_3$**), 0.86 (d, *J* = 6.5 Hz, 3H, C10′-**H$_3$**), 1.23 (app. pd, *J* = 6.5, 2.5 Hz, 2H, C3-**H$_2$**), 1.31 (d, *J* = 2.5 Hz, 3H, C8-**H$_3$**), 1.49 (dhept, *J* = 9.0, 6.5 Hz, 1H, C9-**H**), 1.77 – 1.87 (m, 1H, C6-**H$_a$**H$_b$), 1.97 (br. s, 1H, C3a-**H**), 2.05 – 2.14 (m, 1H, C7-**H**), 2.15 – 2.27 (m, 1H, C6-H$_a$**H$_b$**), 2.51 (ddd, *J* = 6.5, 4.5, 1.5 Hz, 1H, C7a-**H**), 3.54 – 3.63 (m, 1H, C2-**H$_a$**H$_b$), 3.63 – 3.76(m, 1H, C2-H$_a$**H$_b$**), 5.26 (s, 1H, C5-**H**); ^{13}C NMR (101 MHz, C_6D_6) δ 20.4 (C-10), 20.5 (C-8), 21.0 (C-10′), 24.6 (C-6), 26.3 (C-8), 27.2 (C-9), 33.2 (C-3a), 39.5 (C-7), 43.1 (C-7a), 65.5 (C-2), 124.0 (C-5), 132.6 (C-4), 172.1 (C-1); *m/z* ([ESI$^+$]): 209.4.

(+)-Methyl (1*R*,2*R*,6*R*)-6-isopropyl-3-methyl-2-(10-oxoethyl)cyclohex-3-ene-1-carboxylate[129] (+)-239

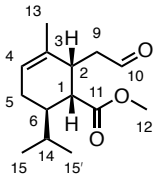

To a solution of (–)-**115** (30 mg, 0.14 mmol) in THF (1.4 mL) under Ar was added KOH (60 mg, 1.0 mmol). The reaction mixture was stirred at RT for 1 h after which time it was cooled to 0 ℃ and quenched with 2 M HCl (1.5 mL). The solution was extracted quickly with EtOAc (3 × 2 mL) and the organic layers were concentrated over K_2CO_3 (30 mg, 0.22 mmol) under a stream of nitrogen to prevent ring closure back to (–)-**115**. The crude residue was redissolved in DMF (0.4 mL) under Ar and K_2CO_3 (30 mg, 0.22 mmol) was added followed by MeI (13 μL, 0.22 mmol). The reaction mixture was stirred for 1 h at RT after which time it was quenched with $NaHCO_3$ (2 mL). The solution was extracted with EtOAc (3 × 2 mL) and the organic layers were washed with $Na_2S_2O_3$ and brine, dried over Na_2SO_4, filtered, and concentrated *in vacuo*. The crude residue was redissolved in CH_2Cl_2 (1.4 mL) under Ar and $NaHCO_3$ (12 mg, 0.14 mmol) was added followed by DMP (0.12 g, 0.29 mmol). The reaction mixture was stirred for 30 mins at RT after which time it was quenched with $Na_2S_2O_3$ (2 mL). The layers were separated, and the aqueous layer was extracted with CH_2Cl_2 (3 × 2 mL). The combined organic layers were washed with $NaHCO_3$ and brine, dried over Na_2SO_4, filtered, and concentrated *in vacuo*. The crude residue was purified by column chromatography (10% EtOAc in pentane) to yield the title compound as a colourless oil (15 mg, 43%). R_f 0.77 (20% EtOAc in pentane);); $[\alpha]_D^{25}$ + 95.7 (*c* 0.55, $CHCl_3$); ν_{max} (thin film)/cm^{-1}: 2959w, 1726s, 1435w, 1371w, 1255w, 1198w, 1161m, 1018w;

^{1}H NMR (400 MHz, $CDCl_3$) δ 0.74 (d, *J* = 6.5 Hz, 3H, C15-**H$_3$**), 0.90 (d, *J* = 6.5 Hz, 3H, C15′-**H$_3$**), 1.64 (app. q, *J* = 2.0 Hz, 3H, C13-**H$_3$**), 1.74 – 1.92 (m, 2H, C5-**H$_a$**H$_b$, C6-**H**), 1.93 – 2.01 (m, 1H, C5-H$_a$**H$_b$**), 2.28 – 2.40 (m, 1H, C9-**H$_a$**H$_b$), 2.61 – 2.68 (m, 1H, C1-**H**), 2.94 – 3.06 (m, 2H, C9-H$_a$**H$_b$**, C2-**H**), 3.60 (s, 3H, C12-**H$_3$**), 5.42 (m, 1H, C4-**H**), 9.70 (app. d, *J* = 1.0 Hz, 1H, C10-**H**); ^{13}C NMR (101 MHz, $CDCl_3$) δ 15.4 (C-15), 21.1 (C-15′), 21.9 (C-13), 23.5 (C-5), 27.8 (C-14), 35.1 (C-6), 35.2 (C-2), 44.7 (C-9), 46.9 (C-1), 51.7 (C-12), 122.5 (C-4), 134.3 (C-3), 175.3 (C-11), 201.2 (C-10); *m/z* ([ESI$^+$]): 261.2 ([M+Na]$^+$); HRMS: 261.1463 found, $C_{14}H_{22}O_3{}^{23}Na$ requires 261.1461.

(*E*)-Triethyl((3-methylhexa-2,4-dien-6-yl)oxy)silane 268a

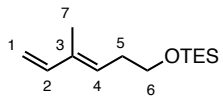

To a solution of alcohol **268** (50 mg, 0.45 mmol) in dry THF (1 mL) was added imidazole (46 mg, 0.70 mmol) as a solution in dry THF (1 mL). The reaction mixture was stirred at RT for 30 mins after which time TESCl (90 μL, 0.54 mmol) was added dropwise over 15 mins. Stirring continued for 4h at RT then the reaction was quenched with water (1 mL) at 0 °C. The layers were separated, and the aqueous layer extracted with EtOAc (3 × 2 mL). The combined organic layers were dried over $MgSO_4$, filtered, and concentrated *in vacuo*. The residue was purified by column chromatography (0%→5% Et_2O in pentane) to give the title compound as a colourless oil (53 mg, 52%). R_f 0.87 (5% Et_2O in pentane); ν_{max} (thin film)/cm^{-1}: 2954m, 2877m, 1742w, 1458w, 1415w, 1381w, 1101s, 1011m, 893m, 743s; ^{1}H NMR (400 MHz, $CDCl_3$) δ 0.60 (q, *J* = 8.0 Hz, 6H, SiC**H$_2$**CH$_3$), 0.96 (t, *J* = 8.0 Hz, 9H, SiCH$_2$C**H$_3$**), 1.75 (s, 3H, C7-**H$_3$**), 2.39 (q, *J* = 7.0 Hz, 2H, C5-**H$_2$**), 3.63 (t, *J* = 7.0 Hz, 2H, C6-**H$_2$**), 4.94 (d, *J* = 10.5 Hz, 1H, C1-**H$_{cis}$**), 5.10 (d, *J* = 17.5 Hz, 1H, C1-**H$_{trans}$**), 5.49 (t, *J* = 7.0 Hz, 1H, C4-**H**), 6.37 (dd,

J = 17.5, 10.5 Hz, 1H, C2-**H**); ^{13}C NMR (101 MHz, $CDCl_3$) δ 4.6 (Si**C**H_2CH_3), 6.9 ($SiCH_2$**C**H_3), 11.9 (C-7), 32.3 (C-5), 62.4 (C-6), 111.0 (C-1), 129.0 (C-4), 135.8 (C-3), 141.6 (C-2); *m/z* ([ESI$^+$]): 227.2 ([M+H]$^+$); HRMS: 227.1827 found, $C_{13}H_{27}O^{28}Si$ requires 227.1826.

(*E*)-*tert*-Butyldimethyl((3-methylhexa-2,4a-dien-6-yl)oxy)silane 268b

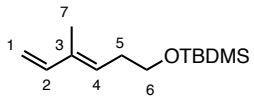

To a solution of alcohol **268** (50 mg, 0.45 mmol) in dry THF (1 mL) was added imidazole (46 mg, 0.70 mmol) as a solution in dry THF (1 mL). The reaction mixture was stirred at RT for 30 mins after which time TBDMSCl (81 mg, 0.54 mmol) was added. Stirring continued for 4 h at 80 °C then the reaction was cooled to 0 °C and quenched with water (1 mL). The layers were separated, and the aqueous layer extracted with EtOAc (3 × 2 mL). The combined organic layers were dried over $MgSO_4$, filtered, and concentrated *in vacuo*. The residue was purified by column chromatography (20% Et_2O in pentane) to give the title compound as a colourless oil (52 mg, 51%). R_f 0.88 (20% Et_2O in pentane); ν_{max} (thin film)/cm^{-1}: 2955w, 2929w, 2858w, 1254m, 1101s, 893m, 835s, 775s; ^{1}H NMR (400 MHz, $CDCl_3$) δ 0.05 (s, 6H, Si(C**H$_3$**)$_2$), 0.89 (s, 9H, SiC(C**H$_3$**)$_3$), 1.75 (s, 3H, C7-**H$_3$**), 2.37 (q, *J* = 7.0 Hz, 2H, C5-**H$_2$**), 3.64 (t, *J* = 7.0 Hz, 2H, C6-**H$_2$**), 4.94 (d, *J* = 10.5 Hz, 1H,C1-**H$_{cis}$**), 5.10 (d, *J* = 17.5 Hz, 1H, C1-**H$_{trans}$**), 5.49 (t, *J* = 7.0 Hz, 1H, C4-**H**), 6.37 (dd, *J* = 17.5, 10.5 Hz, 1H, C2-**H**); ^{13}C NMR (101 MHz, $CDCl_3$) δ –5.1 (Si(**C**H_3)$_2$, 12.0 (C-7), 18.5 (Si**C**$(CH_3)_3$), 26.1 (SiC(**C**H_3)$_3$, 32.2 (C-5), 62.8 (C-6), 111.0 (C-1), 129.1 (C-4), 135.7 (C-3), 141.6 (C-2); *m/z* ([ESI$^+$]): 227.2 ([M+H]$^+$); HRMS: 227.1827 found, $C_{13}H_{27}O^{28}Si$ requires 227.1826.

2-(Propan-5-ylidene)dihydrofuran-1(2*H*)-one[232] **314**

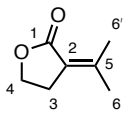

To a solution of freshly distilled DIPA (16.5 mL, 117 mmol) in dry THF (30 mL) was added *n*-BuLi (68 mL, 1.6 M in hexanes, 108 mmol) at –78 ºC. The mixture was warmed to RT over and stirred for 10 minutes after which time it was cooled to –78 ºC and γ-butyrolactone (6.9 mL, 90 mmol) was added dropwise as a solution in THF (20 mL). The reaction was stirred at –78 ºC for 1 h then freshly distilled acetone (13.0 mL, 180 mmol) was added over 20 minutes. The mixture was stirred at –78 ºC for 2 h, then at RT overnight, after which time it was quenched by the addition of solid NH_4Cl (11.0 g) and stirring continued for 30 minutes. The mixture was diluted with EtOAc (50 mL) and enough water was added to dissolve the NH_4Cl. The layers were separated and the aqueous layer was extracted with EtOAc (3 × 30 mL), dried over $MgSO_4$, and concentrated *in vacuo*. The crude residue was redissolved in PhMe (120 mL), conc. H_2SO_4 (0.72 mL, 2.7 mmol) was added and the mixture was stirred at reflux for 1 h. The reaction was diluted with Et_2O (110 mL) and washed sequentially with 1 M HCl (100 mL), sat. aq. $NaHCO_3$ (100 mL), and brine (100 mL). The aqueous layers were neutralised with 3 M NaOH and extracted with Et_2O (3 × 50 mL). The combined organic layers were dried over $MgSO_4$, filtered, and concentrated *in vacuo*, and purified by column chromatography (2:1 pentane:Et_2O) to yield the title compound as a colourless oil (7.00 g, 62%). R_f 0.57 (40% EtOAc in pentane); ν_{max} (thin film)/cm^{-1}: 2986w, 2915w, 1739s, 1667m, 1486w, 1445w, 1373w, 1268m, 1186s, 1031s; ^{1}H NMR (400 MHz, $CDCl_3$) δ 1.87 (s, 3H, C6-**H₃**), 2.25 (t, *J* = 2.0 Hz, 3H, C6′-**H₃**), 2.86 (m, 2H, C3-**H₂**), 4.27 (t, *J* = 7.5 Hz, 2H, C4-**H₂**); ^{13}C NMR (101 MHz, $CDCl_3$) δ 19.8 (C-6),

24.7 (C-6′), 27.8 (C-3), 31.5 (C-2), 64.3 (C-4), 66.0 (C-5); *m/z* ([ESI$^+$]): 127.0 ([M+H]$^+$), 149.0 ([M+Na]$^+$).

4-Methyl-3-(prop-6-en-7-yl)pent-3-en-1-yl acetate[233] 316

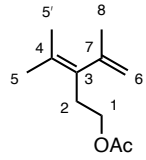

To a solution of lactone **314** (8.6 g, 68 mmol) in dry Et_2O (90 mL) was added MeMgBr (45 mL, 3 M in Et_2O, 136 mmol) at –78 ºC. The mixture was stirred for 30 minutes at –78 ºC and then 2 h at RT (care should be taken when warming reaction up, exothermic addition can lead to build up of pressure through evaporation of solvent) after which time AcCl (14.0 mL, 79 mmol) was added dropwise. The reaction was stirred for 1 h at RT and then quenched with sat. aq. NH_4Cl, the aqueous layer was extracted with Et_2O (3 × 50 mL) and the combined organic layers were dried over $MgSO_4$, filtered, and concentrated *in vacuo* to yield the title compound as a pale yellow oil (11.0 g, 89%). The crude compound was used without further purification. R_f 0.74 (2:1 pentane:Et_2O); ν_{max} (thin film)/cm^{-1}: 3076w, 2963w, 2915w, 1742s, 1446w, 1240s, 1032w, 898w; ^{1}H NMR (400 MHz, $CDCl_3$) δ 1.67 (s, 3H, C5-**H$_3$**), 1.70 (s, 3H, C5′-**H$_3$**), 1.77 (t, *J* = 1.0 Hz, 3H, C8-**H$_3$**), 2.03 (s, 3H, OC(O)C**H$_3$**), 2.42 (t, *J* = 7.5 Hz, 2H, C2-**H$_2$**), 4.03 (t, *J* = 7.5 Hz, 2H, C1-**H$_2$**), 4.57 (s, 1H, C6-**H$_a$**H$_b$), 4.94 (s, 1H, C6-H$_a$**H$_b$**); ^{13}C NMR (101 MHz, $CDCl_3$) δ 19.9 (C-5′), 21.2 (OC(O)**C**H$_3$), 21.9 (C-8), 22.6 (C-5), 30.3 (C-2), 63.2 (C-2), 113.9 (C-6), 128.4 (C-3), 131.9 (C-4), 146.0 (C-7), 171.3 (O**C**(O)CH$_3$).

4-Methyl-3-(prop-6-en-7-yl)pent-3-en-1-ol[234] **317**

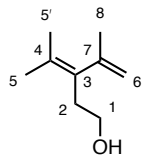

To a solution of acetate **316** (10.8 g, 60.2 mmol) in MeOH (72 mL) was added K_2CO_3 (10.0 g, 72.2 mmol). The mixture was stirred for 9 h at RT after which time it was quenched with sat. aq. NH_4Cl (30 mL) and diluted with Et_2O (30 mL). The layers were separated and the aqueous layer was extracted with Et_2O (3 × 50 mL). The combined organic layers were dried over $MgSO_4$, filtered, and concentrated *in vacuo* to yield the title compound as a pale yellow oil (7.9 g, 93%). The crude compound was used without further purification. R_f 0.31; (2:1 pentane:Et_2O); ν_{max} (thin film)/cm^{-1}: 3358 br. m, 2691s, 2924s, 2875s, 1741w, 1655m, 1445m, 1372m, 1043s, 895m); ^{1}H NMR (400 MHz, $CDCl_3$) δ 1.70 (s, 3H, C5-**H$_3$**), 1.72 (s, 3H, C5′-**H$_3$**), 1.78 (t, *J* = 1.5 Hz, 3H, C8-**H$_3$**), 2.40 (t, *J* = 6.5 Hz, 2H, C2-**H$_2$**), 3.62 (t, *J* = 6.5 Hz, 2H, C1-**H$_2$**), 4.58 (d, *J* = 2.0 Hz, 1H, C6-**H**$_{cis}$H$_{trans}$), 4.96 (dq, *J* = 3.0, 2.0 Hz, 1H, C6-H$_{cis}$**H**$_{trans}$); ^{13}C NMR (101 MHz, $CDCl_3$) δ 20.0 (C-5), 22.0 (C-5′), 22.7 (C-8), 34.1 (C-2), 61.4 (C-1), 113.7 (C-6), 128.7 (C-3), 132.7 (C-4), 146.5 (C-7).

4-Methyl-3-(prop-6-en-7-yl)pent-3-en-1-yl methanesulfonate[235] **318**

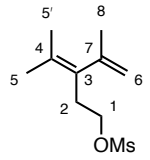

To a solution of alcohol **317** (7.9 mg, 56 mmol) and Et_3N (16.7 mL, 120 mmol) in CH_2Cl_2 (160 mL) was added MsCl (6.0 mL, 78 mmol) at 0 ºC. The reaction was stirred for 2 h at 0 ºC after which time it was quenched with sat. aq. $NaHCO_3$ (100 mL) and

extracted with Et_2O (3 × 75 mL). The combined organic layers were dried over $MgSO_4$, filtered, and concentrated *in vacuo* to yield the title compound as a yellow oil (12.1 g, 99%). The crude compound was used without further purification. R_f 0.36 (2:1 pentane:Et_2O); ν_{max} (thin film)/cm^{-1}: 2915w, 1633w, 1446w, 1353s, 1173s, 950m, 906m; ^1H NMR (400 MHz, $CDCl_3$) δ 1.69 (s, 3H, C5-**H₃**), 1.71 (s, 3H, C5′-**H₃**), 1.77 (t, *J* = 1.0 Hz, 3H, C8-**H₃**), 2.56 (t, *J* = 7.5 Hz, 2H, C2-**H₂**), 2.98 (s, 3H, OSO_2C**H₃**), 4.17 (t, *J* = 7.5 Hz, 2H, C1-**H₃**), 4.59 (dq, *J* = 1.5, 1.0 Hz, 1H, C6-**H*cis***H*trans*), 4.98 (dq, *J* = 3.0, 1.5 Hz, 1H, C6-H*cis***H*trans***); ^{13}C NMR (101 MHz, $CDCl_3$) δ 20.0 (C-5), 21.9 (C-5′), 22.5 (C-8), 30.8 (C-2), 37.6 (RO_3S**C**H_3), 68.4 (C-1), 114.6 (C-6), 129.9 (C-4), 130.5 (C-3), 145.4 (C-7).

4-Methyl-3-(prop-6-en-7-yl)pent-3-en-1-yl bromide 319

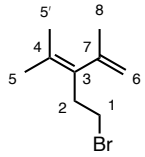

To a solution of mesylate **318** (3.24g, 14.8 mmol) in THF (52 mL) was added anhydrous LiBr (2.58g, 29.7 mmol). The reaction was stirred at reflux for 5 h after which time it was diluted with water (50 mL) and extracted with Et_2O (3 × 30 mL). The combined organic layers were dried over $MgSO_4$, filtered and concentrated *in vacuo*. The crude residue was purified by column chromatography (pentane:Et_2O 3:1) to yield the title compound as a yellow oil (2.20 g, 73%). R_f 0.95 (2:1 pentane:Et_2O); ν_{max} (thin film)/cm^{-1}: 2918w, 2851w, 1444w, 1372w, 1262w, 900w; ^1H NMR (400 MHz, $CDCl_3$) δ 1.68 (s, 3H, C5-**H₃**), 1.70 (s, 3H, C5′-**H₃**), 1.76 (s, 3H, C8-**H₃**), 2.65 (t, *J* = 8.0 Hz, 2H, C2-**H₂**), 3.34 (t, *J* = 8.0 Hz, 2H, C1-**H₂**), 4.61 (s, 1H, C6-**H$_a$**H$_b$), 4.97 (s, 1H, C6-H$_a$**H$_b$**);

^{13}C NMR (101 MHz, $CDCl_3$) δ 19.9 (C-5), 21.9 (C-5′), 22.6 (C-8), 31.5 (C-1), 34.7 (C-2), 114.4 (C-6), 128.9 (C-4), 133.7 (C-3), 145.3 (C-7).

4-Methyl-3-(prop-6-en-7-yl)pent-3-en-1-yl iodide[235] **321**

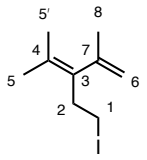

Method A

To a solution of **319** (1.00 g, 4.9 mmol) in dry acetone (25 mL) was added NaI (9.90 g, 66 mmol). The mixture was stirred at reflux for 16 h after which time the reaction was diluted with water (25 mL) and extracted with pentane (3 × 30 mL). The combined organic layers were dried over $MgSO_4$, filtered, and concentrated *in vacuo* to yield the title compound as a yellow oil (1.16 g, 94%). The crude product was used without any further purification.

Method B

To a solution of mesylate **318** (6.3 g, 28.3 mmol) in acetone (56 mL) was added NaI (12.7 g, 85 mmol) and the solution was heated to reflux for 4 h. The mixture was concentrated and redissolved in Et_2O (50 mL) and washed with brine (30 mL). The layers were separated and the organic layer was dried over $MgSO_4$, concentrated, and passed through a silica plug (pentane) to yield the title compound as a yellow oil (5.0 g, 72%). R_f 0.8 (pentane); ν_{max} (thin film)/cm^{-1}: 2923s, 2855m, 2360m, 1456m, 1373w, 1242w, 1166m, 900m; ^{1}H NMR (400 MHz, $CDCl_3$) δ 1.66 (s, 3H, C5-**H$_3$**), 1.68 (s, 3H, C5′-**H$_3$**), 1.75 (t, *J* = 1.0 Hz, 3H, C8-**H$_3$**), 2.67 (t, *J* = 8.0 Hz, 2H, C2-**H$_2$**), 3.11 (t, *J* = 8.0 Hz, 2H, C1-**H$_2$**), 4.62 (dd, *J* = 2.5, 1.5 Hz, 1H, C6-**H**$_{cis}$H$_{trans}$), 4.97 (dt, *J* = 3.0, 1.5

Hz, 1H, C6-H*cis*$\mathbf{H}_{trans}$); ^{13}C NMR (101 MHz, $CDCl_3$) δ 4.8 (C-1), 20.0 (C-5), 22.0 (C-5′), 22.7 (C-8), 35.6 (C-2), 114.5 (C-6), 128.5 (C-4), 135.6 (C-3), 145.1 (C-7).

9-(13-Methyl-9-(prop-12-en-10-yl)pent-9-en-7-yl)cyclohex-2-en-1-one[236] **312**

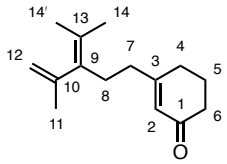

To a solution of iodide **321** (1.16 g, 4.6 mmol) in anhydrous Et_2O (9 mL) at –78 ºC was added *t*-BuLi (5.7 mL, 1.7 M, 9.7 mmol) dropwise. The reaction was stirred at –78 ºC for 15 minutes, then 1 h at RT after which time the mixture was cooled to 0 ºC. 3-ethoxycyclohex-2-en-1-one (1.3 mL, 9.28 mmol) was added and stirring continued for 30 minutes. The reaction was warmed to RT, stirred for 3 h, then quenched with 1 M HCl. The mixture was extracted with Et_2O (3 × 10 mL) and the combined organic layers were dried over $MgSO_4$, filtered, and concentrated *in vacuo*. The crude residue was purified by column chromatography (10% Et_2O in pentane) to yield the title compound as a colourless oil (0.62 g, 60%). ^{1}H NMR (400 MHz, $CDCl_3$) δ 1.66 (s, 6H, C14-$\mathbf{H_3}$, C14′-$\mathbf{H_3}$), 1.76 (s, 3H, C11-$\mathbf{H_3}$), 1.98 (p, *J* = 6.5 Hz, 2H, C5-$\mathbf{H_2}$), 2.16 – 2.28 (m, 4H, C7-$\mathbf{H_2}$, C8-$\mathbf{H_2}$), 2.29 (t, *J* = 6.5 Hz, 2H, C4-$\mathbf{H_2}$), 2.35 (t, *J* = 6.5 Hz, 2H, C6-$\mathbf{H_2}$), 4.56 (dq, *J* = 3.0, 1.0 Hz, 1H, C12-$\mathbf{H}_{cis}$H*trans*), 4.96 (dq, *J* = 3.0, 1.5 Hz, 1H, C12-H*cis*$\mathbf{H}_{trans}$), 5.87 (app. q, *J* = 1.5 Hz, 1H, C2-**H**); ^{13}C NMR (101 MHz, $CDCl_3$) δ 19.8 (C-14), 21.9 (C-14′), 22.7 (C-11), 22.9 (C-5), 28.7 (C-8), 30.0 (C-4), 36.9 (C-7), 37.5 (C-6), 114.0 (C-12), 125.7 (C-2), 126.4 (C-13), 135.3 (C-9), 146.0 (C-10), 166.7 (C-3), 200.1 (C-1); *m/z* ([ESI$^+$]): 219.2 ([M+H]$^+$), 241.2 ([M+Na]$^+$).

3-Ethoxycyclohex-2-en-1-one[237] **295**

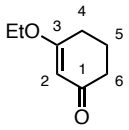

To a solution of 1,3-cyclohexanedione (10.0 g, 89.2 mmol) in EtOH (130 mL) and PhMe (45 mL) was added *p*-TsOH (0.34 g, 1.8 mmol). The reaction was heated to reflux for 16 h after which time it was concentrated *in vacuo*. The residue was diluted with EtOAc and neutralised with 3M NaOH and washed with water. The aqueous layer was extracted with EtOAc (3 × 50 mL), dried over $MgSO_4$, filtered, and concentrated *in vacuo*. The crude residue was purified by distillation to yield the title compound as a colourless liquid (4.24 g, 34%). B.p (111 ºC, 17.5 mbar); ^{1}H NMR (400 MHz, $CDCl_3$) δ 1.35 (t, *J* = 7.0 Hz, 3H, C**H**$_3$CH$_2$O), 1.97 (p, *J* = 6.5 Hz, 2H, C5-**H**$_2$), 2.33 (t, *J* = 6.5 Hz, 2H, C6-**H**$_2$), 2.39 (t, *J* = 6.5 Hz, 2H, C4-**H**$_2$), 3.89 (q, *J* = 7.0 Hz, 2H, CH$_3$C**H**$_2$O), 5.34 (s, 1H, C2-**H**); ^{13}C NMR (101 MHz, $CDCl_3$) δ 14.2 (**C**H$_3$CH$_2$O), 21.4 (C-5), 29.2 (C-4), 36.9 (C-6), 64.3 (CH$_3$**C**H$_2$O), 102.8 (C-2), 178.1 (C-3), 200.0 (C-1); *m/z* ([ESI$^+$]): 141.0 ([M+H]$^+$), 163.0 ([M+Na]$^+$).

2,2-Dimethylcyclohex-1-en-6-yl trifluoromethanesulfonate[238] **324**

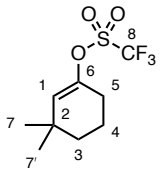

A suspension of CuI (0.12 g, 1.37 mmol) and LiCl (0.50 g, 1.37 mmol) in THF (15 mL) was stirred at RT for 10 minutes after which time it was cooled to –78 ºC and TMSCl (6.1 mL, 48 mmol) and 3-methylcyclohex-2-en-1-one (1.00 g, 9.1 mmol) were added sequentially. Stirring continued for 10 minutes then MeMgBr (3M in THF, 3.6 mL, 10.9

mmol) and, after 20 minutes, anhydrous Et_3N (16 mL, 112 mmol) was added at –78 ºC. The reaction was allowed to warm to RT and stirring continued for 30 minutes after which time the mixture was diluted with pentane (5 mL) and filtered. The filtrate was washed with sat. aq. $NaHCO_3$ and the aqueous layer was extracted with Et_2O (3 × 10 mL). The combined organic layers were dried over $MgSO_4$, filtered and concentrated under a stream of nitrogen. The crude residue was redissolved in DME (48 mL) and, after cooling to –78 ºC, MeLi (1.6 M in Et_2O, 6.1 mL, 9.68 mmol) was added dropwise. The reaction mixture was warmed to 0 ºC and stirring continued for 2 h after which time Comins' reagent (4.75 g, 12.1 mmol) was added as a solution in THF (24 mL). The reaction was stirred at RT for 1 h after which time it was concentrated, redissolved in MeCN:pentane (1:4, 20 mL), and stirred for 10 minutes. The MeCN layer was extracted with pentane (3 × 10 mL) and the combined pentane layers were concentrated *in vacuo*. The crude residue was purified by column chromatography (pentane) to yield the title compound as a colourless oil (0.59g, 25%). R_f 0.17 (pentane); ν_{max} (thin film)/cm^{-1}: 2960w, 1416m 1245m, 1205s, 1041m, 952m, 881m, 849m; ^1H NMR (400 MHz, $CDCl_3$) δ 1.06 (s, 6H, C7-**H_3**, C7′-**H_3**), 1.40 – 1.46 (m, 2H, C3-**H_2**), 1.75 – 1.84 (m, 2H, C4-**H_2**), 2.27 (td, *J* = 6.5, 1.5 Hz, 2H, C5-**H_2**), 5.51 (t, *J* = 1.5 Hz, 1H, C1-**H**); ^{13}C NMR (101 MHz, $CDCl_3$) δ 19.9 (C-4), 27.7 (C-5), 29.4 (C-7, C-7′), 33.1 (C-2), 36.0 (C-3), 128.1 (C-1), 148.3 (C-6).

((2,2-Dimethylcyclohex-1-en-6-yl)methyl)trimethylsilane 325

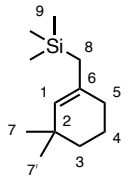

To a suspension of $Pd(PPh_3)_4$ (90 mg, 0.08 mmol) in THF (17 mL) was added vinyl triflate **324** (0.58 g, 2.3 mmol) as a solution in THF at –78 ºC and trimethylsilyl methylmagnesium chloride (1 M in THF, 3.4 mL, 3.4 mmol) was added. The reaction mixture was stirred at RT for 2 h after which time it was quenched with sat. aq. $NaHCO_3$ (30 mL) and extracted with Et_2O (3 × 15 mL). The combined organic layers were dried over $MgSO_4$, filtered, and concentrated under a stream of nitrogen and the crude residue was purified by column chromatography on florisil (pentane) to yield the title compound as a colourless oil (0.23 g, 52%). Characterised as a (1:0.4) mixture of alkene regioisomers due to isomerisation in $CDCl_3$: R_f 0.68 (pentane); ν_{max} (thin film)/cm^{-1}: 2953m, 2928m, 1453w, 1247m, 1160w, 845s; HRMS: not found.

Major regioisomer: ^{1}H NMR (400 MHz, $CDCl_3$) δ 0.00 (s, 9H, Si(C**H₃**)₃), 0.89 (s, 6H, C7-**H₃**, C7′-**H₃**), 1.27 (t, *J* = 6.5 Hz, 2H, C3-**H₂**), 1.36 – 1.41 (m, 2H, C8-**H₂**), 1.67 (app. q, *J* = 2.0 Hz, 2H, C5-**H₂**), 2.01 (m, 2H, C4-**H₂**), 5.16 (m, 1H, C1-**H**); ^{13}C NMR (101 MHz, $CDCl_3$) δ 0.0 (Si(**C**H_3)₃), 24.3 (C-4), 28.9 (C-8), 29.5 (C-7, C-7′), 36.2 (C-3), 46.0 (C-5), 109.2 (C-6), 118.4 (C-1), C-2 was unable to be assigned due to the mixture of regioisomers.

Minor regioisomer: ^{1}H NMR (400 MHz, $CDCl_3$) δ -0.01 (s, 9H, Si(C**H₃**)₃), 0.94 (s, 6H, C7-**H₃**, C7′-**H₃**), 1.36 – 1.38 (m, 2H, C8-**H₂**), 1.53 – 1.57 (m, 2H, C5-**H₂**), 1.57 – 1.63 (m, 1H, C4-**H₂**), 1.82 (t, *J* = 6.5 Hz, 2H, C3-**H₂**), 4.93 – 4.95 (m, 1H, C1-**H**); the ^{13}C NMR spectrum was too weak for assignment.

1-(2,2-Dimethyl-6-methylenecyclohexyl)ethan-1-one 327

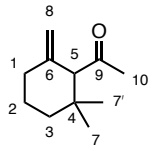

To a solution of silane **325** (50 mg, 0.25 mmol), acetyl chloride (25 μL, 0.32 mmol), and 2,6-di-*tert*-butyl-4-methyl-pyridine (0.56 g, 2.5 mmol) in CH_2Cl_2 (1.5 mL) was added $EtAlCl_2$ (1M in hexanes, 0.32 mL, 0.32 mmol) at –78 ºC. The solution was stirred at –78 ºC for 10 minutes after which time sat. aq. $NaHCO_3$ (1 mL) was added dropwise to the vigorously stirring mixture. The reaction was warmed to RT and sat. aq. Rochelle salt (1 mL) was added and stirring continued for 10 minutes. The mixture was extracted with Et_2O (3 × 2 mL) and the combined organic layers were dried over $MgSO_4$, filtered, and concentrated *in vacuo*. The crude residue was purified by column chromatography (5% EtOAc in pentane) to yield the title compound as a colourless oil (15 mg, 36%). R_f 0.73 (5% EtOAc in pentane); ν_{max} (thin film)/cm^{-1}: 2948m, 1710s, 1642w, 1438w, 1352m, 1152m, 894m; ^{1}H NMR (400 MHz, $CDCl_3$) δ 0.88 (s, 3H, C7-**H$_3$**), 0.96 (s, 3H, C7′-**H$_3$**), 1.17 (dtt, *J* = 13.0, 4.5, 1.0 Hz, 1H, C3-**H$_a$**H$_b$), 1.44 – 1.54 (m, 1H, C2-**H$_a$**H$_b$), 1.58 – 1.68 (m, 1H, C2-H$_a$**H$_b$**), 1.92 – 2.01 (m, 1H, C3-H$_a$**H$_b$**), 2.04 – 2.11 (m, 1H, C1-**H$_a$**H$_b$), 2.14 (s, 3H, C10-**H$_3$**), 2.21 (m, 1H, C1-H$_a$**H$_b$**), 3.09 (s, 1H, C5-**H**), 4.74 (br. s, 1H, C8-**H$_a$**H$_b$), 4.87 (td, *J* = 2.0, 0.5 Hz, 1H, C8-H$_a$**H$_b$**); ^{13}C NMR (101 MHz, $CDCl_3$) δ 23.0, (C-2) 26.9 (C-7), 27.8 (C-7′), 31.7 (C-1), 32.1 (C-10), 35.0 (C-4), 35.3 (C-3), 66.7 (C-5), 112.1 (C-8) 145.1 (C-6), 209.0. (C-9); *m/z* ([ESI$^+$]): 207.2 ([M+H+MeCN]$^+$).

3-Methyl-3-(13-methyl-9-(prop-12-en-10-yl)pent-9-en-7-yl)cyclohex-1-en-1-yl trifluoromethanesulfonate (±)-328

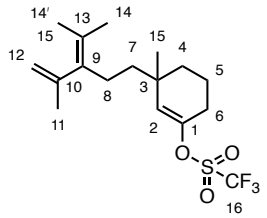

A suspension of anhydrous LiCl (30 mg, 0.69 mmol) and CuI (0.13 g mg, 0.69 mmol) in THF (1.8 mL) was stirred for 10 mins at RT after which time it was cooled to –78 ºC. TMSCl (1.5 mL, 12.1 mmol) was added followed by enone **312** (0.50 g, 2.29 mmol) as a solution in THF (1.8 mL) and stirring continued for 10 mins. MeMgBr (0.70 mL, 4.58 mmol) was added and the reaction was stirred for a further 20 mins after which time it was quenched at –78 ºC with anhydrous Et_3N (3.9 mL, 28.2 mmol) and allowed to warm to room temperature over 30 mins. The mixture was diluted with pentane (5 mL), filtered, and the filtrate washed with $NaHCO_3$. The organic layer was dried over $MgSO_4$, filtered, and concentrated *in vacuo.* The crude was immediately used in the next reaction.

To a solution of crude silyl enol ether (±)-**311** (0.65 g, 2.12 mmol) in DME (12.7 mL) was added MeLi (1.6 M in pentane, 1.6 mL, 2.54 mmol) at –78 ºC. The reaction was warmed to 0 ºC and stirred for 2 h, after which time it was warmed to RT and Comins' reagent (1.30 g, 3.18 mmol) was added as a solution in THF. The mixture was stirred for 2 h then concentrated *in vacuo*. MeCN:pentane 5:1 (10 mL) was added and, after 10 mins, the MeCN layer was extracted with pentane (3 × 10 mL). The pentane layers were concentrated *in vacuo* and the crude residue was purified by column chromatography (pentane) to yield the title compound as a colourless oil (0.64 g, 77%). R_f 0.13 (pentane); ν_{max} (thin film)/cm^{-1}: 2943w, 1417m, 1245m, 1204s, 1142s, 1021w,

890m, 760m; ^{1}H NMR (400 MHz, $CDCl_3$) δ 1.04 (s, 3H, C15-**H$_3$**), 1.25 – 1.42 (m, 4H, C4-**H$_a$**H$_b$, C5-**H$_2$**), 1.48 – 1.56 (m, 2H, C4-H$_a$**H$_b$**), 1.65 (s, 3H, C14-**H$_3$**), 1.65 (s, 3H, C14′-**H$_3$**), 1.74 (dd, *J* = 1.5, 1.0 Hz, 3H, C11-**H$_3$**), 1.76 – 1.84 (m, 2H, C7-**H$_2$**), 2.02 app. (pd, *J* = 13.0, 5.5 Hz, 2H, C8-**H$_2$**), 2.24 – 2.31 (m, 2H, C6-**H$_2$**), 4.53 (dq, *J* = 3.0, 1.0 Hz, 1H, C12-**H$_{cis}$**H$_{trans}$), 4.91 (dq, *J* = 3.0, 1.5 Hz, 1H, C12-H$_{cis}$**H$_{trans}$**), 5.52 (d, *J* = 1.5 Hz, 1H, C2-**H**); ^{13}C NMR (101 MHz, $CDCl_3$) δ 19.6 (C-5), 19.7 (C-14), 21.9 (C-14′), 22.8 (C-11), 26.8 (C-15), 27.8 (C-8), 29.4 (C-6), 33.4 (C-4), 36.0 (C-3), 40.7 (C-7), 113.3 (C-12), 125.3 (C-13), 127.1 (C-2), 136.3 (C-9), 146.5 (C-1), 148.7 (C-10); *m/z* ([ESI$^+$]): 297.2 ([M–CF_3]$^-$); HRMS: 367.1550 found, $C_{17}H_{25}F_3O_3S$ requires 367.1549.

Trimethyl((3-methyl-3-(13-methyl-9-(prop-12-en-10-yl)pent-9-en-7-yl)cyclohex-1-en-1-yl)methyl)silane (±)-308

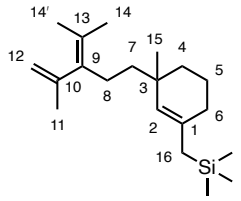

To a suspension of $Pd(PPh_3)_4$ (40 mg, 0.03 mmol) in THF (8 mL) was added vinyl triflate (±)-**328** (0.36 g, 0.98 mmol) as a solution in THF (8 mL) at –78 ºC. Trimethylsilyl methylmagnesium chloride (1M in THF, 1.6 mL, 1.6 mmol) was added dropwise and the reaction was stirred at RT for 2 h after which time it was quenched with sat. aq. $NaHCO_3$ (20 mL). The mixture was extracted with Et_2O (3 × 10 mL) and the combined organic layers were dried with $MgSO_4$, filtered, and concentrated. The crude residue was purified *via* column chromatography with florisil (pentane) to yield the title compound as a colourless oil (0.28 g, 92%). The allylsilane isomerised during the course of the reaction and purification (2.5:1) leading to complex NMR spectra, the peaks corresponding to the major, desired, isomer are reported. ν_{max} (thin film)/cm^{-1}:

3074m, 2952m, 1439w, 1373w, 1257m, 893m, 845s; ^{1}H NMR (400 MHz, $CDCl_3$) δ –0.01 (s, 9H, Si(C**H$_3$**)$_3$), 0.92 (s, 1H, C15-**H$_3$**), 1.23 – 1.35 (m, 3H, C4-**H$_a$**H$_b$, C5-**H$_2$**), 1.38 (d, *J* = 3.5 Hz, 2H, C16-**H$_2$**), 1.44 (td, *J* = 8.0, 4.5 Hz, 1H, C4-H$_a$**H$_b$**), 1.55 – 1.63 (m, 2H, C7-**H$_2$**), 1.63 – 1.69 (m, 6H, C14-**H$_3$**, C14′-**H$_3$**), 1.71 – 1.85 (m, 5H, C8-**H$_2$**, C11-**H$_3$**), 2.03 (dd, *J* = 10.0, 7.5 Hz, 2H, C6-**H$_2$**), 4.53 (br. s, 1H, C12-**H$_a$**H$_b$), 4.89 (br. s, 1H, C12-H$_a$**H$_b$**), 5.16 (s, C2-**H**); ^{13}C NMR (101 MHz, $CDCl_3$) δ –0.92 (Si(**C**H$_3$)$_3$), 19.6 (C-14), 20.1 (C-6), 21.9 (C-14′), 23.0 (C-11), 26.2 (C-4), 27.9 (C-8), 28.1 (C-15), 31.4 (C-16), 34.6 (C-5), 34.7 (C-3), 40.6 (C-7), 112.9 (C-12), 117.8 (C-2), 129.0 (C-13), 134.0 (C-9), 137.4 (C-1), 147.0 (C-10); HRMS: not found.

3-((*Tert*-butyldimethylsilyl)oxy)propan-1-ol[239] 332a

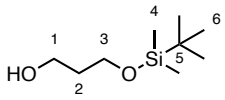

To a suspension of NaH (60% in mineral oil, 1.0 g, 27.7 mmol) in THF (56 mL) was added 1,3-propanediol (2.0 mL, 27.7 mL). The reaction was stirred at RT for 45 minutes after which time TBDMSCl (4.2 g, 27.7 mmol) was added and stirring continued for 45 minutes. The reaction mixture was quenched with sat. aq. $NaHCO_3$ (50 mL) and extracted with Et_2O (3 × 30 mL). The combined organic layers were washed with brine, dried over Na_2SO_4, filtered, and concentrated under a stream of nitrogen. The crude residue was purified by column chromatography (20% EtOAc in pentane) to yield the title compound as a colourless oil (3.4 g, 66%). R_f 0.5 (20% EtOAc in pentane); ^{1}H NMR (400 MHz, $CDCl_3$) δ 0.07 (s, 6H, C4-**H$_3$**), 0.90 (s, 9H, C5-**H$_3$**), 1.77 (p, *J* = 5.5 Hz, 2H, C2-**H$_2$**), 3.80 (t, *J* = 5.5 Hz, 2H, C3-**H$_2$**), 3.83 (t, *J* = 5.5 Hz, 2H, C1-**H$_2$**), ^{13}C NMR (101 MHz, $CDCl_3$) δ –5.4 (C-4), 18.3 (C-5), 26.0 (C-6), 34.3 (C-2), 62.6, 63.1(C-1, C-3); *m/z* ([ESI$^+$]): 191.2 ([M+H]$^+$).

3-((*Tert*-butyldimethylsilyl)oxy)propanal[240] 332b

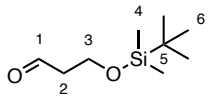

To a solution of oxalyl chloride (1.0 mL, 12.2 mmol) in CH_2Cl_2 (70 mL) was added DMSO (2.3 mL, 32.3 mmol) at – 78 ºC. The reaction was stirred for 30 mins at –78 ºC after which time alcohol **XX** was added as a solution in CH_2Cl_2 (5 mL) and stirring continued for 50 minutes. Et_3N (5.9 mL, 42.1 mmol) was added and the mixture was stirred for 16 h after which time it was quenched with water (50 mL) and extracted with CH_2Cl_2 (3 × 50 mL). The combined organic layers were washed with 1% HCl (100 mL), sat. aq. $NaHCO_3$, and brine, then dried over $MgSO_4$, filtered, and concentrated. The crude residue was purified by column chromatography (pentane → 10% EtOAc in pentane) to yield the title compound as a colourless oil (0.73 g, 38%). R_f 0.48 (10% EtOAc in pentane); ^{1}H NMR (400 MHz, $CDCl_3$) δ 0.06 (s, 6H, C4-**H_2**), 0.88 (s, 9H, C5-**H_3**), 2.59 (td, *J* = 6.0, 2.0 Hz, 2H, C2-**H_2**), 3.99 (t, *J* = 6.0 Hz, 2H, C3-**H_2**), 9.80 (t, *J* = 2.0 Hz, 1H, C1-**H**); ^{13}C NMR (101 MHz, $CDCl_3$) δ -5.3 (C-4), -3.4 (C-5), 18.4 (C-5), 26.0 (C-6), 46.7 (C-2), 57.6 (C-3), 202.2 (C-1); *m/z* ([ESI$^+$]): 211.0 ([M+Na]$^+$).

1-(2,2-Dimethyl-6-oxocyclohexyl)allyl acetate 341

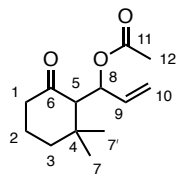

A suspension of CuI (0.6 mg, 0.3 mmol) and LiCl (7.0 mg, 0.3 mmol) in THF (3.2 mL) was stirred at RT for 10 minutes after which time it was cooled to –78 ºC and TMSCl (1.3 mL, 10.6 mmol) and 3-methylcyclohex-2-en-1-one (0.23 mL, 2.0 mmol) were

added sequentially. Stirring continued for 10 minutes then MeMgBr (3M in THF, 0.8 mL, 2.4 mmol) and, after 20 minutes, anhydrous Et_3N (3.4 mL, 24.6 mmol) was added at –78 ºC. The reaction was allowed to warm to RT and stirring continued for 30 minutes after which time the mixture was diluted with pentane (10 mL) and filtered. The filtrate was washed with sat. aq. $NaHCO_3$ and the aqueous layer was extracted with Et_2O (3 × 20 mL). The combined organic layers were dried over $MgSO_4$, filtered and concentrated under a stream of nitrogen. The crude residue was redissolved in THF (5 mL) and, after cooling to –78 ºC, MeLi (1.6 M in Et_2O, 0.5 mL, 0.78 mmol) was added and the reaction warmed to –20 ºC. The mixture was stirred at –20 ºC for 30 minutes after which time it was cooled to –78 ºC and freshly distilled acrolein (70 μL, 1.0 mmol) was added dropwise. Stirring continued for 30 minutes then freshly distilled acetyl chloride (80 μL, 1.1 mmol) was added. The reaction was stirred for a further 15 minutes at –78 ºC then it was warmed to RT while stirring for another 15 minutes. The mixture was quenched with sat. aq. $NaHCO_3$ (5 mL) and extracted with Et_2O (3 × 10 mL). The combined organic layers were dried over Na_2SO_4, filtered, and concentrated *in vacuo* and the crude residue was purified by column chromatography (10% EtOAc in pentane) to yield the title compound as a colourless oil with an unknown minor impurity (58 mg, 14% over two steps). R_f 0.55 (15% EtOAc in pentane); ν_{max} (thin film)/cm^{-1}: 2937w, 1740s, 1710s, 1391w, 1235s, 1020w, 924w; ^{1}H NMR (400 MHz, $CDCl_3$) δ 0.93 (s, 3H, C7-**H$_3$**), 1.06 (s, 3H, C7′-**H$_3$**), 1.52 – 1.62 (m, 1H, C3-**H$_a$**H$_b$), 1.64 – 1.74 (m, 1H, C3-H$_a$**H$_b$**), 1.81 – 1.91 (m, 2H, C2-**H$_2$**), 2.03 (s, 3H, C12-**H$_3$**), 2.18 – 2.33 (m, 2H, C1-**H$_2$**), 2.56 (d, *J* = 8.0 Hz, 1H, C5-**H**), 5.18 (dd, *J* = 10.5, 1.5 Hz, 1H, C10-**H$_{cis}$**H$_{trans}$), 5.30 (dt, *J* = 17.0, 1.5 Hz, 1H, C10-H$_{cis}$**H$_{trans}$**), 5.58 (t, *J* = 8.0 Hz, 1H, C8-**H**), 5.92 (ddd, *J* = 17.0, 10.5, 8.0 Hz, 1H, C9-**H**); ^{13}C NMR (101 MHz, $CDCl_3$) δ 21.6 (C-12), 22.7 (C-2), 25.1 (C-7), 29.0 (C-7′), 38.1 (C-3, 39.0 (C-4), 41.7 (C-1), 64.3 (C-5), 72.5 (C-8), 119.1

(C-10), 135.2 (C-9), 170.1 (C-11), 211.0 (C-6); *m/z* ([ESI$^+$]): 247.2 ([M+Na]$^+$); HRMS: 247.1305 found, $C_{13}H_{20}O_3Na$ requires 247.1305.

5,5-Dimethyl-2,3-divinyl-3,4,5,6,7,8-hexahydro-2*H*-chromene 342

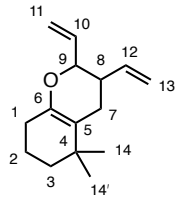

To a suspension of methyltriphenylphosphonium bromide (0.18 g, 0.51 mmol) in THF (0.75 mL) was added KO^{t}Bu (1 M in THF, 0.51 mL, 0.51 mmol) at RT. The mixture was stirred for 1 h after which time ketone **341** (50 mg, 0.26 mmol) was added as a solution in THF (0.75 mL) and stirring continued for 45 minutes. The reaction was quenched with sat. aq. NH_4Cl (5 mL) and extracted with Et_2O (3 × 5 mL), dried over $MgSO_4$, filtered, and concentrated *in vacuo*. The crude residue was purified by column chromatography (5% EtOAc in pentane) to yield the title compound (5 mg, 9%). ν_{max} (thin film)/cm^{-1}: 2929m, 2844w, 1679m, 1458w, 1360w, 1190s, 989m, 918s; ^{1}H NMR (500 MHz, $CDCl_3$) δ 0.98 (s, 3H, C14-**H$_3$**), 1.00 (s, 3H, C14′-**H$_3$**), 1.36 – 1.49 (m, 2H, C3-**H$_2$**), 1.63 – 1.70 (m, 2H, C2-**H$_2$**), 1.90 – 1.96 (m, 1H, C7-**H$_a$**H$_b$), 1.99 – 2.05 (m, 3H, C1-**H$_2$**, C7-H$_a$**H$_b$**), 2.25 – 2.35 (m, 1H, C8-**H**), 3.96 (ddt, *J* = 10.0, 7.0, 1.0 Hz, 1H, C9-**H**), 5.04 – 5.12 (m, 2H, C11-**H$_2$**), 5.20 (ddd, *J* = 10.5, 1.5, 1.0 Hz, 1H, C13-**H$_{cis}$**H$_{trans}$), 5.28 (dt, *J* = 17.0, 1.5 Hz, 1H, C13-H$_{cis}$**H$_{trans}$**), 5.68 (ddd, *J* = 18.0, 10.5, 8.0 Hz, 1H, C12-**H**), 5.83 (ddd, *J* = 17.0, 10.0, 7.5 Hz, 1H, C10-**H**); ^{13}C NMR (126 MHz, $CDCl_3$) δ 19.1 (C-2), 26.1 (C-7), 27.4 (C-14), 28.0 (C-1), 28.5 (C-14′), 33.3 (C-4), 39.3 (C-3), 42.5 (C-8), 78.8 (C-9), 110.6 (C-5), 115.6 (C-13), 117.3 (C-11), 137.3 (C-10), 139.4 (C-12), 145.3 (C-6); *m/z* ([ESI$^+$]): 279.0 ([M+HOD+MeCN+H]$^+$); HRMS: 219.1745 found, $C_{15}H_{23}O$ requires 219.1743.

Ethyl 2,2-dimethyl-6-oxocyclohexane-1-carboxylate[241] 351

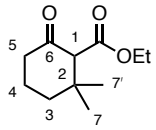

A suspension of CuI (60 mg, 0.3 mmol) and LiCl (7.0 mg, 0.3 mmol) in THF (1.6 mL) was stirred at RT for 10 minutes after which time it was cooled to –78 ºC and TMSCl (1.3 mL, 10.6 mmol) and 3-methylcyclohex-2-en-1-one (0.23 mL, 2.0 mmol) were added sequentially. Stirring continued for 10 minutes then MeMgBr (3 M in THF, 0.8 mL, 2.4 mmol) and, after 20 minutes, anhydrous Et_3N (3.4 mL, 24.6 mmol) was added at –78 ºC. The reaction was allowed to warm to RT and stirring continued for 30 minutes after which time the mixture was diluted with pentane (10 mL) and filtered. The filtrate was washed with sat. aq. $NaHCO_3$ and the aqueous layer was extracted with Et_2O (3 × 20 mL). The combined organic layers were dried over $MgSO_4$, filtered and concentrated under a stream of nitrogen. The crude residue was redissolved in THF (9 mL) and MeLi (0.9 mL, 1.6 M in Et_2O, 1.44 mmol) was added at –78 ºC. The reaction was warmed to 0 ºC and stirred for 2 h after which time the solution was cooled to –78 ºC and ethyl cyanoformate (0.16 mL, 1.57 mmol) was added. The reaction mixture was allowed to warm to RT over 14 h then it was quenched with sat. aq. NH_4Cl (10 mL) and extracted with Et_2O (3 × 10 mL). The combined organic layers were dried over Na_2SO_4, filtered, and concentrated *in vacuo*. The crude residue was purified by column chromatography (10% EtOAc in pentane) to yield the title compound as a colourless oil (180 mg, 45%). R_f 0.48 (10% EtOAc in pentane); ^{1}H NMR (400 MHz, $CDCl_3$) δ 1.33 (t, *J* = 7.0 Hz, 3H, $OCH_2C\mathbf{H_3}$), 1.79 (s, 6H, C7-$\mathbf{H_3}$, C7′-$\mathbf{H_3}$), 1.46 – 1.54 (m, 1H, C3-$\mathbf{H_a}H_b$) 1.82 – 1.99 (m, 3H, C3-$H_a\mathbf{H_b}$, C4-$\mathbf{H_2}$), 2.22 – 2.35 (m, 1H, C5-$\mathbf{H_a}H_b$), 2.62 – 2.71 (m, 1H, C5-$H_a\mathbf{H_b}$), 3.16 (s, 1H, C1-**H**), 4.25 (q, *J* = 7.0 Hz, 2H, $OC\mathbf{H_2}CH_3$); ^{13}C

NMR (101 MHz, $CDCl_3$) δ 14.3 ($OCH_2\mathbf{C}H_3$), 22.1 (C-4), 27.0 (C-7, C-7′), 36.5 (C-3), 39.0 (C-2), 39.6 (C-5), 60.9 ($O\mathbf{C}H_2CH_3$), 67.7 (C-1), 168.9 ($\mathbf{C}O_2Et$), 207.1 (C-6); *m/z* ([ESI^+]): 221.0 ([$M+Na]^+$).

Ethyl 2,2-dimethyl-6-methylenecyclohexane-1-carboxylate[241] 352

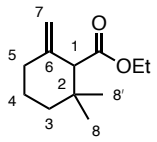

A solution of triphenylmethylphosphonium bromide (0.66 g, 1.9 mmol) and KO′Bu (1.9 mL, 1 M in THF, 1.9 mmol) in THF (4 mL) was heated at reflux for 1 h after which time a solution of ketone **351** (0.17 g, 0.86 mmol) in THF (4 mL) was added. The reaction was stirred for 15 mins and, after cooling to RT, was quenched with sat. aq. NH_4Cl (10 mL). The layers were separated, and the aqueous layer was extracted with Et_2O (3 × 10 mL). The combined organic layers were dried over $MgSO_4$, filtered, and concentrated *in vacuo*. The crude residue was purified by column chromatography (2% EtOAc in pentane) to yield the title compound (42 mg, 24%). R_f 0.65 (5% EtOAc in pentane); ν_{max} (thin film)/cm^{-1}: 2937w, 1729s, 1446w, 1367w, 1323w, 1247w, 1179m, 1144s, 1033m, 896m; ^1H NMR (400 MHz, $CDCl_3$) δ 0.93 (s, 3H, C8-$\mathbf{H_3}$), 0.98 (s, 3H, C8′-$\mathbf{H}_3$), 1.25 (m, 4H, $CO_2CH_2C\mathbf{H_3}$, C3-$\mathbf{H_a}H_b$), 1.46 – 1.59 (m, 1H, C4-$\mathbf{H_a}H_b$), 1.59 – 1.70 (m, 1H, C4-$H_a\mathbf{H_b}$), 1.83 (ddd, *J* = 13.5, 11.0, 4.5 Hz, 1H, C3-$H_a\mathbf{H_b}$), 2.11 (dt, *J* = 13.5, 5.0 Hz, 1H, C5-$\mathbf{H_a}H_b$), 2.42 – 2.53 (m, 1H, C5-$H_a\mathbf{H_b}$), 2.86 (s, 1H, C1-**H**), 4.04 – 4.19 (m, 2H, $CO_2C\mathbf{H_2}CH_3$), 4.73 (d, *J* = 1.5 Hz, 1H, C7-$\mathbf{H_a}H_b$), 4.84 (d, *J* = 1.5 Hz, 1H, C7-$H_a\mathbf{H_b}$); ^{13}C NMR (101 MHz, $CDCl_3$) δ 14.4 ($CO_2CH_2\mathbf{C}H_3$), 22.9 (C-4), 26.6 (C-8), 27.6 (C-8′), 32.3 (C-5), 36.1 (C-3), 60.1 ($CO_2\mathbf{C}H_2CH_3$), 60.2 (C-1), 111.5 (C-7), 144.8 (C-6), 172.7 ($\mathbf{C}O_2CH_2CH_3$).

_N_-Methoxy-_N_,2,2-trimethyl-6-methylenecyclohexane-1-carboxamide 353

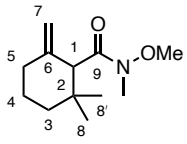

To a solution of MeONHMe.HCl (0.54 g, 5.5 mmol) in THF (2.5 mL) was added *n*-BuLi (6.0 mL, 1.6 M in hexanes, 9.6 mmol) at 0 ºC. The mixture was stirred for 0.5 h then warmed to RT and stirring continued for 0.5 h. Ester **352** (0.27 g, 1.4 mmol) was added as a solution in THF (2 mL) at 0 ºC and the mixture stirred for 0.5 h. The reaction was warmed to RT and stirring continued for 2.5 h after which time the mixture was quenched with sat. aq. NH_4Cl (5 mL). Et_2O (5 mL) was added, the layers were separated, and the aqueous layer was extracted with Et_2O (3 × 5 mL). The combined organic layers were dried over Na_2SO_4, filtered, and concentrated *in vacuo*. The crude residue was purified by column chromatography (pentane → 10% EtOAc in pentane) to yield the title compound as a colourless oil (0.23 g, 79%). R_f 0.28 (10% EtOAc in pentane); ν_{max} (thin film)/cm^{-1}: 2938m, 2867w, 1659s, 1645s, 1440w, 1377m, 1177w, 1004m, 957w, 893m, 837w; ^{1}H NMR (400 MHz, $CDCl_3$) δ 0.93 (s, 3H, C8-**H$_3$**), 0.97 (s, 3H, C8′-**H$_3$**), 1.17 – 1.27 (m, 1H, C3-**H$_a$**H$_b$), 1.45 – 1.59 (m, 1H, C4-**H$_a$**H$_b$), 1.59 – 1.70 (m, 1H, C4-H$_a$**H$_b$**), 1.94 (ddd, *J* = 14.0, 10.5, 4.5 Hz, 1H, C3-H$_a$**H$_b$**), 2.08 (dt, *J* = 13.0, 5.0 Hz, 1H, C5-**H$_a$**H$_b$), 2.43 – 2.55 (m, 1H, C5-H$_a$**H$_b$**), 3.15 (s, 3H, C(*O*)*N*CH$_3$(*O*C**H$_3$**)), 3.67 (s, 3H, C(*O*)*N*C**H$_3$**(*O*CH$_3$)), 4.68 (s, 1H, C7-**H$_a$**H$_b$), 4.83 (s, 1H, C7-H$_a$**H$_b$**); ^{13}C NMR (101 MHz, $CDCl_3$) δ 23.0 (C-4), 26.0 (C-8), 27.9 (C-8′), 32.1 (C(*O*)*N*CH$_3$(*O***C**H$_3$)), 32.7 (C-5), 35.1 (C-2), 36.6 (C-3), 53.6 (C-1), 61.2(C(*O*)*N***C**H$_3$(*O*CH$_3$)), 110.8 (C-7), 146.0 (C-6), 173.7 (**C**(*O*)*N*CH$_3$(*O*CH$_3$)); *m/z* ([ESI$^+$]): 212.2 ([M+H]$^+$), 234.2 ([M+Na]$^+$); HRMS: 212.1645 found, $C_{12}H_{21}NO_2$ requires 212.1645.

(2,2-Dimethyl-1-methylenecyclohexyl)methanol[241] **357**

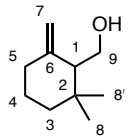

To a suspension of $LiAlH_4$ (80 mg, 2.0 mmol) in THF (1.3 mL) was added a solution of ester **325** (0.10 g, 0.50 mmol) in THF (1.3 mL) at 0 ºC. The reaction was stirred at RT for 48 h after which time it was quenched by adding water (80 μL), aq. NaOH (3 M, 80 μL), and water (0.24 mL) sequentially. After stirring for 20 minutes then $MgSO_4$ was added and stirring continued for another 20 minutes. The mixture was filtered and concentrated under a stream of nitrogen to yield the title compound as a colourless oil which was used in the next step without further purification (50 mg, 63%). R_f 0.13 (5% EtOAc in pentane); ν_{max} (thin film)/cm^{-1}: 3374 br. m, 2930s, 2867m, 1647w, 1439w, 1365w, 1029m, 889m; ^{1}H NMR (400 MHz, $CDCl_3$) δ 0.87 (s, 3H, C8-**H$_3$**), 0.95 (s, 3H, C8′-**H$_3$**), 1.23 – 1.31 (m, 1H, C3-**H$_a$**H$_b$), 1.42 (ddd, *J* = 13.5, 9.5, 5.5 Hz, 1H, C3-H$_a$**H$_b$**), 1.57 (m, 2H, C4-**H$_2$**), 2.04 (dd, *J* = 10.5, 4.5 Hz, 1H, C1-**H**), 2.11 (ddd, *J* = 8.0, 5.0, 1.0 Hz, 2H, C5-**H$_2$**), 3.62 (t, *J* = 10.5 Hz, 1H, C9-**H$_a$**H$_b$), 3.71 (dd, *J* = 10.5, 4.5 Hz, 1, C9-H$_a$**H$_b$**), 4.75 (d, *J* = 2.0 Hz, 1H, C7-**H$_a$**H$_b$), 4.96 (dt, *J* = 2.0, 1.0 Hz, 1H, C7-H$_a$**H$_b$**); ^{13}C NMR (101 MHz, $CDCl_3$) δ 23.3 (C-4), 26.7 (C-8), 28.7 (C-8′), 31.9 (C-5), 34.0 (C-2), 36.5 (C-3), 56.6 (C-1), 59.7 (C-9), 111.9 (C-7), 147.6 (C-6).

2,2-Dimethyl-6-methylenecyclohexane-1-carbaldehyde[241] 358

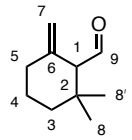

To a solution of alcohol **357** (45 mg, 0.30 mmol) in CH_2Cl_2 (2.7 mL) was added DMP (0.14 g, 0.33 mmol) at 0 ºC. The reaction was warmed to RT and stirred for 2 h after which time it was quenched with $Na_2S_2O_3$ (5 mL). The layers were separated, and the aqueous layer was extracted with Et_2O (3 × 5 mL). The combined organic layers were washed with $NaHCO_3$ (10 mL), dried over $MgSO_4$, filtered, and concentrated under a stream of nitrogen to yield the title compound as a yellow oil which was used in the next step without further purification (37 mg, 77%). R_f 0.35 (5% EtOAc in pentane); ν_{max} (thin film)/cm^{-1}: 2930m, 2868w, 1721s, 1645w, 1440w, 1264w, 1236w, 1118w, 896w, 723w; ^{1}H NMR (400 MHz, $CDCl_3$) δ 0.95 (s, 3H, C8-**H$_3$**), 1.07 (s, 3H, C8′-**H$_3$**), 1.33 – 1.42 (m, 1H, C3-**H$_a$**H$_b$), 1.55 – 1.72 (m, 3H, C3-H$_a$**H$_b$**, C4-**H$_2$**), 2.16 – 2.25 (m, 2H, C5-**H$_2$**), 2.67 (d, *J* = 4.0 Hz, 1H, C1-**H**), 4.69 – 4.71 (s, 1H, C7-**H$_a$**H$_b$), 4.95 (br. s, 1H, C7-H$_a$**H$_b$**), 9.84 (d, *J* = 4.0 Hz, 1H, C9-**H**); ^{13}C NMR (101 MHz, $CDCl_3$) δ 22.8 (C-4), 26.0 (C-8), 28.1 (C-8′), 33.4 (C-5), 34.9 (C-2), 37.5 (C-3), 66.6 (C-1), 112.4 (C-7), 143.5 (C-6), 203.3 (C-9).

(±)-1-(2,2-Dimethyl-6-methylenecyclohexyl)prop-2-en-1-one 340

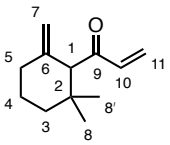

To a solution of aldehyde **358** (35 mg, 0.11 mmol) in Et_2O (0.3 mL) was added vinylmagnesium bromide (0.28 mL, 1 M in THF, 0.28 mmol) at 0 ºC. The reaction was stirred for 1 h at RT after which time it was quenched with sat. aq. NH_4Cl (3 mL) and

extracted with Et_2O (3 × 5 mL). The combined organic layers were dried over $MgSO_4$, filtered, and concentrated under a stream of nitrogen. The crude residue was redissolved in CH_2Cl_2 (0.6 mL) and $NaHCO_3$ (100 mg, 1.1 mmol) and DMP (50 mg, 0.12 mmol) were added sequentially at 0 ºC. The reaction was warmed to RT and stirred for two hours after which time it was quenched with $Na_2S_2O_3$ (3 mL) and extracted with Et_2O (3 × 5 mL). The combined organic layers were washed with sat. aq. $NaHCO_3$ (10 mL), dried over $MgSO_4$, filtered, and concentrated under a stream of nitrogen. The crude residue was purified by column chromatography (pentane → 5% EtOAc in pentane) to yield the title compound as a colourless oil (4.0 mg, 10% over two steps). R_f: 0.51 (5% EtOAc in pentane); ν_{max} (thin film)/cm^{-1}: 2935w, 2878w, 2803w, 1765sw, 1705s, 1397m, 1360m, 1154w, 1049w, 1015w, 748m, 721s; ^{1}H NMR (400 MHz, $CDCl_3$) δ 0.93 (s, 3H, C8-**H$_3$**), 0.96 (s, 3H, C8′-**H$_3$**), 1.18 – 1.24 (m, 1H, C3-**H$_a$**H$_b$), 1.48 – 1.56 (m, 1H, C4-**H$_a$**H$_b$), 1.61 – 1.70 (m, 1H, C4-H$_a$**H$_b$**), 1.98 (ddd, *J* = 13.5, 11.5, 4.5 Hz, 1H, C3-H$_a$**H$_b$**), 2.11 (dt, *J* = 13.5, 4.5 Hz, 1H, C5-**H$_a$**H$_b$), 2.21 – 2.33 (m, 1H, C5-H$_a$**H$_b$**), 3.30 (s, 1H, C1-**H**), 4.71 (s, 1H, C7-**H$_a$**H$_b$), 4.88 (s, 1H, C7-H$_a$**H$_b$**), 5.68 (dd, *J* = 10.5, 1.5 Hz, 1H, C11-**H**$_{cis}$H$_{trans}$), 6.20 (dd, *J* = 17.5, 1.5 Hz, 1H, C11-H$_{cis}$**H**$_{trans}$), 6.41 (dd, *J* = 17.5, 10.5 Hz, 1H, C10-**H**); ^{13}C NMR (101 MHz, $CDCl_3$) δ 23.1 (C-4), 26.8 (C-8), 28.0 (C-8′), 32.1 (C-5), 35.2 (C-2), 36.0 (C-3), 63.6 (C-1), 112.4 (C-7), 127.3 (C-11), 137.6 (C-10), 145.0 (C-6), 200.1 (C-9).

(±)-Ethyl (2*S)-2-methyl-2-(4-methyl-3-(prop-1-en-2-yl)pent-3-en-1-yl)-6-oxocyclohexane-1-carboxylate (±)-359**

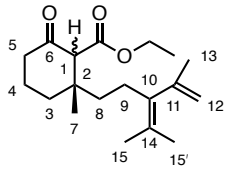

A suspension of CuI (0.26 g, 1.37 mmol) and LiCl (58 mg, 1.37 mmol) in THF (7.2 mL) was stirred for 10 minutes at RT and, after cooling to –78 ºC, TMSCl (6.0 mL, 49 mmol) and enone **312** (2.0 g, 9.2 mmol) as a solution in THF (7.2 mL) were added. Stirring continued for 20 minutes after which time MeMgBr (3.7 mL, 3 M in THF, 11.0 mmol) was added and, after a further 20 minutes, anhydrous Et_3N (12.5 mL, 113 mmol) was added. The reaction was warmed to RT over 30 minutes after which time it was diluted with pentane (20 mL) and filtered. The filtrate was washed with sat. aq. $NaHCO_3$ (20 mL) and the aqueous layer was extracted with pentane (3 × 20 mL). The combined organic layers were dried over $MgSO_4$, filtered, and concentrated under a stream of nitrogen to yield silyl enol ether (±)-**311**. Crude silyl enol ether (±)-**311** was immediately redissolved in dry Et_2O (27 mL) and *n*-BuLi (7.0 mL, 1.6 M in hexanes, 11 mmol) was added at 0 ºC. The reaction was stirred for 2 h at 0 ºC after which time it was cooled to – 78 ºC and ethyl cyanoformate (1.4 mL, 13.7 mmol) was added. The reaction was left to warm to RT over 18 h then it was quenched with sat. aq. NH_4Cl (20 mL). The layers were separated, and the aqueous layer was extracted with Et_2O (3 × 20 mL). The combined organic layers were dried over $MgSO_4$, filtered and concentrated. Purification proved problematic and so the crude residue was used in the next reaction.

(±)-Ethyl (2*S)-2-methyl-2-(4-methyl-3-(prop-1-en-2-yl)pent-3-en-1-yl)-6-methylenecyclohexane-1-carboxylate (±)-360**

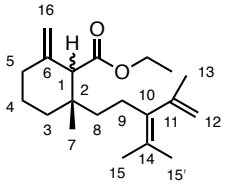

To a solution of triphenylmethylphosponium bromide (6.1 g, 17 mmol) in THF (25 mL) was added KO^{t}Bu (17 mL, 1 M in THF, 17 mmol) and the mixture heated to reflux for 1 h. After this time a solution of crude ketoester (±)-**359** (9.2 mmol, assuming complete conversion in the previous reaction) from the previous reaction in THF (25 mL) was added and stirring continued at reflux for 15 minutes. The reaction was cooled to RT and Et_2O (20 mL) and sat. aq. NH_4Cl (20 mL) was added. The layers were separated and the aqueous layer was extracted with Et_2O (3 × 30 mL). The combined organic layers were dried over $MgSO_4$, filtered, and concentrated *in vacuo*. The crude residue was purified by column chromatography (pentane → 4% EtOAc in pentane) to yield the title compound as a colourless oil which consisted of an inseparable mixture (2:1) of diastereomers (2.2 g, 79% over three steps). R_f 0.45 (5% EtOAc in pentane); ν_{max} (thin film)/cm^{-1}: 2933m, 2868w, 1730s, 1646w, 1436m, 1369w, 1325w, 1158m, 1036w, 894m, 743w, 696w; ^{1}H NMR (400 MHz, $CDCl_3$) (Due to the complexity generated by the mixture of diastereomers in the aliphatic and alicyclic regions, only the diagnostic resonances have been assigned) δ 0.85 (s, 3H, C7-**H$_3$**, major diastereomer), 0.90 (s, 3H, C7-**H$_3$**, minor diastereomer), 1.22 – 1.28 (m, 4H), 1.28 – 1.39 (m, 2H), 1.39 – 1.55 (m, 1H), 1.55 – 1.60 (m, 1H), 1.64 (s, 6H, C15-**H$_3$**, C15′-**H$_3$**, major diastereomer), 1.64 (s, 3H, C15-**H$_3$**, C15′-**H$_3$**, minor diastereomer), 1.74 (s, 3H, C13-**H$_3$**, major diastereomer), 1.75 – 1.85 (m, 1H), 1.90 – 2.01 (m, 2H), 2.00 – 2.18 (m, 2H), 2.42 – 2.56 (m, 1H), 2.92 (s, 1H, C1-**H**, minor diastereomer), 2.94 (s, 1H, C1-**H**, major diastereomer), 4.03 –

4.17 (m, 2H, OC**H₂**CH₃, major diastereomer), 4.03 – 4.17 (m, 2H, OC**H₂**CH₃, minor diastereomer), 4.49 – 4.53 (m, 1H, C12-**Hₐ**Hᵦ, major diastereomer), 4.49 – 4.53 (m, 1H, C12-**Hₐ**Hᵦ, minor diastereomer), 4.73 (dt, *J* = 2.0, 1.0 Hz, 1H, C16-**Hₐ**Hᵦ, major diastereomer), 4.77 (t, *J* = 1.5 Hz, 1H, C16-**Hₐ**Hᵦ, minor diastereomer), 4.83 – 4.86 (m, 1H, C16-Hₐ**Hᵦ**, major diastereomer), 4.83 – 4.86 (m, 1H, C16-Hₐ**Hᵦ**, minor diastereomer), 4.86 – 4.90 (m, 1H, C12-Hₐ**Hᵦ**, major diastereomer), 4.86 – 4.90 (m, 1H, C12-Hₐ**Hᵦ**, minor diastereomer); HRMS: 305.2477 found, $C_{20}H_{32}O_2$ requires 305.2475.

Reduction of ester (±)-360

To a solution of ester (±)-**360** (2.2 g, 7.2 mmol) in THF (37 mL) was added $LiAlH_4$ (1.1 g, 28.9 mmol) at 0 ºC. The reaction stirred at RT for 24 h after which time it was cooled to 0 ºC and diluted with Et_2O (10 mL). Water (1.1 mL), NaOH (3 M, 1.1 mL), and water (3.3 mL) were added sequentially, and the mixture was stirred for 30 mins after which time $MgSO_4$ was added. Stirring continued for 30 mins then the mixture was filtered through celite. The filtrate was concentrated and the crude residue was purified by column chromatography (5% EtOAc in pentane). The diastereomers had similar R_f values so four sequential chromatographic purification steps were carried out in order to maximise the yield of the separate diastereomers.

(±)-(1*R,2*S**)-2-methyl-2-(4-methyl-3-(prop-1-en-2-yl)pent-3-en-1-yl)-6-methylenecyclohexyl)methanol (±)-*trans*-361**

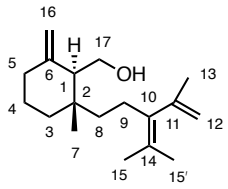

Isolated as a colourless oil (0.69 g, 36%); R_f 0.34 (10% EtOAc) νmax (thin film)/cm^{-1}: 3348 br. w, 2930m, 2866m, 1647w, 1444w, 1376w, 1026m, 892s; ^{1}H NMR (400 MHz, $CDCl_3$) δ 0.85 (d, *J* = 2.5 Hz, 3H, C7-**H$_3$**), 1.19 – 1.40 (m, 4H, C3-**H$_2$**, C8-**H$_2$**), 1.49 – 1.60 (m, 2H, C4-**H$_2$**), 1.65 (s, 6H, C14-**H$_3$**, C14′-**H$_3$**), 1.72 – 1.77 (m, 3H, C11-**H$_3$**), 1.89 – 2.07 (m, 2H, C9-**H$_2$**), 2.09 – 2.20 (m, 3H, C1-**H**, C5-**H$_2$**), 3.62 (t, *J* = 10.5 Hz, 1H, C17-**H$_a$**H$_b$), 3.68 (dd, *J* = 10.5, 5.0 Hz, 1H, C17-H$_a$**H$_b$**), 4.50 – 4.55 (m, 1H, C12-**H$_a$**H$_b$), 4.76 – 4.79 (m, 1H, C16-**H$_a$**H$_b$), 4.87 – 4.91 (m, 1H, C12-H$_a$**H$_b$**), 4.96 (dt, *J* = 2.5, 1.0 Hz, 1H, C16-H$_a$**H$_b$**); ^{13}C NMR (101 MHz, $CDCl_3$) δ 19.6 (C-15), 21.9 (C-15′), 22.8 (C-4), 22.9 (C-13), 23.9 (C-7), 24.9 (C-9), 31.4 (C-5), 33.9 (C-3), 36.1 (C-2), 37.9 (C-8), 54.6 (C-1), 59.6 (C-17), 112.5 (C-16), 113.1 (C-12), 124.8 (C-14), 136.9 (C-10), 146.8 (C-11), 147.4, (C-6); *m/z* ([ESI$^+$]): 263.2 ([M+H]$^+$), 285.2 ([M+Na]$^+$); HRMS: 263.2369 found, $C_{18}H_{31}O$ requires 263.2369.

(±)-(1*S,2*S**)-2-methyl-2-(4-methyl-3-(prop-1-en-2-yl)pent-3-en-1-yl)-6-methylenecyclohexyl)methanol (±)-*cis*-361**

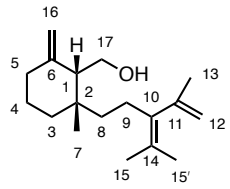

Isolated as a colourless oil (0.33 g, 18%); R_f 0.37 (10% EtOAc); ν_{max} (thin film)/cm^{-1}: 3387 br. w, 3072w, 2931s, 1646w, 1443w, 1376w, 1026w, 892m; ^{1}H NMR (400 MHz, $CDCl_3$) δ 0.93 (s, 2H, C7-**H$_3$**), 1.12 – 1.21 (m, 3H, C3-**H$_a$**H$_h$, C8-**H$_2$**), 1.25 (dt, *J* = 14.0, 4.5 Hz, 1H, C3-H$_a$**H$_b$**), 1.50 – 1.61 (m, 2H, C4-**H$_4$**), 1.64 (s, 3H, C15-**H$_3$**), 1.65 (s, 3H, C15′-**H$_3$**), 1.75 (t, *J* = 1.0 Hz, 3H, C13-**H$_3$**), 1.93 – 2.04 (m, 2H, C9-**H$_2$**), 2.04 – 2.16 (m, 3H, C1-**H**, C5-**H$_2$**), 3.55 – 3.63 (t, *J* = 10.5 Hz 1H, C17-**H$_a$**H$_b$), 3.67 (dd, *J* = 10.5, 4.5 Hz, 1H, C17-H$_a$**H$_b$**), 4.53 (br. s, 1H, C12-**H$_a$**H$_b$), 4.76 (d, *J* = 2.5 Hz, 1H, C16-**H$_a$**H$_b$), 4.90 (br. s, 1H, C12-H$_a$**H$_b$**), 4.95 (d, *J* = 2.5 Hz, 1H, C16-H$_a$**H$_b$**); ^{13}C NMR (101 MHz, $CDCl_3$) δ 19.6 (C-15), 21.8 (C-15′), 22.8 (C-4), 22.9 (C-13), 24.3 (C-9), 24.6 (C-7), 31.5 (C-5), 34.3 (C-3), 36.3 (C-2), 38.1 (C-8), 55.3 (C-1), 59.1 (C-17), 112.6 (C-16), 113.2 (C-12), 124.8 (C-14), 136.8 (C-10), 146.7 (C-11), 147.3 (C-6); *m/z* ([ESI$^+$]): 285.2 ([M+Na]$^+$), HRMS: 263.2370 found, $C_{18}H_{31}O$ requires 263.2369.

(±)-1-((1*R,2*S**)-2-methyl-2-(4-methyl-3-(prop-1-en-2-yl)pent-3-en-1-yl)-6-methylenecyclohexyl)prop-2-en-1-ol (±)-*trans*-336**

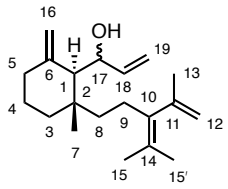

To a solution of alcohol (±)-*trans*-**361** (0.69 g, 2.6 mmol) in CH_2Cl_2 (24 mL) was added DMP (1.20 g, 2.9 mmol) at 0 ºC. The mixture was stirred at 0 ºC for 1 h after which time it was quenched with sat. aq. $Na_2S_2O_3$. The layers were separated and the aqueous layer was extracted with Et_2O (3 × 20 mL). The combined organic layers were dried over $MgSO_4$, filtered, and concentrated *in vacuo*. The crude residue was redissolved in Et_2O (3.2 mL) and vinylmagnesium bromide (5.3 mL, 1 M in THF, 5.3 mmol) was added at 0 ºC. The reaction was stirred at RT for 1 h after which time it was quenched with sat. aq. NH_4Cl (10 mL). The layers were separated and the aqueous layer was extracted with Et_2O (3 × 10 mL). The combined organic layers were dried over $MgSO_4$, filtered, and concentrated *in vacuo*. The crude residue was purified by column chromatography (1% Et_2O in pentane → 5% Et_2O in pentane) to yield the title compound as a colourless oil (0.21 g, 27% over two steps). R_f ; ν_{max} (thin film)/cm^{-1}: 3481 br. w, 2921m, 2869m, 1640w, 1443m, 1372m, 991m, 917m, 892s; ^{1}H NMR (400 MHz, $CDCl_3$) δ 0.98 (s, 3H, C7-**H$_3$**), 1.26 – 1.36 (m, 3H, C3-**H$_a$**H$_b$, C8-**H$_2$**), 1.42 – 1.60 (m, 2H, C4-**H$_2$**), 1.64 (s, 3H, C15-**H$_3$**), 1.65 (s, 3H, C15′-**H$_3$**) 1.70 (dd, *J* = 13.5, 4.5 Hz, 1H, C3-H$_a$**H$_b$**), 1.74 (t, *J* = 1.0 Hz, 3H, C13-**H$_3$**), 1.86 – 1.96 (m, 2H, C9-**H$_2$**), 1.99 (d, *J* = 5.5 Hz, 1H, C1-**H**), 2.14 – 2.28 (m, 2H, C5-**H$_2$**), 4.36 (ddt, *J* = 7.0, 5.5, 1.0 Hz, 1H, C17-**H**), 4.52 (dq, *J* = 3.0, 1.0 Hz, 1H, C12-**H$_a$**H$_b$), 4.63 – 4.66 (m, 1H, C16-**H$_a$**H$_b$), 4.88 (dq, *J* = 3.0, 1.5 Hz, 1H, C12-H$_a$**H$_b$**), 4.93 (t, *J* = 2.0 Hz, 1H, C16-H$_a$**H$_b$**), 5.10 (dt,

J = 10.5, 1.5 Hz, 1H, C19-**H**$_{cis}$H$_{trans}$), 5.21 (dt, *J* = 17.0, 1.5 Hz, 1H, C19-H$_{cis}$**H**$_{trans}$), 5.92 (ddd, *J* = 17.0, 10.5, 7.0 Hz, 1H, C18-**H**); ^{13}C NMR (101 MHz, $CDCl_3$) δ 19.6 (C-15), 21.9 (C-15′), 22.6 (C-8), 22.9 (C-13), 25.0 (C-9), 25.6 (C-7), 33.2 (C-5), 34.0 (C-3), 36.8 (C-2), 37.9 (C-4), 57.5 (C-1), 71.9 (C-17), 113.0 (C-12), 113.5 (C-16), 114.9 (C-19), 124.7 (C-14), 137.0 (C-10), 142.6 (C-18), 146.9 (C-11), 147.5 (C-6); *m/z* ([ESI$^+$]): 311.2 ([M+Na]$^+$); HRMS: 289.2526 found, $C_{20}H_{33}O$ requires 289.2526.

(±)-1-((1*_R_,2_S_*)-2-methyl-2-(4-methyl-3-(prop-1-en-2-yl)pent-3-en-1-yl)-6-methylenecyclohexyl)prop-2-en-1-one (±)-*trans*-306

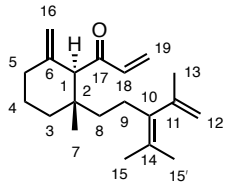

To a solution of allylic alcohol (±)-*trans*-**336** (0.20 g, 0.69 mmol) in CH_2Cl_2 (5.5 mL) was added NaOAc (0.15 g, 1.80 mmol) then PCC (0.30 g, 1.39 mmol). The reaction was stirred for 1 h at RT after which time it was diluted with Et_2O (5 mL) and florisil was added. Stirring continued for 10 minutes then the solution was filtered through celite. The filtrate was concentrated *in vacuo* and the crude residue was purified by column chromatography (2% Et_2O in pentane) to yield the title compound as a colourless oil (0.11 g, 54%). R_f 0.54 (5% EtOAc); ν_{max} (thin film)/cm^{-1}: 2933m, 2867w, 1696m, 1675m, 1653w, 1641w, 1444m, 1395m, 1374w, 1084m, 982m, 890s; ^{1}H NMR (400 MHz, $CDCl_3$) δ 0.93 (s, 3H, C7-**H$_3$**), 1.23 (ddd, *J* = 13.5, 12.0, 5.0 Hz, 1H, C8-**H$_a$**H$_b$), 1.28 – 1.41 (m, 2H, C3-**H$_a$**H$_b$, C8-H$_a$**H$_b$**), 1.44 – 1.54 (m, 1H, C4-**H$_a$**H$_b$), 1.57 – 1.70 (m, 1H, C4-H$_a$**H$_b$**), 1.64 (s, 3H, C15-**H$_3$**), 1.65 (s, 6H, C15′-**H$_3$**), 1.74 (t, *J* = 1.0 Hz, 3H, C13-**H$_3$**), 1.89 – 2.05 (m, 3H, C3-H$_a$**H$_b$**, C9-**H$_2$**), 2.11 (dt, *J* = 13.5, 4.5 Hz, 1H, C5-**H$_a$**H$_b$), 2.30 (dddt, *J* = 13.5, 11.0, 5.5, 1.5 Hz, 1H, C5-H$_a$**H$_b$**), 3.39 (s, 1H,

C1-**H**), 4.51 – 4.54 (m, 1H, C12-**H$_a$**H$_b$), 4.70 (br. s, 1H, C16-**H$_a$**H$_b$), 4.85 – 4.91 (m, 2H, 12-H$_a$**H$_b$**, C16-H$_a$**H$_b$**), 5.67 (dd, *J* = 10.5, 1.5 Hz, 1H, C19-**H$_{cis}$**H$_{trans}$), 6.20 (dd, *J* = 17.5, 1.5 Hz, 1H, C19-H$_{cis}$**H$_{trans}$**), 6.41 (dd, *J* = 17.5, 10.5 Hz, 1H, C18-**H**); ^{13}C NMR (101 MHz, $CDCl_3$) δ 19.6 (C-15) 21.9 (C-15′), 22.6 (C-4), 22.9 (C-13), 23.6 (C-7), 25.0 (C-9), 32.0 (C-5), 32.9 (C-3), 37.2 (C-8), 37.5 (C-2), 62.2 (C-1), 112.7 (C-16), 113.2 (C-12), 125.0 (C-14), 127.3 (C-19), 136.7 (C-10), 137.7 (C-18), 144.8 (C-11), 146.7 (C-16), 200.0 (C-17); *m/z* ([ESI$^+$]): 309.2 ([M+Na]$^+$); HRMS: 287.2371 found, $C_{20}H_{31}O$ requires 287.2369.

(±)-(4a*R,6*R**,12a*S**)-9,12a,13,13-tetramethyl-4-methylene-2,3,4,4a,6,7,8,11,12,12a-decahydro-6,10-methanobenzo[10]annulen-5(1*H*)-one**[219]

(±)-*trans*-132

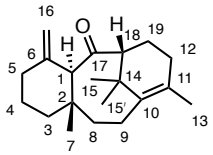

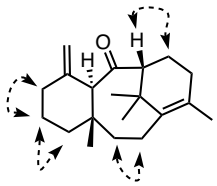

A solution of enone (0.10 gg, 0.35 mmol) in CH_2Cl_2 (1.75 mL) was added to a solution of $BF_3.Et_2O$ (0.28 mL, 2.3 mmol) in CH_2Cl_2 (1.75 mL) at 0 ºC over 1 h. The reaction was stirred at 0 ºC for a further 2 h after which time the mixture was poured into sat. aq. $NaHCO_3$. The layers were separated and the aqueous layer was extracted with CH_2Cl_2 (3 × 5 mL). The combined organic layers were dried over $MgSO_4$, filtered, and concentrated *in vacuo*. The crude residue was purified by column chromatography (0.1% Et_2O in pentane to 1% Et_2O in pentane) to yield the title compound as a pale yellow oil (26 mg, 26%). R_f 0.67 (5% EtOAc); ν_{max} (thin film)/cm^{-1}: 2930s, 2361w, 1694s, 1646w, 1458m, 1377m, 1170w, 1136w, 1112w, 930w, 897m; key COSY correlations are shown, comparison with spectra from previous group work coupled

with the lack of nOe correlations between C1-**H**, C7-**H$_3$** and C1-**H**, C18-**H** allowed characterisation of the relative stereochemistry; ^{1}H NMR (600 MHz, $CDCl_3$) δ 0.94 (s, 3H, C7-**H$_3$**), 1.12 (s, 3H, C15-**H$_3$**), 1.18 (dt, *J* = 13.0, 3.5 Hz, 1H, C3-**H$_a$**H$_b$), 1.24 – 1.31 (m, 1H, C8-**H$_a$**H$_b$) 1.27 (s, 3H, C15′-**H$_3$**), 1.59 – 1.73 (m, 3H, C4-**H$_2$**, C19-**H$_a$**H$_b$), 1.77 – 1.83 (m, 1H, C8-H$_a$**H$_b$**), 1.83 – 1.90 (m, 2H, C3-H$_a$**H$_b$**, C5-**H$_a$**H$_b$), 1.89 (s, 3H, C13-**H$_3$**) 1.91 – 2.03 (m, 2H, C12-**H$_a$**H$_b$, C19-H$_a$**H$_b$**), 2.12 – 2.18 (m, 1H, C9-**H$_a$**H$_b$), 2.25 (dt, *J* = 13.5, 3.0 Hz, 1H, C5-H$_a$**H$_b$**), 2.40 (d, *J* = 8.5 Hz, 1H, C18-**H**), 2.45 – 2.55 (m, 1H, C12-H$_a$**H$_b$**), 2.88 (td, *J* = 14.0, 5.5 Hz, 1H, C9-H$_a$**H$_b$**), 3.78 (s, 1H, C1-**H**), 4.60 (t, *J* = 2.0 Hz, 1H, C16-**H$_a$**H$_b$), 4.73 (t, *J* = 2.0 Hz, 1H, C16-H$_a$**H$_b$**); ^{13}C NMR (151 MHz, $CDCl_3$) δ 18.1 (C-19), 22.3 (C-13), 23.2 (C-4), 23.4 (C-7), 25.1 (C-15), 25.2 (C-9), 29.3 (C-12), 29.8 (C-15′), 35.8 (C-5), 38.4 (C-3), 38.5 (C-14), 39.7 (C-8), 41.4 (C-2), 56.1 (C-1), 62.4 (C-18), 108.2 (C-16), 131.0 (C-11), 137.5 (C-7), 144.2 (C-6), 214.5 (C-17); *m/z* ([ESI$^+$]): 304.4 ([M+NH$_4$]$^+$); HRMS: 287.2370 found, $C_{20}H_{31}O$ requires 287.2369.

(±)-(1*_S_,2_S_*)-2-methyl-2-(4-methyl-3-(prop-1-en-2-yl)pent-3-en-1-yl)-6-methylenecyclohexane-1-carbaldehyde (±)-*cis*362

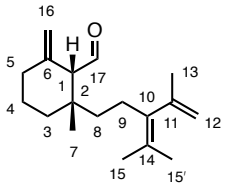

To a solution of alcohol (±)-*cis*-**361** (0.30 g, 1.14 mmol) in CH_2Cl_2 (10 mL) was added DMP (0.53 g, 1.26 mmol) at 0 ºC. The mixture was stirred at 0 ºC for 1 h after which time it was quenched with sat. aq. $Na_2S_2O_3$. The layers were separated and the aqueous layer was extracted with Et_2O (3 × 10 mL). The combined organic layers were dried over $MgSO_4$, filtered, and concentrated *in vacuo*. The crude residue was purified by column chromatography (2% Et_2O in pentane) to yield the title compound as a

colourless oil (0.24 g, 80%). R_f 0.43 (2% Et_2O); ν_{max} (thin film)/cm^{-1}: 2933m, 2867w, 1720s, 1644w, 1443w, 1377w, 894s; ^1H NMR (400 MHz, $CDCl_3$) 0.94 (s, 3H, C7-**H₃**), 1.34 – 1.50 (m, 3H, C3-**H$_a$**H$_b$, C4-**H₂**), 1.56 – 1.62 (m, 1H, C8-**H$_a$**H$_b$), 1.64 (s, 3H, C15-**H₃**), 1.64 (s, 3H, C15′-**H₃**), 1.68 (dd, *J* = 9.0, 4.5 Hz, 1H, C8-H$_a$**H$_b$**), 1.70 – 1.78 (m, 1H, C3-H$_a$**H$_b$**), 1.74 (s, 3H, C13-**H₃**), 2.05 (tt, *J* = 12.0, 7.5 Hz, 2H, C5-**H₂**), 2.14 – 2.30 (m, 2H, C9-**H₂**), 2.79 (d, *J* = 4.5 Hz, 1H, C1-**H**), 4.52 (app. dd, *J* = 2.5, 1.0 Hz, 1H, C12-**H$_a$**H$_b$), 4.75 (d, *J* = 1.0 Hz, 1H, C16-**H$_a$**H$_b$), 4.88 – 4.92 (m, 1H, C12-H$_a$**H$_b$**), 4.94 (br. s, 1H, C16-H$_a$**H$_b$**), 9.87 (d, *J* = 4.5 Hz, 1H, C17-**H**); ^{13}C NMR (101 MHz, $CDCl_3$) δ 19.6 (C-15), 21.9 (C-15′), 22.6 (C-8), 22.6 (C-8) 22.9 (C-13), 23.7 (C-7), 24.8 (C-5), 33.1 (C-9), 34.9 (C-4), 37.8 (C-2), 38.3 (C-4), 66.2 (C-1), 113.3 (C-16), 113.4 (C-12), 125.2 (C-14), 136.5 (C-10), 143.1 (C-11), 146.5 (C-6), 202.7 (C-17); *m/z* ([ESI^+]): 261.2 ([$M+H^+$]); HRMS: 261.2213 found, $C_{18}H_{29}O$ requires 261.2213.

(±)-1-((1*S,2*S**)-2-methyl-2-(4-methyl-3-(prop-1-en-2-yl)pent-3-en-1-yl)-6-methylenecyclohexyl)prop-2-en-1-ol (±)-*cis*-363**

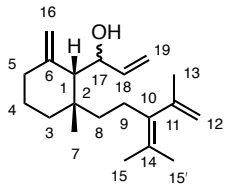

To a solution of aldehyde (±)-*cis*-**362** (0.23 g, 0.90 mmol) in Et_2O (1.1 mL) was added vinylmagnesium bromide (1.8 mL, 1 M in THF, 1.82 mmol) was added at 0 ºC. The reaction was stirred at RT for 1 h after which time it was quenched with sat. aq. NH_4Cl (5 mL). The layers were separated and the aqueous layer was extracted with Et_2O (3 × 5 mL). The combined organic layers were dried over $MgSO_4$, filtered, and concentrated *in vacuo*. The crude residue was purified by column chromatography (2% EtOAc in pentane) to yield the title compound as a colourless oil (0.20 g, 78%). Isolated as a

mixture (10:3) of diastereomers, NMR data reported is from the major diastereomer. ν_{max} (thin film)/cm^{-1}: 3477 br. w, 3072w, 2924m, 2866m, 1640w, 1442m, 1375m, 1123w, 1060w, 991m, 920m, 892s; ^{1}H NMR (400 MHz, $CDCl_3$) δ 0.92 (s, 3H, C7-**H$_3$**), 1.25 – 1.34 (m, 2H, C3-**H$_a$**H$_b$), 1.40 – 1.46 (m, 2H, C8-**H$_2$**), 1.53 – 1.64 (m, 2H, C4-**H$_2$**), 1.66 (s, 3H, C15-**H$_3$**), 1.67 (s, 3H, C15′-**H$_3$**), 1.71 – 1.82 (m, 1H, C3-H$_a$**H$_b$**), 1.77 (dd, *J* = 1.5 Hz, 1.0 Hz, 3H, C13-**H$_3$**) 1.89 (d, *J* = 4.5 Hz, 1H, C1-**H**), 1.94 – 2.03 (m, 1H, C9-**H$_a$**H$_b$), 2.07 – 2.20 (m, 2H, C5-**H$_a$**H$_b$, C9-H$_a$**H$_b$**), 2.28 – 2.40 (m, 1H, C5-H$_a$**H$_b$**), 4.44 (ddt, *J* = 6.5, 4.5, 1.5 Hz, 1H, C17-**H**), 4.56 (dq, *J* = 3.0, 1.0 Hz, 1H, C12-**H$_a$**H$_b$), 4.56 – 4.59 (m, 1H, C16-H$_a$**H$_b$**), 4.89 – 4.93 (m, 2H, C12-H$_a$**H$_b$**, C16-H$_a$**H$_b$**), 5.06 (dt, *J* = 10.0, 1.5 Hz, 1H, C19-**H$_{cis}$**H$_{trans}$), 5.16 (dt, *J* = 17.0, 1.5 Hz, 1H, C19-H$_{cis}$**H$_{trans}$**), 5.92 (app. dddd, *J* = 17.0, 10.0, 6.5, 3.5 Hz, 1H, C18-**H**); ^{13}C NMR (101 MHz, $CDCl_3$) δ 19.6 (C-15), 21.8 (C-15′), 22.9 (C-4), 23.0 (C-13), 24.6 (C-7), 25.2 (C-9), 33.9 (C-3), 34.0 (C-5), 37.1 (C-2), 39.4 (C-8), 58.0 (C-1), 72.4 (C-17), 112.8 (C-16), 113.1 (C-12), 114.4 (C-19), 124.6 (C-14), 137.2 (C-10), 142.3 (C-18), 146.9 (C-11), 147.5 (C-6); *m/z* ([ESI$^+$]): 289.2 ([M+H]$^+$), 311.2 ([M+Na]$^+$); HRMS: 289.2526, $C_{20}H_{33}O$ requires 289.2526.

(±)-1-((1*S,2*S**)-2-methyl-2-(4-methyl-3-(prop-1-en-2-yl)pent-3-en-1-yl)-6-methylenecyclohexyl)prop-2-en-1-one (±)-*cis*-306**

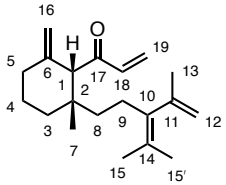

To a solution of allylic alcohol (±)-*cis*-**363** (0.20 g, 0.69 mmol) in CH_2Cl_2 (5.5 mL) was added NaOAc (0.15 g, 1.80 mmol) then PCC (0.30 g, 1.39 mmol). The reaction was stirred for 1 h at RT after which time it was diluted with Et_2O (5 mL) and florisil was

added. Stirring continued for 10 minutes then the solution was filtered through celite. The filtrate was concentrated *in vacuo* and the crude residue was purified by column chromatography (2% Et_2O in pentane) to yield the title compound as a colourless oil (0.12 g, 61%). R_f 0.37 (2% Et_2O); ν_{max} (thin film)/cm^{-1}: 2933m, 2866m, 1696m, 1674m, 1640m, 1611m, 1442m, 1396m, 1376m, 1083m, 981m, 961m, 891s; ^{1}H NMR (400 MHz, $CDCl_3$) δ 0.91 (s, 3H, C7-**H$_3$**), 1.19 – 1.32 (m, 2H, C3-**H$_a$**H$_b$, C8-**H$_a$**H$_b$), 1.39 – 1.55 (m, 3H, C4-**H$_2$**, C8-H$_a$**H$_b$**), 1.58 (s, 3H, C15-**H$_3$**), 1.62 (s, 3H, C15′-**H$_3$**), 1.70 (s, 3H, C13-**H$_3$**), 1.83 (td, *J* = 13.0, 5.0 Hz, 1H, C9-**H$_a$**H$_b$), 2.03 (td, *J* = 13.0, 5.0 Hz, 1H, C9-H$_a$**H$_b$**), 2.08 – 2.22 (m, 3H, C3-H$_a$**H$_b$**, C5-**H$_2$**), 3.34 (s, 1H, C1-**H**), 4.48 (br. s, 1H, C12-**H$_a$**H$_b$), 4.80 (br. s, 1H, C16-**H$_a$**H$_b$), 4.86 (br. s, 1H, C12-H$_a$**H$_b$**), 4.88 – 4.90 (br. s, 1H, C16-H$_a$**H$_b$**), 5.65 (d, *J* = 10.5 Hz, 1H, C19**H$_{cis}$**H$_{trans}$), 6.21 (d, *J* = 17.5 Hz, 1H, C19-H$_{cis}$**H$_{trans}$**), 6.44 (dd, *J* = 17.5, 10.5 Hz, 1H, C18-**H**); ^{13}C NMR (101 MHz, $CDCl_3$) δ 19.6 (C-15), 21.9 (C-15′), 22.8 (C-13), 22.9 (C-4), 23.6 (C-7), 25.3 (C-9), 31.5 (C-5), 33.6 (C-3), 37.8 (C-2), 38.5 (C-8), 62.9 (C-1), 113.2 (C-12), 113.4 (C-16), 124.9 (C-14), 127.4 (C-19), 136.7 (C-10), 137.0 (C-18), 144.6 (C-11), 146.6 (C-6), 199.1 (C-17); *m/z* ([ESI$^+$]): 287.2 ([M+H]$^+$), 309.2 ([M+Na]$^+$); HRMS: 287.2369 found, $C_{20}H_{31}O$ requires 287.2369.

(±)-(4a*R,6*S**,12a*S**)-4,9,12a,13,13-pentamethyl-2,4a,6,7,8,11,12,12a-octahydro-6,10-methanobenzo[10]annulen-5(1*H*)-one[214] (±)-*cis*-131**

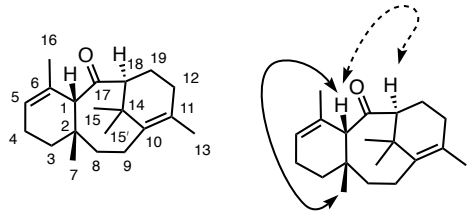

A solution of enone (±)-*cis*-**306** (0.11 g, 0.38 mmol) in CH_2Cl_2 (1.8 mL) was added to a solution of $BF_3.Et_2O$ (0.31 mL, 2.5 mmol) in CH_2Cl_2 (1.8 mL) at 0 ºC over 1 h. The reaction was stirred at 0 ºC for a further 2 h after which time the mixture was poured into sat. aq. $NaHCO_3$. The layers were separated and the aqueous layer was extracted with CH_2Cl_2 (3 × 5 mL). The combined organic layers were dried over $MgSO_4$, filtered, and concentrated *in vacuo*. The crude residue was purified twice by column chromatography (2% EtOAc in pentane then 2% Et_2O in pentane) to yield the title compound as a pale-yellow oil (59 mg, 57%). R_f 0.42 (5% EtOAc); ν_{max} (thin film)/cm^{-1}: 2912m, 1685s, 1457m, 1390w, 1378w, 1305w, 1124m, 1102m, 1030w, 965w, 916w, 857w, 803w, 775w, 731w; ^{1}H NMR (600 MHz, $CDCl_3$) δ 0.85 – 0.90 (m, 1H, C3-**H$_a$**H$_b$), 0.90 (s, 3H, C7-**H$_3$**), 1.10 (s, 3H, C15-**H$_3$**), 1.15 – 1.20 (m, 1H, C8-**H$_a$**H$_b$), 1.27 (s, 3H, C15′-**H$_3$**), 1.53 (app. q, *J* = 2.0 Hz, 3H, C16-**H$_3$**), 1.70 – 1.82 (m, 2H, C3-H$_a$**H$_b$**, C8-H$_a$**H$_b$**), 1.84 (s, 3H, C13-**H$_3$**), 1.95 – 2.07 (m, 4H, C4-**H$_2$**, C19-**H$_2$**), 2.07 – 2.14 (m, 2H, C9-**H$_a$**H$_b$, C12-**H$_a$**H$_b$), 2.43 – 2.46 (m, 1H, C18-**H**), 2.46 – 2.50 (m, 1H, C12-H$_a$**H$_b$**), 2.81 (td, *J* = 13.5, 5.5 Hz, 1H, C9-H$_a$**H$_b$**), 2.94 (s, 1H, C1-**H**), 5.52 (br. s, 1H, C5-**H**); NOESY was used to confirm the stereochemistry of the product, selected NOESY data is shown above (solid line denotes nOe correlation, dashed line denotes lack of nOe correlation); ^{13}C NMR (151 MHz, $CDCl_3$) δ 18.4 (C-19), 22.1 (C-13), 22.2 (C-4), 23.5 (C-7), 24.8 (C-16), 25.0 (C-9), 25.0 (C-15), 28.7 (C-12), 30.0 (C-15′), 33.0

(C-3), 37.8 (C-14), 37.8 (C-2), 40.4 (C-8), 57.1 (C-1), 62.7 (C-18), 123.9 (C-5), 129.8 (C-11), 131.2 (C-6), 136.8 (C-10), 217.9 (C-17); *m/z* ([ESI$^+$]): 287.2 ([M+H]$^+$), 309.2 ([M+Na]$^+$); HRMS: 287.2369 found, $C_{20}H_{31}O$ requires 287.2369.

3,3',5,5'-tetramethyl-[1,1'-biphenyl]-2,2'-diol[223] 365

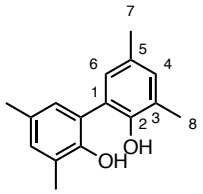

To a solution of $FeSO_4.7H_2O$ (0.7 g, 2.5 mmol) in water (75 mL) was added 2,4-dimethylphenol (6.0 mL, 47 mmol). $Na_2S_2O_5$ (12.0 g, 63 mmol) in water (50 mL) was added over 2 h and the reaction was stirred at RT for 48 h. The mixture was extracted with EtOAc (3 × 100 mL) and the combined organic layers were washed with brine (100 mL), dried over $MgSO_4$, filtered, and concentrated *in vacuo*. The crude residue was passed through a short silica gel column (5% Et_2O in pentane → 20% Et_2O in pentane) and all fractions containing the product were collected and concentrated *in vacuo*. The residue was redissolved in MTBE (7 mL) and pentane (7 mL) was added. The solution was stirred for 12 h to afford a slurry and the product was collection by filtration. The solid product was dried overnight under vacuum to yield the title compound as a white powder (2.6 g, 22%). ν_{max} (thin film)/cm^{-1}: 3371 br. w, 3008w, 2916m, 1478s, 1436m, 1377m, 1322m, 1222s, 1191s, 1155m, 1121m, 1019w, 848s, 793m, 775m, ^{1}H NMR (400 MHz, $CDCl_3$) δ 2.28 (s, 6H, C7-**H$_3$**, C8-**H$_3$**), 5.06 (s, 1H, *O***H**), 6.87 (d, *J* = 2.0 Hz, 1H, Ar**H**), 6.99 – 7.03 (m, 1H, Ar**H**); ^{13}C NMR (101 MHz, $CDCl_3$) δ 16.3 (C-7), 20.6 (C-8), 122.3, 125.3, 128.6, 130.2, 132.2, 149.3 (Ar**C**).

(+)-2,4,8,10-tetramethyl-*N*,*N*-bis((*R*)-1-phenylethyl)dibenzo[*d*,*f*][1,3,2]dioxaphosphepin-6-amine[223] (+)-363

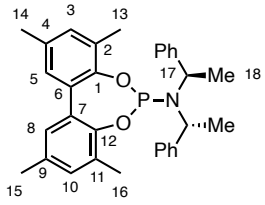

A solution of freshly distilled PCl_3 (0.12 mL, 1.7 mmol) in CH_2Cl_2 (12 mL) was stirred at 0 ºC for 30 minutes after which time Et_3N (1.2 mL, 8.3 mmol) was added followed by a solution of (+)-bis[(*R*)-1-phenethyl]amine (0.38 mL, 1.7 mmol) in CH_2Cl_2 (3 mL). The reaction was warmed to RT and stirring continued for 2 h then a solution of 3,3',5,5'-tetramethyl-[1,1'-biphenyl]-2,2'-diol **365** (0.40 g, 1.7 mmol) in CH_2Cl_2 (3 mL) was added. Stirring continued for another 2 h after which time the mixture was concentrated, redissolved in pentane (15 mL), and filtered. The remaining white solid was washed with cold pentane (5 mL) then purified by column chromatography (5% Et_2O in pentane) to yield the title compound as a white solid (0.55 g, 67%). $[\alpha]_{\mathrm{D}}^{25}$ +264.5 (*c* 1.0, $CHCl_3$); ν_{max} (thin film)/cm^{-1}: 3060w, 3029w, 2970w, 2920w, 2863w, 1478w, 1451w, 1409w, 1377w, 1217m, 1124m, 966w, 928w, 856s, 759m, 697m; ^{1}H NMR (400 MHz, $CDCl_3$) δ 1.61 (d, *J* = 7.0 Hz, 6H, C18-**H**$_3$), 2.00 (s, 3H, Ar-C**H**$_3$), 2.24 (s, 3H, Ar-C**H**$_3$), 2.25 (s, 3H, Ar-C**H**$_3$), 2.38 (s, 3H, Ar-C**H**$_3$), 4.58 (dq, *J* = 14.0, 7.0 Hz, 2H, C17-**H**), 6.90 – 7.04 (m, 14H, Ar**H**); ^{13}C NMR (101 MHz, $CDCl_3$) δ 16.5 (Ar-**C**H_3), 17.5 (Ar-**C**H_3), 20.9 (Ar-**C**H_3), 21.0 (Ar-**C**H_3), 22.2 (C-18), 52.6 (d, $J_{C\text{-}P}$ = 12.0 Hz, C-17), 126.7 (Ar**C**), 127.8 (Ar**C**), 128.1 (d, $J_{C\text{-}P}$ = 3.0 Hz, Ar**C**), 128.3 (d, $J_{C\text{-}P}$ = 4.0 Hz, Ar**C**), 129.4 (Ar**C**), 130.2 (d, $J_{C\text{-}P}$ = 3.0 Hz, Ar**C**), 130.4 (d, $J_{C\text{-}P}$ = 2.0 Hz, Ar**C**), 131.0 (Ar**C**), 131.2 (d, $J_{C\text{-}P}$ = 1.5 Hz, Ar**C**), 131.4 (d, $J_{C\text{-}P}$ = 3.5 Hz, Ar**C**), 132.7

(Ar**C**), 133.4 (Ar**C**), 143.6 (Ar**C**), 147.2 (d, $J_{C\text{-}P}$ = 3.0 Hz, Ar**C**), 148.1 (d, $J_{C\text{-}P}$ = 8.0 Hz, Ar**C**).

(–)-2,4,8,10-tetramethyl-*N*,*N*-bis((*S*)-1-phenylethyl)dibenzo[*d*,*f*][1,3,2]dioxaphosphepin-6-amine[223] (–)-363

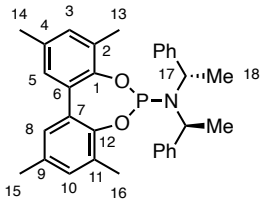

A solution of freshly distilled PCl_3 (0.12 mL, 1.7 mmol) in CH_2Cl_2 (12 mL) was stirred at 0 ºC for 30 minutes after which time Et_3N (1.2 mL, 8.3 mmol) was added followed by a solution of (+)-bis[(*R*)-1-phenethyl]amine (0.38 mL, 1.7 mmol) in CH_2Cl_2 (3 mL). The reaction was warmed to RT and stirring continued for 2 h then a solution of 3,3',5,5'-tetramethyl-[1,1'-biphenyl]-2,2'-diol **365** (0.40 g, 1.7 mmol) in CH_2Cl_2 (3 mL) was added. Stirring continued for another 2 h after which time the mixture was concentrated, redissolved in pentane (15 mL), and filtered. The remaining white solid was washed with cold pentane (5 mL) then purified by column chromatography (5% Et_2O in pentane) to yield the title compound as a white solid (0.57 g, 70%). $[\alpha]_D^{25}$ – 263.5 (*c* 1.0, $CHCl_3$); ν_{max} (thin film)/cm^{-1}: 3060w, 3029w, 2970w, 2920w, 2863w, 1478w, 1451w, 1410w, 1376w, 1246w, 1217m, 1193w, 1124m, 966w, 928w, 856s, 780m, 697m; ^{1}H NMR (400 MHz, $CDCl_3$) δ 1.86 (d, *J* = 7.0 Hz, 6H, C18-**H$_3$**), 2.25 (s, 3H, Ar-C**H$_3$**), 2.48 (s, 3H, Ar-C**H$_3$**), 2.50 (s, 3H, Ar-C**H$_3$**), 2.62 (s, 3H, Ar-C**H$_3$**), 4.83 (dq, *J* = 14.0, 7.0 Hz, 2H, C17-**H**), 7.13 – 7.30 (m, 14H, Ar**H**); ^{13}C NMR (101 MHz, $CDCl_3$) δ 16.5 (Ar-**C**H$_3$), 17.5 (Ar-**C**H$_3$), 20.9 (Ar-**C**H$_3$), 21.0 (Ar-**C**H$_3$), 22.2 (C-18), 52.6 (d, *J* = 12.0 Hz, C-17), 126.7 (Ar**C**), 127.8 (Ar**C**), 128.1 (d, $J_{C\text{-}P}$ = 3.0 Hz, Ar**C**),

128.3 (d, $J_{C\text{-}P}$ = 4.0 Hz, Ar**C**), 129.4 (Ar**C**), 130.2 (d, $J_{C\text{-}P}$ = 3.0 Hz, Ar**C**), 130.4 (d, $J_{C\text{-}P}$ = 2.0 Hz, Ar**C**), 131.0 (Ar**C**), 131.2 (d, $J_{C\text{-}P}$ = 1.5 Hz, Ar**C**), 131.4 (d, $J_{C\text{-}P}$ = 3.5 Hz, Ar**C**), 132.7 (Ar**C**), 133.4 (Ar**C**), 143.6 (Ar**C**), 147.2 (d, $J_{C\text{-}P}$ = 3.0 Hz, Ar**C**), 148.1 (d, $J_{C\text{-}P}$ = 8.0 Hz, Ar**C**).

Ethyl (2*S*)-2-methyl-2-(4-methyl-3-(prop-1-en-2-yl)pent-3-en-1-yl)-6-oxocyclohexane-1-carboxylate 359

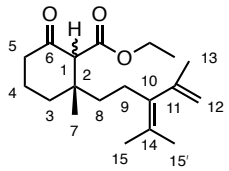

To a solution of copper(I) thiophenecarboxylate (9 mg, 46 μmol), phosphoramidite (+)-**363** (46 mg, 92 μmol), and enone **312** (0.20 g, 0.92 mmol) in freshly degassed Et_2O (4 mL) at –40 ºC was added Me_3Al (0.64 mL, 2 M in hexane, 1.3 mmol) dropwise keeping the temperature between –35 ºC and –40 ºC. The reaction was stirred at –40 ºC for 14 h after which time THF (4 mL) was added slowly keeping the temperature between –35 ºC and –40 ºC and stirring continued for 30 minutes. TMSOTf (0.29 mL, 1.6 mmol) was added dropwise at –40 ºC and, after stirring for another 30 minutes, Et_3N (0.55 mL, 4.0 mmol) was added. The solution was warmed to RT over 2 h after which time it was concentrated to a third volume and poured onto florisil (2.0 g) in pentane (10 mL). The mixture was stirred for 30 minutes then filtered through celite and concentrated. The crude residue was immediately redissolved in Et_2O (2.8 mL) and *n*-BuLi (0.69 mL, 1.6 M in hexanes, 1.0 mmol) was added at 0 ºC. The reaction was stirred for 2 h at 0 ºC after which time it was cooled to – 78 ºC and ethyl cyanoformate (0.14 mL, 1.7 mmol) was added. The reaction was left to warm to RT over 18 h then it was quenched with sat. aq. NH_4Cl (10 mL). The layers were separated, and the aqueous

layer was extracted with Et_2O (3 × 10 mL). The combined organic layers were dried over $MgSO_4$, filtered and concentrated. Purification proved problematic and so the crude residue was used in the next reaction.

Ethyl (2*S*)-2-methyl-2-(4-methyl-3-(prop-1-en-2-yl)pent-3-en-1-yl)-6-methylenecyclohexane-1-carboxylate 360

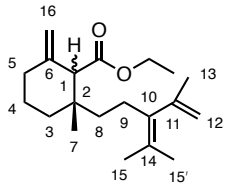

To a solution of triphenylmethylphosphonium bromide (0.72 g, 2.0 mmol) in THF (7 mL) was added KO*t*-Bu (2.0 mL, 1 M in THF, 2.0 mmol) and the mixture heated to reflux for 1 h. After this time a solution of crude ketoester **359** (0.92 mmol, assuming complete conversion in the previous reaction) from the previous reaction in THF (9 mL) was added and stirring continued at reflux for 15 minutes. The reaction was cooled to RT and Et_2O (10 mL) and sat. aq. NH_4Cl (10 mL) was added. The layers were separated and the aqueous layer was extracted with Et_2O (3 × 10 mL). The combined organic layers were dried over $MgSO_4$, filtered, and concentrated *in vacuo*. The crude residue was purified by column chromatography (pentane → 5% EtOAc in pentane) to yield the title compound as a colourless oil which consisted of an inseparable mixture (2:1) of diastereomers (0.15 g, 55% over three steps). Diagnostic data were consistent with that of the racemic analogue (±)-**360**.

(+)-(1*R*,2*S*)-2-methyl-2-(4-methyl-3-(prop-1-en-2-yl)pent-3-en-1-yl)-6-methylenecyclohexyl)methanol (+)-*trans*-361

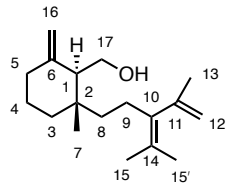

To a solution of ester **360** (0.15 g, 0.50 mmol) in THF (2.5 mL) was added $LiAlH_4$ (75 mg, 2.0 mmol) at 0 ºC. The reaction stirred at RT for 24 h after which time it was cooled to 0 ºC and diluted with Et_2O (5 mL). Water (0.08 mL), NaOH (3 M, 0.08 mL), and water (0.24 mL) were added sequentially, and the mixture was stirred for 30 mins after which time $MgSO_4$ was added. Stirring continued for 30 mins then the mixture was filtered through celite. The filtrate was concentrated and the crude residue was purified by column chromatography (5% EtOAc in pentane) to yield the title compound as a colourless oil (8.0 mg, 6%). $[\alpha]_D^{25}$ +3.0 (*c* 0.8, $CHCl_3$); 26% ee. Other data were consistent with the racemic analogue.

6.3 Enzymatic hydroxylations

General Procedure 1 – Initial Screening

Table 6.1. Components for screening reaction.

Substance	Stock concentration	Volume/µL	Final concentration
Glucose	1 M	50	100 mM
Methyl-cyclodextrin[a]	10 mM	25	500 µM
Substrate[b]	100 mM (EtOH)	5	1 mM
GDH	2 U/µL	10	2 U/mL
$NADP^+$	4 mM	10	80 µM
Enzyme	10 µM	100	2 µM
Phosphate buffer	-	300	200 mM
Total reaction volume		500	

[a]Methyl-cyclodextrin used for reactions with **117** only, volume of phosphate buffer was adjusted for reaction with **115**, **117**, and *trans*-**132** to keep total reaction volume consistent. [b]Substrate *trans*-**132** was added as a 50 mM solution in DMSO (10 µL).

Small scale screens of the substrates were conducted on a 0.5 mL scale in a 24 well plate containing 24 $P450_{BM3}$ mutants (1 per well). These reactions were performed using 200 mM phosphate buffer (pH 7.7) containing 100 mM glucose, 80 µM of nicotinamide adenine dinucleotide phosphate (NADP+), 2 U/mL glucose dehydrogenase (GDH), 5 mM of substrate and 2 µM enzyme. The screening plates were prepared by adding 400 µL of the mixture detailed in Table 1 to each well containing 100 µL of enzyme.

The plates were shaken on a platform shaker for 24 hours at 120 rpm and 20 °C. Each reaction mixture was then transferred into a 1.5 mL microcentrifuge tube, and 300 µL of

ethyl acetate added. The biphasic solution was mixed *via* vortexing for 30 seconds and then centrifuged for 1 minute at 13000 rpm. 150 μL of the organic layer was separated and transferred into a 200 μL glass GC insert. This was analysed by a Thermo Finnigan Trace1300 gas chromatograph equipped with a flame ionisation detector, an AS3000 autosampler and a DB-1 fused silica column (30 m × 0.25 mm i.d. × 0.25 μm film thickness). Helium was used as the carrier gas (1.5 mL/min). For reactions involving **117** the initial oven temperature was 200 °C which was held for 1 min, and then raised at 10 °C/min to 280 °C and kept at this final temperature for 4 mins. For reactions involving **115**, and *trans*-**132** the initial oven temperature was 180 °C which was held for 2 mins, and then raised at 15 °C/min to 300 °C and kept at this final temperature for 2 mins. The initial and the ending oven temperatures, as well as the gradient of temperature change, were adjusted according to the physical properties of substrates.

General Procedure 2 – Preparative scale reactions using P450$_{BM3}$ mutants

All preparative scale reactions were performed in a conical flask at 20 °C using the same ratios of reagents as in **General Procedure 1** (***Table 6.1***). The mixture was left to stir and monitored via GC at regular intervals until deemed appropriate to work up, ranging from 3-24 hours. The reaction mixture was split into falcon tubes with approximately 25 mL into each tube. EtOAc was added to approximately 50 mL and the falcon tubes balanced by adding more EtOAc. The tubes were shaken and then centrifuged for 2 mins at 9500g. The organic layer was pipetted off and the process repeated twice more. The combined organic layers were washed with brine, dried over $MgSO_4$, filtered, and concentrated *in vacuo*. The crude residue was purified by column chromatography.

6.3.1 Growth media and buffers

Table 6.2. Components for media. [a]Components per litre of water. [b]Components per 50 mL solution.

Media	Components
$FB_{glycerol}$[a]	14.7 g K_2HPO_4, 3.6 g NaH_2PO_4, 2.5 g $(NH_4)_2SO_4$, 2.0 g Na_2SO_4, 1.2 g Na_3citrate·$2H_2O$, 0.5 g NH_4Cl, 5 mL glycerol (after autoclaving, add 2.0 mL 1M $NaSO_4·7H_2O$, 3.0 mL trace elements solution, 1.0 mL 10% w/v thiamine·HCl)
Trace elements[a]	0.74 g $CaCl_2·H_2O$, 0.25 g $CoCl_2·6H_2O$, 0.10 g $CuSO_4·5H_2O$, 16.7 g $FeCl_3·6H_2O$, 0.132 g $MnSO_4·4H_2O$, 20.1 g Na_2EDTA, 0.18 g $ZnSO_4·7H_2O$
Induction solution[b]	0.475 g IPTG, 0.84 g δ-ALA·HCl, 0.14 g $FeSO_4·7H_2O$, 0.75 g kanamycin
Phosphate buffer[a]	5.38 g KH_2PO_4, 27.8 g K_2HPO_4

All growth media and buffers were prepared with deionised water (ρ ~ 15 MΩ/cm) from a Millipore ELIX 5-UV system. Media were autoclaved at 121 °C for 30 mins. All components added for bacterial culture growths were first sterilised via a 0.22 μm syringe filter.

6.3.2 *E. Coli* transformation

The pET-28 plasmid bearing the mutant CYP102A1 gene was transformed into BL21.DE3 cells as per manufacturer's instructions, spread onto and LB_{kan} agar plate and incubated in an oven overnight at 37 ℃.

6.3.3 Protein expression, harvest and quantification

A 2 L conical flask containing 500 mL of $FB_{glycerol}$ was autoclaved for 2 hours. Following cooling, 1.2 mL of 1 M MgSO4 (filter sterilized), 1.8 mL of FB trace elements solution (components of which are shown in ***Table 6.2***), 0.6 mL of 10% thiamine HCl solution (filter sterilized) and 0.6 mL of 30 mg/mL kanamycin were added to the flask. The solution was then inoculated with 500 µL of a starter culture containing *E. coli* Bl21.DE3 that had been transformed with the vector. The flask was shaken at 160 rpm and 37 °C for 24 hours. The growth media was then cooled to 20 °C for 1 hour. Protein expression was induced by adding 1 mL of induction solution (filter sterilized, components of which are showing in ***Table 6.2***) and 0.5 g of tryptone. The flask was shaken at 120 rpm for 24 h at 20 ℃ after which time another 1 mL of induction solution and 0.5 g of tryptone were added and shaking continued for 24 h.

The cells were harvested by centrifugation of the growth media at 4,500 rpm for 10 mins at 4 °C. The supernatant was discarded, and the pellet was re-suspended in 10 mL of phosphate buffer and 30 mL deionised water. A spatula tip of lysozyme was added, and the mixture was shaken at 120 rpm for 1 h at 20 ℃. The suspension was transferred to a beaker and the cells were lysed by sonication on ice. The sonication procedure consisted of 10 cycles of 15-second pulses followed by a 30-second cooling period. The lysed suspension was centrifuged for 20 mins at 9500 rpm and 4 °C to remove the cell debris. The supernatant containing the enzyme was purified using ammonium sulfate

fractionation. Sufficient ammonium sulfate to achieve 40% saturation was added (2.33 g/10 mL solution) and the mixture was stirred at 4 °C. Once fully dissolved, the mixture was centrifuged at 9500 rpm and 4 °C for 20 min. The supernatant was poured off and retained and more ammonium sulfate was then added to achieve 60% saturation (1.24 g/10 mL solution). After all the salt had dissolved, the mixture was centrifuged at 9500 rpm and 4 °C for 30 mins and the supernatant was discarded. The pellet was re-suspended in 1.25 mL phosphate buffer and 3.75 mL deionised water overnight at 0 °C. A CO-difference assay was utilised to determine the concentration of P450 enzyme harvested. The 500 µL sample was prepared by diluting the purified P450 enzyme solution 20-fold. Sodium hydrosulphite was added to reduce the heme iron and the UV-Vis spectrum (200–700 nm) was then recorded and used as the baseline. CO was slowly bubbled into the solution and the spectrum of the solution was recorded indicating the protein peak intensity at 450 nm. The concentration of the protein was determined using the following equation:

$$[P450](M) = \frac{(\mathrm{A}_{450} - A_{490}) \times 20}{\varepsilon}$$

where ε, the extinction coefficient is 91,000 M^{-1} cm^{-1}.

General Procedure 3 – Mosher's esterification

To a solution of alcohol (10 µmol) and pyridine-d^5 (40 µmol) in CD_2Cl_2 (0.4 mL) was added (*R*)-(–)-α-methoxy-(trifluoromethyl)phenylacetyl chloride (60 µmol). The reaction was stirred at RT until completion and NMR data were gathered.

6.3.4 Metabolites

(+)-(4a*S*,9*S*,10a*S*)-1,1,4a-Trimethyl-1,2,3,4,4a,9,10,10a-octahydrophenanthren-9-ol (+)-118

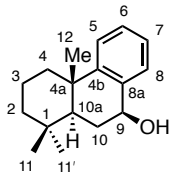

Isolated from reaction of (±)-**117** with RK/T260G. The reaction was carried out as in **General Procedure 2** in 50 mL total reaction volume. The reaction was complete after 24 h. Purified by column chromatography (pentane → 30% Et_2O in pentane). Colourless oil, 5.4 mg, 22%; R_f 0.24 (20% Et_2O in pentane); $[\alpha]_D^{25}$ +44.3 (*c* 0.14, $CHCl_3$); 85% ee; ν_{max} (thin film)/cm^{-1}: 3329w br, 2925s, 2851m, 1462w, 1376w, 1075m, 1018m, 763m, 738m; ^1H NMR (500 MHz, $CDCl_3$) δ 0.95 (s, 3H, C11-**H₃**), 0.96 (s, 3H, C11′-**H₃**), 1.18 – 1.24 (m, 1H, C2-**H$_a$**H$_b$), 1.27 (s, 3H, C12-**H₃**), 1.32 – 1.38 (m, 1H, C4-**H$_a$**H$_b$), 1.38 – 1.43 (m, 1H, C10a-**H**), 1.50 (dtd, *J* = 13.5, 3.5, 1.5 Hz, 1H, C2-H$_a$**H$_b$**), 1.61 (dq, *J* = 13.5, 3.5 Hz, 1H, C3-**H$_a$**H$_b$), 1.66 – 1.72 (m, 1H, C10-**H$_a$**H$_b$), 1.74 – 1.80 (m, 1H, C3-H$_a$**H$_b$**), 2.25 – 2.31 (m, 2H, C4-H$_a$**H$_b$**, C10-H$_a$**H$_b$**), 4.78 – 4.88 (m, 1H, C9-**H**), 7.18 – 7.26 (m, 3H, C5-**H**, C6-**H**, C7-**H**), 7.50 – 7.57 (m, 1H, C8-**H**); ^{13}C NMR (126 MHz, $CDCl_3$) δ 19.3 (C-3), 21.7 (C-11) , 25.5 (C-12), 29.9 (C-1), 30.4 (C-10), 33.3 (C-11′), 38.7 (C-4a), 38.9 (C-4), 41.5 (C-2), 49.3 (C-10a), 71.4 (C-9), 124.6, 126.0 (Ar**C**H), 127.4 (C-8), 127.8 (Ar**C**H) 138.1 (C-8a), 150.1 (C-4b); (EI) MS: 244.1829 found, $C_{17}H_{24}O^+$ requires 244.1827.

(+)-(2*S*,4a*S*,9*S*,10a*R*)-1,1,4a-Trimethyl-1,2,3,4,4a,9,10,10a-octahydrophenanthrene-2,9-diol (+)-206

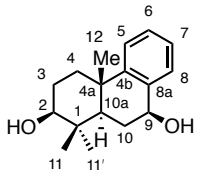

First isolated from reaction of (±)-**117** with RK/T269G. The reaction was carried out as in **General Procedure 2** in 50 mL total reaction volume. The reaction was complete after 24 h. Purified by column chromatography (pentane → Et_2O), 4.2 mg, 16%.

Also isolated from reaction of (±)-**117** with RK/Q403P (10 mg, 38%), GVQ (4.0 mg, 15%), and RK/A328G (11.8 mg, 45%).

White solid; R_f 0.58 (Et_2O); m.p. 64 – 66; $[\alpha]_D^{25}$ +54.1 (*c* 0.21, $CHCl_3$); 96% ee; ν_{max} (thin film)/cm^{-1}: 3348 br. w, 2931w, 2360w, 1456w, 1377w, 1096w, 1072w, 1018m, 926m, 763m, 733s; ^{1}H NMR (500 MHz, $CDCl_3$) δ 0.91 (s, 3H, C11-**H₃**), 1.09 (s, 3H, C11′-**H₃**), 1.27 (s, 3H, C12-**H₃**), 1.34 – 1.40 (m, 1H, C10a-**H**), 1.51 (td, *J* = 13.0, 4.5 Hz, 1H, C4-**H$_a$**H$_b$), 1.69 – 1.75 (m, 1H, C10-**H$_a$**H$_b$), 1.75 – 1.87 (m, 2H, C3-**H₂**), 2.24 – 2.36 (m, 2H, C4-H$_a$**H$_b$**, C10-H$_a$**H$_b$**), 3.30 (app. dt, *J* = 10.0, 4.5 Hz, 1H, C2-**H**), 4.83 (app. dt, *J* = 10.5, 7.5 Hz, 1H, C9-**H**), 7.18 – 7.24 (m, 3H, C6-**H**, C7-**H**, C8-**H**), 7.51 – 7.55 (m, 1H, C5-**H**); ^{13}C NMR (126 MHz, $CDCl_3$) δ 15.6 (C-11), 25.4 (C-12), 28.1 (C-3), 28.3 (C11′), 30.1 (C-10), 37.2 (C-4), 38.4 (C-4a), 38.9 (C-1), 48.5 (C-10a), 71.4 (C-9), 78.6 (C-2), 124.7, 126.3 (C-7, C-8), 127.4 (C-5), 127.9 (C-6), 138.0 (C-8a), 149.2 (C-4b); *m/z* ([ESI$^+$]): 283.0; HRMS: 259.1695 found, $C_{17}H_{23}O_2$ requires 259.1693.

(–)-(4a*R*,9*S*,10*S*,10a*R*)-1,1,4a-Trimethyl-1,2,3,4,4a,9,10,10a-octahydrophenanthrene-9,10-diol (–)-207

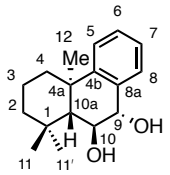

First isolated from reaction of (–)-**117** with RK/T269G. The reaction was carried out as in **General Procedure 2** in 50 mL total reaction volume. The reaction was complete after 24 h.

Also isolated from reaction of (±)-**117** with RK/A328G (3.0 mg, 12%)

Purified by column chromatography (20% Et_2O in pentane → EtOAc). Colourless oil, 1.3 mg, 5%; R_f 0.29 (Et_2O); $[\alpha]_D^{25}$ –49.1 (*c* 0.07, $CHCl_3$); ν_{max} (thin film)/cm^{-1}: 3368 br. w, 2928s, 2361m, 2163s, 2020m, 1978m, 1457w, 1377w, 1261w, 1100w, 979m; ^1H NMR (700 MHz, $CDCl_3$) δ 1.18 (s, 3H, C11′-**H₃**), 1.24 (s, 3H, C11-**H₃**), 1.24 – 1.28 (m, 1H, C2-**H$_a$**H$_b$), 1.30 (s, 3H, C12-**H₃**), 1.36 – 1.42 (m, 1H, C4-**H$_a$**H$_b$), 1.47 (dt, *J* = 14.5, 5.0 Hz, 1H, C2-H$_a$**H$_b$**), 1.57 – 1.63 (m, 2H, C3-**H$_a$**H$_b$, C10a-**H**), 1.74 (qt, *J* = 14.5, 3.0 Hz, 1H, C3-H$_a$**H$_b$**), 2.24 – 2.29 (m, 1H, C4-H$_a$**H$_b$**), 4.15 (app. ddd, *J* = 11.5, 7.0, 3.5 Hz, 1H, C10-**H**), 4.61 (app. t, *J* = 7.0 Hz, 1H, C9-**H**), 7.21 – 7.25 (m, 3H, C5-**H**, C6-**H**, C7-**H**), 7.50 – 7.53 (m, 1H, C8-**H**); ^{13}C NMR (176 MHz, $CDCl_3$) δ 19.0 (C-3), 22.3 (C-11′), 26.7 (C-12), 33.6 (C-1), 36.2 (C-11), 39.1 (C-4), 40.6 (C-4a), 43.4 (C-2), 53.1 (C-10a), 74.8 (C-10), 78.6 (C-9) 124.1, 126.3 (C-5, C-6), 127.2 (C-8), 128.0 (C-7), 135.5 (C-4b), 148.8 (C-8a); *m/z* ([ESI$^+$]): 283.2 ([M+Na]$^+$); HRMS: 283.1670 found, $C_{17}H_{24}O_2{}^{23}Na$ requires 283.1680.

(–)-(4a*R*,10a*R*)-1,1,4a-Trimethyl-1,4,4a,9,10,10a-hexahydrophenanthren-3(2*H*)-one (–)-214

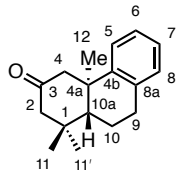

Isolated from reaction of (±)-**117** with GVQ. The reaction was carried out as in **General Procedure 2** in 50 mL total reaction volume. The reaction was complete after 3 h. Purified by column chromatography (pentane → 60% Et_2O in pentane). Colourless oil, 1.2 mg, 5%; R_f 0.52 (20% Et_2O in pentane); $[\alpha]_D^{25}$ –98.3 (*c* 0.06, $CHCl_3$); ν_{max} (thin film)/cm^{-1}: 2957s, 2851m, 1711m, 1261w, 1020w, 798w; ^1H NMR (500 MHz, $CDCl_3$) δ 0.99 (s, 3H, C11-**H₃**), 1.15 (s, 3H, C11′-**H₃**), 1.23 (s, 3H, C12-**H₃**), 1.75 – 1.85 (m, 1H, C10-**H$_a$**H$_b$), 1.94 (dd, *J* = 12.5, 2.0 Hz, 1H, C10a-**H**), 1.98 – 2.05 (m, 1H, C10-H$_a$**H$_b$**), 2.28 (dd, *J* = 13.5, 2.0 Hz, 1H, C2-**H$_a$**H$_b$), 2.38 (d, *J* = 13.5 Hz, 1H, C2-H$_a$**H$_b$**), 2.55 (d, *J* = 13.0 Hz, 1H, C4-**H$_a$**H$_b$), 2.90 – 3.06 (m, 3H, C4-H$_a$**H$_b$**, C9-**H₂**), 7.07 – 7.17 (m, C5-**H**, C6-**H**, C7-**H**, C8-**H**); ^{13}C NMR (126 MHz, $CDCl_3$) δ 19.6 (C-10), 23.1 (C-11), 26.3 (C-12), 30.5 (C-9), 33.4 (C-11′), 38.5 (C-1), 43.1 (C-4a), 50.3 (C-10a), 54.5 (C-4), 56.2 (C-2) 124.6, 126.1, 126.3 (C-5, C-6, C-7), 129.3 (C-8), 135.1 (C-8a), 147.4 (C-4b), 211.3 (C-3); *m/z* ([ESI$^+$]): 243.2 ([M-H]$^+$); 265.2 ([M+Na]$^+$); HRMS: 243.1746 found, $C_{17}H_{23}O$ requires 243.1754.

(–)-(4a*R*,9*R*,10a*R*)-9-Hydroxy-1,1,4a-trimethyl-1,4,4a,9,10,10a-hexahydrophenanthren-3(2*H*)-one (–)-215

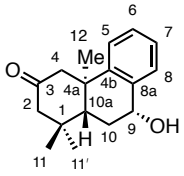

Isolated from reaction of (±)-**117** with GVQ. The reaction was carried out as in **General Procedure 2** in 50 mL total reaction volume. The reaction was complete after 3 h. Purified by column chromatography (pentane → 60% Et_2O in pentane). Colourless oil, 1.5 mg, 6%; R_f 0.37 (60% Et_2O in pentane); $[\alpha]_D^{25}$ –39.4 (*c* 0.10, $CHCl_3$); ν_{max} (thin film)/cm^{-1}: 3412 br. w, 2921s, 2851m, 2191w, 2032w, 1704m, 1463w, 1261m, 1076m, 1020m, 798m; ^{1}H NMR (500 MHz, $CDCl_3$) δ 1.01 (s, 3H, C11-**H$_3$**), 1.17 (s, 3H, C11′-**H$_3$**), 1.30 (s, 3H, C12-**H$_3$**), 1.77 (td, *J* = 12.5, 10.5 Hz, 1H, C10-**H$_a$**H$_b$), 1.98 (dd, *J* = 12.5, 1.5 Hz, 1H, C10a-**H**), 2.26 – 2.37 (m, 2H, C2-**H$_2$**), 2.37 – 2.42 (m, 1H, C10-H$_a$**H$_b$**), 2.51 (dd, *J* = 13.0, 1.0 Hz, 1H, C4-**H$_a$**H$_b$), 2.97 (dd, *J* = 13.0, 2.0 Hz, 1H, C4-H$_a$**H$_b$**), 4.91 (t, *J* = 9.0 Hz, 1H, C9-**H**), 7.12 – 7.17 (m, 1H, C5-**H**), 7.24 – 7.28 (m, 2H, C6-**H**, C7-**H**), 7.55 – 7.61 (m, 1H, C8-**H**); ^{13}C NMR (126 MHz, $CDCl_3$) δ 23.2 (C-11), 26.6 (C-12), 30.6 (C-10), 33.3 (C-11′), 38.3 (C-1), 43.3 (C-4a), 48.8 (C-10a), 54.4 (C-4), 56.0 (C-2), 70.9 (C-9), 124.6 (C-5), 126.8 (C-6), 127.5 (C-8), 128.3 (C-7), 138.0 (C-8a), 147.0 (C-4b), 210.5 (C-3). *m/z* ([ESI$^+$]): 259.2 ([M+H]$^+$), 281.2 ([M+Na]$^+$); HRMS: 259.1695 found, $C_{17}H_{23}O_2$ requires 259.1693.

(+)-(3*R*,4a*R*,9*R*,10a*R*)-1,1,4a-Trimethyl-1,2,3,4,4a,9,10,10a-octahydrophenanthrene-3,9-diol (+)-216

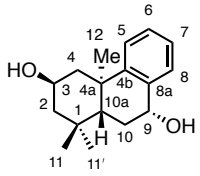

Isolated from reaction of (±)-**117** with GVQ. The reaction was carried out as in **General Procedure 2** in 50 mL total reaction volume. The reaction was complete after 3 h. Purified by column chromatography (pentane → 60% Et_2O in pentane). Colourless oil, 1.1 mg, 4%; R_f 0.13 (60% Et_2O in pentane); $[\alpha]_D^{25}$ +8.7 (*c* 0.15, $CHCl_3$); ν_{max} (thin film)/cm^{-1}: 3323 br. w, 2924m, 2853m, 1723w, 1459w, 1376w, 1259m, 1035s, 1022s, 159s; ^1H NMR (500 MHz, $CDCl_3$) δ 0.99 (s, 3H, C11-**H₃**), 1.06 (s, 3H, C11′-**H₃**), 1.17 (s, 3H, C12-**H₃**), 1.22 – 1.29 (m, 1H, C2-**H$_a$**H$_b$), 1.36 (t, *J* = 11.5 Hz, 1H, C4-**H$_a$**H$_b$), 1.69 (dd, *J* = 12.0, 3.0 Hz, 1H, C10a-**H**), 1.91 (ddd, *J* = 12.5, 4.5, 2.0 Hz, 1H, C2-H$_a$**H$_b$**), 1.92 – 2.07 (m, 2H, C10-**H₂**), 2.65 (ddd, *J* = 11.5, 4.0, 2.5 Hz, 1H, C4-H$_a$**H$_b$**), 4.09 (tt, *J* = 12.5, 4.0 Hz, 1H, C3-**H**), 4.87 (d, *J* = 3.0 Hz, 1H, C9-**H**), 7.22 (dd, *J* = 7.0, 1.5 Hz, 1H, C6-**H**), 7.28 (dd, *J* = 7.5, 1.5 Hz, 1H, C7-**H**), 7.31 (dd, *J* = 7.0, 1.5 Hz, 1H, C5-**H**), 7.36 (dd, *J* = 7.5, 1.5 Hz, 1H, C8-**H**); ^{13}C NMR (126 MHz, $CDCl_3$) δ 22.7 (C-11), 25.2 (C-12), 28.5 (C-10), 33.3 (C-11′), 34.5 (C-1), 40.0 (C-4a), 44.1 (C-10a), 47.5 (C-4), 50.9 (C-2), 65.7 (C-3), 68.2 (C-9), 124.4 (C-5), 126.5 (C-6), 128.6 (C-7), 130.3 (C-8), 136.2 (C-8a), 149.1 (C-4b); *m/z* ([ESI$^+$]): 283.1 ([M+Na]$^+$); HRMS: 283.1670 found, $C_{17}H_{24}O_2{}^{23}Na$ requires 283.1669.

(3*R*,4a*R*,10a*R*)-1,1,4a-Trimethyl-1,2,3,4,4a,9,10,10a-octahydrophenanthren-3-ol

217

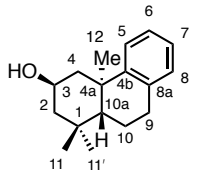

Isolated from reaction of (–)-**117** with GVQ. The reaction was carried out as in **General Procedure 2** in 50 mL total reaction volume. The reaction was complete after 3 h. Purified by column chromatography (pentane → 40% EtOAc in pentane). Colourless oil, 1.2 mg, 5%; R_f 0.29 (20% EtOAc in pentane); ^{1}H NMR (500 MHz, $CDCl_3$) δ 0.98 (s, 3H, C11′-**H$_3$**), 1.02 (s, 3H, C11-**H$_3$**), 1.15 – 1.21 (m, 1H, C2-**H$_a$**H$_b$), 1.22 (s, 3H, C12-**H$_3$**), 1.31 – 1.39 (m, 2H, C4-**H$_a$**H$_b$, C10a-**H**), 1.71 (tdd, *J* = 13.0, 11.0, 7.0 Hz, 1H, C10-**H$_a$**H$_b$), 1.83 – 1.95 (m, 2H, C2-H$_a$**H$_b$**, C10-H$_a$**H$_b$**), 2.61 – 2.71 (m, 1H, C4-H$_a$**H$_b$**), 2.81 – 3.03 (m, 2H, C9-**H$_2$**), 4.07 (td, *J* = 11.5, 5.0 Hz, 1H, C3-**H**), 7.04 – 7.07 (m, 1H, C5-**H**), 7.09 (td, *J* = 7.0, 1.5 Hz, 1H, C7-**H**), 7.11 – 7.16 (m, 1H, C6-**H**), 7.28 (d, *J* = 1.5 Hz, 1H, C8-**H**); ^{13}C NMR (126 MHz, $CDCl_3$) δ 18.9 (C-10), 22.7 (C-11′), 25.8 (C-12), 30.3 (C-9), 33.5 (C-11), 35.0 (C-1), 39.6 (C-4a), 48.0 (C-4), 49.7 (C-10a), 51.0 (C-2), 65.8 (C-3), 124.2 (C-8), 125.7 (C-7), 125.9 (C-6), 129.3 (C-5), 135.0 (C-8a), 149.2 (C-4b).

(+)-(3a*R*,7*R*,7a*R*)-7-Isopropyl-1-oxo-2,3,3a,6,7,7a-hexahydro-1*H*-isochromene-4-carbaldehyde[128] **(+)-125**

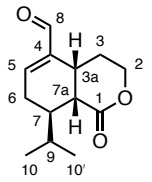

Isolated from reaction with (±)-**115** with GVQ. Colourless oil, 1.0 mg, 8%; $[\alpha]_{D}^{25}$ +84.5 (*c* 0.08, $CHCl_3$); 80% ee. The reaction was carried out as in **General Procedure 2** in 50 mL total reaction volume. The reaction was complete after 5 h.

Isolated from reaction with (±)-**115** with KSK19/IA for 5 h. Colourless oil, 2.1 mg, 17%, 66 % ee. The reaction was carried out as in **General Procedure 2** in 50 mL total reaction volume. The reaction was complete after 5 h.

Purified by column chromatography (pentane → 40% EtOAc in pentane). R_f 0.37 (30% EtOAc in pentane); ν_{max} (thin film)/cm^{-1}: 2925m, 2850w, 1717m, 1684s, 1261m, 1087m, 1023m, 799m; ^{1}H NMR (500 MHz, CD_3CN) δ 0.92 (d, *J* = 6.5 Hz, 3H, C10-**H$_3$**), 0.94 (d, *J* = 6.5 Hz, 3H, C10′-**H$_3$**), 1.51 (dp, *J* = 8.5, 6.5 Hz, 1H, C9-**H**), 1.78 – 1.88 (m, 1H, C3-**H$_a$**H$_b$), 2.01 – 2.05 (m, 1H, C7-**H**), 2.26 (dtd, *J* = 14.5, 6.5, 3.5 Hz, 1H, C3-H$_a$**H$_b$**), 2.35 – 2.42 (m, 1H, C6-**H$_a$**H$_b$), 2.46 (app. ddt, *J* = 20.0, 5.5, 3.0 Hz, C6-H$_a$**H$_b$**), 2.89 (ddd, *J* = 6.5, 5.5, 1.0 Hz, 1H, C7a-**H**), 3.08 (q, *J* = 6.5 Hz, 1H, C3a-**H**), 4.14 (ddd, *J* = 11.5, 6.5, 4.5 Hz, 1H, C2-**H$_a$**H$_b$), 4.25 (ddd, *J* = 11.5, 8.5, 3.5 Hz, 1H, C2-H$_a$**H$_b$**), 6.95 (ddd, *J* = 5.5, 3.5, 1.5 Hz, 1H, C5-**H**), 9.37 (s, 1H, C8-**H**); ^{13}C NMR (126 MHz, CD_3CN) δ 19.8 , (C-10), 21.1 (C-10′), 26.4 (C-6), 27.3 (C-3), 28.0 (C-9), 28.5 (C-3a), 39.3 (C-7), 41.8 (C-7a), 67.3 (C-2), 142.7 (C-4), 152.8 (C-5), 174.0 (C-1), 194.4 (C-8); *m/z* ([ESI$^+$]): 223.2 ([M+H]$^+$). 245.0 ([M+Na]$^+$); HRMS: 223.1333 found, $C_{13}H_{19}O_3$ requires 223.1323.

(+)-(3a*S*,7*S*,7a*S*)-4-(hydroxymethyl)-7-isopropyl-2,3,3a,6,7,7a-hexahydro-1*H*-isochromen-1-one[128] **(+)-124**

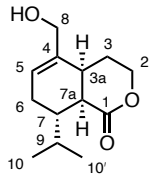

Isolated from reaction with (±)-**115** with GVQ. Colourless oil; 2.5 mg, 18%; $[\alpha]_{\mathrm{D}}^{25}$ +42.5 (*c* 0.25, $CHCl_3$); 18% ee. The reaction was carried out as in **General Procedure 2** in 50 mL total reaction volume. The reaction was complete after 5 h.

Isolated from reaction with (±)-**115** with KSK19/IA. Colourless oil, 3.8 mg, 27%, 71% ee. The reaction was carried out as in **General Procedure 2** in 50 mL total reaction volume. The reaction was complete after 5 h.

Purified by column chromatography (pentane → 40% EtOAc in pentane). ν_{max} (thin film)/cm^{-1}: 3444 br. m, 2960m, 2866m, 1718s, 1262m, 1021m, 799w; ^{1}H NMR (500 MHz, CD_3CN) δ 0.93 (t, *J* = 6.5 Hz, 6H, C10-**H$_3$**, C10′-**H$_3$**), 1.60 (ddt, *J* = 13.5, 9.0, 6.5 Hz, 1H, C9-**H**), 1.86 – 1.93 (m, 2H, C3-**H$_a$**H$_b$, C7-**H**), 2.04 – 2.08 (m, 2H, C3-H$_a$**H$_b$**, C6-**H$_a$**H$_b$), 2.09 – 2.12 (m, 1H, C6-H$_a$**H$_b$**), 2.70 (dd, *J* = 6.5, 5.0 Hz, 1H, ***O*H**), 2.82 – 2.86 (m, 2H, C3a-**H**, C7a-**H**), 3.90 (dd, *J* = 13.0, 5.0 Hz, 1H, C8-**H$_a$**H$_b$), 3.99 – 4.04 (m, 1H, C8-H$_a$**H$_b$**), 4.16 (ddd, *J* = 11.0, 8.5, 4.0 Hz, 1H, C2-H$_a$**H$_b$**), 4.20 – 4.28 (m, 1H, C2-H$_a$**H$_b$**), 5.72 (br. t, *J* = 4.0 Hz, 1H, C5-**H**); ^{13}C NMR (126 MHz, CD_3CN) δ 20.5 (C-10), 21.2 (C-10′), 24.6 (C-6), 26.6 (C-3), 27.6 (C-9), 30.3 (C-3a), 40.2 (C-7), 43.0 (C-7a), 64.5 (C-8), 67.4 (C-2), 124.3 (C-5), 138.7 (C-4), 174.5 (C-1); *m/z* ([ESI$^+$]): 247.0 ([M+Na]$^+$); HRMS: 247.1306 found, $C_{13}H_{20}O_3{}^{23}Na$ requires 247.1305.

(+)-(3a*S*,7*R*,7a*R*)-7-(9-hydroxypropan-9-yl)-4-methyl-2,3,3a,6,7,7a-hexahydro-1*H*-isochromen-1-one[128] **(+)-126**

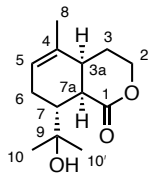

Isolated from reaction with (±)-**115** with GVQ. Colourless oil, 3.6 mg, 16%; $[\alpha]_{D}^{25}$ +77.2 (*c* 0.14, $CHCl_3$); 43% ee. The reaction was carried out as in **General Procedure 2** in 50 mL total reaction volume. The reaction was complete after 5 h.

Isolated from reaction with (±)-**115** with KSK19/IA for 5 h. Colourless oil, 2.7 mg, 12%, 57% ee. The reaction was carried out as in **General Procedure 2** in 50 mL total reaction volume. The reaction was complete after 5 h.

Purified by column chromatography (pentane → 40% EtOAc in pentane). ν_{max} (thin film)/cm^{-1}: 3389br. w, 2966m, 2945m, 2870w, 2837w, 1488m, 1477m, 1447m, 1375w, 1091m, 1032s, 1007m, 935w, 761s, 723m; ^{1}H NMR (400 MHz, $CDCl_3$) δ 1.29 (s, 3H, C10-**H$_3$**), 1.50 (s, 3H, C10′-**H$_3$**), 1.60 (ddt, *J* = 15.0, 7.5, 6.5 Hz, 1H, C3-**H$_a$**H$_b$), 1.76 (dt, *J* = 2.5, 1.5 Hz, 3H, C8-**H$_3$**), 1.78 – 1.84 (m, 1H, C3-H$_a$**H$_b$**), 1.97 – 2.05 (m, 1H, C6-**H$_a$**H$_b$), 2.09 – 2.20 (m, 2H, C6-H$_a$**H$_b$**, C7-**H**), 2.59 (app. d, *J* = 6.5 Hz, 1H, C3a-**H**), 2.64 (dd, *J* = 13.5, 6.5 Hz, 1H, C7a-**H**), 3.73 (app. ddq, *J* = 17.5, 12.0, 6.5 Hz, 2H, C2-**H$_2$**), 5.38 – 5.43 (m, 1H, C5-**H**); ^{13}C NMR (126 MHz, $CDCl_3$) δ 21.5 (C-10), 22.3 (C-8), 26.1 (C-6), 28.0 (C-10′), 34.2 (C-3), 35.1 (C-3a), 42.4 (C-7), 46.0 (C-7a), 61.8 (C-2), 86.4 (C-9), 120.3 (C-5), 138.5 (C-4), 177.3 (C-1); *m/z* ([ESI$^+$]): 247.2 ([M+Na]$^+$).

(+)-(3a*R*,6*R*,7*R*,7a*S*)-6-Hydroxy-7-isopropyl-4-methyl-2,3,3a,6,7,7a-hexahydro-1*H*-isochromen-1-one[128] **(+)-116**

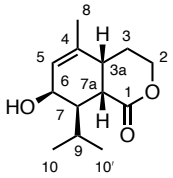

Isolated from reaction with (±)-**115** with R19/A330W for 5 h. Purified by column chromatography (pentane → 40% EtOAc in pentane). Colourless oil, 4.9 mg, 25%; R_f 0.59 (50% EtOAc in pentane); $[\alpha]_D^{25}$ +8.6 (*c* 0.14, $CHCl_3$); ^{1}H NMR (400 MHz, $CDCl_3$) δ 0.99 (d, *J* = 6.5 Hz, 3H, C10-**H₃**), 1.13 (d, *J* = 6.5 Hz, 3H, C10′-**H₃**), 1.72 (app. td, *J* = 1.5, 1.0 Hz, 3H, C8-**H₃**), 1.74 – 1.87 (m, 1H, C3-**H$_a$**H$_b$), 1.88 – 1.97 (m, 1H, C9-**H**), 2.03 – 2.08 (m, 1H, C3-H$_a$**H$_b$**), 2.08 – 2.14 (m, 1H, C7-**H**), 2.58 (q, *J* = 7.0 Hz, 1H, C3a-**H**), 3.00 (t, *J* = 7.0 Hz, 1H, C7a-**H**), 4.20 – 4.38 (m, 2H, C2-**H₂**), 4.42 (app. tq, *J* = 3.0, 1.5 Hz, 1H, C6-**H**), 5.61 (app. dt, *J* = 3.0, 1.5 Hz, 1H, C5-**H**); ^{13}C NMR (101 MHz, $CDCl_3$) δ 20.8 (C-8), 21.9 (C-10), 22.0 (C-10), 25.8 (C-3), 26.9 (C-9), 35.6 (C-3a), 41.3 (C-7a), 44.5 (C-7), 66.4 (C-6), 66.8 (C-2), 127.4 (C-5), 136.3 (C-4), 173.9 (C-1); *m/z* ([ESI$^+$]): 225.1 ([M+H]$^+$).

(+)-(4a*R,6*R**,12a*S**)-9,12a,13,13-Tetramethyl-4-methylene-1,2,3,4,4a,6,7,11,12,12a-decahydro-6,10-methanobenzo[10]annulene-5,8-dione (+)-367**

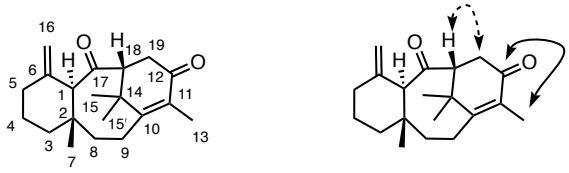

Isolated from reaction with (±)-*trans*-**132** with GV/AI. The reaction was carried out as in **General Procedure 2** in 40 mL total reaction volume using a 50 mM stock solution of (±)-*trans*-**132**. After 24 h the reaction was incomplete and so addition of glucose, $NADP^+$, GDH, and GV AI was repeated. The reaction was complete after 48 h. Purified by column chromatography (1% Et_2O in pentane → EtOAc). White solid, 0.7 mg, 6%. $[\alpha]_D^{25}$ +7.4 (*c* 0.07, $CHCl_3$); C3-**H₂**, C4-**H₂** and C-3, C-4 have been omitted from NMR data due to the complexity of the aliphatic region precluding clear characterisation, key HMBC (solid arrow) and COSY (dashed arrow) correlations are shown; ^{1}H NMR (600 MHz, $CDCl_3$) δ 0.93 (s, 3H, C7-**H₃**), 1.19 (s, 3H, C15-**H₃**), 1.33 – 1.36 (m, 1H, C8-**H$_a$**H$_b$), 1.37 (s, 3H, C15′-**H₃**), 1.77 – 1.89 (m, 1H, C8-H$_a$**H$_b$**), 1.91 – 2.00 (m, 1H, C5-**H$_a$**H$_b$), 2.04 (s, 3H, C13-**H₃**), 2.21 (d, *J* = 15.0 Hz, 1H, C5-H$_a$**H$_b$**), 2.34 – 2.40 (m, 1H, C9-H$_a$**H$_b$**), 2.53 (d, *J* = 9.0 Hz, 1H, C18-**H**), 2.54 – 2.64 (m, 1H, C19-**H$_a$**H$_b$), 3.01 (dd, *J* = 19.0, 9.0 Hz, 1H, C19-H$_a$**H$_b$**), 3.61 (td, *J* = 14.0, 5.5 Hz, 1H, C9-H$_a$**H$_b$**), 3.78 (s, 1H, C1-**H**), 4.60 (d, *J* = 1.5 Hz, 1H, C16-**H$_a$**H$_b$), 4.76 (d, *J* = 1.5 Hz, 1H, C16-H$_a$**H$_b$**); ^{13}C NMR (151 MHz, $CDCl_3$) δ 21.1 (C-13), 23.0 (C-7), 24.6 (C-15), 25.8 (C-19), 27.7 (C-9), 28.7 (C-15′), 35.3 (C-5), 38.8 (C-8), 40.5 (C-14), 41.3 (C-2), 56.0 (C-1), 62.7 (C-18), 108.3 (C-16), 130.1 (C-11), 144.1 (C-6), 158.8 (C-10), 171.0 (C-12), 212.9 (C-17); *m/z* ([ESI^+]): not found; HRMS: 301.2162 found, $C_{20}H_{29}O_2$ requires 301.2162.

(4a*R,6*S**,7*S**,12*S**,12a*R**)-7,12-Dihydroxy-9,12a,13,13-tetramethyl-4-methylene-2,3,4,4a,6,7,8,11,12,12a-decahydro-6,10-methanobenzo[10]annulen-5(1*H*)-one 368**

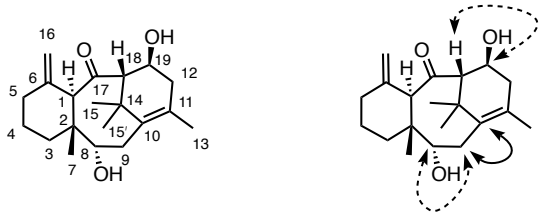

Isolated from reaction with (±)-*trans*-**132** with RK/A328G. The reaction was carried out as in **General Procedure 2** in 50 mL total reaction volume using a 50 mM stock solution of (±)-*trans*-**132**. After 24 h the reaction was incomplete and so addition of glucose, $NADP^+$, GDH, and RK/A328G was repeated. The reaction was complete after 48 h. Purified by column chromatography to yield a 2:1 mixture of compounds (pentane → EtOAc). White solid, 1.8 mg, 14%. The major component was able to be fully characterised. $[\alpha]_D^{25}$ +32.2 (*c* 0.18, $CHCl_3$), C3-**H₂** and C4-**H₂** have been omitted from NMR data due to the complexity of the aliphatic region precluding clear characterisation, key HMBC (solid arrow) and COSY (dashed arrow) correlations are shown, nOe couplings were observed between C19-**H**, C1-**H** and C8-**H**, C7-**H₃** in the NOESY spectrum allowing characterisation of the relative stereochemistry. ^{1}H NMR (600 MHz, $CDCl_3$) δ 1.11 (s, 3H, C7-**H₃**), 1.27 (s, 3H, C15-**H₃**), 1.31 (s, 3H, C15′-**H₃**), 1.79 – 1.94 (m, 1H, C5-**H$_a$**H$_b$), 1.96 (s, 3H, C13-**H₃**), 2.41 (s, 1H, C18-**H**), 2.47 – 2.53 (m, 1H, C9-**H$_a$**H$_b$), 2.54 – 2.62 (m, 1H, C12-**H$_a$**H$_b$), 2.65 (dd, *J* = 18.0, 8.5 Hz, 1H, C12-H$_a$**H$_b$**), 2.88 (dd, *J* = 13.5, 11.5 Hz, 1H, C9-H$_a$**H$_b$**), 3.47 (s, 1H, C1-**H**), 3.91 (dd, *J* = 11.5, 5.5 Hz, 1H, C8-**H**), 4.08 (dd, *J* = 8.5, 6.0 Hz, 1H, C19-**H**), 4.62 (app. q, *J* = 1.5 Hz, 1H, C16-**H$_a$**H$_b$), 4.81 (app. q, *J* = 1.5 Hz, 1H, C16-H$_a$**H$_b$**); ^{13}C NMR (151 MHz, $CDCl_3$) δ 19.9 (C-7), 22.5 (C-13), 25.8 (C-15), 30.3 (C-15′), 35.3 (C-9), 36.4 (C-5), 39.1 (C-14), 41.5 (C-12), 46.7 (C-2), 58.1 (C-1), 65.6 (C-19), 73.5 (C-18), 76.4 (C-6),

109.8 (C-16), 131.7 (C-11), 136.8 (C-10), 142.6 (C-6), 211.4 (C-17); *m/z* ([ESI$^+$]): 319.2 ([M+H]$^+$), 341.2 ([M+Na]$^+$); HRMS: 319.2268 found, $C_{20}H_{31}O_3$ requires 319.2268.

(4a*R,6*R**,12*S**,12a*R**)-12-Hydroxy-9,12a,13,13-tetramethyl-4-methylene-2,3,4,4a,6,7,8,11,12,12a-decahydro-6,10-methanobenzo[10]annulen-5(1*H*)-one 369**

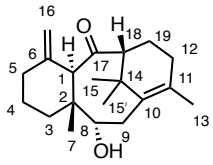

Minor component isolated alongside **368**. The regiochemistry of the alcohol was tentatively assigned due to the similarity of the C**H***O*H coupling constants to the major compound. The COSY spectrum showed coupling of C8-**H** to two diastereomeric CH_2 resonances which, according to the HSQC, belonged to the same carbon. Determination of the relative stereochemistry was assigned based on the major component, only diagnostic signals are reported. ^{1}H NMR (600 MHz, $CDCl_3$) δ 3.61 (s, 1H, C1-**H**), 4.02 (dd, *J* = 12.0, 5.0 Hz, 1H, C8-**H**), 4.60 (app. q, *J* = 1.5 Hz, 1H, C16-**H**$_a$H$_b$), 4.89 (app. q, *J* = 1.5 Hz, 1H, C16-H$_a$**H**$_b$); ^{13}C NMR (151 MHz, $CDCl_3$) δ 55.3 (C-1), 76.0 (C-8), 110.3 (C-16), 213.3 (C-17).

(4a*R,6*S**,7*S**,11*S**,12a*S**)-7,11-Dihydroxy-9,12a,13,13-tetramethyl-4-methylene-2,3,4,4a,6,7,8,11,12,12a-decahydro-6,10-methanobenzo[10]annulen-5(1*H*)-one 370**

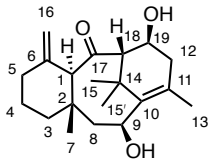

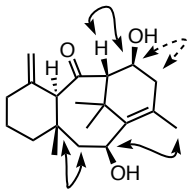

Isolated from reaction with (±)-*trans*-**132** with RK/A328G. The reaction was carried out as in **General Procedure 2** in 50 mL total reaction volume using a 50 mM stock solution of (±)-*trans*-**132**. After 24 h the reaction was incomplete and so addition of glucose, $NADP^+$, GDH, and RK/A328G was repeated. The reaction was complete after 48 h. Purified by column chromatography to yield a 2:1 mixture of compounds (pentane → EtOAc). White solid, 0.3 mg, 2.4%. The major component was able to be fully characterised. $[\alpha]_D^{25}$ +53.6 (*c* 0.03, $CHCl_3$), C3-**H₂** and C4-**H₂** have been omitted from NMR data due to the complexity of the aliphatic region precluding clear characterisation, key HMBC (solid arrow) and COSY (dashed arrow) correlations are shown, presence of a nOe coupling between C19-**H**, C1-**H** and lack of a nOe coupling between C9-**H**, C7-**H₃** in the NOESY spectrum allowed characterisation of the relative stereochemistry. ^{1}H NMR (600 MHz, $CDCl_3$) δ 1.09 (s, 3H, C7-**H₃**), 1.20 (s, 3H, C15-**H₃**), 1.36 (s, 3H, C15′-**H₃**), 1.69 – 1.73 (m, 1H, C8-**H$_a$**H$_b$), 1.70 (s, 3H, C13-**H₃**), 1.73 – 1.79 (m, 1H, C5-**H$_a$**H$_b$), 2.01 – 2.05 (m, 1H, C5-H$_a$**H$_b$**), 2.09 (dd, *J* = 16.0, 9.5 Hz, 1H, C12-**H$_a$**H$_b$), 2.26 (app. s, 1H, C18-**H**), 2.30 (dd, *J* = 15.0, 5.0 Hz, 1H, C8-H$_a$**H$_b$**), 2.45 (dd, *J* = 16.0, 9.5 Hz, 1H, C12-H$_a$**H$_b$**), 3.31 (s, 1H, C1-**H**), 4.03 (dt, *J* = 11.0, 5.0 Hz, 1H, C9-**H**), 4.23 (td, *J* = 9.5, 4.5 Hz, 1H, C19-**H**), 4.69 (d, *J* = 1.5 Hz, 1H, C16-**H$_a$**H$_b$), 4.93 (app. q, *J* = 1.5 Hz, 1H,C16-H$_a$**H$_b$**); ^{13}C NMR (151 MHz, $CDCl_3$) δ 19.7 (C-15), 24.9 (C-15′), 25.0 (C-13), 30.1 (C-7), 35.7 (C-5), 35.9 (C-8), 37.5 (C-12), 38.6 (C-14),

45.6 (C-2), 57.3 (C-1), 65.0 (C-19), 70.8 (C-18), 75.9 (C-9), 110.8 (C-16), 134.3 (C-10), 140.5 (C-11), 142.8 (C-6), 210.8 (C-17); *m/z* ([ESI$^+$]): 319.2 ([M+H]$^+$), 341.2 ([M+Na]$^+$); HRMS: 341.2087 found, $C_{20}H_{31}O_3Na$ requires 341.2087.

(+)-(4a*R,6*R**,8*R**,12*S**,12a*R**)-8,12-dihydroxy-9,12a,13,13-tetramethyl-4-methylene-2,3,4,4a,6,7,8,11,12,12a-decahydro-6,10-methanobenzo[10]annulen-5(1*H*)-one (+)-371**

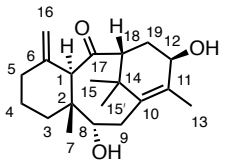

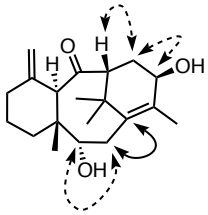

Isolated from reaction with (±)-*trans*-**132** with RK/A328G. The reaction was carried out as in **General Procedure 2** in 50 mL total reaction volume using a 50 mM stock solution of (±)-*trans*-**132**. After 24 h the reaction was incomplete and so addition of glucose, NADP$^+$, GDH, and RK/A328G was repeated. The reaction was complete after 48 h. Purified by column chromatography (pentane → EtOAc) to yield the title compound as a white solid (0.6 mg, 4.7%). $[\alpha]_D^{25}$ +19.3 (*c* 0.06, $CHCl_3$), key HMBC (solid arrow) and COSY (dashed arrow) correlations are shown, presence of a nOe coupling between C7-**H$_3$**, C8-**H** and C12-**H**, C13-**H$_3$** in the NOESY spectrum allowed characterisation of the relative stereochemistry. ^{1}H NMR (600 MHz, $CDCl_3$) δ 1.12 (s, 3H, C7-**H$_3$**), 1.26 (s, 3H, C15-**H$_3$**), 1.38 (s, 3H, C15′-**H$_3$**), 1.48 (td, *J* = 13.5, 4.5 Hz, 1H, C3-**H$_a$**H$_b$), 1.60 (tt, *J* = 13.5, 4.5 Hz, 1H, C4-**H$_a$**H$_b$), 1.66 – 1.73 (m, 1H, C4-H$_a$**H$_b$**), 1.73 – 1.79 (m, 1H, C3-H$_a$**H$_b$**), 1.85 (td, *J* = 13.5, 4.5 Hz, 1H, C5-**H$_a$**H$_b$), 1.99 (s, 3H, C13-**H$_3$**), 2.12 (ddd, *J* = 16.0, 7.5, 3.5 Hz, 1H, C19-**H$_a$**H$_b$), 2.20 (dd, *J* = 16.0, 9.0 Hz, 1H, C19-H$_a$**H$_b$**), 2.30 (dd, *J* = 13.5, 4.5 Hz, 1H, C5-H$_a$**H$_b$**), 2.57 – 2.63 (m, 1H, C9-**H$_a$**H$_b$),

2.58 (d, *J* = 7.5 Hz, 1H, C18-**H**), 2.86 (dd, *J* = 13.0, 11.5 Hz, 1H, C9-H_a**H_b**), 3.67 (s, 1H, C1-**H**), 3.92 – 3.98 (m, 1H, C8-**H**), 4.21 (d, *J* = 9.0 Hz, 1H, C12-**H**), 4.62 (app. q , *J* = 1.5 Hz, 1H, C16-**H_a**H_b), 4.80 (app. q, *J* = 1.5 Hz, 1H, C16-H_a**H_b**); ^{13}C NMR (151 MHz, $CDCl_3$) δ 19.8 (C-7), 20.7 (C-13), 22.6 (C-4), 25.4 (C-15), 30.4 (C-3), 30.5 (C-19), 34.5 (C-15′), 36.0 (C-9), 36.6 (C-5), 37.6 (C-14), 46.6 (C-2), 56.9 (C-1), 66.8 (C-18), 71.5 (C-12), 75.9 (C-8), 109.3 (C-16), 133.5 (C-11), 142.1 (C-10), 143.2 (C-6), 213.4 (C-17); *m/z* ([ESI$^+$]): 319.2 ([M+H]$^+$), 341.2 ([M+Na]$^+$); HRMS: 341.2087 found, $C_{20}H_{31}O_3Na$ requires 341.2087.

7 Bibliography

(1) Chatt, J.; Davidson, J. M. *J. Chem. Soc.* **1965**, *111*, 843.

(2) Mbuvi, H. M.; Woo, L. K. *Organometallics* **2008**, *27* (4), 637.

(3) Flores-Gaspar, A.; Gutiérrez-Bonet, Á.; Martin, R. *Org. Lett.* **2012**, *14* (20), 5234.

(4) Lebel, H.; Huard, K.; Lectard, S. *J. Am. Chem. Soc.* **2005**, *127* (41), 14198.

(5) O'Hanlon, J. A.; Ren, X.; Morris, M.; Wong, L. L.; Robertson, J. *Org. Biomol. Chem.* **2017**, *15* (41), 8780.

(6) Rogge, T.; Kaplaneris, N.; Chatani, N.; Kim, J.; Chang, S.; Punji, B.; Schafer, L. L.; Musaev, D. G.; Wencel-Delord, J.; Roberts, C. A.; Sarpong, R.; Wilson, Z. E.; Brimble, M. A.; Johansson, M. J.; Ackermann, L. *Nat. Rev. Methods Prim.* **2021**, *1* (1), 43.

(7) Barton, D. H. R.; Beaton, J. M.; Geller, L. E.; Pechet, M. *J. Am. Chem. Soc.* **1960**, *82* (10), 2640.

(8) Barton, D. H. R.; Beaton, J. M. *J. Am. Chem. Soc.* **1960**, *82* (10), 2641.

(9) Stateman, L. M.; Nakafuku, K. M.; Nagib, D. A. *Synthesis* **2018**, *50* (8), 1569.

(10) Friese, F. W.; Mück-Lichtenfeld, C.; Studer, A. *Nat. Commun.* **2018**, *9* (1), 2808.

(11) Hakimelahi, G. H.; Li, P. C.; Moosavi-Movahedi, A. A.; Chamani, J.; Khodarahmi, G. A.; Ly, T. W.; Valiyev, F.; Leong, M. K.; Hakimelahi, S.; Shia, K. S.; Chao, I. *Org. Biomol. Chem.* **2003**, *1* (14), 2461.

(12) Snieckus, V. *Chem. Rev.* **1990**, *90* (6), 879.

(13) Watanabe, M.; Sahara, M.; Kubo, M.; Furukawa, S.; Billedeau, R. J.; Snieckus, V. *J. Org. Chem.* **1984**, *49* (5), 742.

(14) Clark, R. D.; Jahangir, J. *J. Org. Chem.* **1989**, *54* (5), 1174.

(15) Hughes, J. M. E.; Gleason, J. L. *Angew. Chem., Int. Ed.* **2017**, *56* (36), 10830.

(16) Basu, D.; Kumar, S.; V, S. S.; Bandichhor, R. *J. Chem. Sci.* **2018**, *130* (6), 71.

(17) Rej, S.; Das, A.; Chatani, N. *Coord. Chem. Rev.* **2021**, *431*, 213683.

(18) Sambiagio, C.; Schönbauer, D.; Blieck, R.; Dao-Huy, T.; Pototschnig, G.; Schaaf, P.; Wiesinger, T.; Zia, M. F.; Wencel-Delord, J.; Besset, T.; Maes, B. U. W.; Schnürch, M. *Chem. Soc. Rev.* **2018**, *47* (17), 6603.

(19) Dailler, D.; Danoun, G.; Baudoin, O. *Angew. Chem., Int. Ed.* **2015**, *54* (16), 4919.

(20) Kudashev, A.; Baudoin, O. *Chem. - Eur. J.* **2021**, *27* (70), 17688.

(21) Sharpe, R. J.; Johnson, J. S. *J. Am. Chem. Soc.* **2015**, *137* (15), 4968.

(22) Park, Y.; Kim, Y.; Chang, S. *Chem. Rev.* **2017**, *117* (13), 9247.

(23) Harris, R. J.; Park, J.; Nelson, T. A. F.; Iqbal, N.; Salgueiro, D. C.; Bacsa, J.; MacBeth, C. E.; Baik, M. H.; Blakey, S. B. *J. Am. Chem. Soc.* **2020**, *142* (12), 5842.

(24) Liu, Y.; You, T.; Wang, T. T.; Che, C. M. *Tetrahedron* **2019**, *75* (44), 130607.

(25) Zhu, R. Y.; Liu, L. Y.; Yu, J. Q. *J. Am. Chem. Soc.* **2017**, *139* (36), 12394.

(26) He, J.; Shao, Q.; Wu, Q.; Yu, J. Q. *J. Am. Chem. Soc.* **2017**, *139* (9), 3344.

(27) Wang, P. L.; Li, Y.; Wu, Y.; Li, C.; Lan, Q.; Wang, X. S. *Org. Lett.* **2015**, *17* (15), 3698.

(28) Rao, W. H.; Zhan, B. B.; Chen, K.; Ling, P. X.; Zhang, Z. Z.; Shi, B. F. *Org. Lett.* **2015**, *17* (14), 3552.

(29) Borpatra, P. J.; Deka, B.; Deb, M. L.; Baruah, P. K. *Org. Chem. Front.* **2019**, *6* (20), 3445.

(30) Plietker, B.; Röske, A. *Catal. Sci. Tech.* **2019**, *9* (16), 4188.

(31) Nunewar, S.; Kumar, S.; Talakola, S.; Nanduri, S.; Kanchupalli, V. *Chem. - Asian J.* **2021**, *16* (5), 443.

(32) He, J.; Hamann, L. G.; Davies, H. M. L.; Beckwith, R. E. J. *Nat. Commun.* **2015**, *6*, 5943.

(33) Hong, B.; Li, C.; Wang, Z.; Chen, J.; Li, H.; Lei, X. *J. Am. Chem. Soc.* **2015**, *137* (37), 11946.

(34) Hayashi, H.; Uchida, T. *Eur. J. Org. Chem.* **2020**, *8*, 909.

(35) Paradine, S. M.; White, M. C. *J. Am. Chem. Soc.* **2012**, *134* (4), 2036.

(36) Mack, J. B. C.; Bedell, T. A.; Deluca, R. J.; Hone, G. A. B.; Roizen, J. L.; Cox, C. T.; Sorensen, E. J.; Du Bois, J. *J. Chem. Educ.* **2018**, *95* (12), 2243.

(37) Abrams, D. J.; Provencher, P. A.; Sorensen, E. J. *Chem. Soc. Rev.* **2018**, *47* (23), 8925.

(38) Nambu, H.; Noda, N.; Niu, W.; Fujiwara, T.; Yakura, T. *Asian J. Org. Chem.* **2015**, *4* (11), 1246.

(39) Fleming, J. J.; Du Bois, J. *J. Am. Chem. Soc.* **2006**, *128* (12), 3926.

(40) Ye, Q.; Qu, P.; Snyder, S. A. *J. Am. Chem. Soc.* **2017**, *139* (51), 18428.

(41) Liu, C.; Chen, R.; Shen, Y.; Liang, Z.; Hua, Y.; Zhang, Y. *Angew. Chem., Int. Ed.* **2017**, *56* (28), 8187.

(42) Davies, H. M. L.; Morton, D. *Chem. Soc. Rev.* **2011**, *40* (4), 1857.

(43) Bedell, T. A.; Hone, G. A. B.; Valette, D.; Yu, J. Q.; Davies, H. M. L.; Sorensen, E. J. *Angew. Chem., Int. Ed.* **2016**, *55* (29), 8270.

(44) Chen, M.; White, M. *Science* **2007**, *318* (5851), 783.

(45) White, M. C.; Zhao, J. *J. Am. Chem. Soc.* **2018**, *140*, 13988.

(46) Howell, J. M.; Feng, K.; Clark, J. R.; Trzepkowski, L. J.; White, M. C. *J. Am. Chem. Soc.* **2015**, *137* (46), 14590.

(47) Klas, K.; Tsukamoto, S.; Sherman, D. H.; Williams, R. M. *J. Org. Chem.* **2015**, *80* (23), 11672.

(48) Shepherd, E. D.; Hallside, M. S.; Sutro, J. L.; Thompson, A.; Hutchings, M.; Burton, J. W. *Tetrahedron* **2020**, *76* (11), 130981.

(49) Li, C.; Zhang, R.; Wang, J.; Wilson, L. M.; Yan, Y. *Trends Biotechnol.* **2020**, *38* (7), 729.

(50) Maurer, S. C.; Kühnel, K.; Kaysser, L. A.; Eiben, S.; Schmid, R. D.; Urlacher, V. B. *Adv. Synth. Catal.* **2005**, *347* (7–8), 1090.

(51) Black, W. B.; Zhang, L.; Mak, W. S.; Maxel, S.; Cui, Y.; King, E.; Fong, B.; Sanchez Martinez, A.; Siegel, J. B.; Li, H. *Nat. Chem. Biol.* **2020**, *16* (1), 87.

(52) Dewick, P. M. *Nat. Prod. Rep.* **2002**, *19* (2), 181.

(53) Helfrich, E. J. N.; Lin, G. M.; Voigt, C. A.; Clardy, J. *Beilstein J. Org. Chem.* **2019**, *15* (1), 2889.

(54) Kanda, Y.; Nakamura, H.; Umemiya, S.; Puthukanoori, R. K.; Murthy Appala, V. R.; Gaddamanugu, G. K.; Paraselli, B. R.; Baran, P. S. *J. Am. Chem. Soc.* **2020**, *142* (23), 10526.

(55) Chen, K.; Baran, P. S. *Nature* **2009**, *459* (7248), 824.

(56) Sheldon, R. A.; Brady, D.; Bode, M. L. *Chem. Sci.* **2020**, *11* (10), 2587.

(57) Bell, E. L.; Finnigan, W.; France, S. P.; Hepworth, L. J.; Lovelock, S. L.; Hayes, M. A.; Osuna, S.; Romero, E.; Ryan, K. S.; Turner, N. J.; Flitsch, S. L. *Nat. Rev. Methods Prim.* **2021**, *1*, 46.

(58) Chowdhury, R.; Maranas, C. D. *AIChE J.* **2020**, *66* (3), e16847.

(59) Li, F.; Zhang, X.; Renata, H. *Curr. Opin. Chem. Biol.* **2019**, *49*, 25.

(60) Zwick, C. R.; Renata, H. *Nat. Prod. Rep.* **2020**, *37* (8), 1065.

(61) Kling, A.; Lukat, P.; Almeida, D. V; Bauer, A.; Fontaine, E.; Sordello, S.; Zaburannyi, N.; Herrmann, J.; Wenzel, S. C.; König, C.; Ammerman, N. C.; Barrio, M. B.; Borchers, K.; Bordon-Pallier, F.; Brönstrup, M.; Courtemanche,

G.; Gerlitz, M.; Geslin, M.; Hammann, P.; Heinz, D. W.; Hoffmann, H.; Klieber, S.; Kohlmann, M.; Kurz, M.; Lair, C.; Matter, H.; Nuermberger, E.; Tyagi, S.; Fraisse, L.; Grosset, J. H.; Lagrange, S.; Müller, R. *Science* **2015**, *348* (6239), 1106.

(62) Zwick, C. R.; Renata, H. *J. Org. Chem.* **2018**, *83* (14), 7407.

(63) Kaluzna, I.; Schmitges, T.; Straatman, H.; Van Tegelen, D.; Müller, M.; Schürmann, M.; Mink, D. *Org. Process Res. Dev.* **2016**, *20* (4), 814.

(64) Behrendorff, J. B. Y. H.; Huang, W.; Gillam, E. M. J. *Biochem. J.* **2015**, *467* (1), 1.

(65) Fessner, N. D. *ChemCatChem* **2019**, *11* (9), 2226.

(66) Loskot, S. A.; Romney, D. K.; Arnold, F. H.; Stoltz, B. M. *J. Am. Chem. Soc.* **2017**, *139* (30), 10196.

(67) Hong, B.; Luo, T.; Lei, X. *ACS Cent. Sci.* **2020**, *6* (5), 622.

(68) Sigel, A.; Sigel, H.; Sigel, R. K. O. *Metal Ions in Life Sciences*; John Wiley & Sons Ltd, 2007; Vol. 3.

(69) Urlacher, V. B.; Eiben, S. *Trends Biotechnol.* **2006**, *24* (7), 324.

(70) Suzuki, K.; Stanfield, J. K.; Shoji, O.; Yanagisawa, S.; Sugimoto, H.; Shiro, Y.; Watanabe, Y. *Catal. Sci. Technol.* **2017**, *7* (15), 3332.

(71) Yosca, T. H.; Ledray, A. P.; Ngo, J.; Green, M. T. *J. Biol. Inorg. Chem.* **2017**, *22* (2–3), 209.

(72) Zanger, U. M.; Schwab, M. *Pharmacol. Ther.* **2013**, *138* (1), 103.

(73) Bertea, C. M.; Schalk, M.; Karp, F.; Maffei, M.; Croteau, R. *Arch. Biochem. Biophys.* **2001**, *390* (2), 279.

(74) Carlson, J. C.; Li, S.; Gunatilleke, S. S.; Anzai, Y.; Burr, D. A.; Podust, L. M.; Sherman, D. H. *Nat. Chem.* **2011**, *3* (8), 628.

(75) Helliwell, C. A.; Chandler, P. M.; Poole, A.; Dennis, E. S.; Peacock, W. J. *Proc. Natl. Acad. Sci. U. S. A.* **2001**, *98* (4), 2065.

(76) Kim, S. Y.; Zhao, P.; Igarashi, M.; Sawa, R.; Tomita, T.; Nishiyama, M.; Kuzuyama, T. *Chem. Biol.* **2009**, *16* (7), 736.

(77) Greule, A.; Stok, J. E.; De Voss, J. J.; Cryle, M. J. *Nat. Prod. Rep.* **2018**, *35* (8), 757.

(78) Finnigan, J. D.; Young, C.; Cook, D. J.; Charnock, S. J.; Black, G. W. *Adv. Protein Chem. Struct. Biol.* **2020**, *122*, 289.

(79) Matson, R. S.; Hare, R. S.; Fulco, A. J. *Biochim. Biophys. Acta, Lipids Lipid Metab.* **1977**, *487* (3), 487.

(80) Fulco, A. J. *Annu. Rev. Pharmacol. Toxicol.* **1991**, *31* (1), 177.

(81) Whitehouse, C. J. C.; Bell, S. G.; Wong, L.-L. *Chem. Soc. Rev.* **2012**, *41* (3), 1218.

(82) Miura, Y.; Fulco, A. J. *J. Biol. Chem.* **1974**, *249* (6), 1880.

(83) Brummund, J.; Müller, M.; Schmitges, T.; Kaluzna, I.; Mink, D.; Hilterhaus, L.; Liese, A. *J. Biotechnol.* **2016**, *233*, 143.

(84) Pflug, S.; Richter, S. M.; Urlacher, V. B. *J. Biotechnol.* **2007**, *129* (3), 481.

(85) Boddupalli, S. S.; Estabrook, R. W.; Peterson, J. A. *J. Biol. Chem.* **1990**, *265* (8), 4233.

(86) Narhi, L. O.; Fulco, A. J. *J. Biol. Chem.* **1987**, *262* (14), 6683.

(87) Nakayama, N.; Takemae, A.; Shoun, H. *J. Biochem.* **1996**, *119* (3), 435.

(88) Correddu, D.; Di Nardo, G.; Gilardi, G. *Trends Biotechnol.* **2021**, *39* (11), 1184.

(89) Groves, J. T. In *Cytochrome P450: Structure, Mechanism, and Biochemistry: Third edition*; Springer US: Boston, MA, 2005; pp 1–43.

(90) Theorell, H.; Ehrenberg, A.; Chance, B. *Arch. Biochem. Biophys.* **1952**, *37* (1),

237.

(91) Rittle, J.; Green, M. T. *Science* **2010**, *330* (6006), 933.

(92) Haines, D. C.; Tomchick, D. R.; Machius, M.; Peterson, J. A. *Biochemistry* **2001**, *40* (45), 13456.

(93) Noble, M. A.; Miles, C. S.; Chapman, S. K.; Lysek, D. A.; Mackay, A. C.; Reid, G. A.; Hanzlik, R. P.; Munro, A. W. *Biochem. J.* **1999**, *339* (2), 371.

(94) Li, H.; Poulos, T. L. *Nat. Struct. Biol.* **1997**, *4* (2), 140.

(95) Huang, W. C.; Westlake, A. C. G.; Maréchal, J. D.; Joyce, M. G.; Moody, P. C. E.; Roberts, G. C. K. *J. Mol. Biol.* **2007**, *373* (3), 633.

(96) Yeom, H.; Sligar, S. G. *Arch. Biochem. Biophys.* **1997**, *337* (2), 209.

(97) Clark, J. P.; Miles, C. S.; Mowat, C. G.; Walkinshaw, M. D.; Reid, G. A.; Daff, S. N.; Chapman, S. K. *J. Inorg. Biochem.* **2006**, *100* (5–6), 1075.

(98) Chen, Z.; Ost, T. W. B.; Schelvis, J. P. M. *Biochemistry* **2004**, *43* (7), 1798.

(99) Klein, M. L.; Fulco, A. J. *J. Biol. Chem.* **1993**, *268* (10), 7553.

(100) Joyce, M. G.; Ekanem, I. S.; Roitel, O.; Dunford, A. J.; Neeli, R.; Girvan, H. M.; Baker, G. J.; Curtis, R. A.; Munro, A. W.; Leys, D. *FEBS J.* **2012**, *279* (9), 1694.

(101) Schmitz, L. M.; Rosenthal, K.; Lütz, S. *Biotechnol. Bioeng.* **2019**, *116* (12), 3469.

(102) Venkataraman, H.; de Beer, S. B. A.; van Bergen, L. A. H.; van Essen, N.; Geerke, D. P.; Vermeulen, N. P. E.; Commandeur, J. N. M. *ChemBioChem* **2012**, *13* (4), 520.

(103) Alworth, W. L.; Xia, Q. W.; Lin, H. M. *FASEB J.* **1997**, *11* (9SS), 90.

(104) Bloom, J. D.; Meyer, M. M.; Meinhold, P.; Otey, C. R.; MacMillan, D.; Arnold, F. H. *Curr. Opin. Struct. Biol.* **2005**, *15* (4), 447.

(105) Reetz, M. T. *J. Org. Chem.* **2009**, *74* (16), 5767.

(106) Strohmeier, G. A.; Pichler, H.; May, O.; Gruber-Khadjawi, M. *Chem. Rev.* **2011**, *111* (7), 4141.

(107) Li, Q. S.; Schwaneberg, U.; Fischer, P.; Schmid, R. D. *Chem. - Eur. J.* **2000**, *6* (9), 1531.

(108) Whitehouse, C. J. C.; Bell, S. G.; Wong, L. L. *Chem. - Eur. J.* **2008**, *14* (35), 10905.

(109) Whitehouse, C. J. C.; Bell, S. G.; Tufton, H. G.; Kenny, R. J. P.; Ogilvie, L. C. I.; Wong, L. L. *Chem. Commun.* **2008**, No. 8, 966.

(110) Li, Y.; Wong, L. L. *Angew. Chem., Int. Ed.* **2019**, *58* (28), 9551.

(111) Chen, W.; Fisher, M. J.; Leung, A.; Cao, Y.; Wong, L. L. *ACS Catal.* **2020**, *10* (15), 8334.

(112) Acevedo-Rocha, C. G.; Gamble, C. G.; Lonsdale, R.; Li, A.; Nett, N.; Hoebenreich, S.; Lingnau, J. B.; Wirtz, C.; Fares, C.; Hinrichs, H.; Deege, A.; Mulholland, A. J.; Nov, Y.; Leys, D.; McLean, K. J.; Munro, A. W.; Reetz, M. T. *ACS Catal.* **2018**, *8* (4), 3395.

(113) Ren, X.; Yorke, J. A.; Taylor, E.; Zhang, T.; Zhou, W.; Wong, L. L. *Chem. - Eur. J.* **2015**, *21* (42), 15039.

(114) Zhang, K.; Shafer, B. M.; Demars, M. D.; Stern, H. A.; Fasan, R. *J. Am. Chem. Soc.* **2012**, *134* (45), 18695.

(115) Le-Huu, P.; Heidt, T.; Claasen, B.; Laschat, S.; Urlacher, V. B. *ACS Catal.* **2015**, *5* (3), 1772.

(116) Le, T. K.; Jang, H. H.; Nguyen, H. T. H.; Doan, T. T. M.; Lee, G. Y.; Park, K. D.; Ahn, T.; Joung, Y. H.; Kang, H. S.; Yun, C. H. *Enzyme Microb. Technol.* **2017**, *97*, 34.

(117) Lewis, J. C.; Bastian, S.; Bennett, C. S.; Fu, Y.; Mitsuda, Y.; Chen, M. M.;

Greenberg, W. A.; Wong, C. H.; Arnold, F. H. *Proc. Natl. Acad. Sci. U. S. A.* **2009**, *106* (39), 16550.

(118) Singh, R.; Bordeaux, M.; Fasan, R. *ACS Catal.* **2014**, *4* (2), 546.

(119) Renata, H.; Wang, Z. J.; Kitto, R. Z.; Arnold, F. H. *Catal. Sci. Technol.* **2014**, *4* (10), 3640.

(120) Shoji, O.; Aiba, Y.; Watanabe, Y. *Acc. Chem. Res.* **2019**, *52* (4), 925.

(121) Zilly, F. E.; Acevedo, J. P.; Augustyniak, W.; Deege, A.; Reetz, M. T. *Angew. Chem., Int. Ed.* **2011**, *50* (12), 2720.

(122) Banks, R. E.; Tatlow, J. C. *J. Fluor. Chem.* **1986**, *33* (1–4), 227.

(123) Karasawa, M.; Stanfield, J. K.; Yanagisawa, S.; Shoji, O.; Watanabe, Y. *Angew. Chem., Int. Ed.* **2018**, *57* (38), 12264.

(124) Suzuki, K.; Stanfield, J. K.; Shoji, O.; Yanagisawa, S.; Sugimoto, H.; Shiro, Y.; Watanabe, Y. *Catal. Sci. Technol.* **2017**, *7* (15), 3332.

(125) Zehentgruber, D.; Urlacher, V. B.; Lütz, S. *J. Mol. Catal. B Enzym.* **2012**, *84*, 62.

(126) Archelas, A.; Fourneron, J. D.; Furstoss, R.; Cesario, M.; Pascard, C. *J. Org. Chem.* **1988**, *53* (8), 1797.

(127) Henrot, M.; Richter, M. E. A.; Maddaluno, J.; Hertweck, C.; De Paolis, M. *Angew. Chem., Int. Ed.* **2012**, *51* (38), 9587.

(128) Syntrivanis, L. D.; Wong, L. L.; Robertson, J. *Eur. J. Org. Chem.* **2018**, *2018* (45), 6369.

(129) Chen, X. T.; Bhattacharya, S. K.; Zhou, B.; Gutteridge, C. E.; Pettus, T. R. R.; Danishefsky, S. J. *J. Am. Chem. Soc.* **1999**, *121* (28), 6563.

(130) Eghtesadi, F.; Moridi Farimani, M.; Hazeri, N.; Valizadeh, J. *Springerplus* **2016**, *5*, 1068.

(131) Teixeira, A. P.; Batista, O.; Fátima Simões, M.; Nascimento, J.; Duarte, A.; De

La Torre, M. C.; Rodríguez, B. *Phytochemistry* **1997**, *44* (2), 325.

(132) Peters, R. J. *Nat. Prod. Rep.* **2010**, *27* (11), 1521.

(133) Zhang, G. J.; Li, Y. H.; Jiang, J. D.; Yu, S. S.; Qu, J.; Ma, S. G.; Liu, Y. B.; Yu, D. Q. *Tetrahedron* **2013**, *69* (3), 1017.

(134) Chen, Y. C.; Li, Y. C.; You, B. J.; Chang, W. Te; Chao, L. K.; Lo, L. C.; Wang, S. Y.; Huang, G. J.; Kuo, Y. H. *Molecules* **2013**, *18* (1), 682.

(135) Moujir, L. M.; Seca, A. M. L.; Araujo, L.; Silva, A. M. S.; Barreto, M. C. *Fitoterapia* **2011**, *82* (2), 225.

(136) Hirasawa, Y.; Izawa, E.; Matsuno, Y.; Kawahara, N.; Goda, Y.; Morita, H. *Bioorg. Med. Chem. Lett.* **2007**, *17* (21), 5868.

(137) González, M. A. *Tetrahedron* **2015**, *71* (13), 1883.

(138) Son, K. H.; Oh, H. M.; Choi, S. K.; Han, D. C.; Kwon, B. M. *Bioorg. Med. Chem. Lett.* **2005**, *15* (8), 2019.

(139) Matsumoto, T.; Ohsuga, Y.; Harada, S.; Fukui, K. *Bull. Chem. Soc. Jpn.* **1977**, *50* (1), 266.

(140) Alvarez-Manzaneda, E.; Chahboun, R.; Alvarez, E.; Ramos, J. M.; Guardia, J. J.; Messouri, I.; Chayboun, I.; Mansour, A. I.; Dahdouh, A. *Synthesis* **2010**, *2010* (20), 3493.

(141) Cai, W.; Huang, S.; Wu, J.; Song, Z.; Xin, Z.; Li, J.; Xue, X. *J. Org. Chem.* **2020**, *85*, 6718.

(142) Snitman, D. L.; Himmelsbach, R. J.; Watt, D. S. *J. Org. Chem.* **1978**, *43* (25), 4758.

(143) Ireland, R. E.; Kierstead, R. C. *J. Org. Chem.* **1966**, *31* (8), 2543.

(144) Meyer, W. L.; Clemans, G. B.; Manning, R. A. *J. Org. Chem.* **1975**, *40* (25), 3686.

(145) Bhar, S. S.; Ramana, M. M. V. *J. Org. Chem.* **2004**, *69* (25), 8935.

(146) Kametani, T.; Kondoh, H.; Tsubuki, M.; Honda, T. *J. Chem. Soc., Perkin Trans. 1* **1990**, *1*, 5.

(147) Burnell, R. H.; Côté, C.; Girard, M. *J. Nat. Prod.* **1993**, *56* (4), 461.

(148) Wendt, K. U.; Schulz, G. E.; Corey, E. J.; Liu, D. R. *Angew. Chem. Int. Ed.* **2000**, *39* (16), 2812.

(149) Surendra, K.; Corey, E. J. *J. Am. Chem. Soc.* **2012**, *134* (29), 11992.

(150) Samanta, R. C.; Yamamoto, H. *J. Am. Chem. Soc.* **2017**, *139* (4), 1460.

(151) Ishihara, K.; Ishibashi, H.; Yamamoto, H. *J. Am. Chem. Soc.* **2001**, *123* (7), 1505.

(152) Surendra, K.; Rajendar, G.; Corey, E. J. *J. Am. Chem. Soc.* **2014**, *136* (2), 642.

(153) Saito, Y.; Goto, M.; Nakagawa-Goto, K. *Org. Lett.* **2018**, *20* (3), 628.

(154) Zhang, C. L.; Bie, P. Y.; Peng, X. J.; Pan, X. F. *J. Chin. Chem. Soc.* **2003**, *50* (3 A), 429.

(155) Jana, C. K.; Scopelliti, R.; Gademann, K. *Synthesis* **2010**, *13*, 2223.

(156) Milanova, R.; Moore, M.; Hirai, Y. *J. Nat. Prod.* **1994**, *57* (7), 882.

(157) Guo, J.; Zhou, Y. J.; Hillwig, M. L.; Shen, Y.; Yang, L.; Wang, Y.; Zhang, X.; Liu, W.; Peters, R. J.; Chen, X.; Zhao, Z. K.; Huang, L. *Proc. Natl. Acad. Sci. U. S. A.* **2013**, *110* (29), 12108.

(158) Youn, S. W.; Pastine, S. J.; Sames, D. *Org. Lett.* **2004**, *6* (4), 581.

(159) Lin, S. C.; Chein, R. J. *J. Org. Chem.* **2017**, *82* (3), 1575.

(160) Isse, A. A.; Lin, C. Y.; Coote, M. L.; Gennaro, A. *J. Phys. Chem. B* **2011**, *115* (4), 678.

(161) Baker, K. V.; Brown, J. M.; Hughes, N.; Skarnulis, A. J.; Sexton, A. *J. Org. Chem.* **1991**, *56* (2), 698.

(162) Narute, S.; Parnes, R.; Toste, F. D.; Pappo, D. *J. Am. Chem. Soc.* **2016**, *138* (50),

16553.

(163) Turner, H. M.; Patel, J.; Niljianskul, N.; Chong, J. M. *Org. Lett.* **2011**, *13* (21), 5796.

(164) Crusco, A.; Bordoni, C.; Chakroborty, A.; Whatley, K. C. L.; Whiteland, H.; Westwell, A. D.; Hoffmann, K. F. *Eur. J. Med. Chem.* **2018**, *152*, 87.

(165) Ishibashi, H.; Ishihara, K.; Yamamoto, H. *J. Am. Chem. Soc.* **2004**, *126* (36), 11122.

(166) Biedermann, F.; Nau, W. M.; Schneider, H. J. *Angew. Chem., Int. Ed.* **2014**, *53* (42), 11158.

(167) Nakagawa, O.; Shimoda, K.; Izumi, S.; Hirata, T. *J. Label. Compd. Radiopharm.* **2000**, *43* (13), 1301.

(168) Hashimoto, S.; Itoh, A.; Kitagawa, Y.; Hisashi, Y.; Nozaki, H. *J. Am. Chem. Soc.* **1977**, *99* (12), 4192.

(169) Surendra, K.; Qiu, W.; Corey, E. J. *J. Am. Chem. Soc.* **2011**, *133* (25), 9724.

(170) Tian, Y.; Xu, X.; Zhang, L.; Qu, J. *Org. Lett.* **2016**, *18* (2), 268.

(171) Burnell, R. H.; Caron, S. *Can. J. Chem.* **1992**, *70* (5), 1446.

(172) Wu, S.; Snajdrova, R.; Moore, J. C.; Baldenius, K.; Bornscheuer, U. T. *Angew. Chem., Int. Ed.* **2021**, *60* (1), 88.

(173) Fenical, W.; Jensen, P. R.; Lindel, T. Eleutherobin and analogs thereof. US5473057A, November 9, 1995.

(174) Lin, Y.; Bewley, C. A.; Faulkner, D. J. *Tetrahedron* **1993**, *49* (36), 7977.

(175) D'Ambrosio, M.; Guerriero, A.; Pietra, F. *Helv. Chim. Acta* **1987**, *70* (8), 2019.

(176) D'Anbrosio, M.; Guerriero, A.; Pietra, F. *Helv. Chim. Acta* **1988**, *71* (5), 964.

(177) Lindel, T.; Jensen, P. R.; Fenical, W.; Long, B. H.; Casazza, A. M.; Carboni, J.; Fairchild, C. R. *J. Am. Chem. Soc.* **1997**, *119* (37), 8744.

(178) Yang, C. P. H.; Horwitz, S. B. *Int. J. Mol. Sci.* **2017**, *18* (8).

(179) Akhmanova, A.; Steinmetz, M. O. *Nat. Rev. Mol. Cell Biol.* **2008**, *9* (4), 309.

(180) Risinger, A. L.; Giles, F. J.; Mooberry, S. L. *Cancer Treat. Rev.* **2009**, *35* (3), 255.

(181) Kikkawa, M.; Ishikawa, T.; Nakata, T.; Wakabayashi, T.; Hirokawa, N. *J. Cell Biol.* **1994**, *127* (6 II), 1965.

(182) Jordan, M. A.; Wilson, L. *Nat. Rev. Cancer* **2004**, *4* (4), 253.

(183) Nogales, E. *Annu. Rev. Biophys. Biomol. Struct.* **2001**, *30*, 397.

(184) Mitchison, T.; Kirschner, M. *Nature* **1984**, *312* (5991), 237.

(185) Rodionov, V. I.; Borisy, G. G. *Science* **1997**, *275* (5297), 215.

(186) Wani, M. C.; Taylor, H. L.; Wall, M. E.; Coggon, P.; Mcphail, A. T. *J. Am. Chem. Soc.* **1971**, *93* (9), 2325.

(187) Schiff, P. B.; Fant, J.; Horwitz, S. B. *Nature* **1979**, *277* (5698), 665.

(188) Bollag, D. M.; McQueney, P. A.; Zhu, J.; Hensens, O.; Koupal, L.; Liesch, J.; Goetz, M.; Lazarides, E.; Woods, C. M. *Cancer Res.* **1995**, *55* (11), 2325.

(189) Goodin, S.; Kane, M. P.; Rubin, E. H. *J. Clin. Oncol.* **2004**, *22* (10), 2015.

(190) Long, B. H.; Carboni, J. M.; Wasserman, A. J.; Cornell, L. A.; Casazza, A. M.; Jensen, P. R.; Lindel, T.; Fenical, W.; Fairchild, C. R. *Cancer Res.* **1998**, *58* (6), 1111 LP.

(191) Chen, X.-T.; Zhou, B.; Bhattacharya, S. K.; Gutteridge, C. E.; Pettus, T. R. R.; Danishefsky, S. J. *Angew. Chem. Int. Ed.* **1998**, *37* (6), 789.

(192) Nicolaou, K. C.; Van Delft, F.; Ohshima, T.; Vourloumis, D.; Xu, J.; Hosokawa, S.; Pfefferkorn, J.; Kim, S.; Li, T. *Angew. Chem., Int. Ed.* **1997**, *36* (22), 2520.

(193) Nicolaou, K. C.; Ohshima, T.; Hosokawa, S.; Van Delft, F. L.; Vourloumis, D.; Xu, J. Y.; Pfefferkorn, J.; Kim, S. *J. Am. Chem. Soc.* **1998**, *120* (34), 8674.

(194) Nicolau, K. C.; Xu, J. Y.; Kim, S.; Ohshima, T.; Hosokawa, S.; Pfefferkorn, J. *J. Am. Chem. Soc.* **1997**, *119* (46), 11353.

(195) Nicolaou, K. C.; Xu, J. Y.; Kim, S.; Pfefferkorn, J.; Ohshima, T.; Vourloumis, D.; Hosokawa, S. *J. Am. Chem. Soc.* **1998**, *120* (34), 8661.

(196) Trost, B. M.; Tasker, A. S.; Rüther, G.; Brandes, A. *J. Am. Chem. Soc.* **1991**, *113* (2), 670.

(197) Castoldi, D.; Caggiano, L.; Panigada, L.; Sharon, O.; Costa, A. M.; Gennari, C. *Chem. - Eur. J.* **2005**, *12* (1), 51.

(198) Caggiano, L.; Castoldi, D.; Beumer, R.; Bayón, P.; Telser, J.; Gennari, C. *Tetrahedron Lett.* **2003**, *44* (43), 7913.

(199) Castoldi, D.; Caggiano, L.; Panigada, L.; Sharon, O.; Costa, A. M.; Gennari, C. *Angew. Chem., Int. Ed.* **2005**, *44* (4), 588.

(200) Ritter, N.; Metz, P. *Synlett* **2003**, *2003* (15), 2422.

(201) Jung, M. E.; Huang, A.; Johnson, T. W. *Org. Lett.* **2000**, *2* (13), 1835.

(202) Kim, P.; Nantz, M. H.; Kurth, M. J.; Olmstead, M. M. *Org. Lett.* **2000**, *2* (13), 1831.

(203) Britton, R.; Roberge, M.; Berisch, H.; Andersen, R. J. *Tetrahedron Lett.* **2001**, *42* (16), 2953.

(204) Britton, R.; De Silva, E. D.; Bigg, C. M.; McHardy, L. M.; Roberge, M.; Andersen, R. J. *J. Am. Chem. Soc.* **2001**, *123* (35), 8632.

(205) Nicolaou, K. C.; Winssinger, N.; Vourloumis, D.; Ohshima, T.; Kim, S.; Pfefferkorn, J.; Xu, J. Y.; Li, T. *J. Am. Chem. Soc.* **1998**, *120* (42), 10814.

(206) Nicolaou, K. C.; Kim, S.; Pfefferkorn, J.; Xu, J.; Ohshima, T.; Hosokawa, S.; Vourloumis, D.; Li, T. *Angew. Chem., Int. Ed.* **1998**, *37* (10), 1418.

(207) Taillefumier, C.; Chapleur, Y. *Can. J. Chem.* **2000**, *78* (6), 708.

(208) Shing, T. K. M.; Ying, T. *Tetrahedron* **1990**, *46* (6), 2187.

(209) Saito, A.; Ito, H.; Taguchi, T. *Org. Lett.* **2002**, *4* (26), 4619.

(210) Holton, R. A. Semi-synthesis of taxane derivatives using metal alkoxides and oxazinones. US5254703A, April 6, 1992.

(211) Tong, Y.; Luo, Y. F.; Gao, W. *Phytochem. Rev.* **2021**, 10.1007/s11101.

(212) Bringi, V.; Kadkade, P. G.; Prince, C. L.; Roach, B. L. Enhanced production of taxol and taxanes by cell cultures of Taxus species. US7264951B1, May 22, 2007.

(213) Walls, L. E.; Martinez, J. L.; del Rio Chanona, E. A.; Rios-Solis, L. *Biotechnol. J.* **2021**, 2100414.

(214) Mendoza, A.; Ishihara, Y.; Baran, P. S. *Nat. Chem.* **2012**, *4* (1), 21.

(215) Hu, Y.-J.; Gu, C.-C.; Wang, X.-F.; Min, L.; Li, C.-C. *J. Am. Chem. Soc.* **2021**, *143* (42), 17862.

(216) Ishihara, Y.; Baran, P. S. *Synlett* **2010**, *2010* (12), 1733.

(217) Wilde, N. C.; Isomura, M.; Mendoza, A.; Baran, P. S. *J. Am. Chem. Soc.* **2014**, *136* (13), 4909.

(218) Hosomi, A.; Sakurai, H. *J. Am. Chem. Soc.* **1977**, *99* (5), 1673.

(219) Ishihara, Y.; Mendoza, A.; Baran, P. S. *Tetrahedron* **2013**, *69* (27–28), 5685.

(220) Mander, L. N.; Sethi, S. P. *Tetrahedron Lett.* **1983**, *24* (48), 5425.

(221) Crabtree, S. R.; Chu, W. L. A.; Mander, L. N. *Synlett* **1990**, *1990* (03), 169.

(222) Bonnert, R. V.; Jenkins, P. R. *J. Chem. Soc. Perkin Trans. 1* **1989**, No. 3, 413.

(223) Mistry, N.; Fletcher, S. P. *Adv. Synth. Catal.* **2016**, *358* (15), 2489.

(224) Li, Y.; Li, Q. *Org. Lett.* **2012**, *14* (17), 4362.

(225) Ghosh, S.; Ghatak, U. R. *Tetrahedron* **1992**, *48* (35), 7289.

(226) Slegeris, R.; Dudley, G. B. *Tetrahedron* **2016**, *72* (26), 3666.

(227) Gremaud, L.; Alexakis, A. *Angew. Chem., Int. Ed.* **2012**, *51* (3), 794.

(228) Peixoto, P. A.; El Assal, M.; Chataigner, I.; Castet, F.; Cornu, A.; Coffinier, R.; Bosset, C.; Deffieux, D.; Pouységu, L.; Quideau, S. *Angew. Chem., Int. Ed.* **2021**, *60* (27), 14967.

(229) Ruiz, B. M.; Geurts, K.; Fernández-Ibáñez, M. Á.; Horst, B. Ter; Minnaard, A. J.; Feringa, B. L. *Org. Lett.* **2007**, *9* (24), 5123.

(230) Shing, T. K. M.; Ying, T. *Tetrahedron* **1990**, *46* (6), 2187.

(231) Syntrivanis, L. D.; Robertson, J. *Eur. J. Org. Chem.* **2017**, *2017* (33), 4916.

(232) Fesenko, A. A.; Shutalev, A. D. *Tetrahedron* **2016**, *72* (20), 2560.

(233) Hitchcock, S. A.; Houldsworth, S. J.; Pattenden, G.; Pryde, D. C.; Thomson, N. M.; Blake, A. J. *J. Chem. Soc. - Perkin Trans. 1* **1998**, No. 19, 3181.

(234) Phillips, A. J.; Morris, J. C.; Abell, A. D. *Tetrahedron Lett.* **2000**, *41* (15), 2723.

(235) Winkler, J. D.; Kim, H. S.; Kim, S. *Tetrahedron Lett.* **1995**, *36* (5), 687.

(236) Kanda, Y.; Ishihara, Y.; Wilde, N. C.; Baran, P. S. *J. Org. Chem.* **2020**, *85* (16), 10293.

(237) Zhou, M.; Liu, T. L.; Cao, M.; Xue, Z.; Lv, H.; Zhang, X. *Org. Lett.* **2014**, *16* (13), 3484.

(238) Ishihara, K.; Nakano, K. *J. Am. Chem. Soc.* **2007**, *129* (29), 8930.

(239) Lou, S.; Westbrook, J. A.; Schaus, S. E. *J. Am. Chem. Soc.* **2004**, *126* (37), 11440.

(240) Li, X.; Lantrip, D.; Fuchs, P. L. *J. Am. Chem. Soc.* **2003**, *125* (47), 14262.

(241) Mosaferi, S.; Jelley, R. E.; Fedrizzi, B.; Barker, D. *Tetrahedron Lett.* **2020**, *61* (51), 152642.

8 Appendices

8.1 (±)-117 screening data

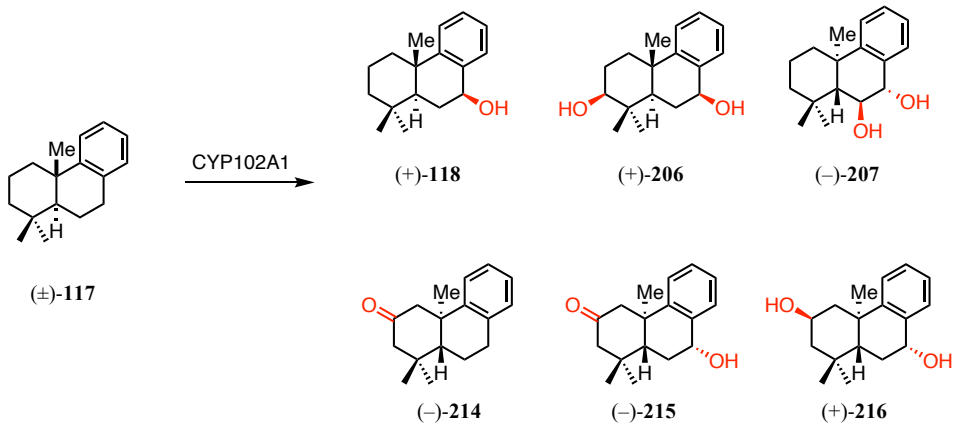

Table 8.1. Table showing conversions and yields for screening of (±)-**117** against 44 CYP102A1 variants.

Mutant	Conv.	(+)-**117** + (–)-**214**	(–)-**207**	(–)-**215**	(+)-**216**	(+)-**206**
GVQ	**100%**	**13%**	**13%**	**12%**	**11%**	**38%**
RK P329G A330P	**98%**	**-**	**4%**	**-**	**-**	**43%**
K19 F87V	**98%**	**17%**	**-**	**8%**	**14%**	**24%**
RK A184I S270G	**98%**	**6%**	**-**	**11%**	**-**	**15%**
RK A184I T260G	**97%**	**-**	**6%**	**-**	**-**	**-**
RKA V78I	**97%**	**8%**	**8%**	**-**	**-**	**45%**
RK S270G	**97%**	**5%**	**11%**	**6%**	**-**	**32%**
KSK19 AM	**96%**	**-**	**-**	**-**	**-**	**16%**
RK A184I T269G	**96%**	**-**	**-**	**10%**	**-**	**18%**
RP F87V	**96%**	**12%**	**-**	**6%**	**15%**	**33%**
RK	**96%**	**5%**	**-**	**-**	**-**	**29%**
RK A328G P329G A330G	**95%**	**6%**	**-**	**-**	**-**	**8%**
RK T269G	**95%**	**-**	**11%**	**-**	**-**	**33%**
GVQ A264G P329G A330W	**94%**	**10%**	**-**	**-**	**14%**	**14%**
GVQ A264G P329G A330P	**93%**	**7%**	**-**	**-**	**8%**	**31%**
KSK19 F81W	**93%**	**7%**	**-**	**-**	**-**	**25%**
GV A184I	**92%**	**15%**	**-**	**-**	**5%**	**25%**
K19 F87V Q403P	**91%**	**28%**	**-**	**5%**	**18%**	**20%**
RK L262G	**91%**	**-**	**9%**	**-**	**-**	**38%**
GVQ A264G	**90%**	**14%**	**-**	**-**	**8%**	**13%**
RK A184I L262G	**89%**	**-**	**-**	**-**	**-**	**24%**
RK W90V	**89%**	**11%**	**-**	**-**	**-**	**27%**
K19 F87V A264G	**89%**	**17%**	**-**	**-**	**7%**	**11%**
RK A328G	**88%**	**9%**	**-**	**-**	**-**	**7%**
KSK19 I263A	**87%**	**15%**	**-**	**-**	**-**	**5%**

RK Q403P	**86%**	**5%**	-	-	-	**9%**
RK P329G A330W	**86%**	**7%**	**11%**	-	-	**23%**
RK A264G	**84%**	**10%**	-	-	-	**22%**
RLYF KSK19 A184I	**82%**	**13%**	-	-	-	**14%**
RK T260G	**80%**	**25%**	-	-	-	**10%**
KSK19 IG	**77%**	**5%**	-	-	-	**10%**
RK A328G A264G	**75%**	**6%**	-	-	-	-
RK G265GG	**66%**	**17%**	-	-	-	**7%**
RK A328G I263G A264G	**60%**	**6%**	-	-	-	**8%**
KSK19 A82M I263G	**57%**	**8%**	-	-	-	-
GVQ I263G A264G	**57%**	**20%**	-	-	-	-
KSK19 A82M E267F	**48%**	-	-	-	-	**17%**
GV A184I I263G A264G	**47%**	**26%**	-	-	-	-
RP H171L I263G A184I	**41%**	**10%**	-	-	-	-
K19 FV A184I	**41%**	**12%**	-	-	-	-
RK I263G P329G A330W	**36%**	-	-	-	-	**6%**
RK I263G	**0%**	-	-	-	-	-
RK I263G A264G	**0%**	-	-	-	-	-
RK I263G P329G A330P	**0%**	-	-	-	-	-

8.2 (±)-115 screening data

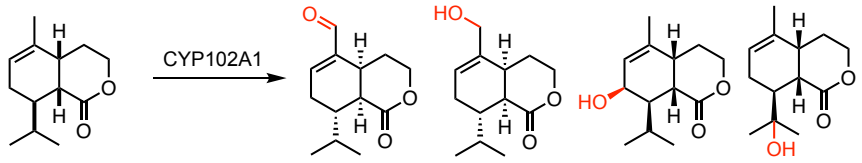

(±)-**115** (+)-**125** (+)-**124** (+)-**116** (+)-**126**

Table 8.2. Table showing conversions and yields for screening of (±)-**115** against 48 CYP102A1 variants.

Mutant	Conversion	(+)-**125**	(+)-**124**	(+)-**116**	(+)-**126**
KSK19/IG	**100%**	**31%**	**56%**	-	**13%**
KSK19/F81W	**100%**	**21%**	-	-	**79%**
R19/A328L/A184I	**100%**	-	**100%**	-	-
RLYF/KSK19/A184I	**100%**	-	-	-	**100%**
GVQ/I263G/V78L	**100%**	**16%**	**5%**	-	**8%**
RLYF/KSK19	**100%**	**9%**	**23%**	**5%**	**63%**
RT2	**100%**	-	**13%**	**72%**	-
GVQ/A264G	**100%**	**14%**	**44%**	**13%**	**27%**
K19/F87V/A264G	**100%**	-	**48%**	**17%**	**35%**
GVQ/A330W	**100%**	-	-	-	**100%**
RLYF/KSK19/I263G	**100%**	**53%**	**32%**	-	**15%**
I263G	**100%**	**17%**	**83%**	-	-

RK/A328G/P329G/A330G	**100%**	**7%**	**29%**	**8%**	**47%**
RP/V78I/E267V	**100%**	**5%**	**47%**	**10%**	**27%**
RT2/A330P/V78I/A184I	**99%**	**-**	**33%**	**-**	-
RLYF/K19	**98%**	**-**	**29%**	**52%**	**-**
RK/I263G/A264G	**98%**	**24%**	**47%**	**-**	**27%**
RK/A328G/A264G	**98%**	**3%**	**15%**	**16%**	**36%**
K19/F87V/A328V	**97%**	**8%**	**76%**	**5%**	**3%**
GVQ	**97%**	**17%**	**42%**	**7%**	**29%**
RK/G265GG	**96%**	**8%**	**24%**	**6%**	**27%**
RP/H171L/I263G	**96%**	**-**	**94%**	**-**	-
RK/A328L	**96%**	**12%**	**66%**	**9%**	**8%**
RP/A82M/I263A	**95%**	**-**	**30%**	**26%**	**-**
KSK19/I263A	**94%**	**20%**	**49%**	**-**	**26%**
RKA/S72W	**88%**	**-**	**57%**	**-**	**31%**
RK/A328G	**86%**	**-**	-	**23%**	**55%**
KSK19/A82M/E267F	**86%**	**-**	**48%**	**5%**	**16%**
R19/A330W	**83%**	**-**	**39%**	**34%**	**-**
R19/A328L/I263A	**82%**	**-**	**73%**	**-**	-
WT	**70%**	**-**	**19%**	**41%**	**-**
RKA/V78I	**61%**	**15%**	**11%**	**4%**	**19%**
KU3/A330P/A328I	**60%**	**2%**	**50%**	**-**	-
RP/IA/EV	**60%**	**-**	**45%**	**-**	**15%**
R19/F87I/L437LV	**59%**	**-**	**46%**	**-**	-
KSK19/A82M/I263G	**52%**	**-**	**34%**	**4%**	**8%**
R19FI	**51%**	**7%**	**35%**	**8%**	**-**
K19/F87V/E267V	**50%**	**8%**	**36%**	**-**	-
GVQ/I263G/A82M	**41%**	**-**	**32%**	**-**	-
K19/F87V/E267V/V78I	**31%**	**6%**	**25%**	**-**	-
RP/F87V	**10%**	**-**	**6%**	**-**	-
K19/F87V	**0%**	**-**	-	-	-
K19/F87V/Q403P	**0%**	**-**	-	-	-
GV/A184I	**0%**	**-**	-	-	-
RP/F87V/V78I	**0%**	**-**	-	-	-
GVQ/I263G/A328L	**0%**	**-**	-	-	-
GVQ/IG	**0%**	**-**	-	-	-
KSK19/AM	**0%**	**-**	-	-	-

8.3 (±)-*trans*-132 screening data

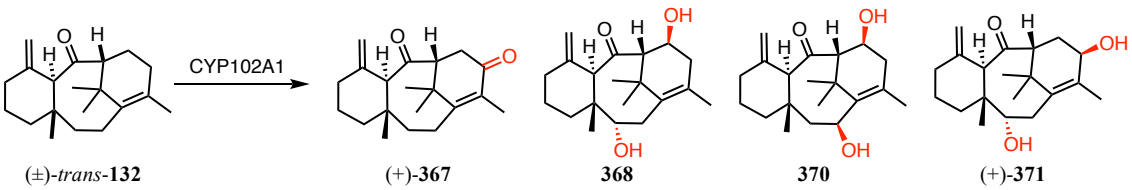

(±)-*trans*-**132** (+)-**367** **368** **370** (+)-**371**

Table 8.3. Table showing conversions and yields for screening of (±)-**132** against 48 CYP102A1 variants.

Variant	Conversion	(+)-**367**	(+)-**371**	**368**	**370**	Other
KSK19/E267V	**91%**	-	-	-	-	**9%**
GVQ/A328G	**90%**	**3%**	-	**2%**	-	**5%**
GVQ	**89%**	**1%**	-	-	-	**11%**
GLQ/I263G/A328G	**86%**	**1%**	-	-	-	**13%**
GVQ/A330W	**84%**	**2%**	-	**1%**	**4%**	**8%**
RKA/V78I	**81%**	**6%**	-	-	-	**13%**
RLYF/KSK19/A184I	**71%**	**1%**	**1%**	**2%**	-	**24%**
RK/A328L	**69%**	**3%**	-	-	-	**28%**
KSK19/I263A	**65%**	**9%**	-	**8%**	**3%**	**14%**
KU3/AP/IA	**64%**	-	-	-	-	**36%**
RP/A82M/I263A	**64%**	**2%**	-	-	-	**34%**
KSK19/I263G	**62%**	**3%**	-	-	-	**35%**
KSK19/A264G	**60%**	**2%**	-	-	-	**38%**
RP/H171L/I263G/A184I	**60%**	**2%**	-	-	-	**38%**
R19/A328L/I263A	**51%**	**2%**	-	-	-	**47%**
WT	**47%**	-	-	-	-	**53%**
K19/F87V/Q403P	**45%**	**11%**	-	**5%**	-	**40%**
RK/A328G	**44%**	**2%**	**4%**	**14%**	**12%**	**24%**
VQ/S72G/A330W	**44%**	**3%**	-	**2%**	-	**52%**
RP/I263A/E267V	**43%**	-	-	-	-	**57%**
RP/H171L/I263G	**42%**	**2%**	-	-	-	**56%**
RK/F81W/T269G/A328G	**42%**	**4%**	**3%**	**3%**	-	**49%**
KU3/AP/S72W	**42%**	**1%**	-	-	-	**57%**
RK/A328G/A264G	**41%**	**3%**	**3%**	**2%**	-	**51%**
GVQ/I263G/A328L	**40%**	**24%**	-	-	-	**36%**
GQ/IG/AL	**38%**	**1%**	-	-	-	**61%**
RK/A328G/P329G/A338G	**36%**	**5%**	**1%**	**3%**	-	**55%**
KSK19/A82M/I263G	**35%**	-	-	**3%**	-	**62%**
GV/A183I/I263G/A328G	**34%**	**2%**	-	-	**0%**	**63%**
KT2/L188G/I263G	**34%**	**2%**	-	-	-	**64%**
GVQ/A264G	**34%**	**1%**	-	-	-	**65%**
KSK19/F81W	**34%**	**3%**	**1%**	**12%**	**2%**	**48%**
A330P	**33%**	-	-	-	-	**67%**

RT2/S72G/A330W	**31%**	**1%**	**-**	**-**	**-**	**68%**
RK/T260G	**30%**	**2%**	**-**	**-**	**-**	**68%**
RLYF/K19	**30%**	**1%**	**-**	**-**	**-**	**69%**
KSK19/IG	**28%**	**5%**	**2%**	**7%**	**-**	**57%**
R19/FI	**28%**	**-**	**-**	**-**	**-**	**72%**
KSK19/E267V/V78I	**27%**	**-**	**-**	**-**	**-**	**73%**
GV/A184I	**26%**	**5%**	**1%**	**10%**	**-**	**58%**
R19/S72G/A330W	**25%**	**-**	**-**	**-**	**-**	**75%**
R19/A330W	**25%**	**-**	**-**	**-**	**-**	**75%**
R19/F87I/L437LV	**25%**	**3%**	**-**	**-**	**-**	**72%**
RLYF/KSK19	**25%**	**3%**	**2%**	**8%**	**2%**	**60%**
GVQ/I263G	**25%**	**2%**	**-**	**-**	**-**	**73%**
RKAI/TG/A328G	**23%**	**3%**	**1%**	**1%**	**-**	**72%**
RK/S72W/A328I	**23%**	**7%**	**-**	**-**	**-**	**70%**
K19/F87V	**23%**	**-**	**-**	**-**	**-**	**77%**

8.4 CYP102A1 variant mutation list

Table 8.4. Table showing mutations for the plate 1 variants used for screening with tricycle (±)-**117**.

Variant	**Mutations**
GV/A184I	A74G/F87V/A184I
GV/A184I/I263G/A264G	A74G/F87V/A184I/I263G/A264G
GVQ	A74G/F87V/L188Q
GVQ/A264G	A74G/F87V/L188Q/A264G
K19/FV/A184I	F87V/H171L/A184I/Q307H/N319Y
GVQ/I263G/A264G	A74G/F87V/L188Q/I263G/A264G
K19/F87V	F87V/H171L/Q307H/N319Y
K19/F87V/A264G	F87V/H171L/A264G/Q307H/N319Y
K19/F87V/Q403P	F87V/H171L/Q307H/N319Y/Q403P
KSK19/A82M/E267F	A82M/F87A/H171L/E267F/Q307H/N319Y
KSK19/A82M/I263G	A82M/F87A/H171L/I263G/Q307H/N319Y
KSK19/F81W	F81W/F87A/H171L/Q307H/N319Y
KSK19/I263A	F87A/H171L/I263A/Q307H/N319Y
RK	R47L/Y51F/F87A/H171L/Q307H/N319Y
RK/A264G	R47L/Y51F/F87A/H171L/A264G/Q307H/N319Y

RK/A328G	R47L/Y51F/F87A/H171L/Q307H/N319Y/A328G
RK/A328G/A264G	R47L/Y51F/F87A/H171L/A264G/Q307H/N319Y/A328G
RK/A328G/I263G/A264G	R47L/Y51F/F87A/H171L/I263G/A264G/Q307H/N319Y/A328G
RK/A328G/P329G/A330G	R47L/Y51F/F87A/H171L/Q307H/N319Y/A328G/P329G/A330G
RK/W90V	R47L/Y51F/F87A/W90V/H171L/Q307H/N319Y
RK/G265GG	R47L/Y51F/F87A/H171L/G265GG/Q307H/N319Y
RK/I263G	R47L/Y51F/F87A/H171L/I263G/Q307H/N319Y
RK/I263G/A264G	R47L/Y51F/F87A/H171L/I263G/A264G/Q307H/N319Y
RK/I263G/P329G/A330P	R47L/Y51F/F87A/H171L/I263G/Q307H/N319Y/P329G/A330P

Table 8.5. Table showing mutations for the plate 2 variants used for screening with tricycle (±)-**117**.

Variant	**Mutations**
RK I263G P329G A330W	R47L/Y51F/F87A/H171L/I263G/Q307H/N319Y/P329G/A330W
RK P329G A330P	R47L/Y51F/F87A/H171L/Q307H/N319Y/P329G/A330P
RK P329G A330W	R47L/Y51F/F87A/H171L/Q307H/N319Y/P329G/A330W
RK Q403P	R47L/Y51F/F87A/H171L/Q307H/N319Y/Q403P
RKA V78I	R47L/Y51F/V78I/F87A/H171L/Q307H/N319Y/A328I
RLYF KSK19 A184I	R47L/Y51F/F87A/H171L/A184I/Q307H/N319Y
RP F87V	R47L/Y51F/F87V/I401P
GVQ A264G P329G A330P	A74G/F87V/L188Q/A264G/P329G/A330P
GVQ A264G P329G A330W	A74G/F87V/L188Q/A264G/P329G/A330P
KSK19 AM	A82M/F87A/H171L/Q307H/N319Y
KSK19 IG	F87A/H171L/I263G/Q307H/N319Y
RP H171L I263G A184I	R47L/Y51F/H171L/A184I/I263G/I401P
RK T260G	R47L/Y51F/F87A/H171L/T260G/Q307H/N319Y
RK L262G	R47L/Y51F/F87A/H171L/L262G/Q307H/N319Y
RK T269G	R47L/Y51F/F87A/H171L/T269G/Q307H/N319Y
RK S270G	R47L/Y51F/F87A/H171L/S270G/Q307H/N319Y
RK A184I T260G	R47L/Y51F/F87A/H171L/A184I/T260G/Q307H/N319Y
RK A184I L262G	R47L/Y51F/F87A/H171L/A184I/L262G/Q307H/N319Y

RK A184I T269G	R47L/Y51F/F87A/H171L/A184I/T269G/Q307H/N319Y
RK A184I S270G	R47L/Y51F/F87A/H171L/A184I/S270G/Q307H/N319Y

Table 8.6. Table showing mutations for the plate 1 variants used for screening with lactone (±)-**115**.

Variant	**Mutations**
R19/A330W	R47L/Y51F/H171L/Q307H/N319Y/A330W
KSK19/IG	F87A/H171L/I263G/Q307H/N319Y
GVQ	A74G/F87V/L188Q
R19/FI	R47L/Y51F/F87I/H171L/Q307H/N319Y
K19/F87V	F87V/H171L/Q307H/N319Y
K19/F87V/E267V	F87V/H171L/E267V/Q307H/N319Y
KSK19/A82M/I263G	A82M/F87A/H171L/I263G/Q307H/N319Y
K19/F87V/A328V	F87V/H171L/Q307H/N319Y/A328V
KSK19/F81W	F81W/F87A/H171L/Q307H/N319Y
KSK19/I263A	F87A/H171L/I263A/Q307H/N319Y
K19/F87V/Q403P	F87V/H171L/Q307H/N319Y/Q403P
KU3/A328I/A330P	N239H/I259V/A276T/A328I/A330P
R19/A184I/A328L	R47L/Y51F/H171L/A184I/Q307H/N319Y/A328I
RK/A328G	R47L/Y51F/F87A/H171L/Q307H/N319Y/A328G
RLYF/K19	R47L/Y51F/H171L/Q307H/N319Y
RLYF/KSK19/A184I	R47L/Y51F/F87A/H171L/A184I/Q307H/N319Y
GVQ/V78L/I263G	A74G/V78L/F87V/L188Q/I263G
RLYF/KSK19	R47L/Y51F/F87A/H171L/Q307H/N319Y
GV/A184I	A74G/F87V/A184I
RT2	R47L/Y51F/A191T/N239H/I259V/A276T/L353I
RK/I263G/A264G	R47L/Y51F/F87A/H171L/I263G/A264G/Q307H/N319Y
RT2/V78I/A184I/A330P	R47L/Y51F/V78I/A184I/A191T/N239H/I259V/A276T/A330P/L353I
RK/G265GG	R47L/Y51F/F87A/H171L/G265GG/Q307H/N319Y
RP/H171L/I263G	R47L/Y51F/H171L/I263G/I401P

Table 8.7. Table showing mutations for the plate 2 variants used for screening with lactone (±)-**115**.

Variant	Mutations
RP/IA/EV	R47L/Y51F/I263A/E267V/I401P
RKA/S72W	R47L/Y51F/S72W/F87A/H171L/Q307H/N319Y/A328I
WT	WT
GVQ/IG	A74G/F87V/L188Q/I263G
GVQ/A264G	A74G/F87V/L188Q/A264G
K19/F87V/A264G	F87V/H171L/A264G/Q307H/N319Y
K19/V78I/F87V/E267V	V78I/F87V/H171L/E267V/Q307H/N319Y
KSK19/A82M/E267F	A82M/F87A/H171L/E267F/Q307H/N319Y
KSK19/AM	A82M/F87A/H171L/Q307H/N319Y
RK/A328L	R47L/Y51F/F87A/H171L/Q307H/N319Y/A328L
RK/A264G/A328G	R47L/Y51F/F87A/H171L/A264G/Q307H/N319Y/A328G
RKA/V78I	R47L/Y51F/V78I/F87A/H171L/Q307H/N319Y/A328I
R19/F87I/L437LV	R47L/Y51F/F87I/H171L/Q307H/N319Y/L437LV
GVQ/A330W	A74G/F87V/L188Q/A330W
RLYF/KSK19/I263G	R47L/Y51F/F87A/H171L/I263G/Q307H/N319Y
GVQ/A82M/I263G	A74G/A82M/F87V/L188Q/I263G
RP/A82M/I263A	R47L/Y51F/A82M/I263A/I401P
RP/F87V	R47L/Y51F/F87V/I401P
RP/V78I/F87V	R47L/Y51F/V78I/F87V/I401P
I263G	I263G
GVQ/I263G/A328L	A74G/F87V/L188Q/I263G/A328L
RK/A328G/P329G/A330G	R47L/Y51F/F87A/H171L/Q307H/N319Y/A328G/P329G/ A330G
RP/V78I/E267V	R47L/Y51F/V78I/E267V/I401P
R19/I263A/A328L	R47L/Y51F/H171L/I263A/Q307H/N319Y/A328L

Table 8.8. Table showing mutations for the plate 1 variants used for screening with taxane (±)-*trans*-**132**.

Variant	Mutations
R19/A330W	R47L/Y51F/H171L/Q307H/N319Y/A330W
KSK19/I263G	F87A/H171L/I263G/Q307H/N319Y
GVQ	A74G/F87V/L188Q
R19/F87I	R47L/Y51F/F87I/H171L/Q307H/N319Y
KSK19	F87V/H171L/Q307H/N319Y
KSK19/E267V	F87V/H171L/E267V/Q307H/N319Y
K19/A82M/F87A/I263G	A82M/F87A/H171L/I263G/Q307H/N319Y
GV/A184I/I263G/A328G	A74G/F87V/A184I/I263G/A328G
K19/F81W/F87A	F81W/F87A/H171L/Q307H/N319Y
K19/F87A/I263A	F87A/H171L/I263A/Q307H/N319Y
KU3/A184I/A330P	N239H/I259V/A276T/A328I/A330P/A328I
KU3/S72W/A330P	S72W/N239H/I259V/A276T/A330P
GQ/I263G/A328L	A74G/L188Q/I263G/A328L
RK/A328G	R47L/Y51F/F87A/H171L/Q307H/N319Y/A328G
R19	R47L/Y51F/F87V/H171L/Q307H/N319Y
RK/A184I	R47L/Y51F/H171L/Q307H/N319Y
KT2/L188G/I263G	R47L/Y51F/L188G/A191T/N239H/I259V/I263G/A276T/L353I
RK	R47L/Y51F/F87A/H171L/Q307H/N319Y
GV/A184I	A74G/F87V/A184I
KSK19/Q403P	F87V/H171L/Q307H/N319Y/Q403P
RK/A184I/T269G/A328G	R47L/Y51F/F87A/H171L/A184I/T269G/Q307H/N319Y/A32G
RK/A328L	R47L/Y51F/F87A/H171L/Q307H/N319Y/A328L
RT2/S72G/A330W	R47L/Y51F/A191T/N239H/I259V/A276T/L353I
RP/H171L/I263G	R47L/Y51F/H171L/I263G/I401P

Table 8.9. Table showing mutations for the plate 2 variants used for screening with taxane (±)-*trans*-**132**.

Variant	Mutations
RP/I263A/E267V	R47L/Y51F/I263A/E267V/I401P
RK/S72W/A328I	R47L/Y51F/S72W/F87A/H171L/Q307H/N319Y/A328I
WT	WT
GVQ/I263G	A74G/F87V/L188Q/I263G
GVQ/A264G	A74G/F87V/L188Q/A264G
KSK19/A264G	F87V/H171L/A264G/Q307H/N319Y
KSK19/E267V/V78I	V78I/F87V/H171L/E267V/Q307H/N319Y
A330P	A330P
KSK19/I263G	F87V/H171L/I263G/Q307H/N319Y
RK/F81W/T269G/A328G	R47L/Y51F/F81W/F87A/H171L/T269G/Q307H/N319Y/A328G
RK/A328G/A264G	R47L/Y51F/F87A/H171L/A264G/Q307H/N319Y/A328G
RKA/V78I	R47L/Y51F/V78I/F87A/H171L/Q307H/N319Y/A328I
R19/F87I/L437LV	R47L/Y51F/F87I/H171L/Q307H/N319Y/L437LV
GVQ/A330W	A74G/F87V/L188Q/A330W
R19/S72G/A330W	R47L/Y51F/S72G/H171L/Q307H/N319Y/A330W
GVQ/A328G	A74G/F87V/L188Q/A328G
RP/A82M/I263A	R47L/Y51F/A82M/I263A/I401P
RK/T260G	R47L/Y51F/F87A/H171L/T260G/Q307H/N319Y
RP/H171L/I263G/A184I	R47L/Y51F/H171L/I263G/A328I/I401P
VQ/S72G/A330W	S72G/F87V/L188Q/A330W
GVQ/I263G/A328L	A74G/F87V/L188Q/I263G/A328L
RK/A328G/P329G/A330G	R47L/Y51F/F87A/H171L/Q307H/N319Y/A328G/P329G/A330G
GLQ/I263G/A328G	A74G/F87V/L188Q/I263G/A328G
R19/A328L/I263A	R47L/Y51F/H171L/I263A/Q307H/N319Y/A328L

8.5 Chapter 2 – selected spectra

118:

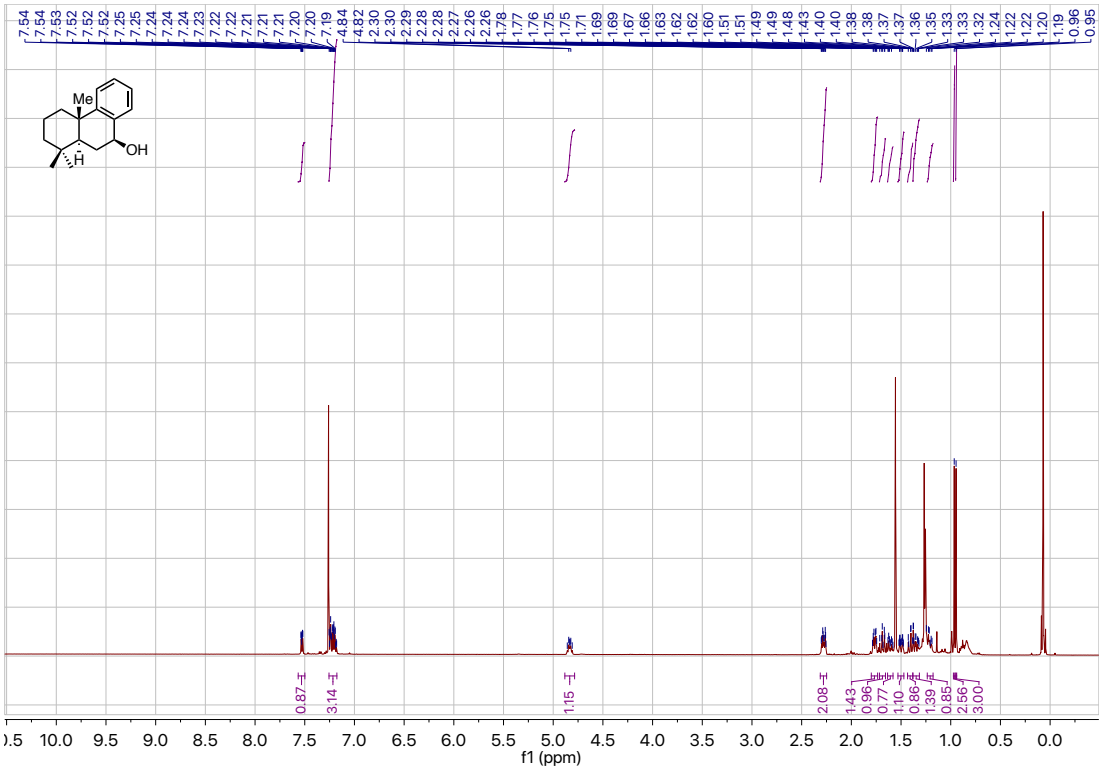

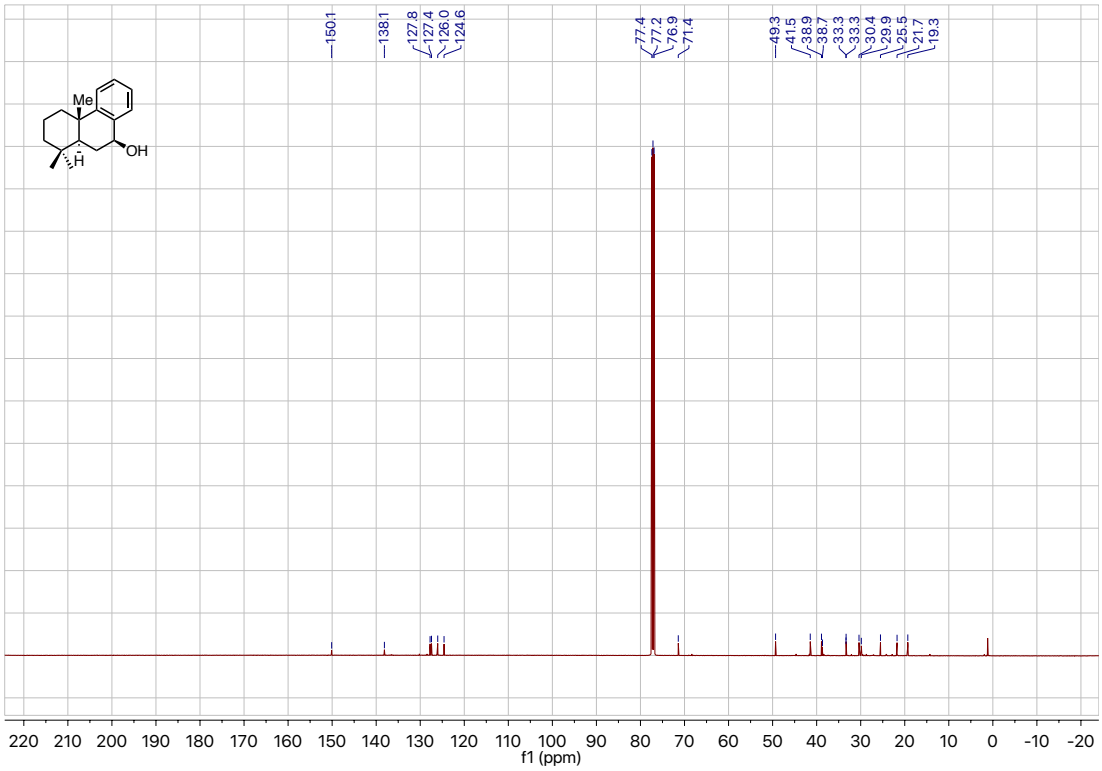

206:

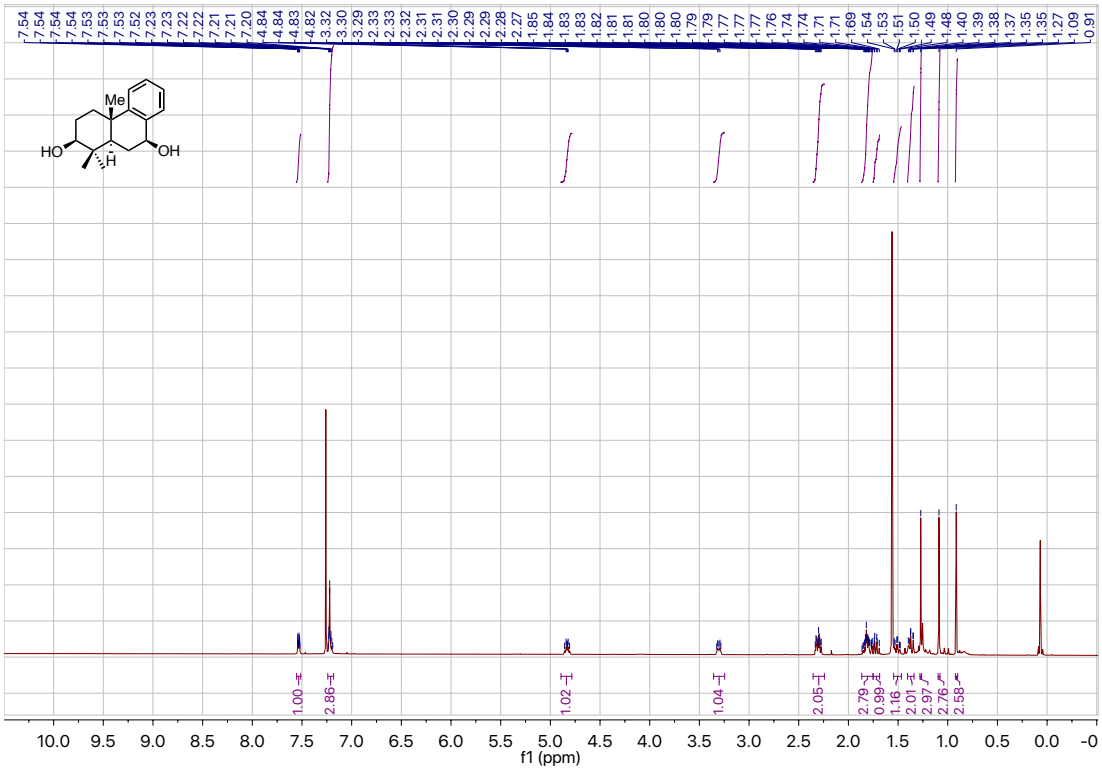

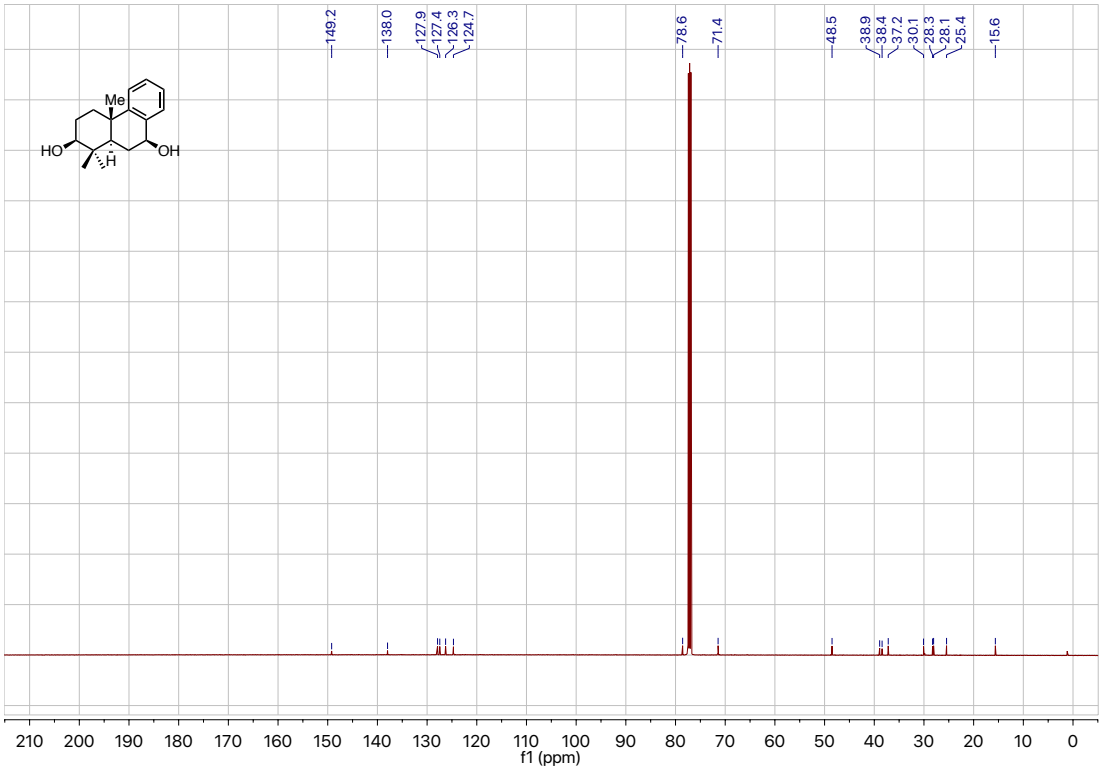

207:

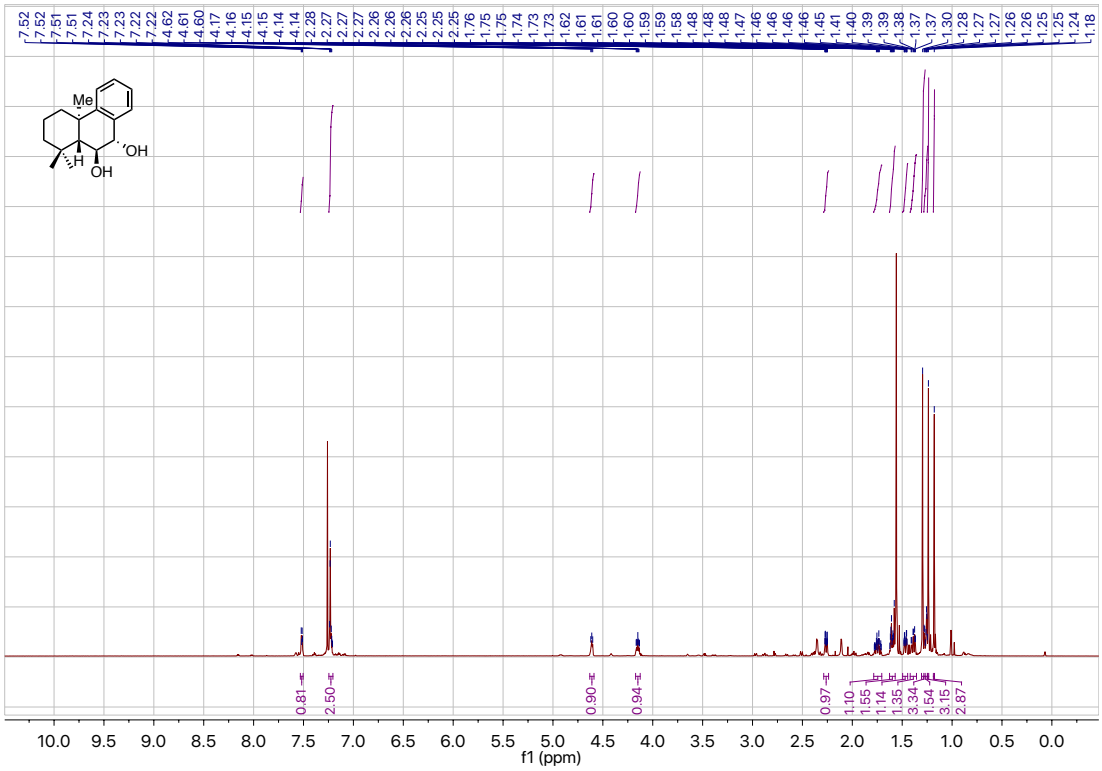
Me
H
OH
OH
f1 (ppm)

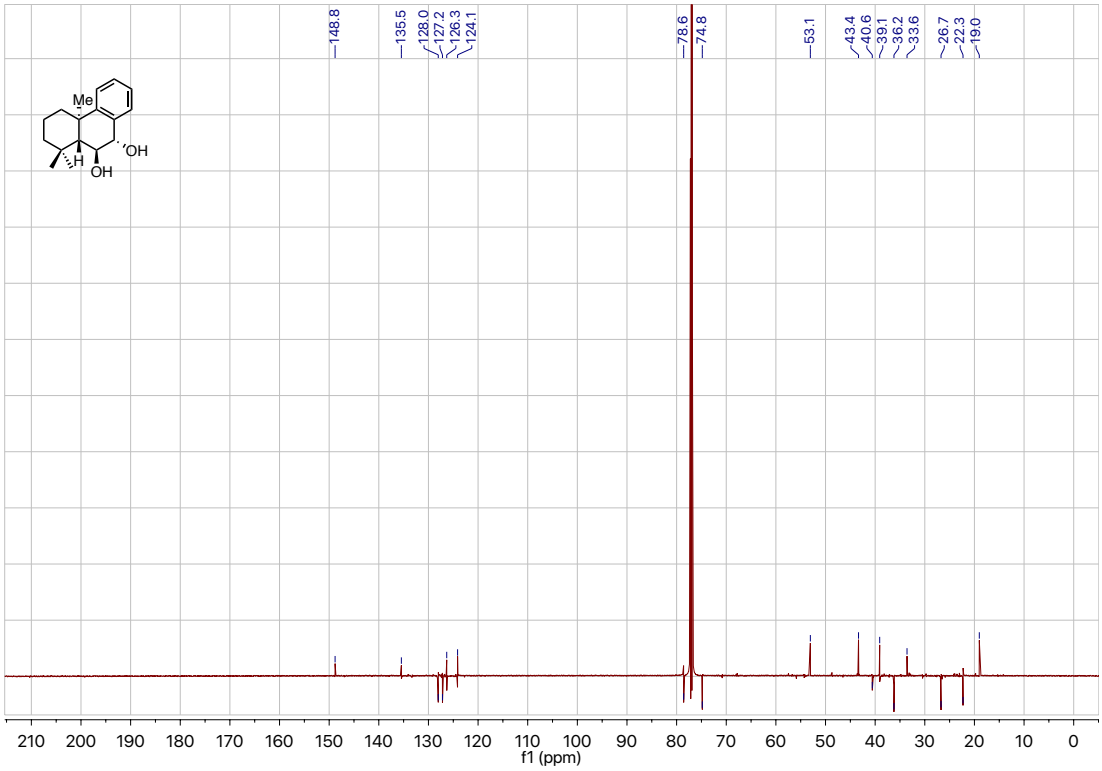
Me
H
OH
OH
148.8
135.5
128.0
127.2
126.3
124.1
78.6
74.8
53.1
43.4
40.6
39.1
36.2
33.6
26.7
22.3
19.0
f1 (ppm)

214:

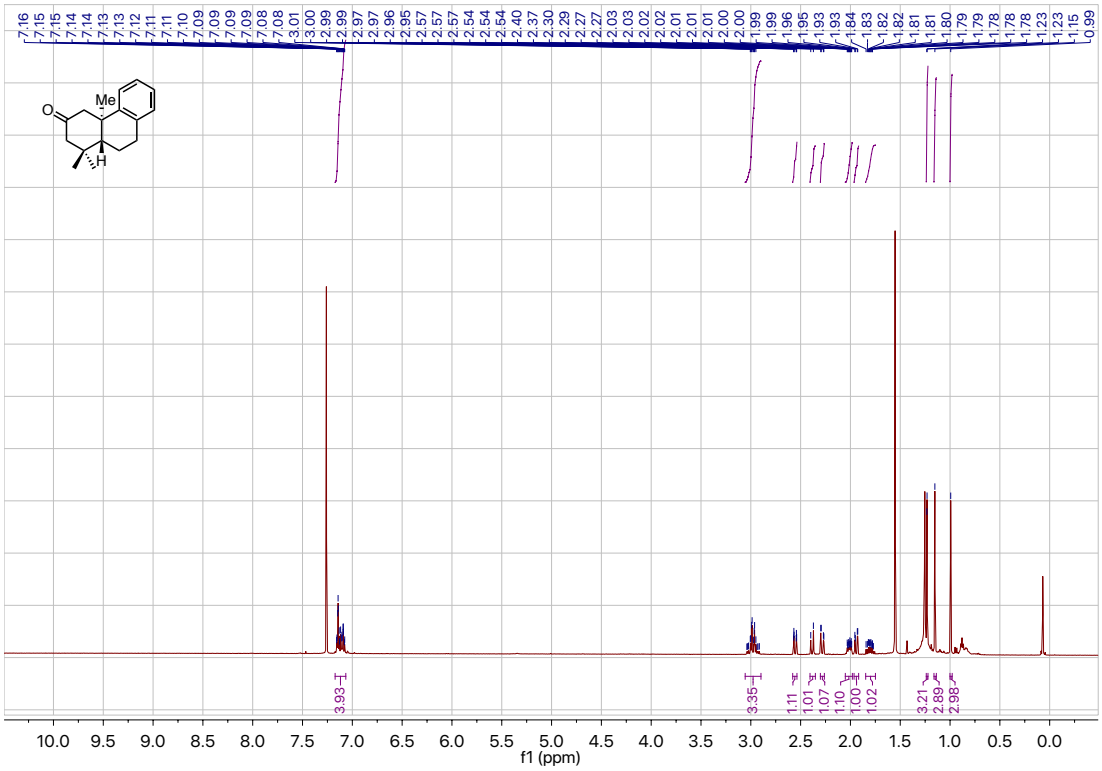

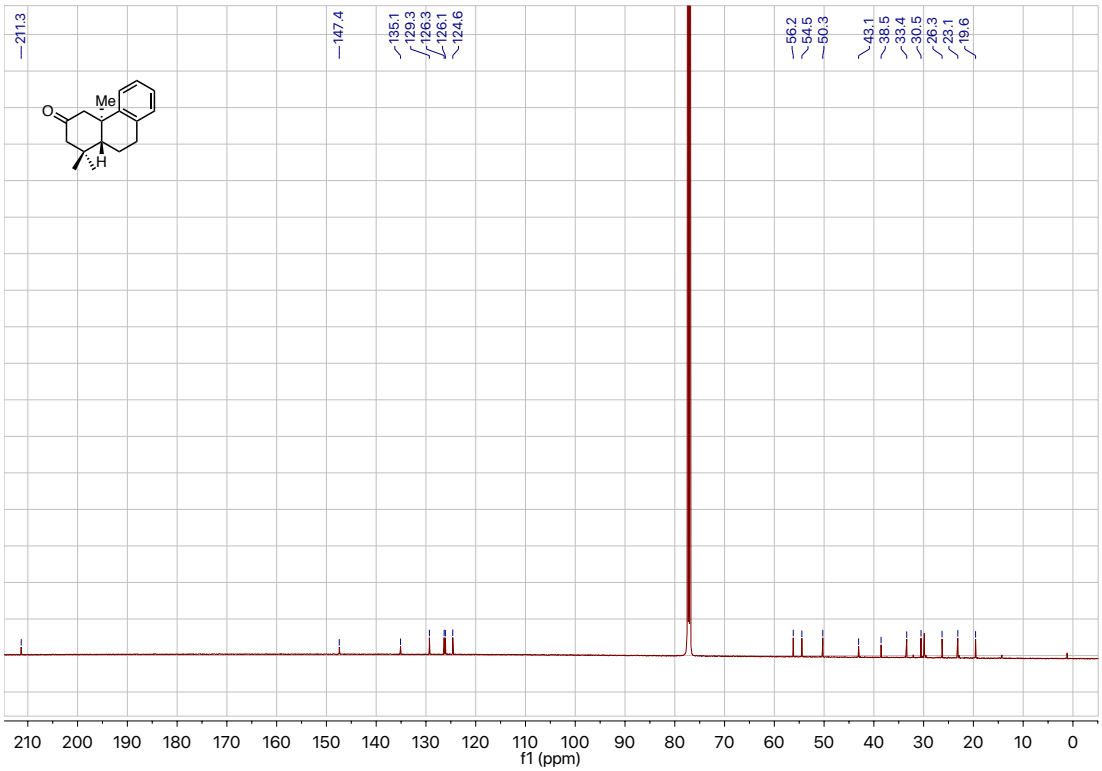

215:

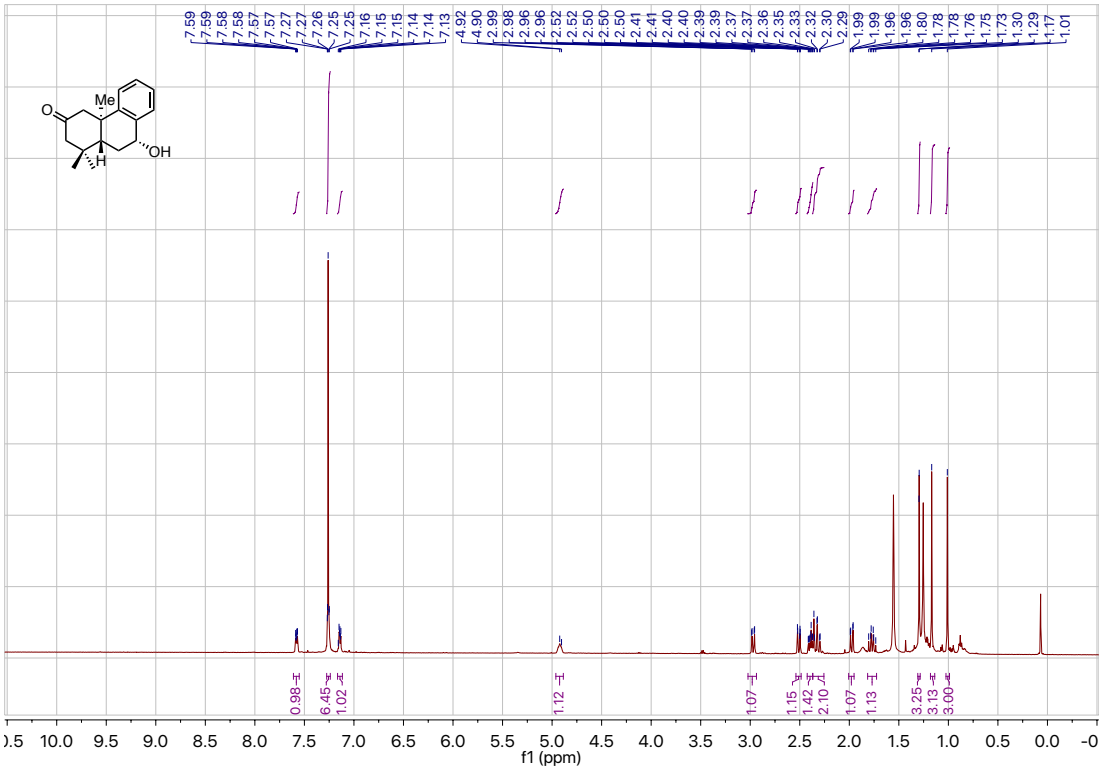

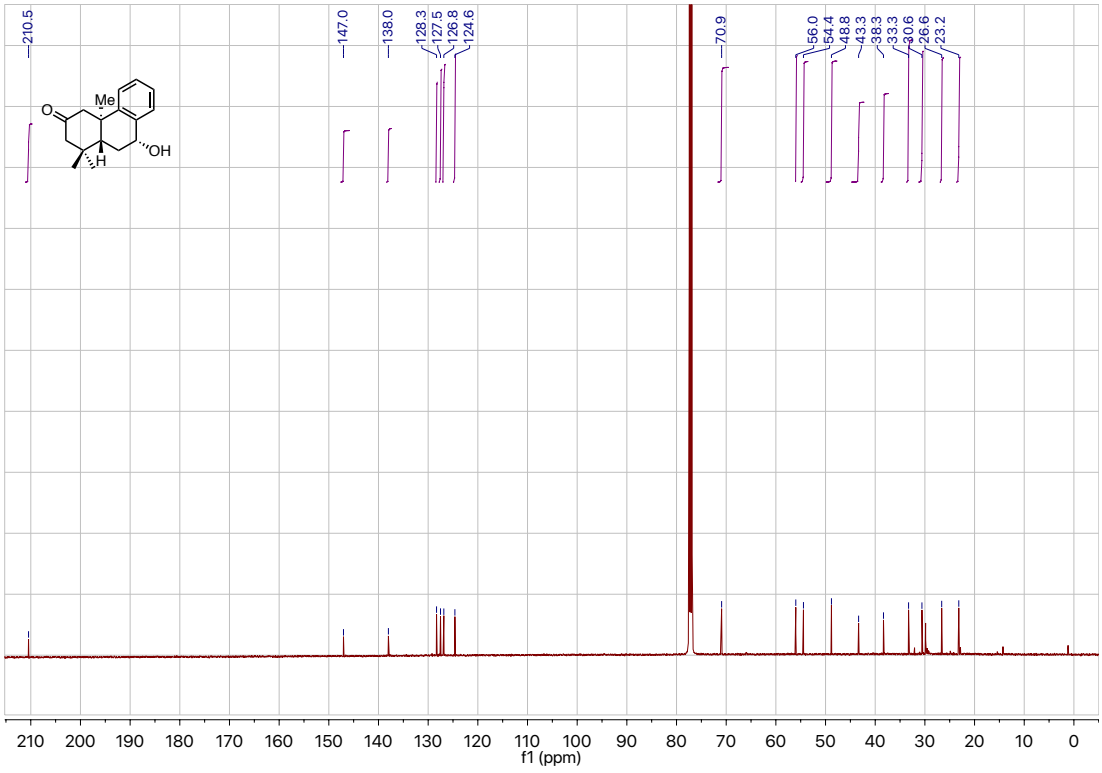

216:

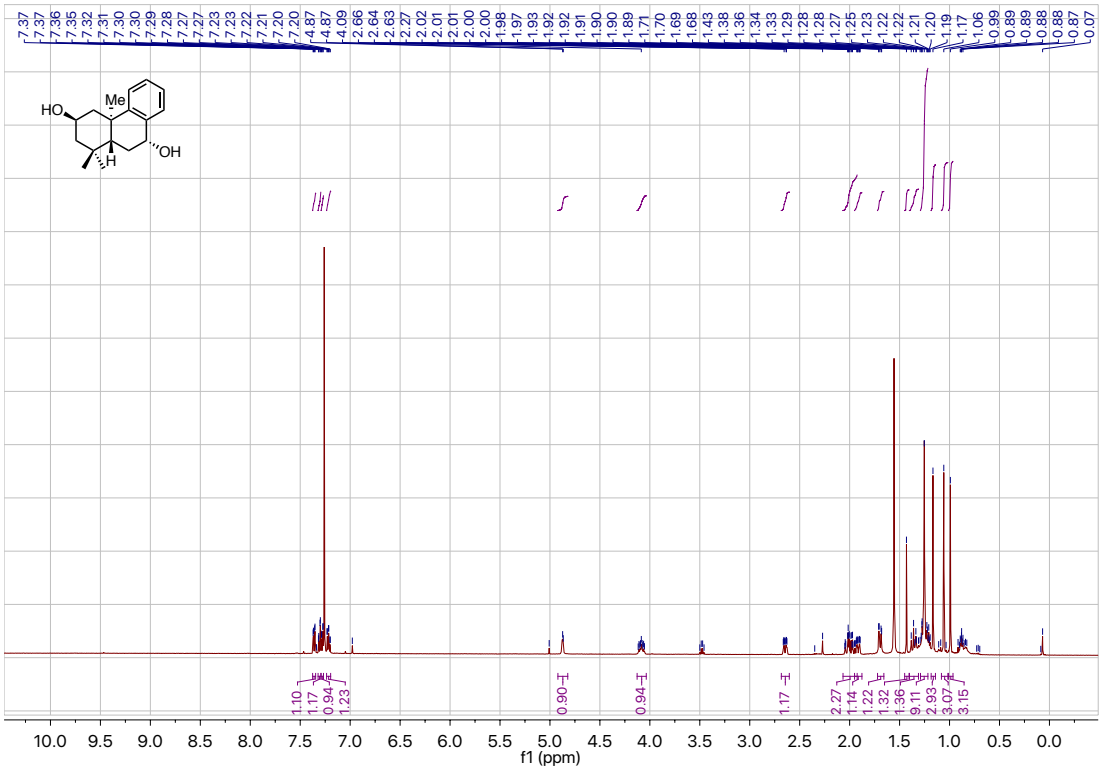
HO
Me
H
OH
f1 (ppm)

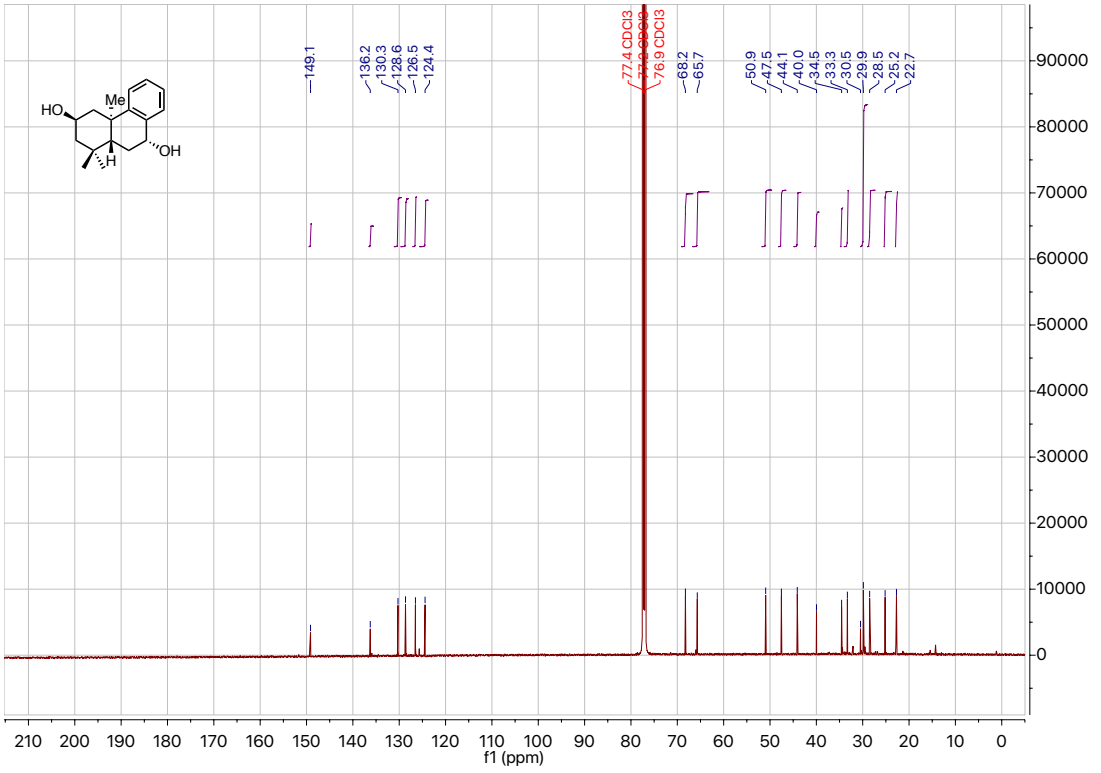
HO
Me
H
OH
149.1
136.2
130.3
128.6
126.5
124.4
77.4 CDCl3
76.9 CDCl3
68.2
65.7
50.9
47.5
44.1
40.0
34.5
33.3
30.5
29.9
28.5
25.2
22.7
f1 (ppm)

8.6 Chapter 3 – selected spectra

125:

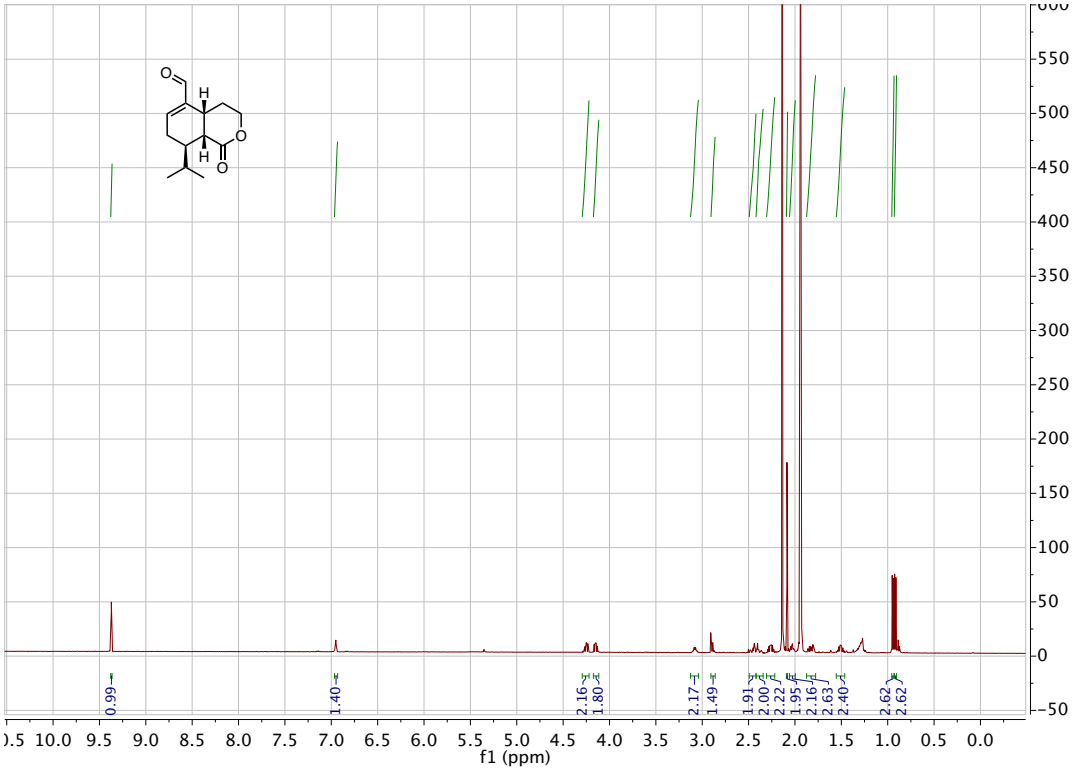

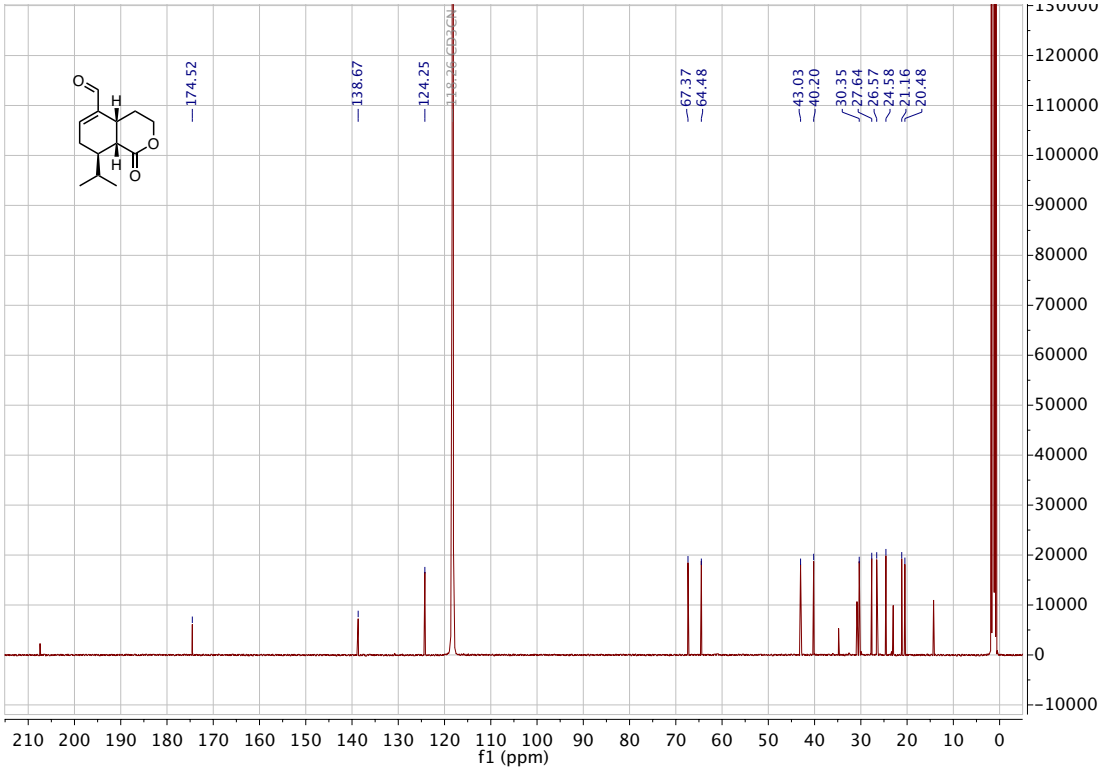

124:

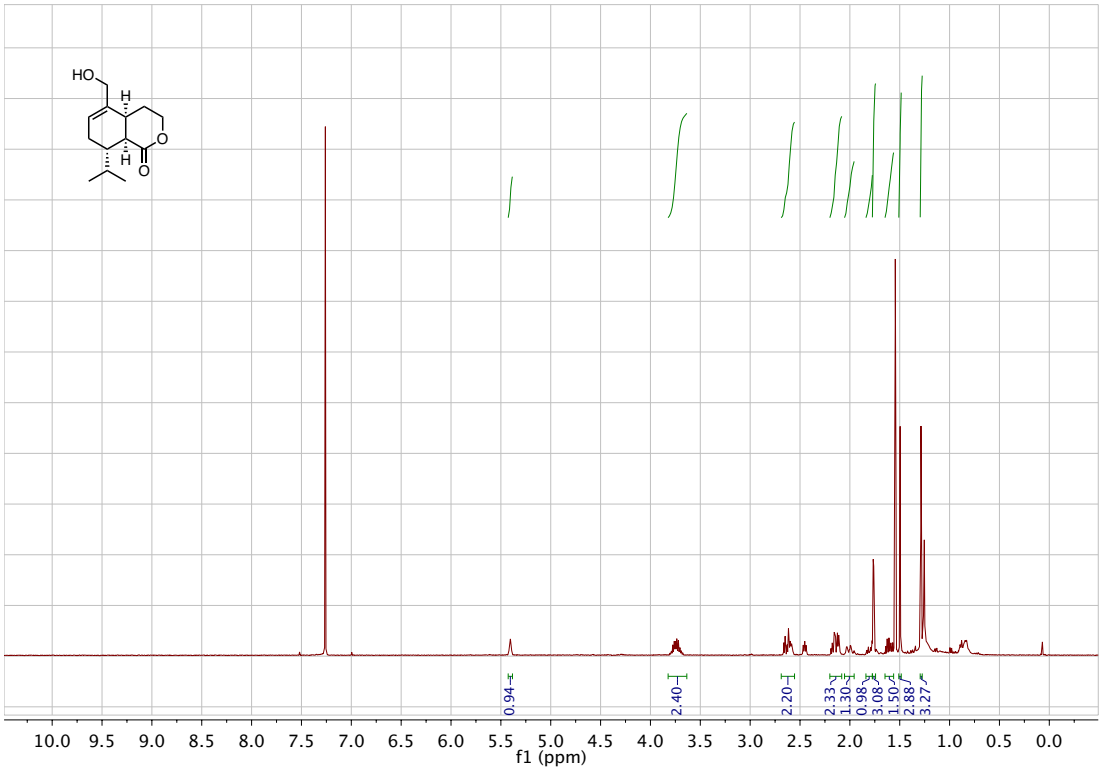
HO
H
O
H
O
0.94
2.40
2.20
2.33
1.30
0.98
3.08
1.50
2.88
3.27
10.0 9.5 9.0 8.5 8.0 7.5 7.0 6.5 6.0 5.5 5.0 4.5 4.0 3.5 3.0 2.5 2.0 1.5 1.0 0.5 0.0
f1 (ppm)

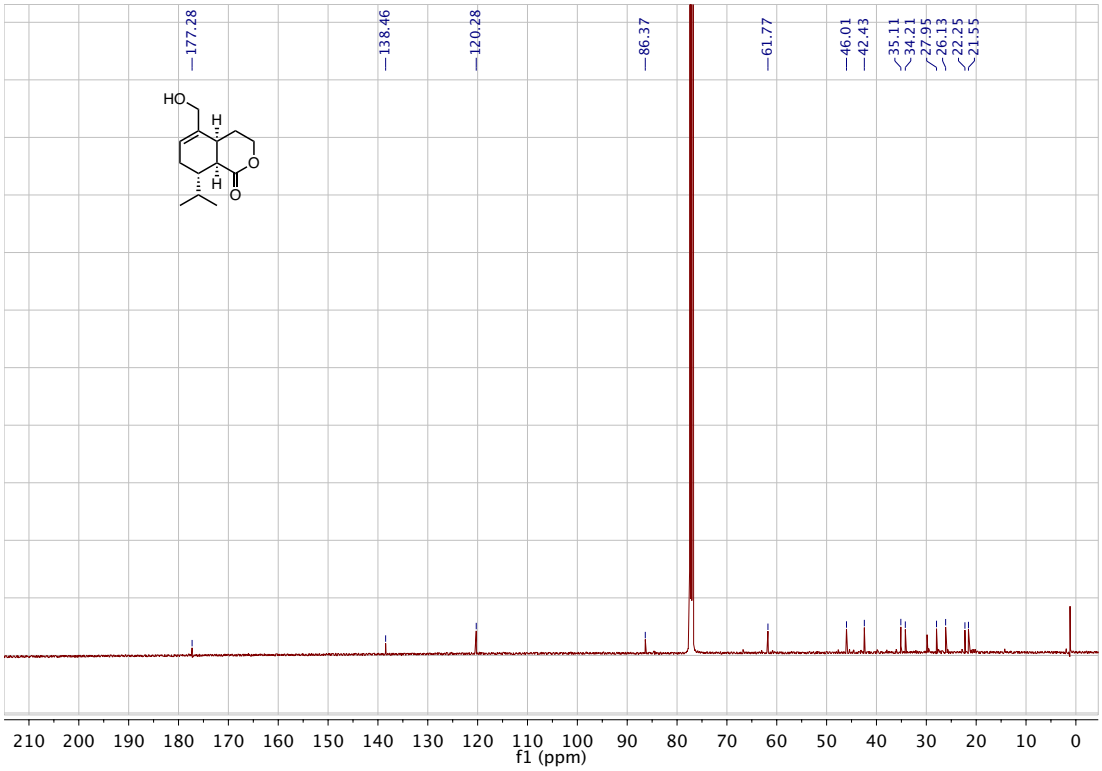
177.28
138.46
120.28
86.37
61.77
46.01
42.43
35.11
34.21
27.95
26.13
22.25
21.55
HO
H
O
H
O
210 200 190 180 170 160 150 140 130 120 110 100 90 80 70 60 50 40 30 20 10 0
f1 (ppm)

126:

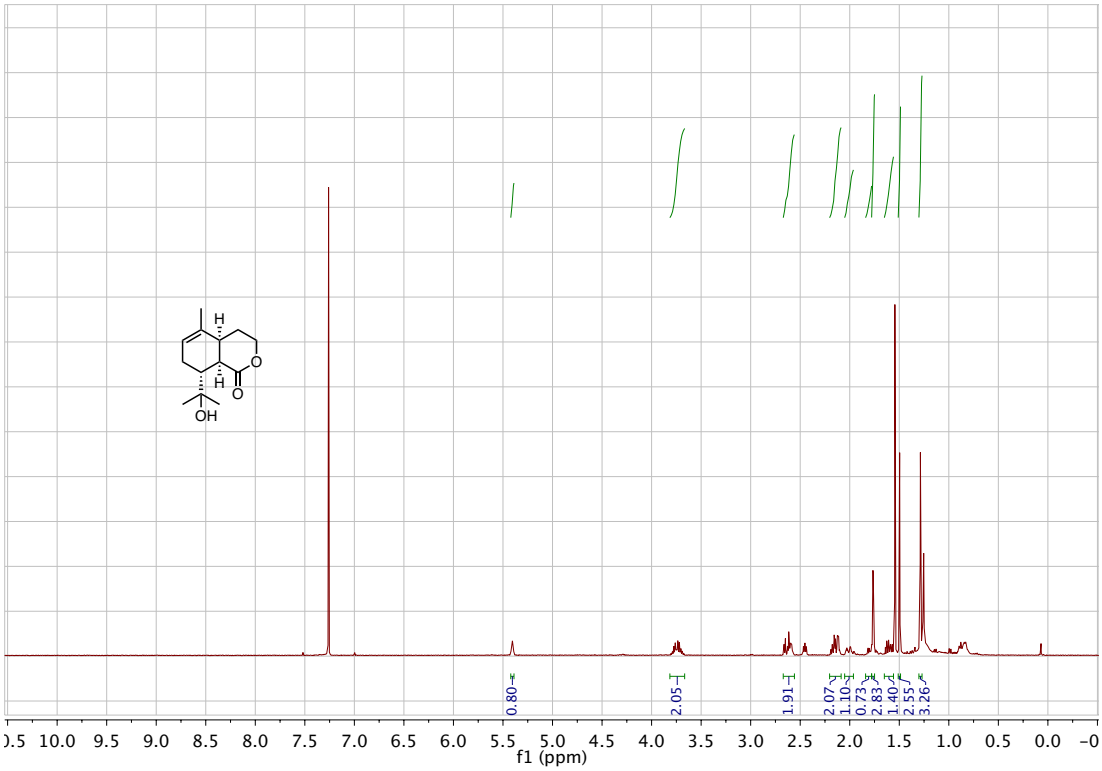
H
O
H
O
OH
0.80
2.05
1.91
2.07
1.10
0.73
2.83
1.40
2.55
3.26
f1 (ppm)

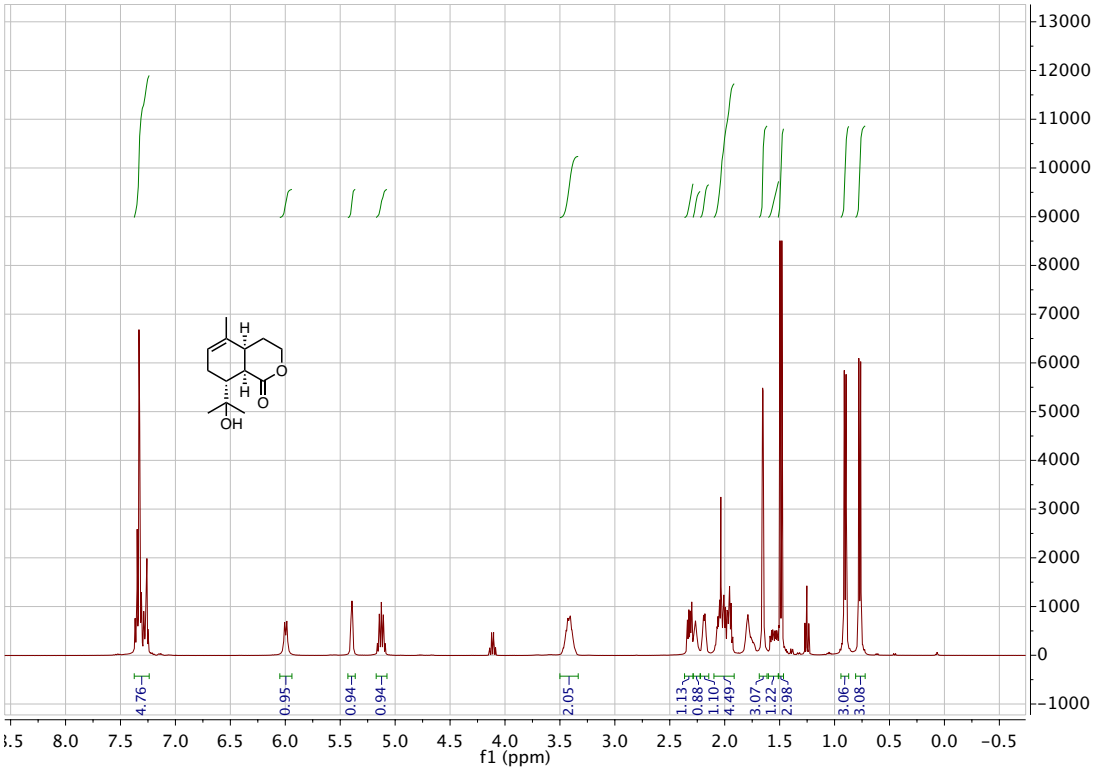
H
O
H
O
OH
4.76
0.95
0.94
0.94
2.05
1.13
0.88
1.10
4.49
3.07
1.22
2.98
3.06
3.08
f1 (ppm)

116:

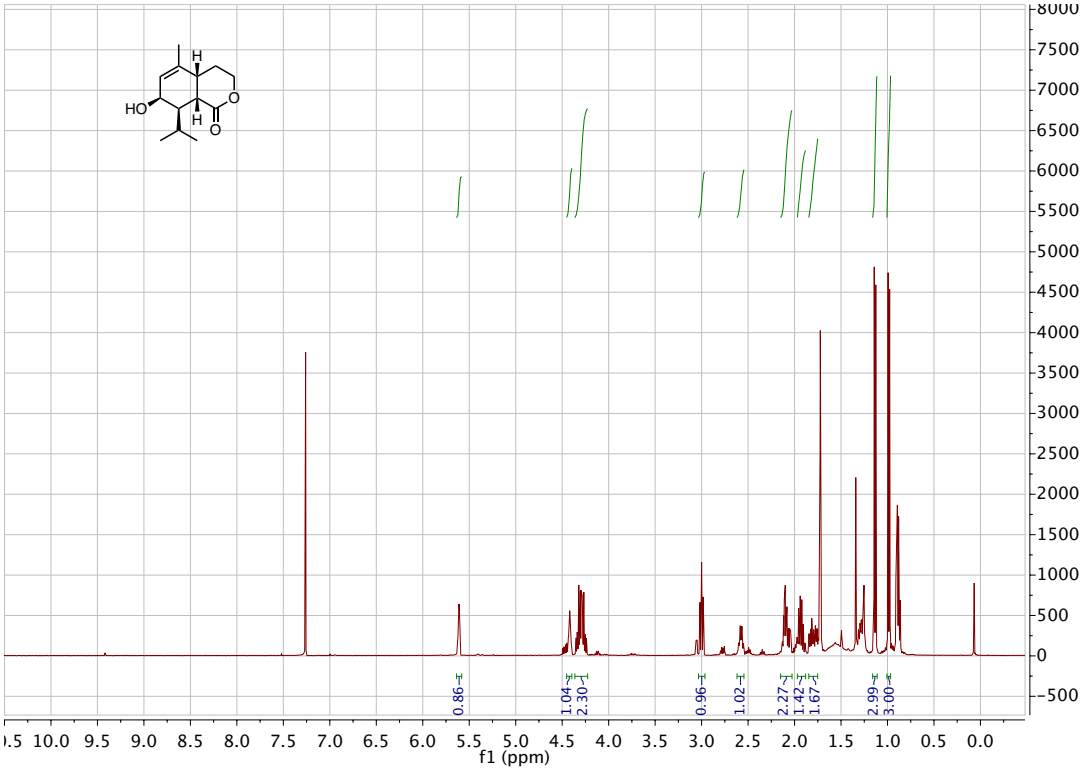
HO
H
O
H
O
0.86
1.04
2.30
0.96
1.02
2.27
1.42
1.67
2.99
3.00
f1 (ppm)

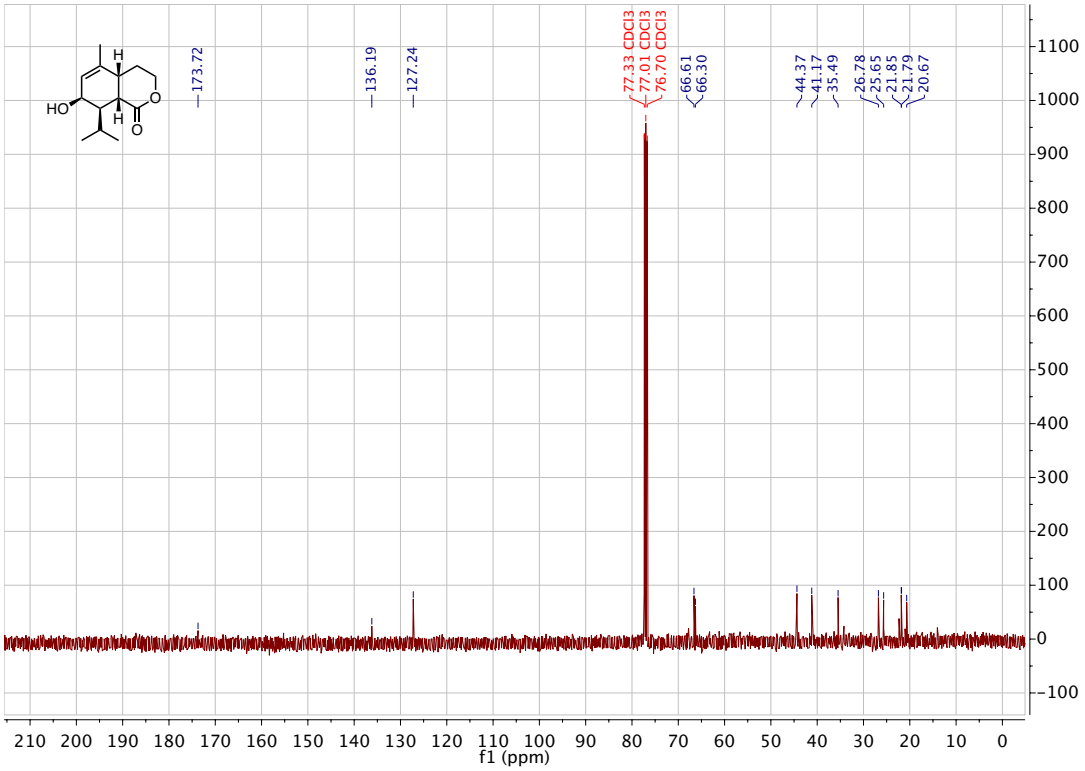
HO
H
O
H
O
173.72
136.19
127.24
77.33 CDCl3
77.01 CDCl3
76.70 CDCl3
66.61
66.30
44.37
41.17
35.49
26.78
25.65
21.85
21.79
20.67
f1 (ppm)

8.7 Chapter 4 – selected spectra

Trans-**132**:

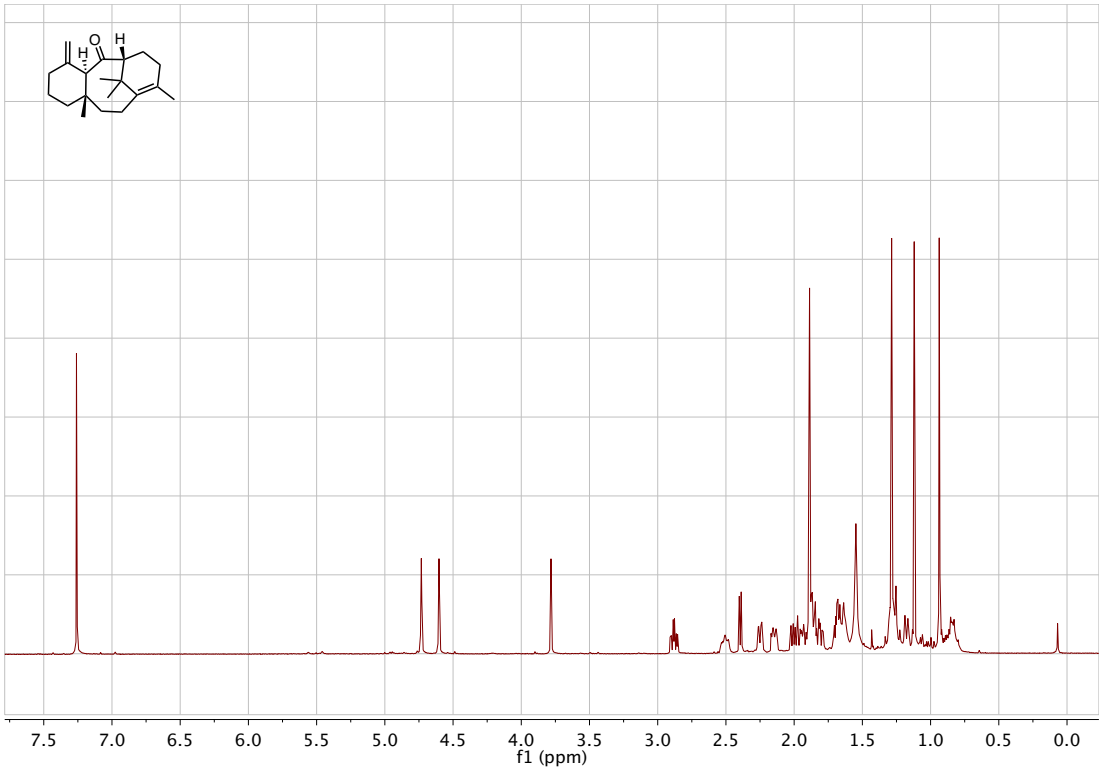

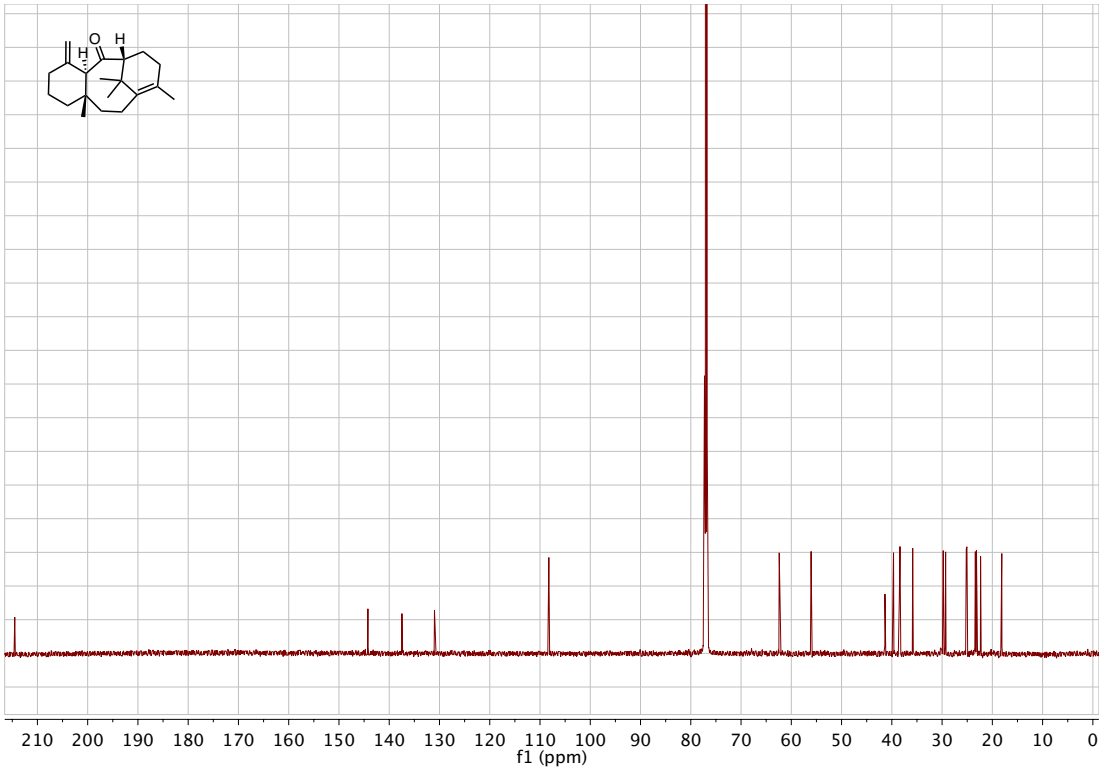

Cis-**131**:

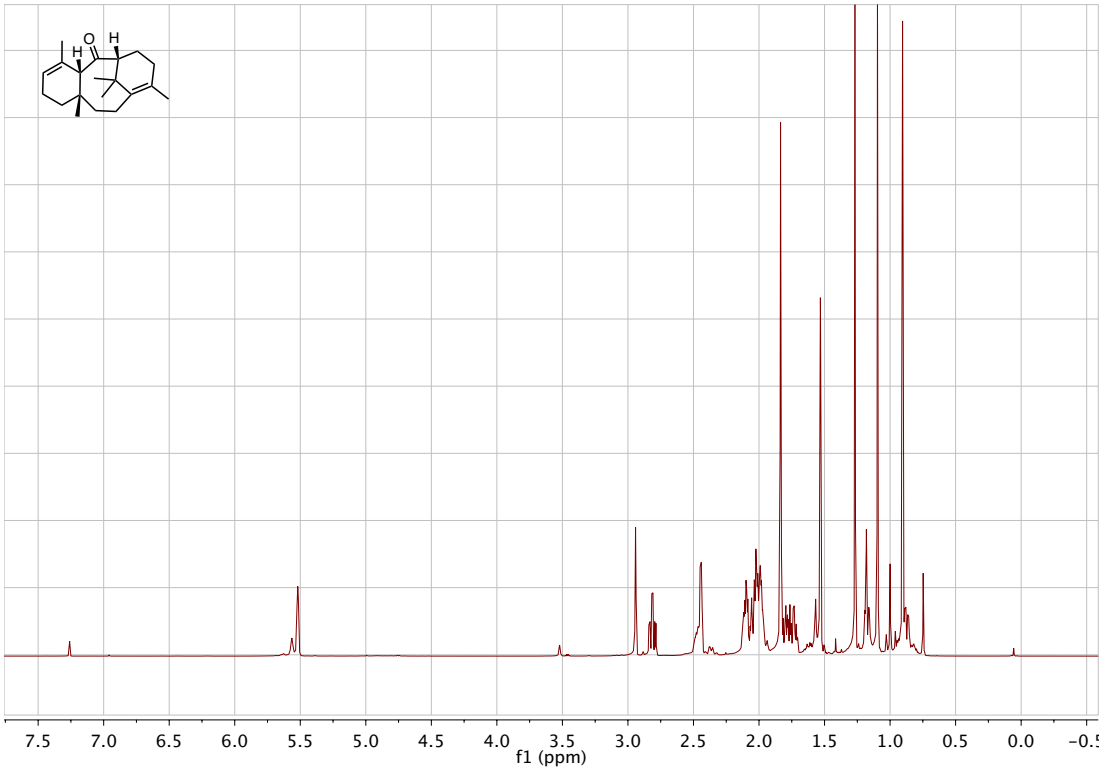
O
H
H
7.5 7.0 6.5 6.0 5.5 5.0 4.5 4.0 3.5 3.0 2.5 2.0 1.5 1.0 0.5 0.0 -0.5
f1 (ppm)

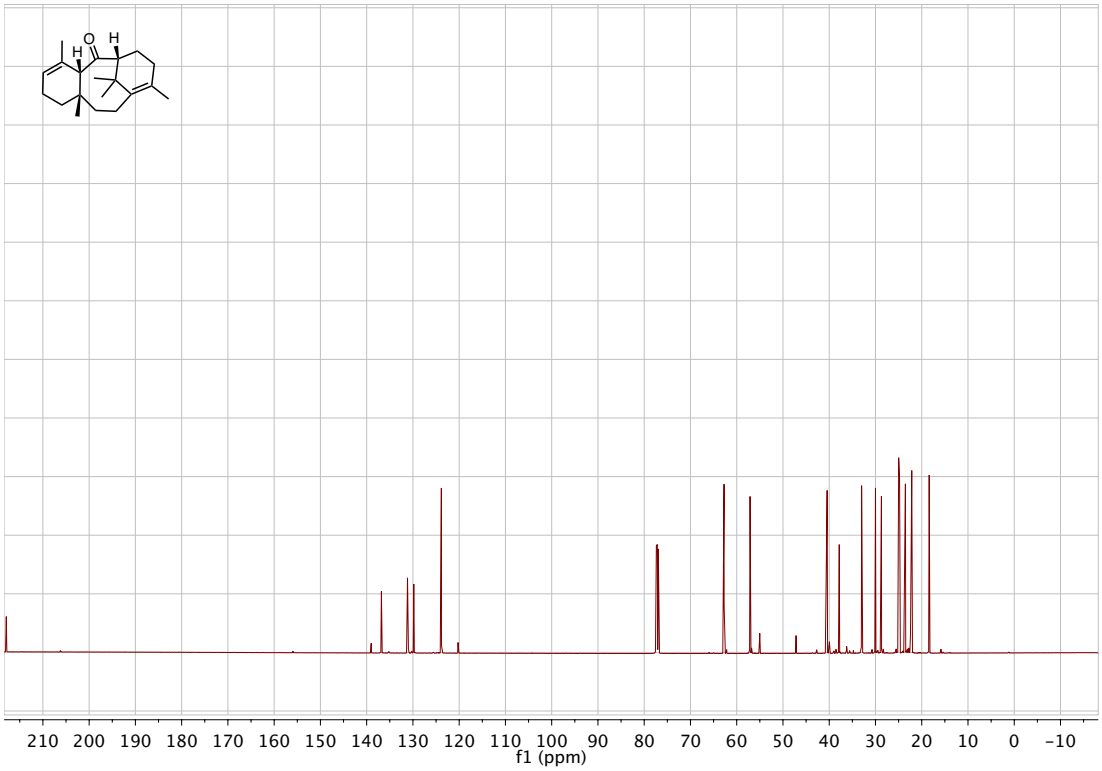
O
H
H
210 200 190 180 170 160 150 140 130 120 110 100 90 80 70 60 50 40 30 20 10 0 -10
f1 (ppm)

367:

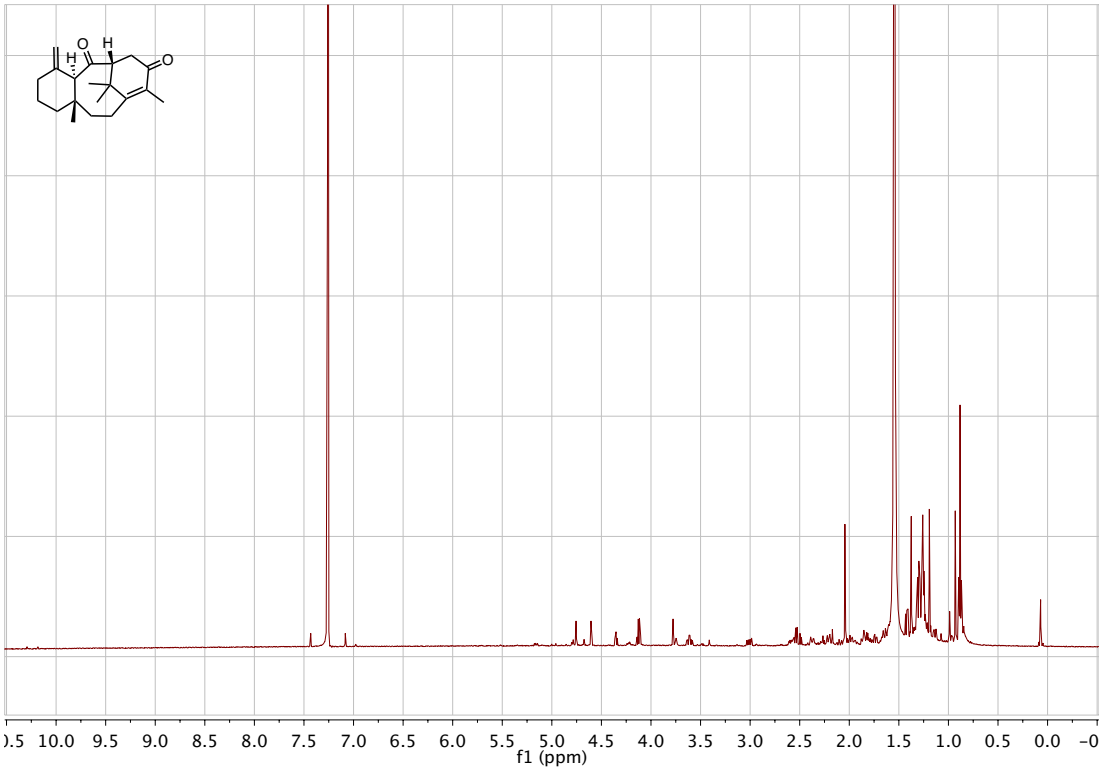
O
H
H
O
10.0 9.5 9.0 8.5 8.0 7.5 7.0 6.5 6.0 5.5 5.0 4.5 4.0 3.5 3.0 2.5 2.0 1.5 1.0 0.5 0.0
f1 (ppm)

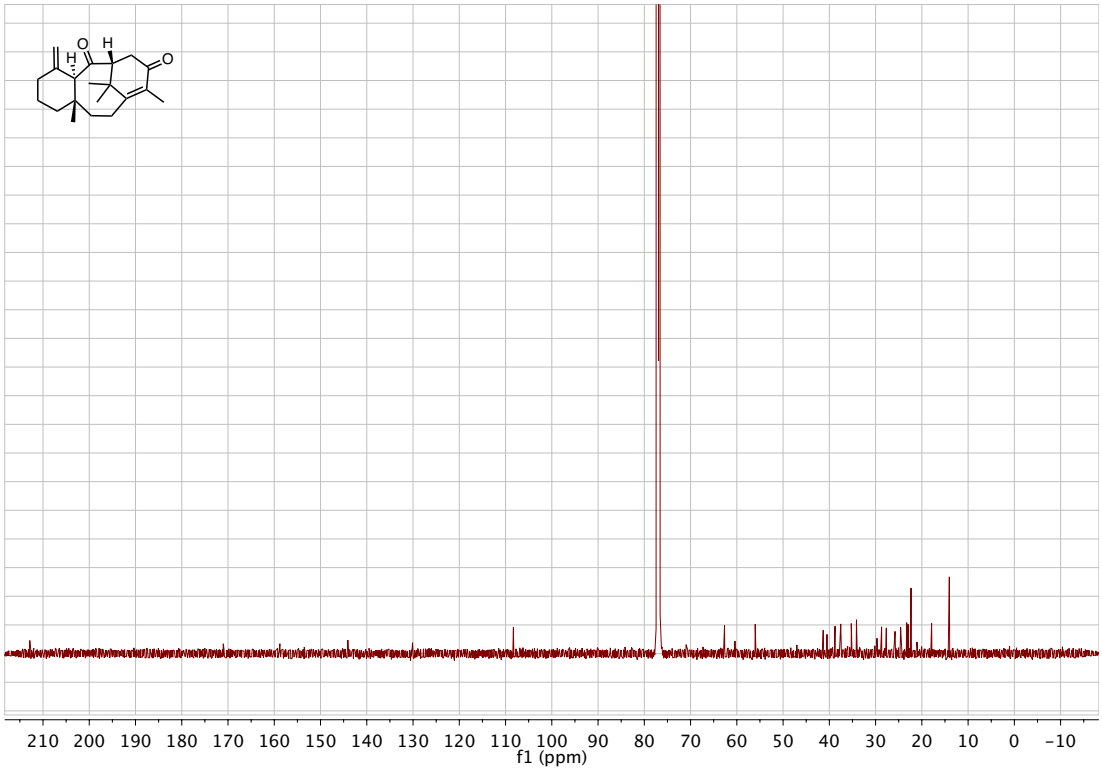
O
H
H
O
210 200 190 180 170 160 150 140 130 120 110 100 90 80 70 60 50 40 30 20 10 0 -10
f1 (ppm)

368:

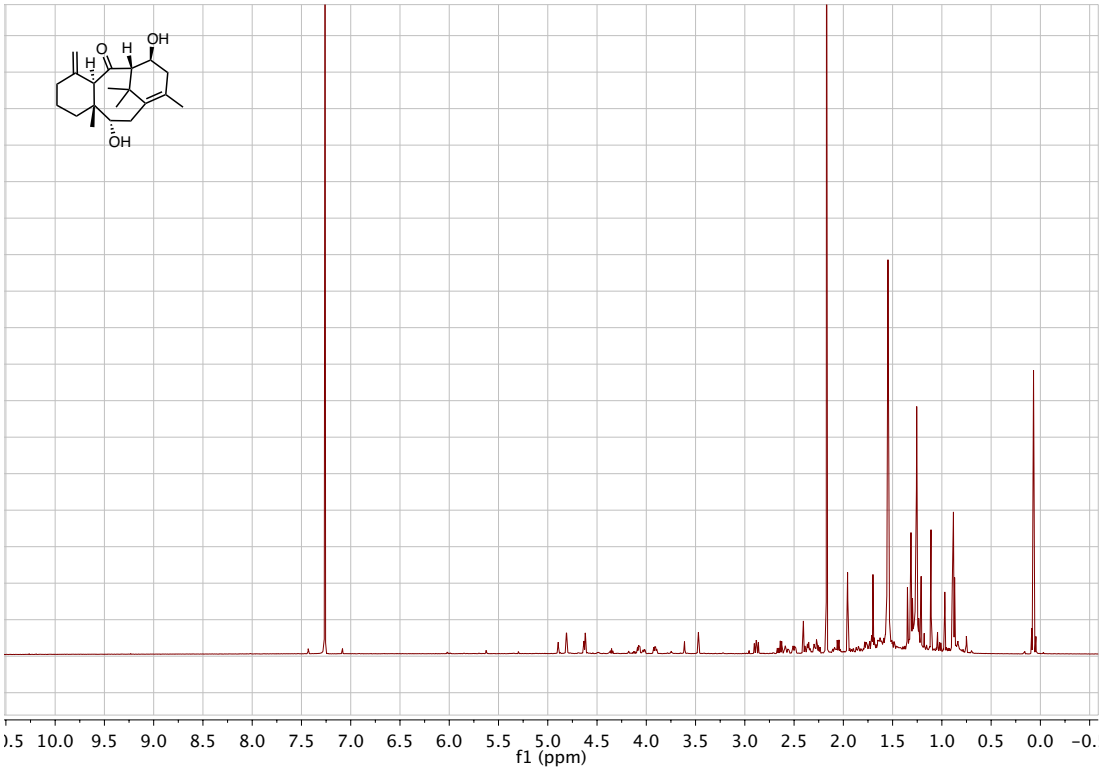
O
H
H
OH
OH
10.0 9.5 9.0 8.5 8.0 7.5 7.0 6.5 6.0 5.5 5.0 4.5 4.0 3.5 3.0 2.5 2.0 1.5 1.0 0.5 0.0
f1 (ppm)

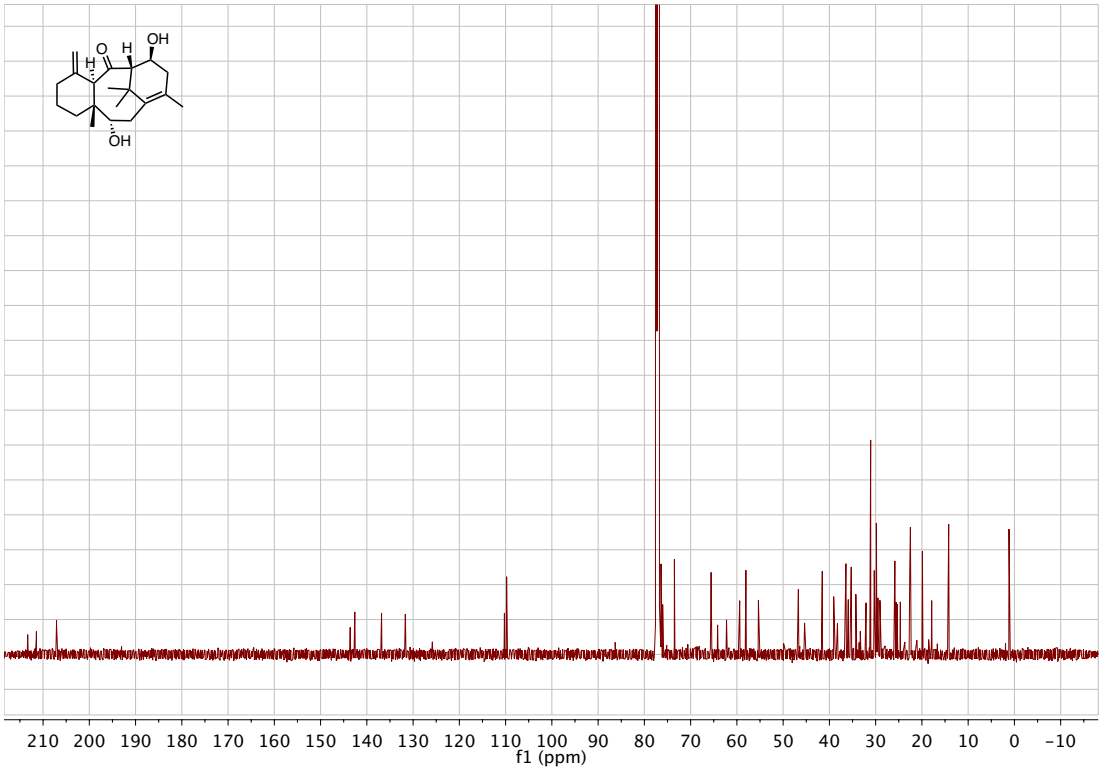
O
H
H
OH
OH
210 200 190 180 170 160 150 140 130 120 110 100 90 80 70 60 50 40 30 20 10 0 -10
f1 (ppm)

370:

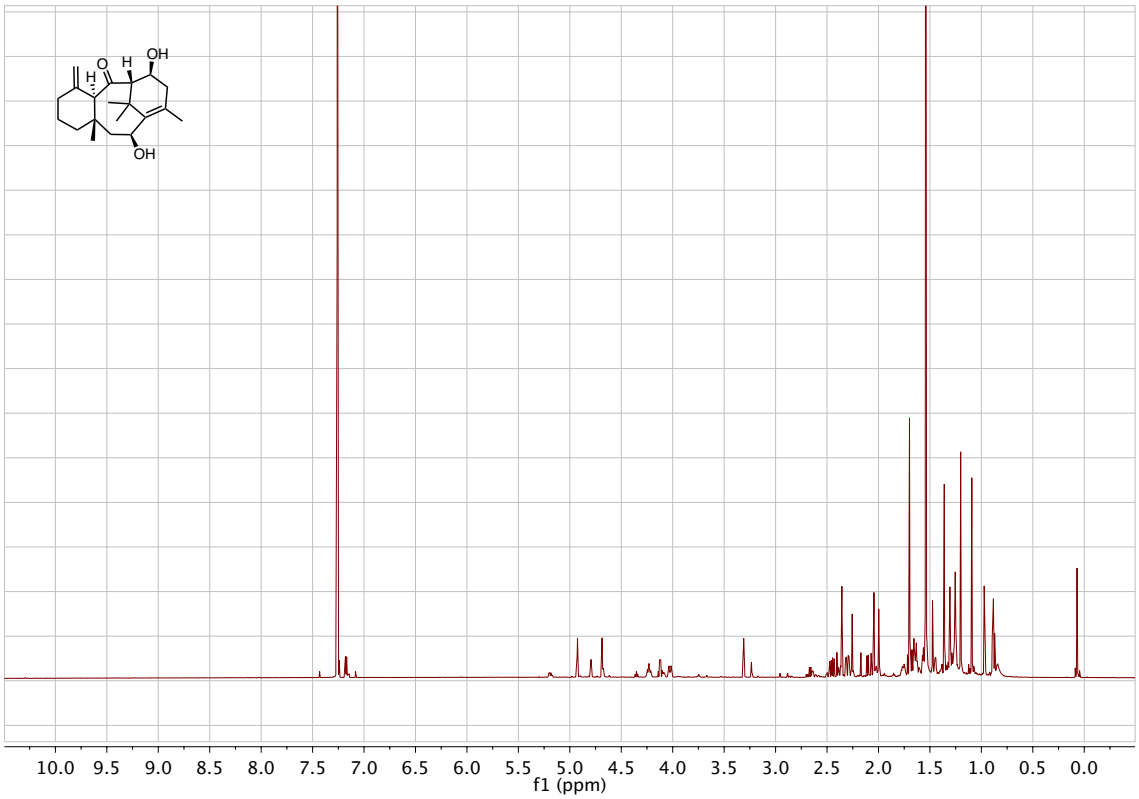
O
H
OH
H
OH
10.0 9.5 9.0 8.5 8.0 7.5 7.0 6.5 6.0 5.5 5.0 4.5 4.0 3.5 3.0 2.5 2.0 1.5 1.0 0.5 0.0
f1 (ppm)

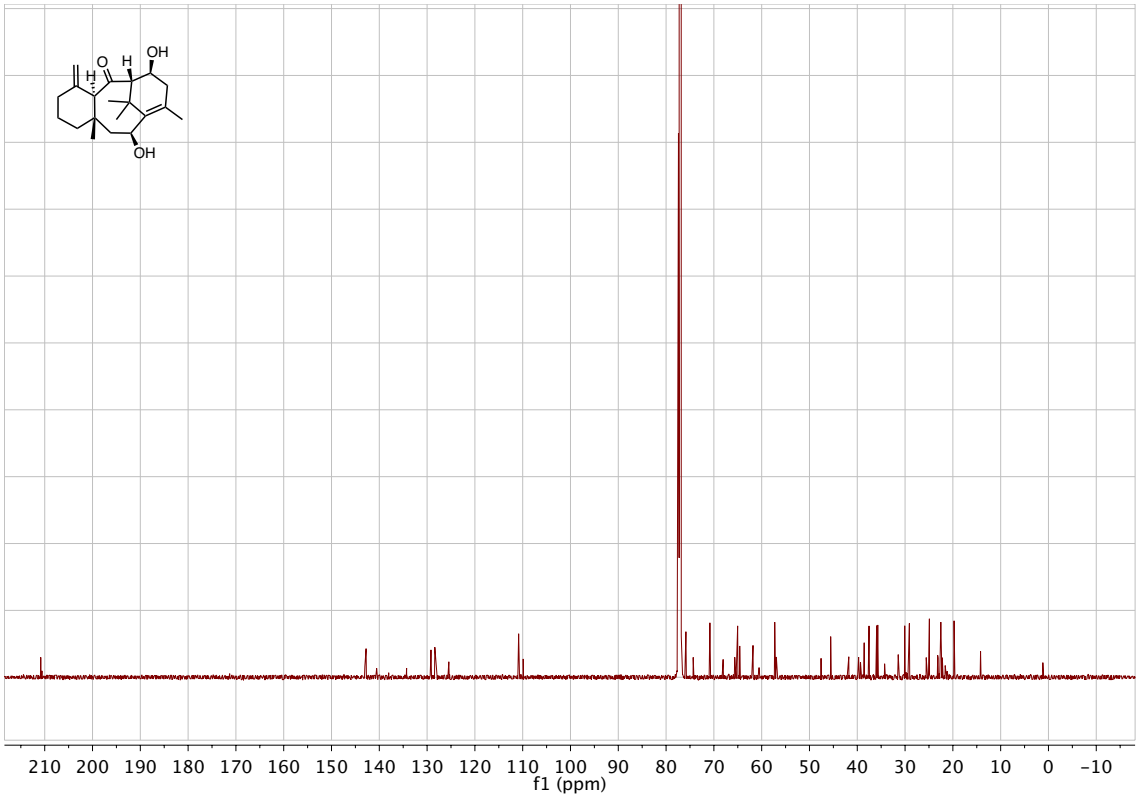
O
H
OH
H
OH
210 200 190 180 170 160 150 140 130 120 110 100 90 80 70 60 50 40 30 20 10 0 -10
f1 (ppm)

371:

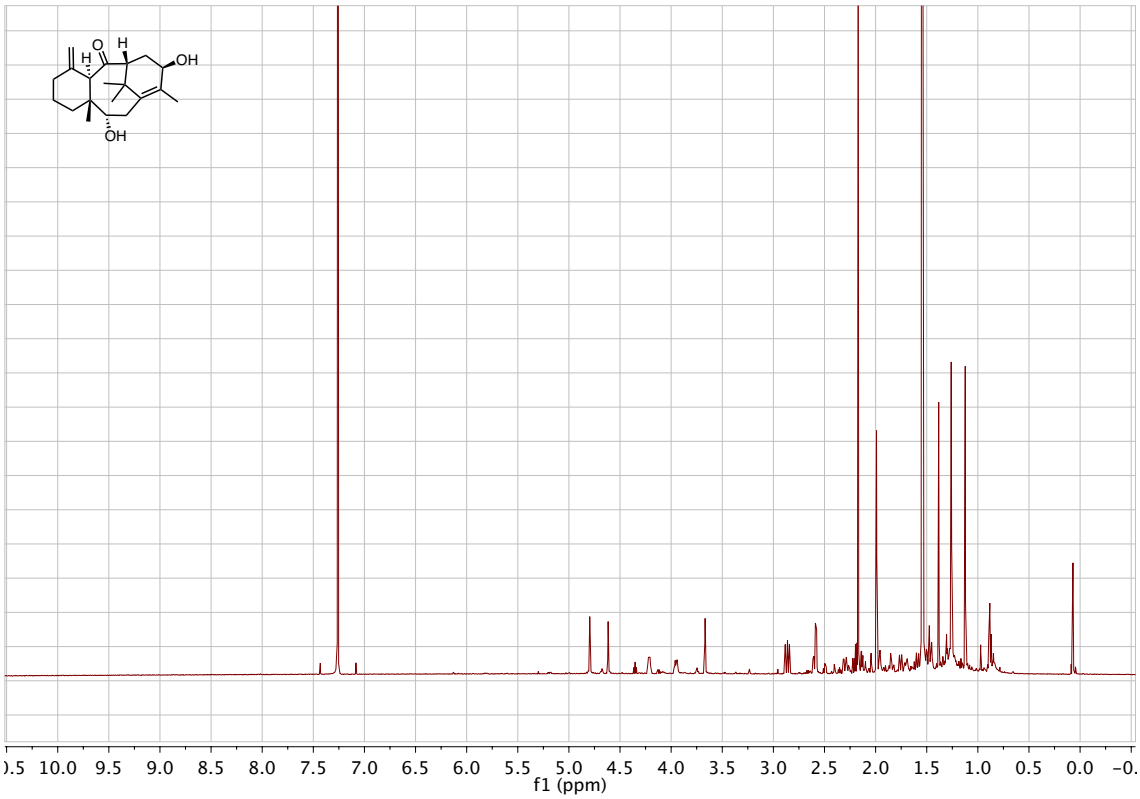
O
H
H
OH
OH
10.0 9.5 9.0 8.5 8.0 7.5 7.0 6.5 6.0 5.5 5.0 4.5 4.0 3.5 3.0 2.5 2.0 1.5 1.0 0.5 0.0
f1 (ppm)

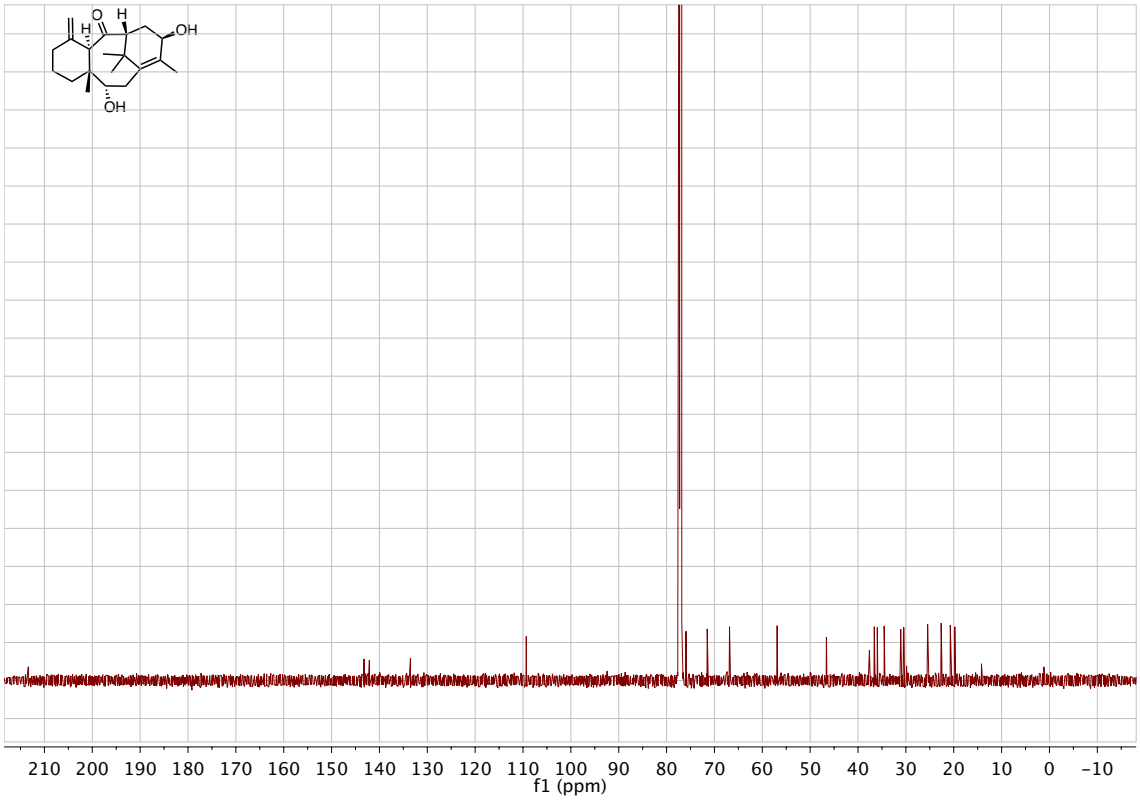
O
H
H
OH
OH
210 200 190 180 170 160 150 140 130 120 110 100 90 80 70 60 50 40 30 20 10 0 -10
f1 (ppm)